

Strengthening of damaged reinforced concrete beams by external fiber glass plates.

Badr Mohammed Naji Ghaleb

Civil Engineering

July 1992

Abstract

The main theme of this thesis has focused on the use of external fiber glass plates to strengthen damaged flexure and shear beams.

The work was divided into four parts, with the first part dealing with the selection of the fiber glass material for the proposed repair out of two recommended composites by the local manufacturer to provide the highest strength and ductility.

The second part of the thesis addressed the study of the effect of thermal cycling on the bond strength between the fiber glass plates and the epoxy glue.

The third part, studied the performance of repairing flexure reinforced concrete beams after damaging them to a level loading corresponding to 10 mm central deflection. The level of damage was decided upon after testing two control beams to failure. These beams were then repaired using external fiber glass plates of different thicknesses.

The fourth part of the studyh evaluated the performance of R.C. shear beams strengthened with external web reinforcement of the fiber glass. Two control beams were tested upon failure. It was decided then to damage the beams upto the appearance of the first shear crack in the shear span. Three repair techniques were tried in the form of side plates (wings), strips and a newly suggested technique in the form of U-jacket.

A criterion to evaluate the plate thickness to be used for repair any beam in reality was presented based on the ultimate flexural capacity of the section as well as the maximum interface shear and normal stresses at the plate ends.

Strengthening of Damaged Reinforced Concrete Beams By External Fiber Glass Plates

by

Badr Mohammed Naji Ghaleb

A Thesis Presented to the

FACULTY OF THE COLLEGE OF GRADUATE STUDIES

KING FAHD UNIVERSITY OF PETROLEUM & MINERALS

DHAHRAN, SAUDI ARABIA

In Partial Fulfillment of the
Requirements for the Degree of

MASTER OF SCIENCE

In

CIVIL ENGINEERING

July, 1992

INFORMATION TO USERS

This manuscript has been reproduced from the microfilm master. UMI films the text directly from the original or copy submitted. Thus, some thesis and dissertation copies are in typewriter face, while others may be from any type of computer printer.

The quality of this reproduction is dependent upon the quality of the copy submitted. Broken or indistinct print, colored or poor quality illustrations and photographs, print bleedthrough, substandard margins, and improper alignment can adversely affect reproduction.

In the unlikely event that the author did not send UMI a complete manuscript and there are missing pages, these will be noted. Also, if unauthorized copyright material had to be removed, a note will indicate the deletion.

Oversize materials (e.g., maps, drawings, charts) are reproduced by sectioning the original, beginning at the upper left-hand corner and continuing from left to right in equal sections with small overlaps. Each original is also photographed in one exposure and is included in reduced form at the back of the book.

Photographs included in the original manuscript have been reproduced xerographically in this copy. Higher quality 6" x 9" black and white photographic prints are available for any photographs or illustrations appearing in this copy for an additional charge. Contact UMI directly to order.

U·M·I

University Microfilms International
A Bell & Howell Information Company
300 North Zeeb Road, Ann Arbor, MI 48106-1346 USA
313/761-4700 800/521-0600

0001

Order Number 1355312

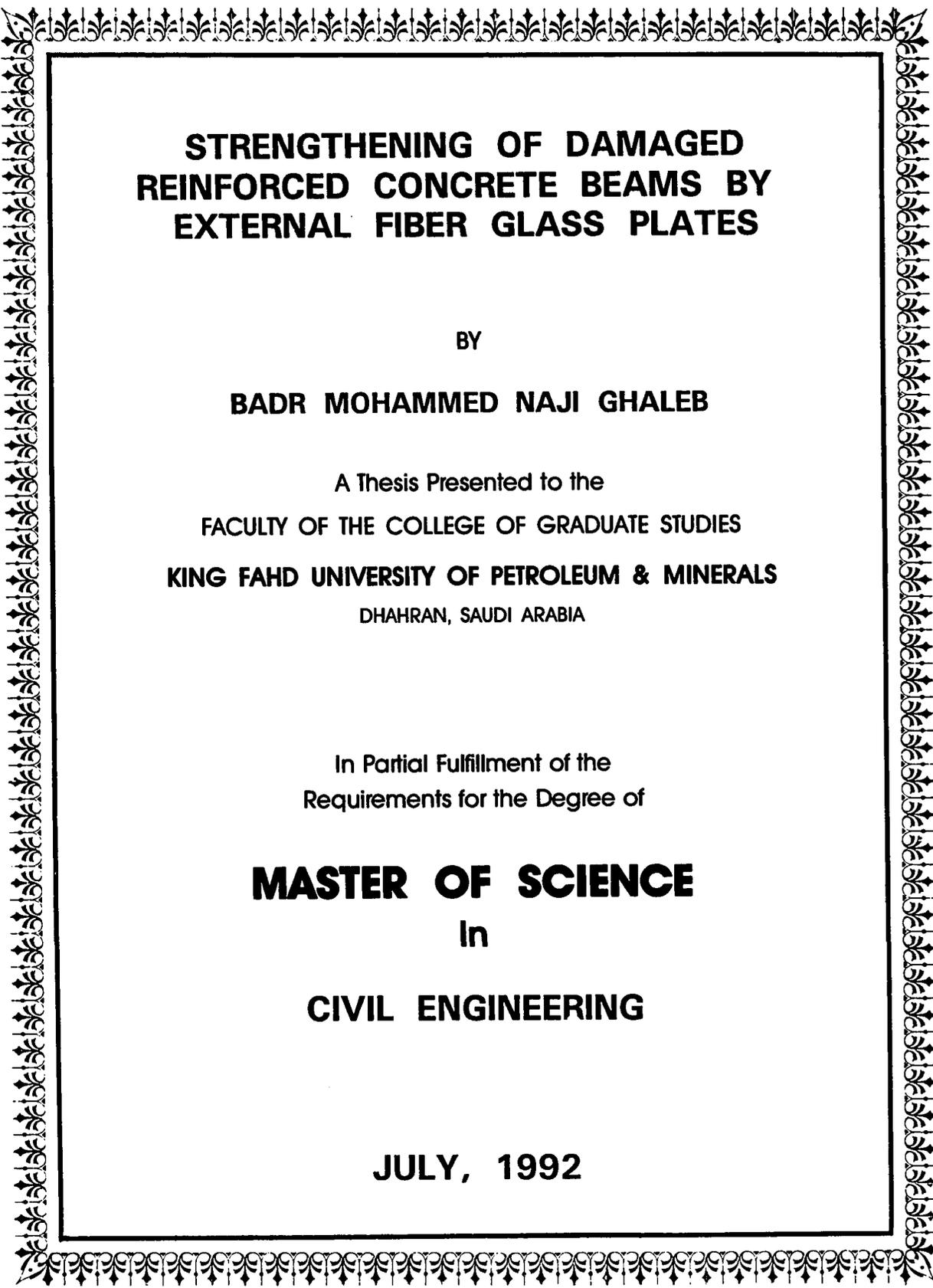
**Strengthening of damaged reinforced concrete beams by external
fiber glass plates**

Ghaleb, Badr Mohammad Naji, M.S.

King Fahd University of Petroleum and Minerals (Saudi Arabia), 1992

U·M·I
300 N. Zeeb Rd.
Ann Arbor, MI 48106





**STRENGTHENING OF DAMAGED
REINFORCED CONCRETE BEAMS BY
EXTERNAL FIBER GLASS PLATES**

BY

BADR MOHAMMED NAJI GHALEB

A Thesis Presented to the
FACULTY OF THE COLLEGE OF GRADUATE STUDIES
KING FAHD UNIVERSITY OF PETROLEUM & MINERALS
DHAHRAN, SAUDI ARABIA

In Partial Fulfillment of the
Requirements for the Degree of

MASTER OF SCIENCE

In

CIVIL ENGINEERING

JULY, 1992

KING FAHD UNIVERSITY OF PETROLEUM & MINERALS

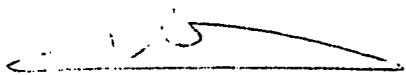
DHAHRAN, SAUDI ARABIA

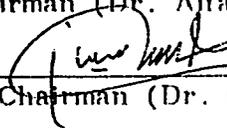
COLLEGE OF GRADUATE STUDIES

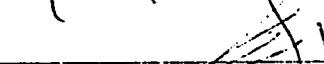
This thesis, written by **BADR MOHAMMED NAJI GHALEB** under the direction of his Thesis Advisor, and approved by his Thesis Committee, has been presented to and accepted by the Dean of the College of Graduate Studies, in partial fulfillment of the requirements for the degree of

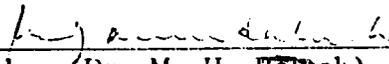
MASTER OF SCIENCE IN CIVIL ENGINEERING

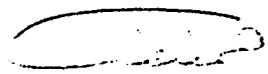
Thesis Committee


Chairman (Dr. Alfarabi M. Sharif)


Co-Chairman (Dr. G. J. Al-Sulaimani)


Member (Dr. I. A. Basunbul)

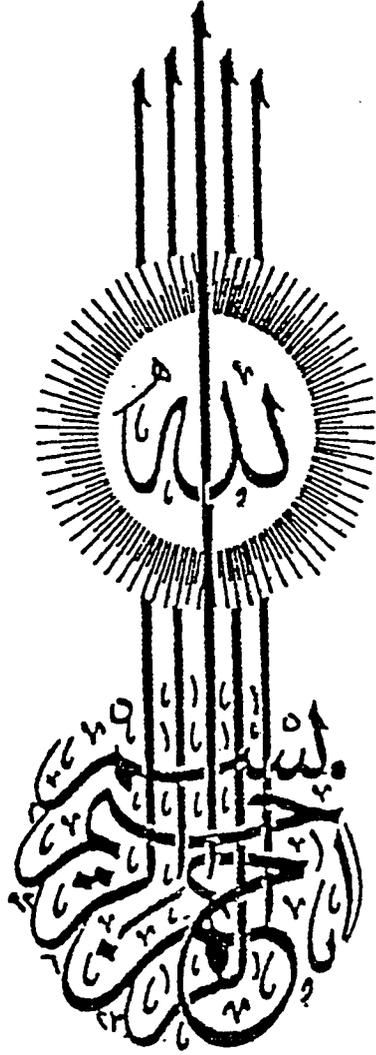

Member (Dr. M. H. Baluch)


Dr. Hamdan Al-Ghamdi
Department Summer Chairman


Dr. Ala H. Al-Rabeh
Dean College of Graduate Studies

Date : July, 1992.





سُبْحَانَكَ لَا عِلْمَ لَنَا إِلَّا مَا عَلَّمْتَنَا إِنَّكَ أَنْتَ الْعَلِيمُ الْحَكِيمُ

مَسَدَاتُ اللَّهِ الْعَظِيمِ

الإهداء إلى الأجابة :

الوالدين العزيزين
زوجتي الوفية وأولادي الأعزاء

الذين شاركوني المعاناة أثناء فترة دراستي وقاسوا
أوقاتاً صعبة من خلال تضحياتهم المستمرة .

*Dedicated to my beloved parents
and my wife and children, who made
the ultimate sacrifice and fought
through hard times to make things
possible for me.*

ACKNOWLEDGEMENT

All praise, thanks and gratitude first and last be to Almighty Allah, who helped me to complete this task.

I wish to express my deep gratitude and sincere appreciation to my beloved parents, wife and children for their sacrifice, encouragement and understanding for leaving them during my study.

Acknowledgment is due to King Fahd University of Petroleum and Minerals for extending all the facilities and support for this research.

I wish to express my sincere appreciation and deepest gratitudes to Dr. Alfarabi Sharif who served as my major thesis advisor and has been a constant source of help, and encouragement during this study with open heart and without any time and potential limitations.

Also, I greatly appreciate the guidance and invaluable cooperation provided by Dr. Ghazi J. Al-Sulaimani who served as a co-advisor. Thanks and appreciation for the frequent attention and encouragement provided by Dr. Islem Basunbul and Prof. Mohammad H. Baluch who served as committee members.

Special thanks to engineer Ahmad Sami and Amiantit Company for providing the fiber glass plates throughout the research program.

TABLE OF CONTENTS

	<i>Page</i>
Acknowledgement	ii
List of Tables	vii
List of Figures	ix
List of Plates	xiv
Abstract (English)	xvii
Abstract (Arabic)	xviii
1. INTRODUCTION	
1.1 General	1
1.2 Strengthening Needs	4
1.3 Repair By Plate Bonding	5
1.4 History of Plate Bonding	8
1.5 Scope and Objectives	11

2. LITERATURE REVIEW

2.1	Introduction	13
2.2	Epoxy Resin	24
2.2.1	Introduction	
2.2.2	Historical Background of Epoxy	24

3. EXPERIMENTAL PROGRAM

3.1	General	28
3.2	Material Properties of Fiber Glass	30
3.2.1	General	30
3.2.2	Selection of Fiber Glass Type	31
3.3	Effect of Thermal Cycling on Bond Strength	34
3.4	Manufacturing of Beam Specimens	45
3.5	Preloading of Beams	50
3.6	Repair of Beams	56
3.6.1	Flexure Beams	60
3.6.2	Shear Beams	70

4. THEORITICAL CALCULATIONS

4.1	General	88
4.2	Ultimate Flexural Capacity	88
4.3	Ultimate Shear Capacity	92

5. RESULTS & DISCUSSIONS

5.1	Selection of the Repair Material	95
5.2	Effect of Thermal Cycling on Bond Strength	97
5.3	Flexural Damaged Repair	102
5.3.1	<i>Modes of Failures</i>	102
5.3.2	<i>Ductility Measurements</i>	115
5.3.2.1	Moment Vs. Curvature	135
5.3.2.2	Rigidity	135
5.3.3	<i>Load Vs. Deflection</i>	149
5.3.4	<i>Load Vs. Strain</i>	159
5.4	Shear Damaged Repair	172

5.4.1	<i>Modes of Failures</i>	179
5.4.2	<i>Load Vs. Deflection</i>	188
5.4.3	<i>Load Vs. Strain</i>	209
6.	DESIGN CONSIDERATION FOR REPAIR IN FLEXURE	
6.1	<i>General</i>	214
6.2	EVALUATION OF THE PLATE THICKNESS	214
7.	CONCLUSIONS	227
8.	REFERENCES	230

APPENDIX

LIST OF TABLES

<i>Table</i>		<i>Page</i>
3.1	Composition of Fiber Glass Types	31
3.2	Flexure and Shear Beams Details.....	46
3.3	Flexurally Damaged Beams	68
3.4	Shear Repaired Beams	87
5.1	Basic Properties of Concrete.....	99
5.2	Effect of Thermal Cycling on Bond Strength	100
5.3	Theoretical Flexural Capacities and Ultimate Loads carried of Flexure beams)	116
5.4	Comparasion of controlled and Repaired Flexural Beams	129
5.5	Ductility and Strength Ratios of Flexural Beams for Different Plate Thicknesses	136
5.6	Stiffness values of Flexural Beams	150
5.7	Theoretical Capacities and Average Experimental Loads	152
5.8	Failure Loads and Strength Improvements	157
5.9	Theoretical Ultimate Strength of Flexure Beams Specimens	161
5.10	Experimental and Theoretical Ultimate Loads of Shear Beams.....	202
5.11	Improvements in the Ultimate Capacity and Ductility	204
5.12	Theoretical Ultimate Strength of Shear Beam Specimens	205
5.13	Comparasion of Experimental and Theoretical Loads for Wings and Strips	210
6.1	Numerical Examples Data.....	222

6.2	Results of Numerical Examples	225
6.3	Comparison Between Experimental and Theoretical Loads	226

LIST OF FIGURES

<i>Figure</i>		<i>Page</i>
3.1	General Testing Program.....	29
3.2	Tension Test Specimens.....	32
3.3	Preparation of Pull-out Test Specimens.....	37
3.4	Pull-out Specimens.....	41
3.5	Pull-out Set-up.....	42
3.6	Schematic diagram of the Pull-out Set-up	43
3.7	Forces acting on the Glue Layer	44
3.8	General Chart Diagram for Repair Beam Specimens	47
3.9	Reinforcement Details of Flexure Beams	48
3.10	Reinforcement Details of Shear Beams	49
3.11	Load Configuration Used in Testing the Beam Specimens	58
3.12	Supporting I-Steel Beam and Loading Frame.....	60
3.13	Locations of Strain Gauges.....	61
3.14	Chart Diagram for Repair Flexure Beams	67
3.15	Repair Sequences of Flexure Beams	69
3.16	Flexure Beams Repaired with I-Jacket.....	71
3.17	Chart Diagram for Repair Shear beams.....	74
3.18	Repair Sequence of Shear beams Using Wings	77
3.19	Repair Sequence of Shear Beams Using Strips.....	78
3.20	Shear Beams Repaired Using U-Jacket	79
4.1	Strain Compatibility Diagram	89

5.1	Stress-Strain Curves for Fiber Glass Types and concrete	96
5.2	Stress-Strain Curves for Steel and Fiber Glass ..	98
5.3	Reduction (%) in Bond Strength Vs. Number of Thermal Cycles	101
5.4	System of Forces Acting in the Epoxy Layer Between the Plate and the Beam	107
5.5	Applied Load Vs. Central Deflection for Unrepaired and Repaired Beams (Only Plates)	120
5.6	Applied Load Vs. Central Deflection for Unrepaired and Repaired beams (Plates + Anchor Bolts)	121
5.7	Applied Load Vs. Central Deflection for Unrepaired and Repaired Beams (Anchored Plates + Wings)	122
5.8	Applied Load Vs. Central Deflection for Unrepaired and Repaired Beams (Plate only).....	123
5.9	Applied Load Vs. Central Deflection for Unrepaired and Repaired Beams (Plates + Anchor Bolts)	124
5.10	Applied Loads Vs. Central Deflection for Unrepaired Repaired Beams (Anchored Plates + Wings)	125
5.11	Applied Load Vs. Central Deflection for Unrepaired and Repaired Beams (Plates only).....	126
5.12	Applied Load Vs. Central Deflection for Unrepaired and Repaired Beams (I-Jacket)	127
5.13	Ductility Ratio Vs. Plate Thickness (Plates only).	130
5.14	Ductility Ratio Vs. Plate Thickness (Plates + Anchor Bolts)	131
5.15	Ductility Ratio Vs. Plate Thickness (Plates + Anchor Bolts + Wings).....	132
5.16	Strength Ratio Vs. Plate Thickness (Plates only)	137

5.17	Strength Ratio Vs. Plate Thickness (Plates + Anchor Bolts)	138
5.18	Strength Ratio Vs. Plate Thickness (Anchor Bolts + Wings).....	139
5.19	Moment Vs. Curvature (Plate only)	140
5.20	Moment Vs. Curvature (Plate only)	141
5.21	Moment Vs. Curvature (Plate only)	142
5.22	Moment Vs. Curvature (Plate + Bolts)	143
5.23	Moment Vs. Curvature (Plate + Bolts)	144
5.24	Moment Vs. Curvature (Anchored Plate + Wings) .	145
5.25	Rigidity Vs. Plate Thickness (Plate only)	146
5.26	Rigidity Vs. Plate Thickness (Plate + Anchor Bolts)	147
5.27	Rigidity Vs. Plate Thickness (Anchored Plate + Wings)	148
5.28	Load Vs. Central Deflection for Beams Repaired with Different Types of Repair	151
5.29	Load Vs. Central Deflection for Beams Repaired with Different Types of Repair	154
5.30	Load Vs. Central Deflection for Beams Repaired with Different Plate Thicknesses	156
5.31	Load Vs. Central Deflection for Beams Repaired with Anchored Plates	158
5.32	Load Vs. Central Deflection for Beams Repaired with Anchored Plates + Wings.....	160
5.33	Strain Distribution Along the Plate Length at Different Load Levels (2 mm Plates)	162
5.34	Strain Distribution Along the Plate Length at Different Load Levels (3 mm Plates)	163
5.35	Strain Distribution Along the Plate Length at 40 kN load for Beams Repaired with Different Plate Thicknesses	165

5.36	Strain Distribution Along the Plate Length at 60 kN load for Beams Repaired with Different Plate Thicknesses	166
5.37	Strain Distribution Along the Plate Length at 40 kN load for Beams Repaired with Different Repair Types	167
5.38	Strain Distribution Along the Plate Length at 60 kN load for Beams Repaired with Different Repair Types	168
5.39	Strain Distribution Along the Plate Length at 40 kN load for Beams Repaired with Different Repair Types	169
5.40	Strain Distribution Along the Plate Length at 60 kN load for Beams Repaired with Different Repair Types	170
5.41	Load Vs. Strain at the Plate Center for Beams Repaired with Different Plate Thicknesses.....	171
5.42	Load Vs. Rebar Strain at 120 mm from the Beam end (plate only)	173
5.43	Load Vs. Rebar Strain at 230 mm from the Beam end (plate only)	174
5.44	Load Vs. Rebar Strain at 120 mm from the Beam end (plate only)	175
5.45	Load Vs. Rebar Strain at 230 mm from the Beam end (plate only)	176
5.46	Load Vs. Rebar Strain at the Middle of the Rebar (Plate only)	177
5.47	Load Vs. Plate Strain at 230 mm from the Beam end (Plate only)	178
5.48	Load Vs. Central Deflection for Unrepaired and Repaired Beams with Wings Only	191
5.49	Load Vs. Central Deflection for Unrepaired and Repaired Beams with Wings and Bottom Plate	192
5.50	Load Vs. Central Deflection for Unrepaired and Repaired Beams with Wings and	

	Anchpred Plate	193
5.51	Load Vs. Central Deflection for Unrepaired and Repaired Beams with Strips Only	195
5.52	Load Vs. Central Deflection for Unrepaired and Repaired Beams with Strips and Bottom Plate Only	196
5.53	Load Vs. Central Deflection for Unrepaired and Repaired Beams with Strips and Bottom Anchored Plate	197
5.54	Load Vs. Central Deflection for Unrepaired and Repaired Beams with Strips Only	198
5.55	Load Vs. Central Deflection for Beams Repaired with Wings and U-Jacket.....	199
5.56	Load Vs. Central Deflection for Beams Repaired with Different Repair Types Using Strips	201
5.57	Load Vs. Central Deflection for Comparison Between Beams Repaired with Wings and Strips Only.....	206
5.58	Load Vs. Central Deflection for Comparison Between Beams (with bottom Plates) Repaired with Wings and Strips	207
5.59	Load Vs. Central Deflection for Comparison Between Beams (with Anchored Bottom Plates) Repaired with Wings and Strips.....	208
5.60	Load Vs. Strain for Beams Repaired with Strips Only	211
5.61	Load Vs. Rebar Strains at Different Locations for Beam Repaired with U-Jacket	213
6.1	Peeling Force at the end of the Plate	215
6.2	Stress-Strain Curves for Fiber Glass Plates.....	216
6.3	Idealized Stress-Strain Curve for Steel and Fiber Glass.....	217

LIST OF PLATES

<i>Plates</i>	<i>Page</i>
3.1 Fiber Glass Spesimen Under Axial Tension	33
3.2 Pull-out Specimens in the Oven for Heat-Cool Cycling.....	35
3.3 Stirring the Two Components of the Epoxy Sepa- rately	38
3.4 Applying Pressure on the Plate for Seven Days ..	39
3.5 A Pull-out Specimen Subjected to Pull-out Test ..	40
3.6 Testing the Cylinders (75 * 150 mm) for Com- pressive Strength Using TONIPAC Machine.....	51
3.7 Testing Cylinders (150 * 300 mm) for Plotting Stress-Strain Curve for Concrete Using an Extensiometer.....	52
3.8 Testing Prisms (150 * 150 * 500 mm) for Evaluat- ing the Modulus of Rupture.....	53
3.9 A Control Flexure Beam Tested Upto Failure	54
3.10 A Control Shear Beam Tested Upto Failure.....	55
3.11 Preloading Shear Beam Upto the Appearance of the First Crack.....	57
3.12 The INSTRON Machine and Acquisition System Used in Testing the Beam Specimens.....	59
3.13 Roughening the Beam Surfaces Using Sand Blast- ing Machine	63
3.14 Application of the epoxy on the Beam Surface Using a Pait Brush	64
3.15 Application of the Epoxy on the Plate surface using a pait brush	65
3.16 Placing the Fiber Glass Plate on the Beam Sur- face and Pressing With Hands to Force Excess Epoxy out From All Sides.....	66

3.17	The I-Shaped Fiber Glass Jacket Used to Repair Beam FJ	72
3.18	Steel Anchor Bolts Used to Anchor the Plate Ends	73
3.19	The U-Shaped Fiber Glass Jacket Used to Repair Beam SJ	80
3.20	A Complete U-Channel Fiber Glass Before Cutting It into 420 mm U-Jackets	81
3.21	Application of the Epoxy to the Beam Surfaces Using a Brush	83
3.22	Encasement of the Shear Span of the Beam with the U-Jacket	84
3.23	Holding the U-Jacket From Sides Using C-Clamps	85
3.24	Resting the Beam on Concrete Blocks to Provide a Uniform Pressure on the U-Jacket Surface Utilizing the Beam Own Weight	86
5.1	Failure Mode of Control Group (Ripping off the Concrete)	103
5.2	Failure Mode of Group (1) after 30 Thermal Cycles (Failure is in the Glue/Concrete Interface)	104
5.3	Failure Mode of Group (2) and Group 3 after 60 and 120 Thermal Cycles (Failure is in the Glue/Plate Interface)	105
5.4	Failure Mode of Beams FP3 (Plate Separation With the Concrete Cover)	109
5.5	Failure Mode of Beams FPB3 (Diagonal Tension Crack and Debonding of the Plate)	110
5.6	Failure Mode of Beams FPBW3 (Debonding of the Plate)	111
5.7	Failure Mode of Beam FJ (Rupturing of the Plate Followed by Diagonal Crack at the Point of Rupture)	113
5.8	Failure Mode of Beams FP2 (Separation of the Plate and the Concrete Cover Followed by	

	Crushing of the Concrete)	114
5.9	Failure Mode of Beams FPB2 (Diagonal Tension Crack followed by Debonding of the Plate)	117
5.10	Failure Mode of Beams FPBW2 (Crushing of Concrete)	118
5.11	Failure Mode of Beams FP1 (Rupturing of the Plate Followed by Crushing of Concrete)	119
5.12	Failure Mode of Beams SW (Formation of Longitudinal Crack at the Beam Soffit Causing Transverse Splitting)	180
5.13	Failure Mode of Beams SWP (Separation at the End of the Bottom Plate Followed With Ripping Off the Wings With Chunks of Concrete)	182
5.14	Failure Mode of Beams SWPB (Transverse Opening at the end of the Beam)	183
5.15	Failure Mode of Beams SS (Formation of Longitudinal Crack at the Beam Soffit Causing Transverse Splitting)	185
5.16	Failure Mode of Beams SSP (Ripping of the Wing With Concrete and Subsequent Plate Separation) .	186
5.17	Failure Mode of Beams SSPB (Ripping of the Wings and Concrete)	187
5.18	Failure Mode of Beams SJ (Flexural Failure by Crushing of Concrete)	189
5.19	Shear Span of Beam (SJ) After Failure by Crushing of Concrete in the Constant Moment Region Concrete)	190

Thesis Abstract

Full Name : Badr Mohammed Naji Ghaleb
Title of Study : Strengthening of Damaged Reinforced Concrete Beams by External Fiber Glass Plates
Major Field : Civil Engineering (Structures)
Date of Degree : July 1992

The main theme of this thesis has focused on the use of external fiber glass plates to strengthen damaged flexure and shear beams.

The work was divided into four parts, with the first part dealing with the selection of the fiber glass material for the proposed repair out of two recommended composites by the local manufacturer to provide the highest strength and ductility.

The second part of the thesis addressed the study of the effect of thermal cycling on the bond strength between the fiber glass plates and the epoxy glue.

The third part, studied the performance of repairing flexure reinforced concrete beams after damaging them to a level loading corresponding to 10 mm central deflection. The level of damage was decided upon after testing two control beams to failure. These beams were then repaired using external fiber glass plates of different thicknesses.

The fourth part of the study evaluated the performance of R.C. shear beams strengthened with external web reinforcement of the fiber glass. Two control beams were tested upon failure. It was decided then to damage the beams upto the appearance of the first shear crack in the shear span. Three repair techniques were tried in the form of side plates (wings), strips and a newly suggested technique in the form of U-jacket.

A criterion to evaluate the plate thickness to be used for repair any beam in reality was presented based on the ultimate flexural capacity of the section as well as the maximum interface shear and normal stresses at the plate ends.

خلاصة الرسالة

- اسم الطالب : بدر محمد ناجي غالب .
عنوان الدراسة : تقوية جسور خرسانية مسلحة متضررة باستخدام ألواح خارجية من الألياف الزجاجية (الفايبرجلاس)
التخصص : هندسة مدنية (إنشاءات)
تاريخ الشهادة : يوليو ١٩٩٢ م .

يتلخص الهدف الرئيسي لهذه الرسالة في استخدام مادة الألياف الزجاجية (الفايبرجلاس) في تقوية جسور متضررة قصياً وعزماً بطريقة الربط بقطعة فايبرجلاس واستخدام مادة الإيبوكسي اللاصقة .
ينقسم هذا البحث إلى أربعة أجزاء ، الجزء الأول يتعلق بتقييم الخواص الميكانيكية لمادة الفايبرجلاس بهدف إختيار نوعية مادة الإصلاح المراد استخدامها في هذا البحث على أساس إعطاء أقصى قوة وأعلى مرونة .
الجزء الثاني يتعلق بدراسة تأثير التغيرات الحرارية على قوة التماسك بين أنواع الفايبرجلاس ومادة الإيبوكسي .
في الجزء الثالث تم إخضاع ٢٤ جسراً (صممت للإنتيبار العزمي) إلى إنعطاف مركزي مساو لـ ١٠ مم بعد إختبار عينتين إلى النهاية القصوى للإنعطاف .
قيمت بعد ذلك إمكانية إصلاح هذه الجسور باستخدام ألواح مختلفة السماكة إضافة إلى استخدام براغي التثبيت للتغلب على مشكلة الإنفصال الذي يحدث عند أطراف الألواح .
كما تم استخدام طريقة جديدة للتغلب على هذه المشكلة باستخدام غلاف من الفايبرجلاس على شكل حرف (I) .
بحث الجزء الرابع في إخضاع ٢٠ جسراً (صممت للإنتيبار القصي) إلى مستوى تحميل ينتج عنه ظهور أول صدع قصي في منطقة مديد القص . تم بعد ذلك إصلاح هذه الجسور باستخدام ألواح جانبية وشرائح من الفايبرجلاس .
كما تم تطبيق طريقة جديدة تتلخص في تغليف منطقة مديد القص بغلاف من الفايبرجلاس على شكل حرف (U) .
هذا وقد تم إختبار جميع الجسور بطريقة التصرف العزمي تحت قوتين عند نهاية الثلث الوسط من الجسر في كل إتجاه .
في نهاية البحث تم إقتراح طريقة لإختيار وتصميم السُمك الأمثل للألواح المراد استخدامها في إصلاح الجسور المتضررة عزماً .
تتلخص هذه الطريقة في إختيار معدل السماكة الدنيا والسماكة القصوى والمسببة لتمزق الألواح وإنفصالها تحت تأثير الإجهاد القصي عند نهاية اللوح على التوالي .

درجة الماجستير في العلوم
جامعة الملك فهد للبترول والمعادن
الظهران ، المملكة العربية السعودية
يوليو ١٩٩٢ م

Chapter 1

INTRODUCTION

1.1 GENERAL

It is known that reinforced concrete is highly durable material under normal conditions, but concrete structures in the Gulf countries have shown earlier sign of distress and deterioration within a short time of completion. Some of these problems, in which structures have shown sign of distress within a short time are caused by dynamic loading, impact loading, static over loading, creep or thermal gradient, shrinkage, corrosion of reinforcement and/or sulfate attack. Most of these problems have resulted from the lack of understanding the nature of local materials and the execution of either private or public projects without considering the nature and the effect of the environmental conditions such as high humidity and high ambient temperature.

Cracks in Concrete

The cracks in concrete is an inherent feature which cannot be completely prevented but can only be controlled and minimized. Plain concrete is well known for its high compressive strength and weakness in tension. A plain concrete member subjected to flexure would therefore crack at low load and fail suddenly. The perform-

ance of such member is conventionally improved by using tensile reinforcing bars. During their lives concrete structures will experience cracks patterns. These cracks either minor or major in nature and some times the structure may indicate both minor and major cracks.

Major cracks are signs of distress and indicators of structural problems and they require immediate attention. Minor cracks are often tolerable from the point of view of strength and can be ignored unless when the structure is located in aggressive environment which will result in corrosion of reinforcement. In mild exposure conditions, mild cracks can be tolerated, however, they are not acceptable from a durability point of view in severe environments which are characterized by high temperatures and high humidity. Concrete elements that exhibit distress by cracking or excessive deflection in such environment require immediate repair to prevent further degradation and to restore the integrity of the structure. The cracks which are existing in a structure might be one or a combination of the following:

- a) Dormant Cracks: which are stable and remain as they are, e.g. cracks resulting from shrinkage and drying.
- b) Active Cracks: which are growing in width, e.g. cracks resulting from corrosion of reinforcement or differential settlement.

- c) Live Cracks: which close and open because of loading and unloading, e.g. cracks occurring in bridge decks or structural members.

Cracks in Flexural Members

a) Flexure Cracks:

The study of crack formation, behavior of cracks under increasing load, and control of cracking is necessary for proper design of reinforced concrete structures. In flexural members, cracks develop under working loads and since concrete is weak in tension, reinforcement is placed in the cracked tension zone to resist the tension force produced by the external loads. Flexural cracks develop where the stress at the extreme tension fibres exceeds the modulus of rupture of concrete.

b) Shear Cracks:

Inclined cracks can develop in the webs of reinforced concrete beams either as extensions of flexural cracks or occasionally as independent cracks such as flexure shear cracks. For them to occur the moment must be larger than the cracking moment and the shear must be rather large. The cracks run at angles of about 45° with the beam axis and probably start at the top of a flexure crack. The approximately vertical flexure cracks are not dangerous unless there is a critical combination of shear stress and fle-

xure stress occurring at the top of one of the flexure cracks. Occasionally an inclined crack will develop independently in a beam, even though no flexure cracks are in that locality. Such cracks are called web shear cracks.

1.2 STRENGTHENING NEEDS

In practice, situations arise where existing concrete structures or part of them may, for a variety of reasons be found to be inadequate and need to be strengthened. The inadequacy may be due to one or more of the following:

- 1) Poor performance under service loading in the form of excessive deflections and cracking.
- 2) Construction faults or poor construction practice: which may mean that the concrete cross section or the cross sectional area of the reinforcement originally calculated are not achieved or individual reinforcing bars are incorrectly placed.
- 3) Design faults: This may be in the form of mistakes in calculating the loads, bending moments, shear forces ... etc. It also may be due to incorrect calculations of steel cross sectional area.
- 4) Excessive deterioration due to corrosion may result in

reduction of internal reinforcement cross section.

- 5) Changing the use of structure may produce internal force that exceeds its limiting capacity, or alternatively it may arise from requirements to increase the imposed loading above the original design load.

In such circumstances, there are two possible solutions; i.e. demolish and rebuild or carry out a program of strengthening, when such situations arise, it has to be considered whether it is more economical to replace the member or to strengthen it. The choice between these alternatives depends on many important factors, such as basic materials and labor costs, time during which the structure is out of commission, and disruption of other facilities. In the present economic climate, the second alternative is becoming more attractive, particularly if a simple, quick strengthening technique is available.

1.3 REPAIR BY PLATE BONDING

It is sometimes necessary to modify existing structures in order that they will satisfy the design requirements of any future loading. The modification may be needed to increase the strength of the structure and/or to improve its performance under service conditions. In structural engineering, the maintenance, repair and upgrading of existing concrete structures is just as important and

technical as the design and construction of new structures. Upgrading of structures usually involves strengthening of an existing structure to satisfy a higher ultimate load and/or more stringent serviceability requirements. Such work may be needed to overcome the problems resulting from the changes in the design criteria, such as the imposed loading, or due to deficiencies in the existing structures, such as displaced reinforcement bars.

A number of techniques have been used in the past to achieve the desired improvement, some of the most common methods are:

- 1) Replacing non-structural toppings with structural toppings, or lighter material.
- 2) Introducing extra supports.
- 3) Adding extra reinforcement by stapling and guniting.
- 4) Prestressing either externally or internally.

The cost of such work and the time and disruption can often be considerable. Evacuation of all or part of a building, or road closures in the case of bridges, may be necessary while the work is carried out and these all added to the cost.

In recent years, the development of strong epoxy glue has led to another technique which has great potential in the field of

upgrading structures. Basically the technique involves gluing steel plates to the surface of the concrete. The plates then act compositely with the original member and help to carry the live loading.

Efficient repair requires that special attention should be given to the following:

- Understanding the main cause of the cracks
- The correct choice of repair method
- The selection of the material to be used for that purpose.

Different repair techniques were developed successfully in Western countries to strengthen a given structure or part of one, depending on the type of construction and the given situation. In the past, concrete bridges were strengthened by additional beams or props. In recent years, with the development of strong structural adhesives, external epoxy-coated steel plates are now recognized to be an effective and convenient method of improving structures performances under service loads or to increase their ultimate strength, stiffness, and hence, deflections, and also on the initiation and development of cracks. Advantages of this technique include:

- 1) Avoiding the problems with headrooms because the additional construction depth would be in the range of few

millimeters.

- 2) Site disturbance of the function of structure is kept to minimum because the strengthening operation can be carried out relatively quickly and simply. Also, due to the fact that the technique is a dry process, there will be no damage to the adjacent structural elements.
- 3) Minimum additional loading due to the self weight of the plate and the epoxy.

1.4 HISTORY OF PLATE BONDING

Despite of the limited test data available on the plated beams, the method has been used effectively to strengthen a variety of structures. Some cases from the actual practice will be presented here.

The postal (PTT) building department after the investigation of the construction condition of the Fusslistrasse Telephone Exchange in Zurich, came to the conclusion that neither operating nor economic considerations justify the demolition of the building. They decided that the building should be strengthened to meet the new functional needs. The first floor above the ground had to be reinforced on top, the floor above that from underneath. In addition, the reduction of room height in the latter case had to be

kept to a minimum. The only way to solve this difficult problem was the use of relatively new bonding method, namely steel plate bonding technique.

The technique of plate bonding was also applied to strengthen the shopping center at Spreitenbach. In order to increase the admissible loading of about 2300 m² of the floor above the underground grage, a total of 216 steel plate 6 mm thick, 100 to 200 mm wide and 6600 to 7900 mm were bonded to the underside of the floor slab. In Contraves AG, Zurich, modifications at two locations at the edge of a mushroom slab reduced the floor's admissible load. To restore the original load-bearing capacity, it was reinforced with bonded steel plates arranged in a crosswise pattern. A total of 26 steel plates were 6 mm thick, 120 mm wide and 6600 mm long. The lower layer plates had 12 mm thickness, 120 mm width and 7300 mm length. The plates in the lower layer were milled out by 6 mm in the intersection points to accommodate the upper 6 mm plates.

In 1974, ALBA Aluminum Smelter, Bahrain, was strengthened by plate bonding technique.

The prefabricated concrete frames serve as supports for the melting ladles in addition they transmit the materials handling loads to the foundations soil. Because these handling loads proved substantially greater than assumed in the calculation, crack devel-

oped in the frame cross-beam. Thus it became necessary to increase the total reinforcement cross-section. In all, 700 concrete frames had a single steel plate of 8 mm thickness, 280 mm width and 2850 mm length bonded to the underside of the cross beam. Afterwards, the cracks were injected with epoxy resin.

This technique was used efficiently in linking the Swiss Industries Fair, parking garage Basle, which was opened in 1975, to one of the existing exhibition by means of escalator. To do this, it was necessary to break out an opening of 1.7 x 3.15 m in the 40 cm thick, mesh-reinforced concrete wall adjacent to the parking garage. To replace the reinforcing mesh removed, a steel plate frame 15 mm thick was bonded to the concrete wall on both sides of the opening. These frames act as shear reinforcement.

A shortcoming of the plate bonding technique using steel plates is the danger of corrosion at the epoxy-steel interface, which adversely affects the bond strength. An effective way of eliminating the corrosion problem is to replace steel plates with corrosion-resistant synthetic material such as Fiber Glass Plates. In severe environments such as those prevailing in some areas of the Middle East in which the climatic environment is characterized by high ambient temperature and variable humidity. Such climatic conditions would damage the repaired interface and eventually lead to the failure of the repair members. In this work another proposed material is aimed at developing an alternative to use the

steel plates as external reinforcing medium. The new material is the glass reinforced-plastic in which it is intended to evaluate the strengthening of damaged concrete beams by external fiber glass plates. This repair scheme if proven satisfactory would be suitable for the repair of damaged beams subjected to corrosive environment.

1.5 SCOPE AND OBJECTIVES

The problem of strengthening damaged existing structures and damaged R.C. flexural members in particular is that it is susceptible to corrosion. When the external bonded steel plate is corroded, the epoxy-steel interface is disintegrated which adversely affects the bond strength. Thus the overall objectives of this study is to use the corrosion-resistant fiber glass plates in lieu of steel plates to strengthen flexurally damaged and shear damaged reinforced concrete beams. The evaluation of the fiber glass plates to repair damaged beams in shear and flexure was carried out under static loading.

The detailed objectives of this study can be summarized as follows:

- 1) Evaluate mechanical properties of fiber glass plates and make a choice based on strength and ductility.

- 2) Effect of thermal cycling on the degradation of bond strength.
- 3) Repair of flexurally damaged beams
- 4) Repair of shear damaged beams
- 5) Use of anchoring scheme to eliminate plate separation.

Chapter 2

LITERATURE REVIEW

2.1 INTRODUCTION

Although in the past, very small test data was available on the plate bonding technique, even then this technique was used to strengthen the existing concrete structures. External strengthening of existing highway bridges using epoxy-bonded steel plates are now being accepted as an efficient and convenient way of improving the serviceability performance and/or ultimate strength of concrete existing structures. There is a growing need to strengthen damaged reinforced concrete structures which applies both to buildings and to bridges and other structures. The bonded reinforcement method is characterized by:

- Excellent adaptability to existing geometry
- Negligible reduction of overhead heights and clearance
- The fact that it is a dry building process which is completed quickly with no damage to adjacent structural elements.

In order to investigate the performance of members strengthened by this technique, research work, on the glued plate

technique were started in late 1960s and early 1970s [1-10]. In Japan, well over 200 bridges had been strengthened in this way by 1975 [11]. (The large number of under-strength bridges was mainly due to a big increase in the intensity of heavy truck traffic since the bridges were designed).

The first major application to bridges in the United Kingdom was in 1975 when a group of four bridges at an interchange on the M5 motorway at Quinton needed to be strengthened to cater for increased traffic loads [12]. This technique was used to strengthen the underpass CD126 below autoroute running to the south from Paris [14].

Bresson has reported the use of bonded plates to strengthen a series of pre-stressed concrete elements of double-T sections, where the plates were glued to the sides of the element [15], the ground and the first four levels of telephone exchange in Zurich [16,17]. In United Kingdom the technique was used in 1975 to strengthen the soffits of two pairs of motorway under bridges at Quinton and later in 1977 to strengthen the decks of two defective concrete bridges on M25-M20 interchange at Swanley, Kent [18].

Irwin [19], in 1975, studied the use of the plate bonding technique for strengthening beams in flexure when he proposed two reinforced concrete beams, one with bonded steel plate and one without. After testing the beams up to failure, the results indi-

cated that the crack widths of the plated beams were significantly reduced to half of those on the unplated beams whilst the moment capacity did not seem increased to any great degree.

Macdonald [20], studied the use of glued steel plates for strengthening four reinforced concrete beams. The plates were bonded to the tension flanges of the beams by epoxy-resin. This study focused on the effects of variation as adhesive properties, joint in the plates, plate thickness variation and load cycling. The results showed that the load to produce a crack of a certain width in a plated beam was approximately double loads to produce the same size-crack in the unplated beam, but with no significant increase in the load carrying capacity.

From observation, in all cases, failure to the plated beam occurred by horizontal shear in the concrete adjacent to the steel plate commencing at the free end. Also, after plate separation, subsequent failure usually occurs by compression of the concrete at a loads similar to the failure loads of an unplated beam.

In 1980, Raithby [12], carried out full scale loading tests on one half of the center span of one of the four bridges forming the interchange on the M5 motorway at Quinton, before and after strengthening showed that the required improvements had been achieved. Also, laboratory tests indicated that the performance could be improved further by better detail design of the plates and

further research is needed for further application.

For a long-term behavior, a protective treatment of the steel surface against corrosion is very essential. For the objective of studying the long-term behavior of reinforced concrete structures strengthened with externally bonded reinforcement, the Swiss Federal Laboratories for Materials Testing and Research (MPA) started in 1973 a special program of testing reinforced concrete beams strengthened by externally bonded steel plates, with a planned observation period of at least 15 years.

In 1976 Calder [13], carried out exposure tests to investigate the possibility of deterioration of the bond between steel and concrete due to prolonged exposure to the weather in a series of long-term exposure tests on plain concrete beams which were 508 mm long with a square cross section of 102 mm strengthened with a mild steel plate (500 mm, 38 mm wide and 3 mm deep) bonded to one face using a structural epoxy adhesive. Some of the test specimens are subjected to sustained flexural loading while they are exposed, others remain unloaded. The specimens were exposed on racks at three exposure sites representing high rainfall rural clean air, highly polluted industrial and coastal marine environment. Specimens were also kept in a controlled laboratory environment under conditions of constant temperature and humidity (20°C and 65% RH).

After various periods of exposure, test beams are subjected to four-point bending and the strength and stiffness are compared with similar beams which have been kept in an air-conditioned laboratory.

Compared with the beams which had been kept in the laboratory for two years, the exposed beams showed a slight loss in strength, although the mean strength still exceeded the original strengths. Results of the exposure tests to date suggest that further attention needs to be given to alternative surface treatments.

In 1980, Jones [21], studied the behavior of the concrete beams strengthened by steel plates bonded by the epoxy glue to the tensile face of the beam. Two types of glue and two types of steel plates with different yield strengths were used and the effect of the glue thickness, plate lapping, multiple plates and of pre-cracking prior to bonding were investigated. The effects of variables on the deflection, concrete strain distribution, cracking behavior, steel strain, mode of failure, load at the first crack and ultimate strength were discussed.

Results showed that the use of external reinforcement in the form of steel plates glued to the tension face of plain and reinforced concrete beams increases the range of elastic behavior, increases the flexural stiffness at all loads, and consequently reduces deflections at corresponding loads, enhances the ultimate

flexural capacity and increases the ductility of flexural failure.

Jones et al. [23], carried out a testing program consisting of 24 reinforced concrete beams to investigate the effect of glued plates on the cracking behavior of reinforced concrete beams strengthened with such plates. The variables studied include plate thickness, glue thickness, layered plates, and lapped plates. These investigations showed that the propagation of crack away from the tensile faces was delayed, also the numbers of cracks developed and the mean ultimate spacing of these cracks were relatively insensitive to the application of plates.

The results also showed that for the same level of loadings, the mean crack width were considerably reduced by plating.

A comprehensive testing program has been carried out in 1987 by Swamy [22], to investigate the effect of glued steel plates on the first crack load, cracking behavior, serviceability loads, and structural deformations of reinforced concrete beams strengthened with such plates on the tension face.

The results showed that the plated beams have enhanced flexural stiffness which control cracking and deformation at all load levels until failure, reduce cracking and structural deformation. The reduction in cracking and deformation increased with increasing the plate thickness. However, the stiffening effect is much greater in controlling cracking; further, the structural effect is

far greater than if the bar area had been increased by the same area as the plates. Provided the adhesive, is chosen carefully and proper gluing techniques are followed, the plated beams show the beam action and composite behavior right up to failure. The glued plates can increase the ultimate capacity by up to 15%.

There is, however, a limitation on plate thickness beyond which premature brittle shear/bond failure occurs without achieving the full flexural capacity and ensuring ductility.

In 1988, a study was carried out by Jones [25], to investigate the problem of anchorage at the ends of the plate glued to the tensile face of the reinforced concrete beams. A simple theoretical study of the force systems at the plate/glue and the glued concrete interfaces was presented. This suggested that high stress concentrations and peeling forces were present at the end of the plates when composite beam was loaded in flexure.

Tests carried out to investigate the effectiveness of different anchorages were described in detail and the results from these tests confirmed that, at the ends of the plates, interface stress concentration exist, which have limiting peak values in the range of $\sqrt{2}$ * tensile splitting strength of the concrete.

Theoretical interface bond stresses, based on simple elastic behavior, were found to have no consistent relationship to the

measured peak values. However, if maximum (unreduced) plate thickness was always used in these calculations, a simple method was proposed for obtaining a reasonable assessment of the peak stress. The efficiency of different anchorage details was discussed, and it is shown that the use of the additional glued anchor plates gave the best results. These anchorage plates overcame the problem of anchorage failure and enabled the full theoretical flexural strength to be achieved, together with ductile behavior.

In 1989, Swamy [25], conducted a testing program to investigate the applicability of the plate bonding technique to strengthen structurally damaged reinforced concrete beams. Two types of strengthened beams were tested. In the first, beams loaded up to 70% of their flexural capacity were unloaded and strengthened in the unloaded state. In the second, beams also loaded up to 70% of their flexural strength were reinforced with bonded plates while under load.

The structural behavior of these two types of strengthened beam is reported in terms of deflection, concrete and steel strain, cracking behavior, flexural stiffness and strength. It was shown that strengthening by bonding steel plates, of significantly cracked beams was structurally efficient and that the plated beams were restored to stiffness and strength values superior to those of the original unplated beams.

The data showed that complete confidence and reliability can be placed in applying the technique to structurally damaged members. The repaired composite beams are able to preserve their structural integrity and maintain composite action until failure. Further, the composite structural system obeyed the simple laws of mechanism right up to failure.

Basunbul et al. [26], reported that steel plate bonding repair technique leads to an increase in strength but concomitantly with considerable reduction in ductility of the repaired beams, regardless of the level of damage.

Another proposed material is aimed at developing an alternative to the use of steel plates as external reinforcing medium in view of ubiquitous occurrence of corrosion in all structural elements, making use of steel in conjunction with concrete in the Gulf environment.

The proposed new material conceived for flexural bonding in glass fiber reinforced plastics (GFRP) which can be produced to yield strength as high as steel, albeit at reduced ductility. A successful incorporation of use of fiber glass as repair material for reinforced concrete could be a panacea for at least some of the ills associated with the inevitable problems of corrosion in the presence of steel reinforced concrete. The plate bonding technique using fiber glass plates to strengthen damaged reinforced concrete beams

was not known before 1990. Also, the information regarding the use of the fiber glass plates to strengthen the reinforced concrete beams was very limited.

In 1990, Saadatmanesh [27], carried out a testing program in which four reinforced concrete beams strengthened with epoxy-bonded fiber glass (F.G.) plates and one beam was not strengthened and was used as a control beam. Result showed that strengthening reinforced concrete beams with epoxy bonded fiber glass plates appears to be a feasible way of increasing the load carrying capacity of existing bridges. Also, the flexural strength and stiffness of reinforced concrete beams can be increased by bonding fiber glass plates to the tension flange using epoxy, and the behavior of beams strengthened in this way is very similar to the behavior of beams strengthened with steel plates.

Ehsani [28], carried out a testing program in which he investigated the feasibility of strengthening small and large-scale reinforced concrete beams with Glass-Fiber-Reinforced-Plastic (GFRP) plates. The results indicate great potential for the use of the proposed strengthening technique in civil engineering structures.

Saadatmanesh [29], reported that the flexural strength of reinforced concrete beams can be significantly increased by gluing fiber glass plates to the tension face. In addition, the epoxy

bonded plates improved the cracking behavior of the beams by delaying the formation of visible cracks and reducing crack widths at higher load levels.

Philip [30], carried out a testing program in which he investigated the effect of different anchoring systems on the ultimate strength and the mode of failure. The anchoring systems were, anchoring the ends of the plate using an unequal leg fiber glass angle, bonding full-height FRP plates to the sides of the beam at the plate ends and then connecting these to the plate using bonded fiber glass angles and replacing the plate with a pair of angles bonded along the underside of the beam.

The results showed that there was a remarkable increase in the ultimate strength. Also, the crack patterns shifted from several widely spaced and large width cracks to many more closely spaced narrower cracks.

In 1989, Robert [31], developed a simple approximate procedure for predicting the shear and normal stress concentrations in the adhesive layer of plated reinforced concrete beams assuming full composite action. The results showed satisfactory correlation with available test data and with rigorous analytical solution based on partial interaction theory.

2.2 EPOXY RESINS

2.2.1 Introduction

Epoxy-resins have been used very widely for many applications all over the world to repair buildings, dams and bridges for more than two decades. There are so many papers written on the use of epoxy-resin for repairing, strengthening and rehabilitation of structures. Results showed a good performance of epoxy materials used to repair concrete structures.

2.2.2 Historical Background of Epoxy

The word "epoxy" is a Greek description of the chemical symbol for the family of epoxies. The word "epoxy" is of Greek derivation. The word "epo" which means "on the other side of", was combined by "oxygen", which described the presence of the oxygen atom in the molecular structure. In short, the word is a Greek description of the chemical symbol for the family of epoxy [30].

The first practical application of epoxy resins took place in Germany and Switzerland in 1930s, with some experiments were done in the U.S. The first known patent on epoxy was issued to Dr. Pierre Casan in Switzerland in 1936.

In 1939, Greenlee developed several basic epoxy systems, many of which are used today as adhesives and coatings. First

interest in the use of epoxy in the construction industry as an adhesive was in 1948 and it showed satisfactory results in bonding two pieces of hardened concrete [30].

The production of epoxy-resin started in the late 1940s, and in 1950s it was produced commercially and was available in the market for use.

In 1954, the California Highway Department became interested in epoxies as a bonding agent for raised traffic lane markers on concrete highways. The successful utilization of an epoxy as a bonding agent encouraged the extension of research into the field of structural repair of concrete and the eventual application of an epoxy polysulfide polymer, as a bonding material for joining new concrete to old [30].

Epoxy concrete was first used as a wearing course in the repair popouts and spoiled areas on the surfaces of various concrete bridge decks in California in 1957. Presently epoxies are used widely with concrete in the form of bonding agents, adhesives, coatings, paints, repair materials, epoxy mortar and concrete, wearing surfaces and seal coats [30].

Several investigations have been carried out on the uses and applications of epoxy compounds with concrete. American Concrete Institute Committee 503 [30], published a report which provides a detailed review of literature on epoxy history, chemical

and physical properties of epoxy, characteristics, precautions, guidelines to users, uses and preparing surfaces for repair.

Schultz [31], 1981, listed the properties and specifications of epoxies used in concrete repair. These standard specifications were published in 1978 and they are:

- ASTM C881 on epoxy-resin-base bonding system for concrete
- ASTM C882 on bond strength of epoxy resin systems
- ASTM C883 on effective shrinkage of epoxy resin systems used with concrete.
- ASTM C884 on thermal compatibility between concrete and epoxy resin overlays.

Advantages of Epoxy Resins

There are many advantages of using epoxies in concrete. Some of the properties of epoxies which make them desirable for use in concrete are:

- 1) Adhesion; epoxies form excellent and very strong bond with concrete.
- 2) Versatility; exhibited by a wide range of their physical and chemical properties.

- 3) High resistance to the attack of acids, oils, alkalis and solvents.
- 4) Rapid hardening, low shrinkage and highly impermeable to water.

Chapter 3

EXPERIMENTAL PROGRAM

3.1 General

In this research work, an extensive and elaborated experimental program was carried out to attain the objective specified earlier. The work was divided into four main phases as follows: (Fig.3.1)

Part A: Selection of the fiber glass material for the proposed repair out of two recommended composites by the local manufacturer to provide high strength and ductility. Several specimens were tested under axial tension to evaluate the stress-strain behavior of the material.

Part B: Casting twelve 50 x 125 x 150mm prisms to evaluate the effect of thermal cycling on durability of the glue and consequently on the bond strength between the epoxy layer and the fiber glass plate.

Part C: Casting twenty six reinforced concrete flexure beams designed to fail in flexure to evaluate the performance of the repaired flexurally damaged reinforced concrete beams using externally bonded fiber glass plates.

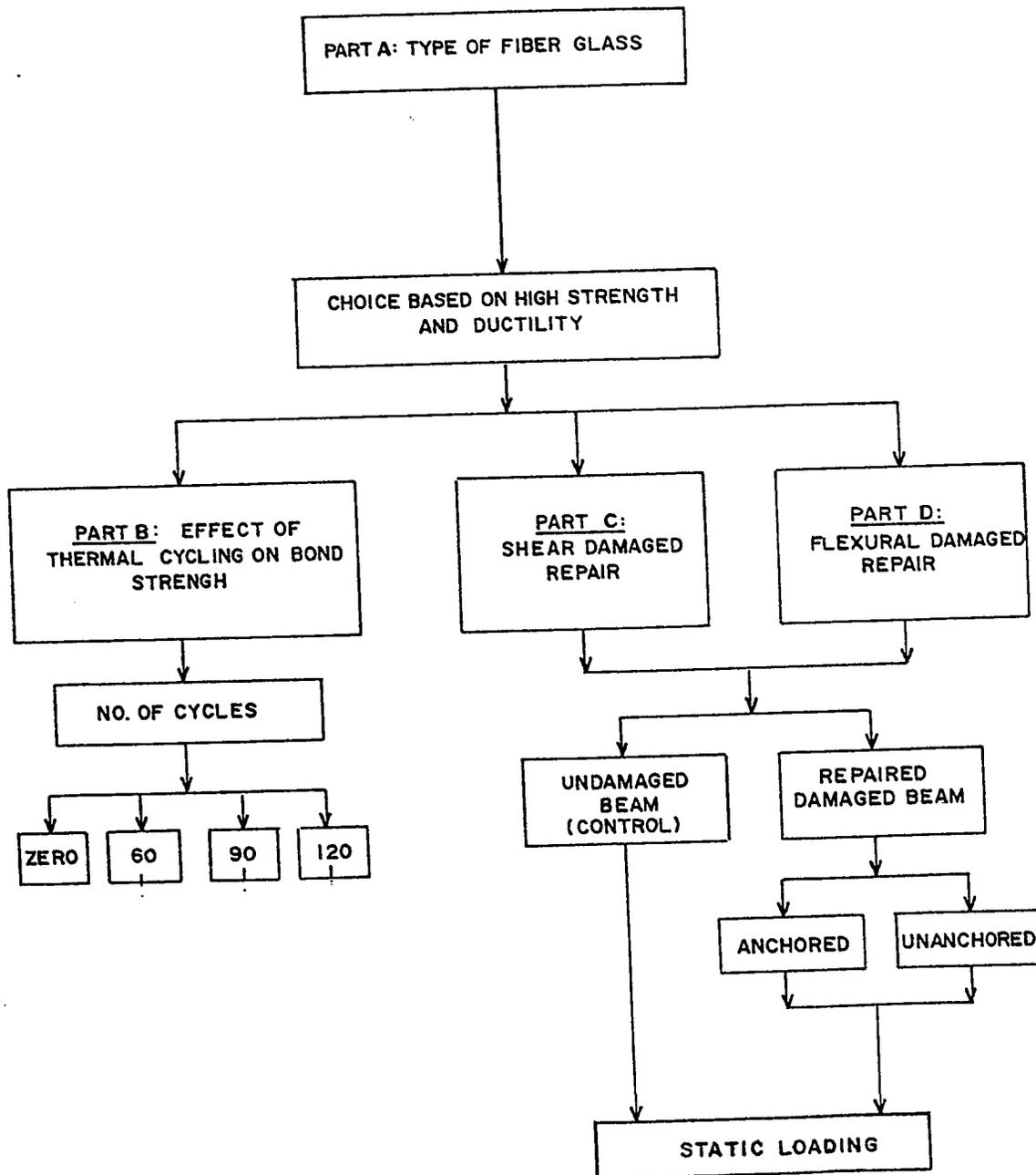


Fig.3.1 General Testing Program

Part D: Casting twenty four reinforced concrete beams designed to fail in shear to evaluate the performance of the damaged reinforced concrete shear beams using external web reinforcement.

3.2 Material Properties of Fiber Glass

3.2.1 General

The fiber glass material used in this research was in the form of plates manufactured by the hand lay-up method which is considered the oldest but, the simplest and the most common technique. The most common fiber glass are:

Woven Roving:

Woven roving are a coarse fabric made by weaving on twisted rovings almost in plain weave. The use of woven rovings enables the highest glass content and therefore strengthens, to be achieved.

Chopped Strand Mat (CSM):

Chopped strand mat consists of chopped glass strands 25-30 mm in length, distributed in random pattern in the plane of the mat and held together by a small amount of resin binder. The glass content obtainable with this form of reinforcement is considerably less than that using woven roving materials.

3.2.2 Selection of Fiber Glass Type

Two different types of fiber glass material were recommended by the local manufacturer as mentioned earlier. Table 3.1 shows the composition of the two types. Three specimens of each type were prepared in accordance with ASTM standard (ASTM-E8) and a strain gauge was fixed on the middle of each specimen to record the strain in the specimen during testing Fig. 3.2.

Table 3.1: Composition of Fiber Glass Types

Fiberglass Type	Woven Rovings (Layer)	Chopped Strand Mat (Layer)	Surface Mat (Layer)
Type (I)	2	2	1
Type (II)	3	-	1

All specimens were tested under axial tension using INSTRON machine, Plate 3.1.

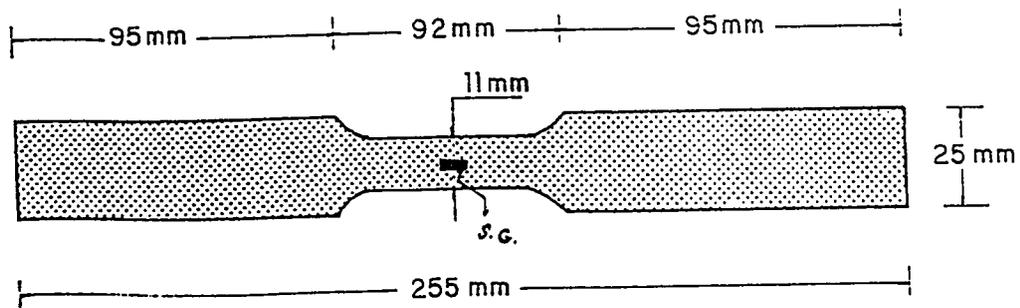


Fig.3.2 Tension Test Specimen

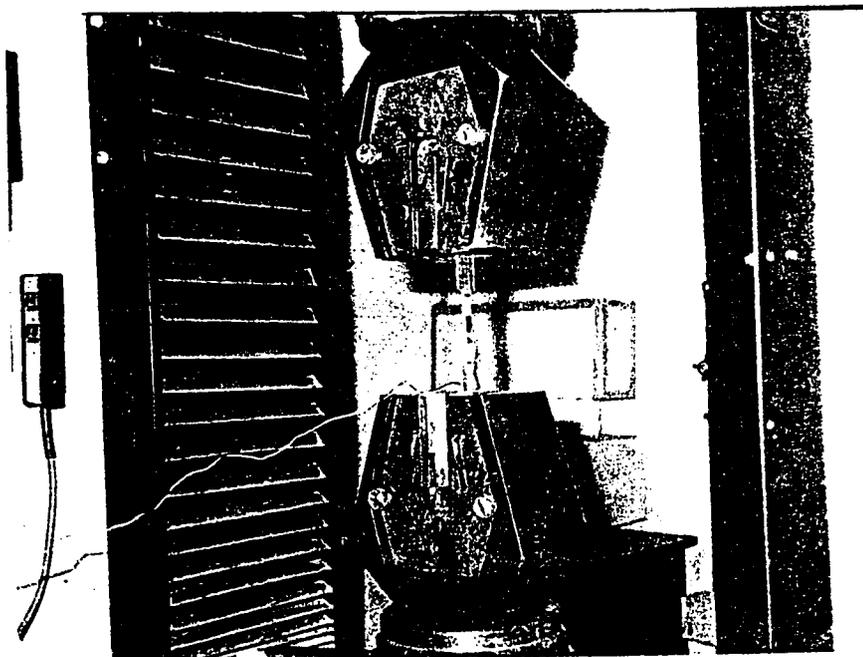


plate 3.1: Fiber Glass Specimen Under Axial Tension

3.3 Effect of Thermal Cycling on Bond Strength

To evaluate the effect of thermal cycling on durability of the glue and consequently the bond strength between fiber glass plates and concrete surface, a total of twelve pullout specimens consisting of concrete prisms 50 x 125 x 150mm and twenty four fiber glass plates were prepared and divided into four groups, each group consists of three specimens.

Group (1), Group 2) and Group (3) were subjected to 60, 90 and 120 heat and cool cycles, respectively. Group 4 was kept under laboratory conditions as controlled specimens.

One heat cycle consisted of heating the specimens upto 80°C for about six hours and cooling them for another six hours, thereby completing two heat-cool cycles per day. The temperature was raised gradually till it reached a maximum temperature of 80°C in four hours. The oven was maintained at 80°C for two hours, and then the temperature was gradually decreased to room temperature for two hours, before another heat-cycle was initiated, Plate 3.2.

The upper half of both sides of each prisms were covered with masking tape except an area of 50 x 75mm which is to be glued to the fiber glass plates. Twenty four 3.0 x 75 x 175mm fiber glass plates were prepared and covered with the masking tape from one side only. A contact area of 50 x 75mm was kept

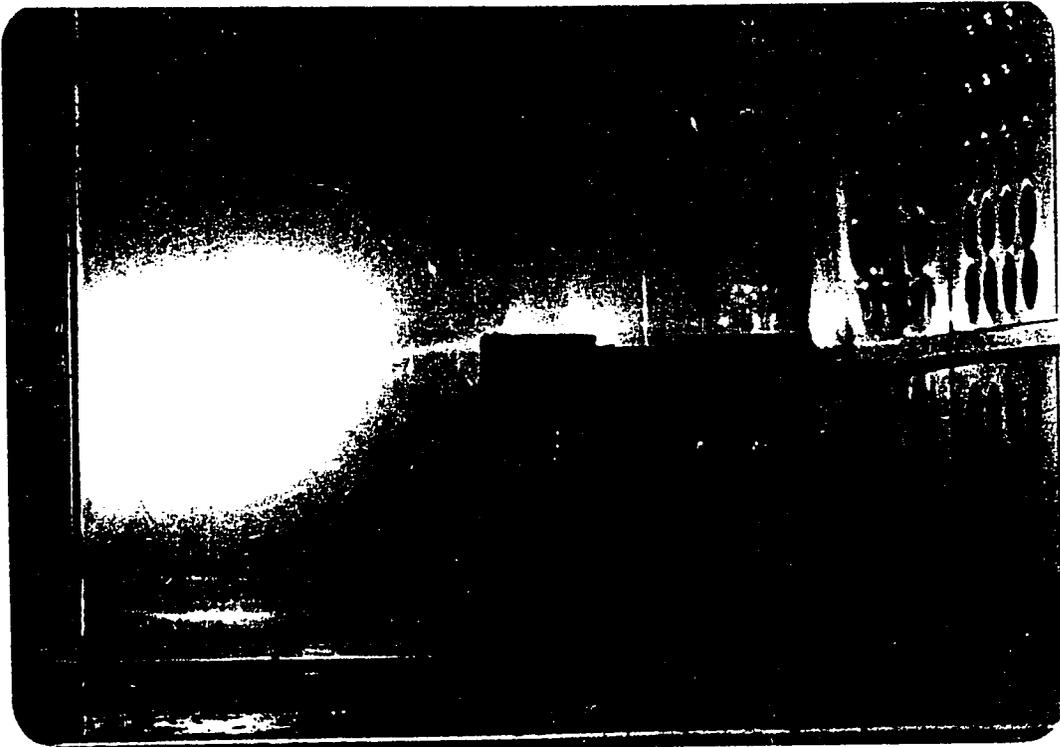


plate 3.2: Pullout Specimens in the Oven for Heat-Cool Cycling

uncovered at the end of the plate (Fig. 3.3).

In order to achieve a good bond between the concrete surface and the fiber glass plates, the area to be bonded was roughened using ordinary hammer-axe and the surface of the concrete was then cleaned using air pressure.

The structural adhesive used to bond the fiber glass plates was EP-CA resin (white) and EP-CA hardener (black). The mixing operation started by stirring the content of each then followed by mixing two parts of the resin to one part of the hardener (by volume). The two components were mixed thoroughly to obtain a gray colour mix, Plate 3.3.

The adhesive was applied to both the concrete and plate surfaces. The epoxy layer thickness was controlled by small metal spacers of 1mm diameter and 5mm length. The plate was then applied and pressed by hand to force the excess epoxy out from all sides. Then, the plate was held in position by a uniformly distributed pressure obtained by a concrete cylinder (75 x 150mm). The pressure was maintained for seven days, Plate 3.4. Similarly, another plate was bonded to the other face of the prism (see Fig. 3.4). All the prisms were left to cure for another seven days before they were subjected to the pullout test using the pullout set up as shown in Plate 3.5 and Figs. 3.4 through 3.7.

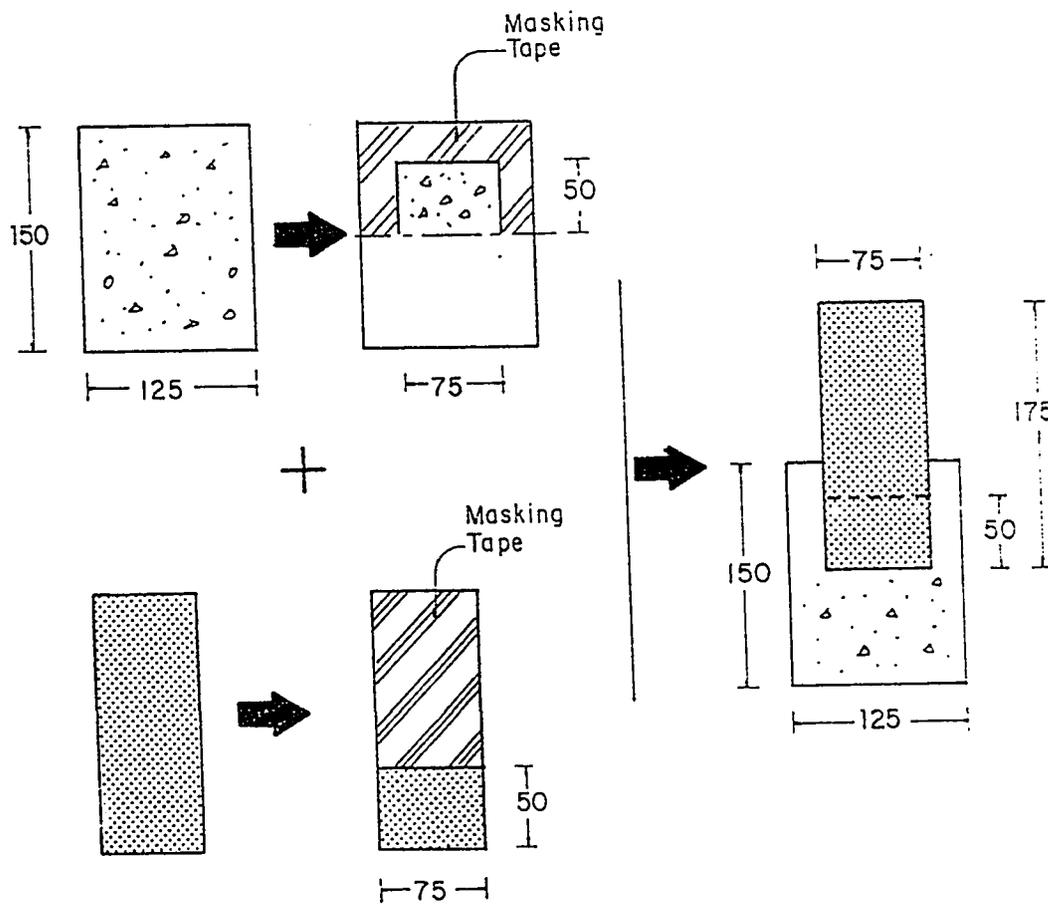


Fig.3.3 Preparation of Pull-out test Specimen

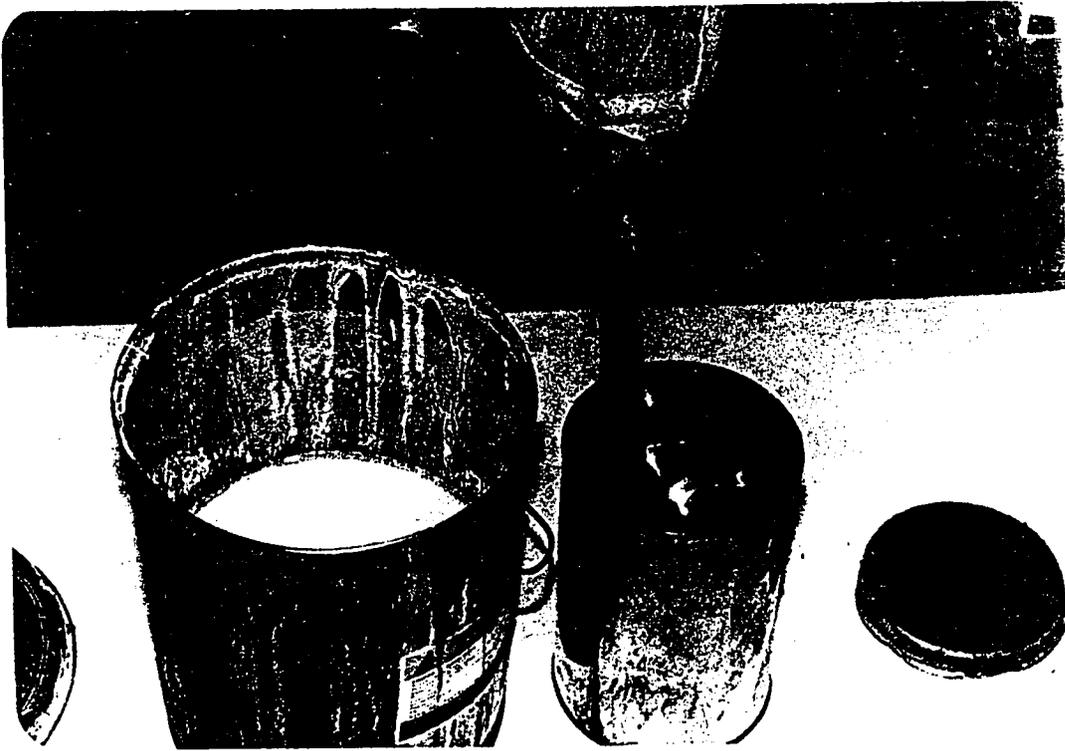


Plate 3.3: Stirring the Two Components of the Epoxy Separately

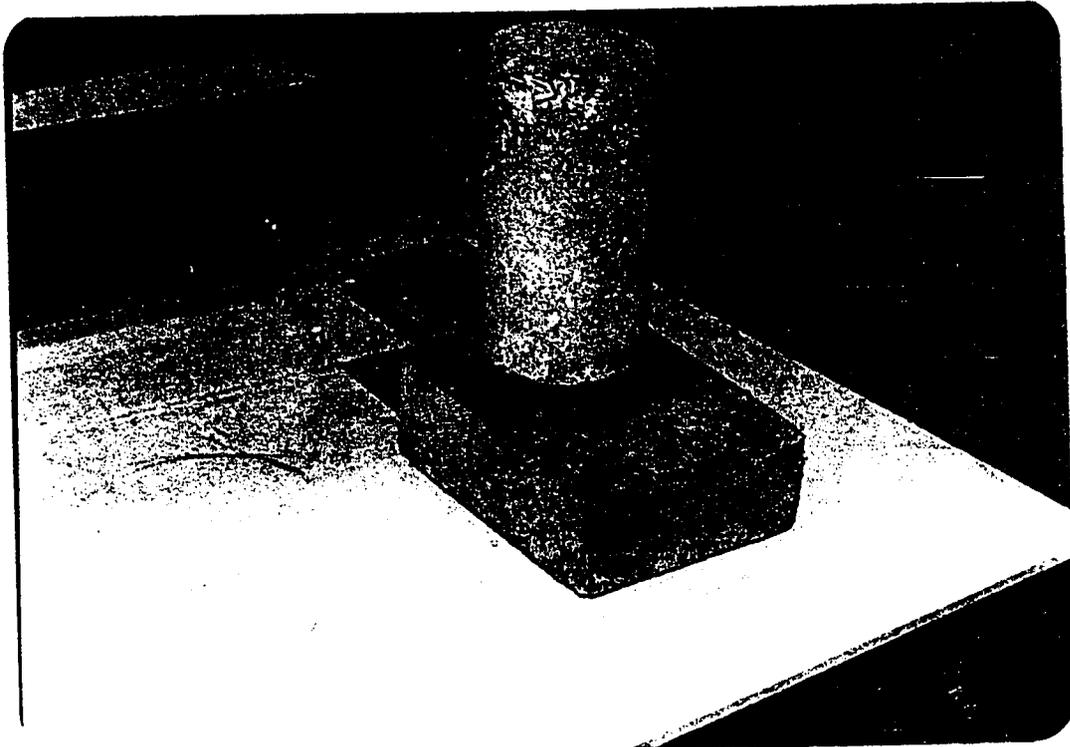


Plate 3.4: Applying Pressure on the plates for Seven days

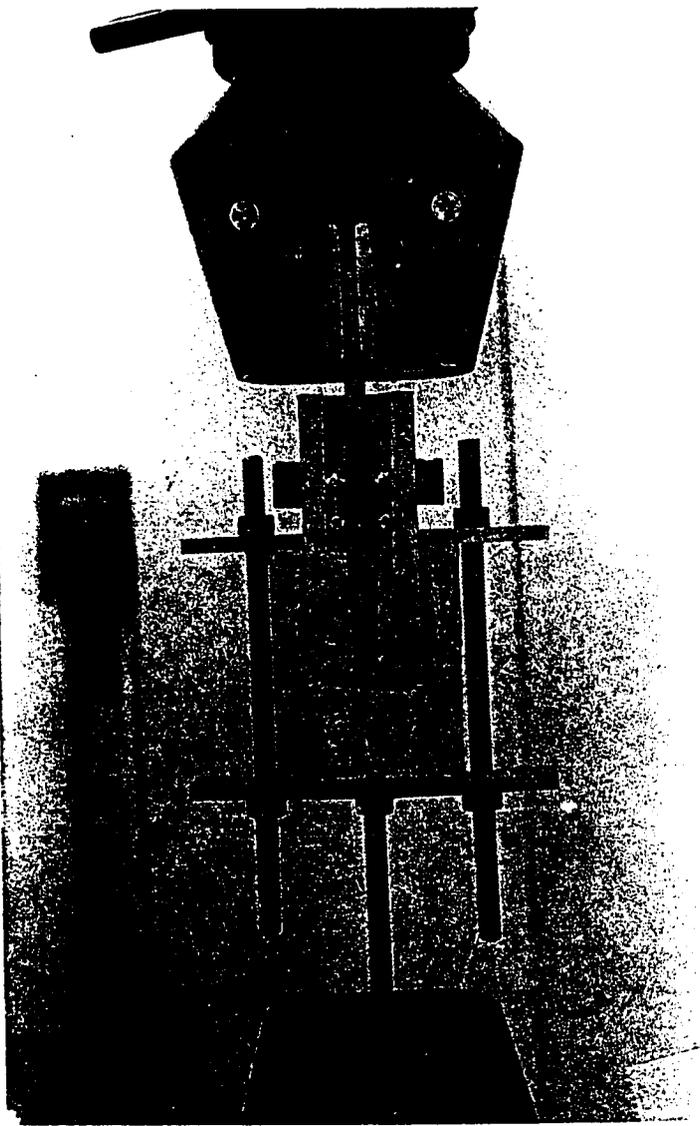
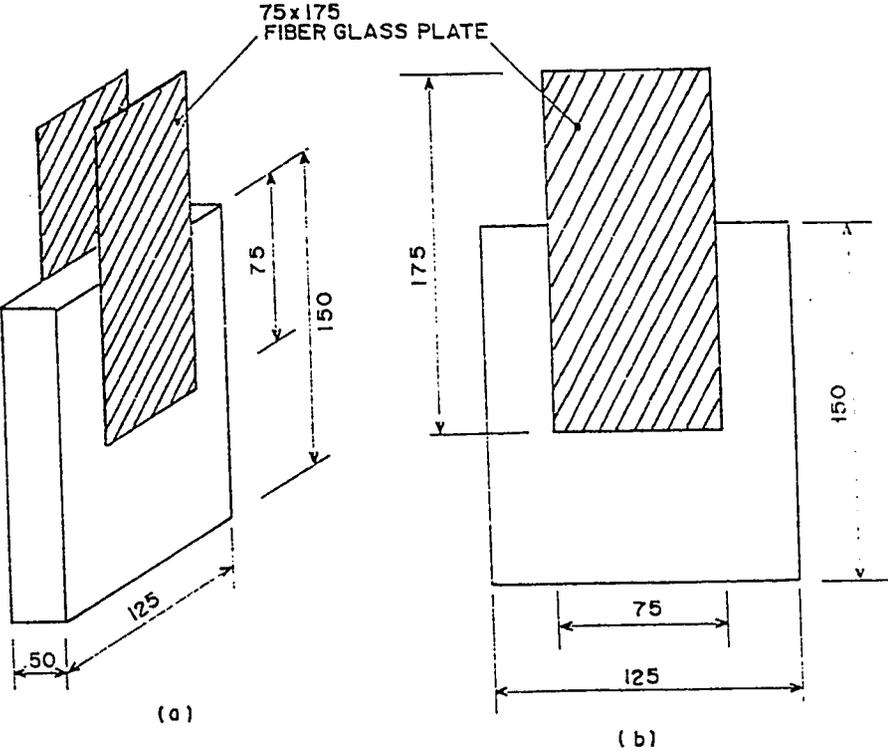


Plate 3.5: A pullout Specimen Under Testing



All dimensions in mm.

Fig.3.4 Pull-out Test Specimen

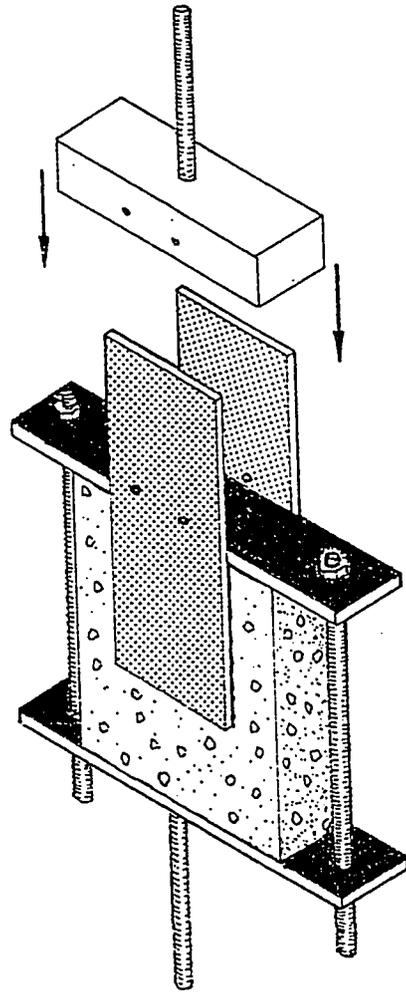


Fig.3.5 Pull-out Set up

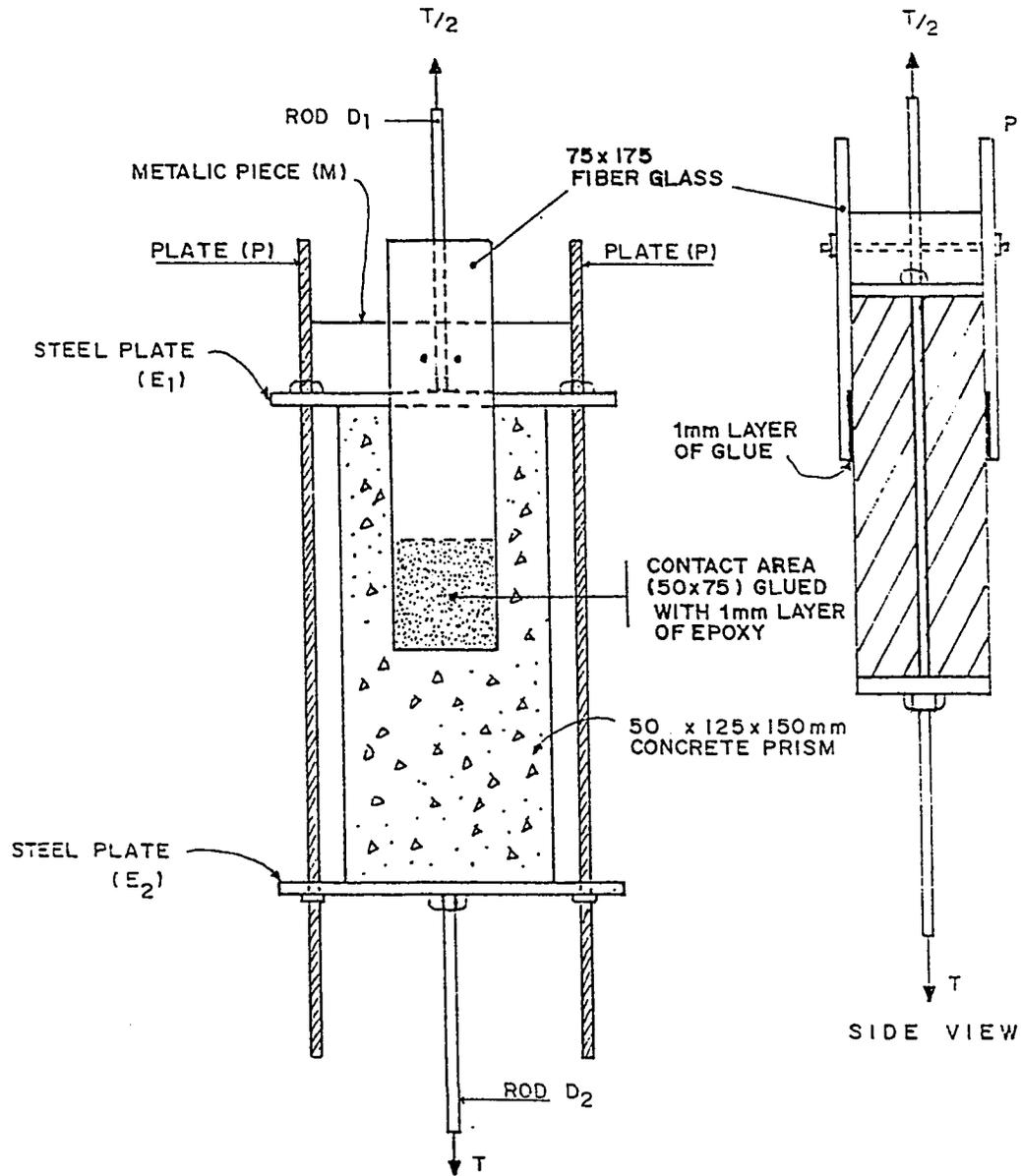


Fig.3.6 Schematic diagram of the pull out set up

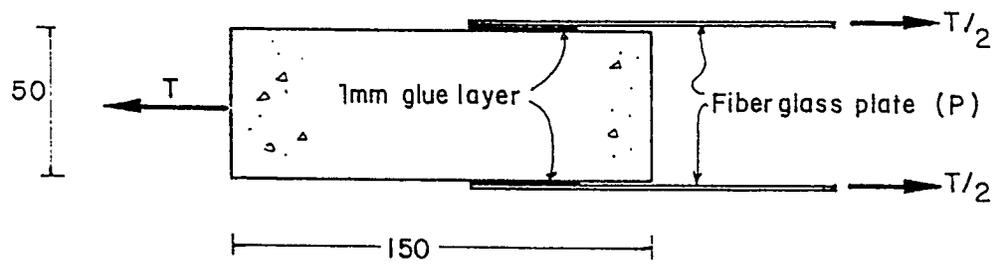


Fig. 3.7: Forces Acting on the Glue Layer

PLEASE NOTE

Page(s) not included with original material
and unavailable from author or university.
Filmed as received.

45

University Microfilms International

Table 3.2: Flexure and Shear Beams Details

Item	Flexure Beams	Shear Beams
Concrete Dimension	150 * 150 * 1250 mm	150 * 150 * 1250 mm
ρ_p	0.0037	0.0037
ρ_s	0.0093	0.0200
Reifts.	2 ϕ 10 mm	3 ϕ 12 mm
Web Rfts.	ϕ 6 mm	ϕ 6 mm
Spacing	60 mm c/c	200 mm c/c

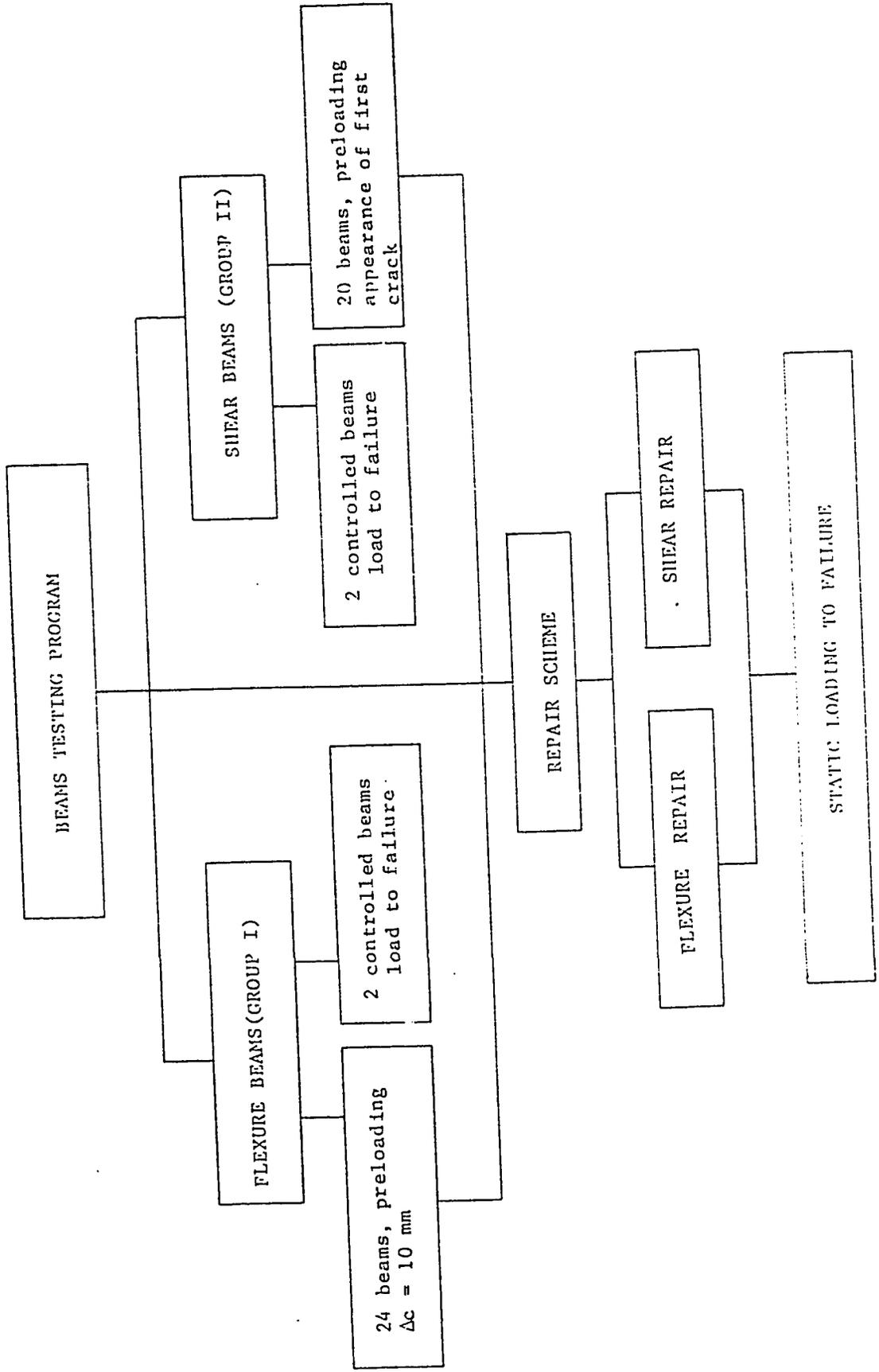
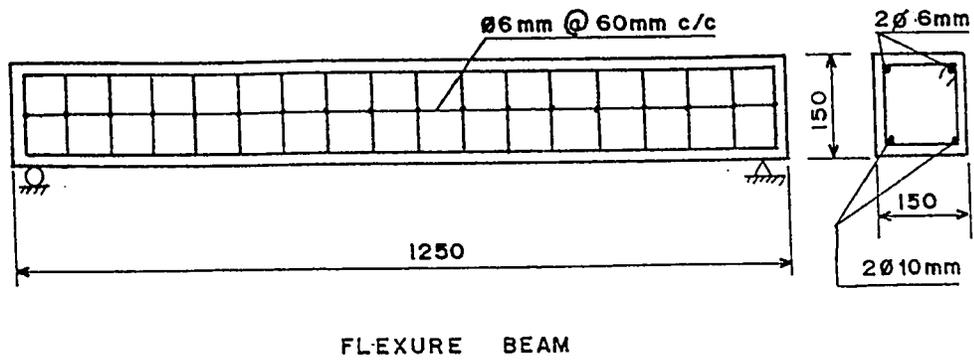


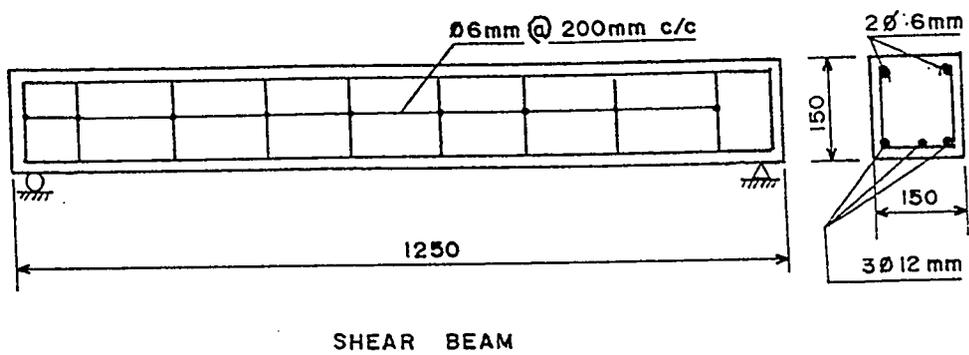
Fig. 3.8: General Chart Diagram for Repaired Beams Specimens



NOTE:

1. All dimensions are in mm.
2. Clear cover = 25mm from all sides.

Fig. 3.9: Reinforcement details for Flexure Beams

**NOTE:**

1. All dimensions are in mm .
2. Clear cover = 25mm from all sides .

Fig. 3.10: Reinforcement details for Shear Beams

($\rho_s = 0.02 < \rho_b = 0.037$). To ensure shear failure, 6mm diameter mild steel stirrups at 200mm spacing were adopted.

Prior to preparing the steel cages consisting of the longitudinal bars and stirrups, the bars were wire brushed to remove the millscale of the external surface. The steel cages of both flexure and shear beams were then prepared, and the spacers of the main steel were checked (25mm) from all sides.

Concrete basic properties of these beams were evaluated using cylinders and prisms. Fourteen 75 mm cylinders were cast for compressive strength, two cylinders 150mm in diameter by 300mm long were cast for plotting concrete stress-strain diagram, and four prisms 150 x 150 x 500mm were cast for evaluating the modulus of rupture, Plates 3.6 through 3.8 respectively. All specimens were cast in three layers and thoroughly vibrated after each layer in accordance with ASTM Standards C192 using electrical internal vibrator. All specimens were moist cured for 14 days.

3.5 Preloading of Beams

All beams were preloaded to a predetermined level to simulate badly damaged beams in practice. The preloading levels for both flexure and shear beams were decided upon after testing the control beams of both types to failure, Plates 3.9 and 3.10. It



Plate 3.6: Testing 75mm*150mm Cylinder for Concrete compressive Strength Using TONIPAC Machine.

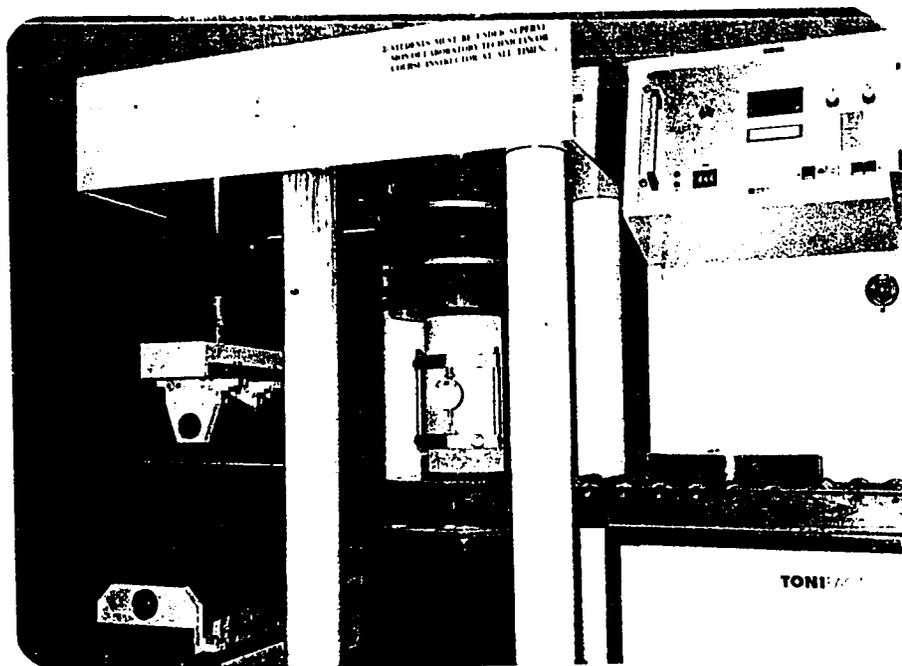


Plate 3.7: Testing 150mm*300mm Cylenders for Plotting Concrete Stress-Strain Curve using a Ccompressometer.



Plate 3.8: Testing 150mm*150mm Concrete Prisms for Evaluating the Modulus of Rupture.

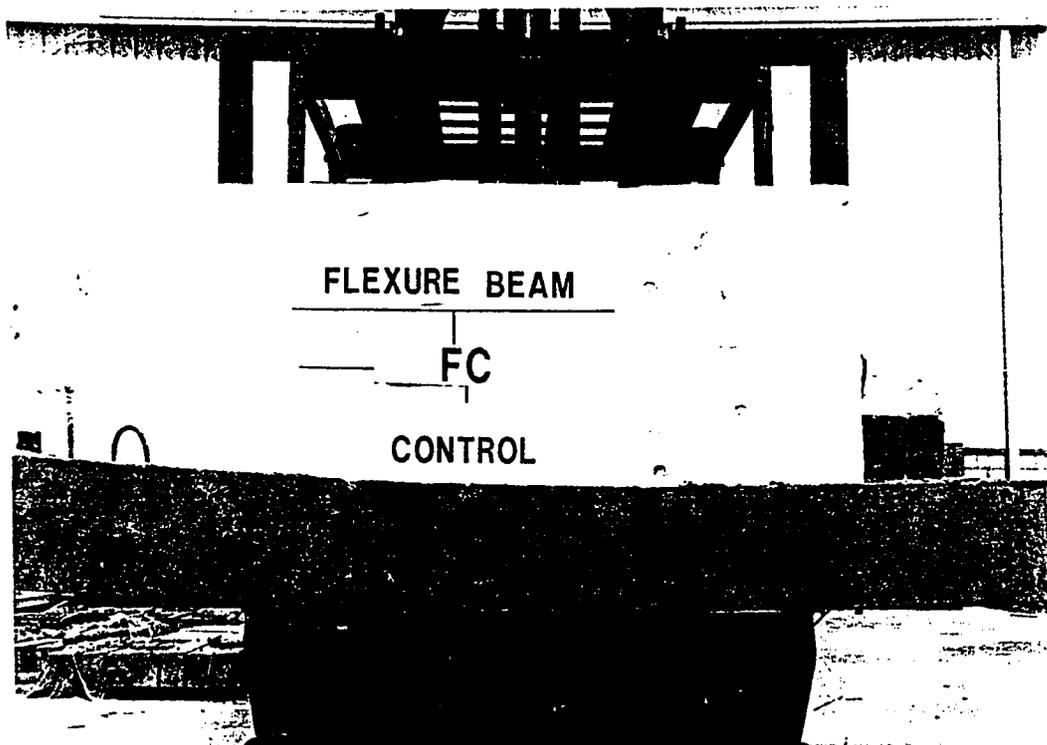


Plate 3.9: A Control Flexure beam Tested upto Failure,aluting

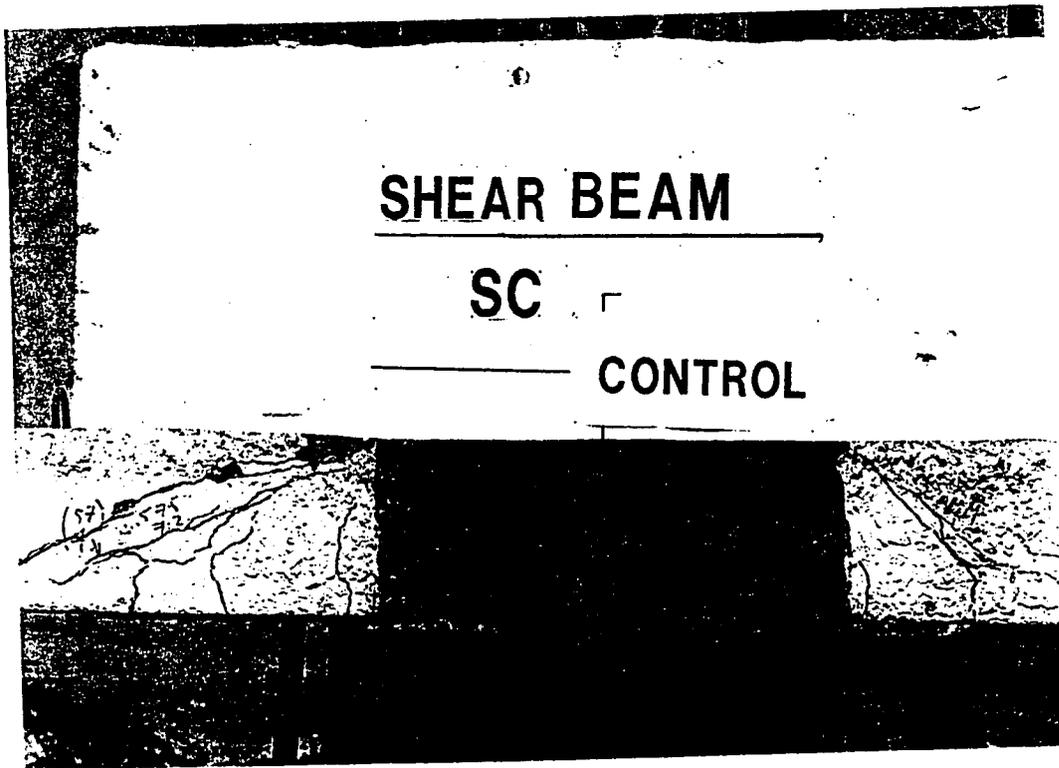


Plate 3.10: A Control Shear Beam Tested upto Failure.

was then decided to load the flexural beams to obtain 10 mm central deflection, while shear beams were preloaded upto the appearance of the first shear crack. To facilitate the crack viewing, the shear beams were white-washed one day prior to preloading, Plate 3.11

All beams were tested under two points load Fig. 3.11 using INSTRON machine of 25 tons capacity. A portable data logger and a personal computer were used to record the outputs directly from the load cell as shown in Plate 3.12.

Loading was applied at a rate of 1 mm/min and readings were taken every 1 kN. The loading frame is shown in Fig. 3.12. Deflections were measured at three central points using the Linear Variable Differential Transducers (LVDT's).

Strain gauges were mounted at top of concrete and rebars to measure the respective strain, Fig. 3.13 shows the locations of strain gauges.

3.6 Repair of Beams

All damaged beams were strengthened either for flexure or shear according to their types. Several repair modes were used to strengthen the flexural as well as the shear beams. Prior to the application of the repair techniques, beam surfaces were roughened

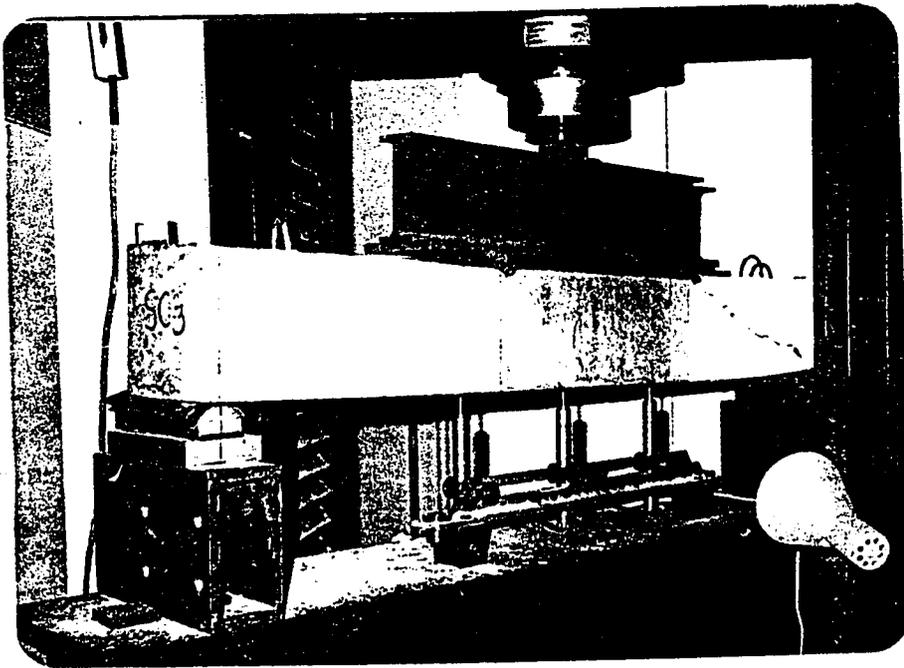


Plate 3.11: Damaging Shear beams upto the Appearance of the First Crack.

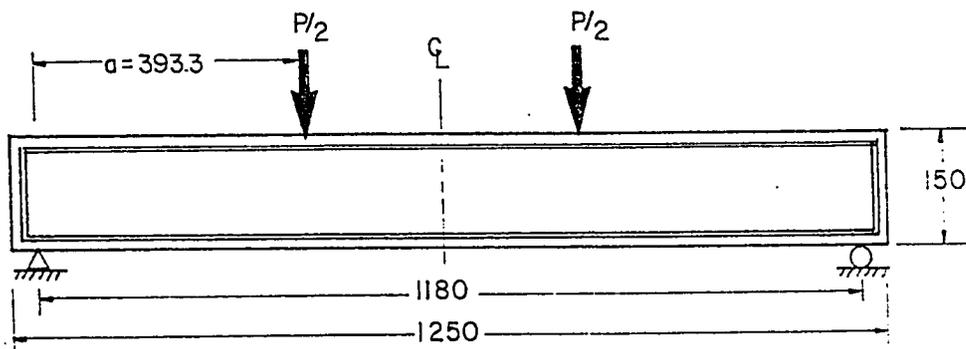


Fig.3.11 Load configuration used in testing the beam specimens

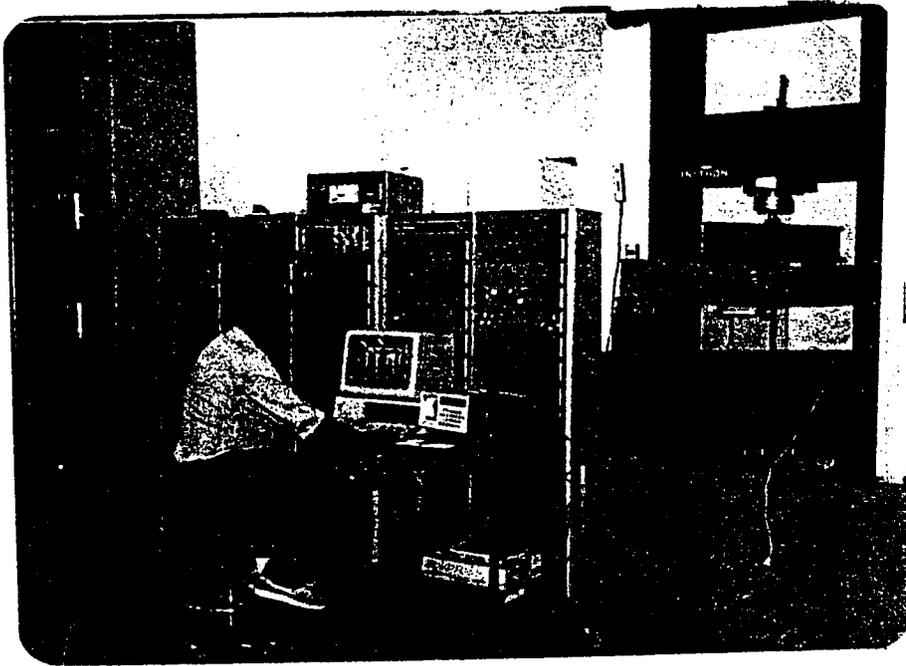


Plate 3.12: The INSTRON Machine and the Acquisition System
Used in Testing the Beam Specimens.

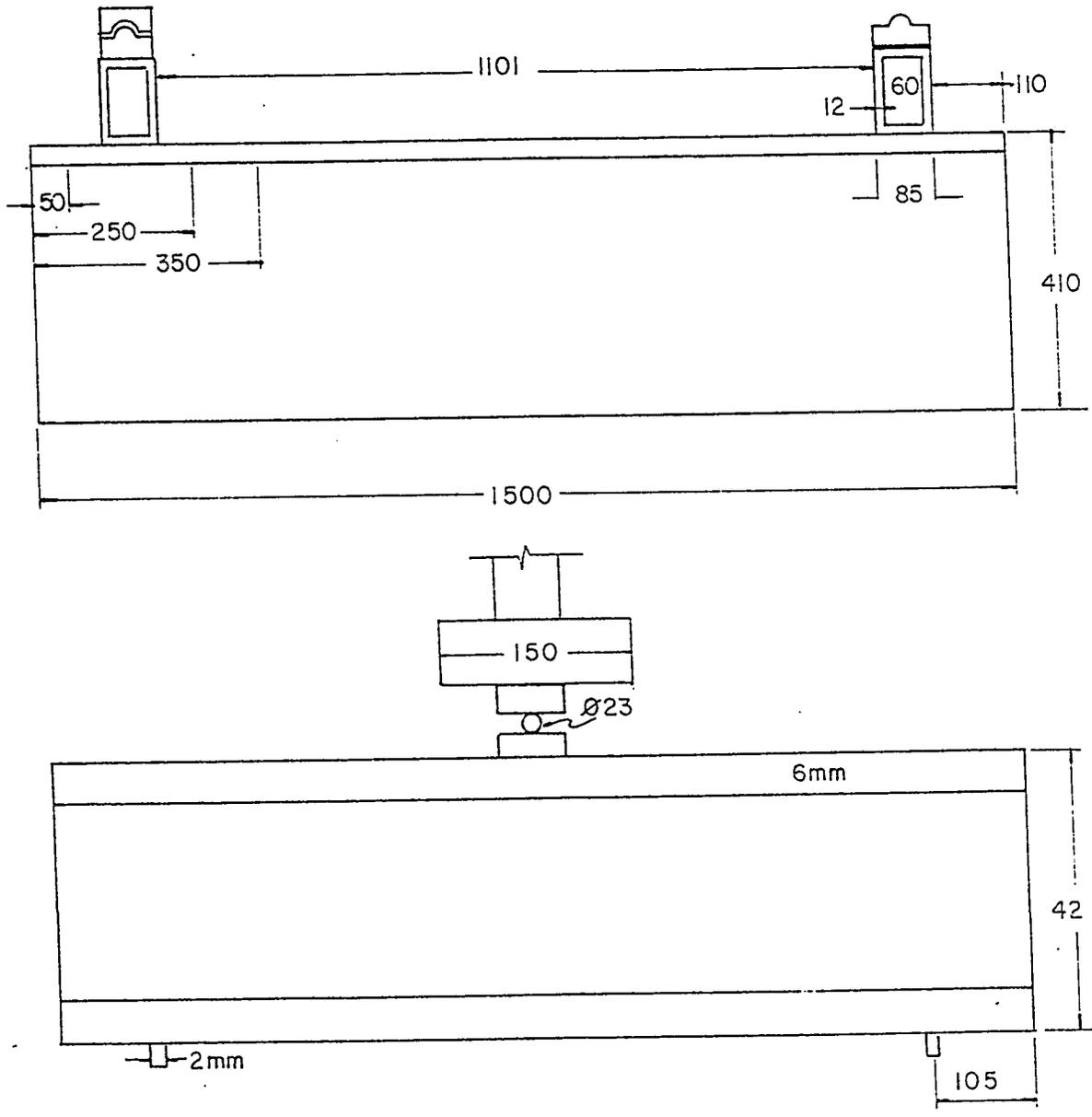


Fig.3.12 Supporting I-Steel beam and Loading frame

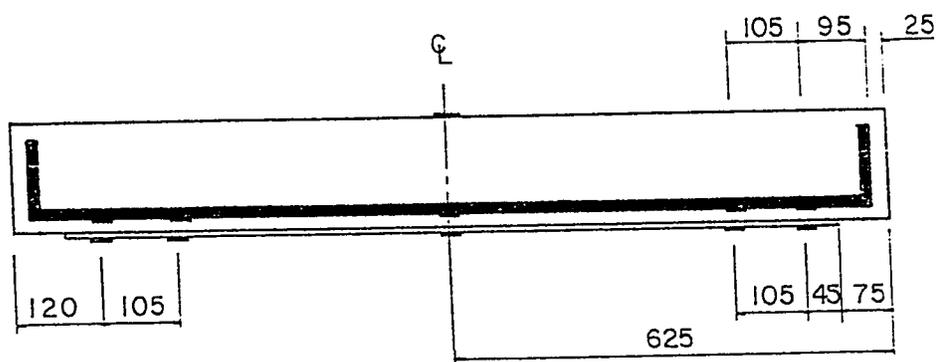


Fig.3.13 Location of strain gauges

using sand blasting machine to ensure a good bond between the concrete surface and the fiber glass plates Plate 3.13. The repair material were then bonded as mentioned earlier in Section 3.3. The sequence of glueing the fiber glass plates is shown in the plates 3.14 through 3.16. Strain gauges were fixed at soffit of plates to record the respective strain.

3.6.1 Flexure Beams

This part of the experimental program deals with the repair of beams failing in flexure. Twenty four reinforced concrete beams were strengthened using three different thicknesses (3mm, 2mm and 1mm) as shown in Fig. 3.14. anchor bolts were also used to prevent premature failure and insure ductile behavior. Beams FP3, FP2 and FP1 were strengthened using fiber glass plates with 3mm, 2mm and 1mm thickness, respectively.

An end anchorage system in the form of steel bolts was applied to beam FPB3 and FPB2 to prevent premature failure caused by separation of plate ends. Furthermore, side plates (wings) were used to confine the shear span of beams FPBW3 and FPBW2 against diagonal tension cracks initiating at the plate curtailment. Table 3.3 and Fig. 3.15 show the repaired flexure beams and the sequence of repair, respectively.

A new repair scheme in the form of I-shaped fiber glass jacket was suggested to overcome the problem of both plate separa-

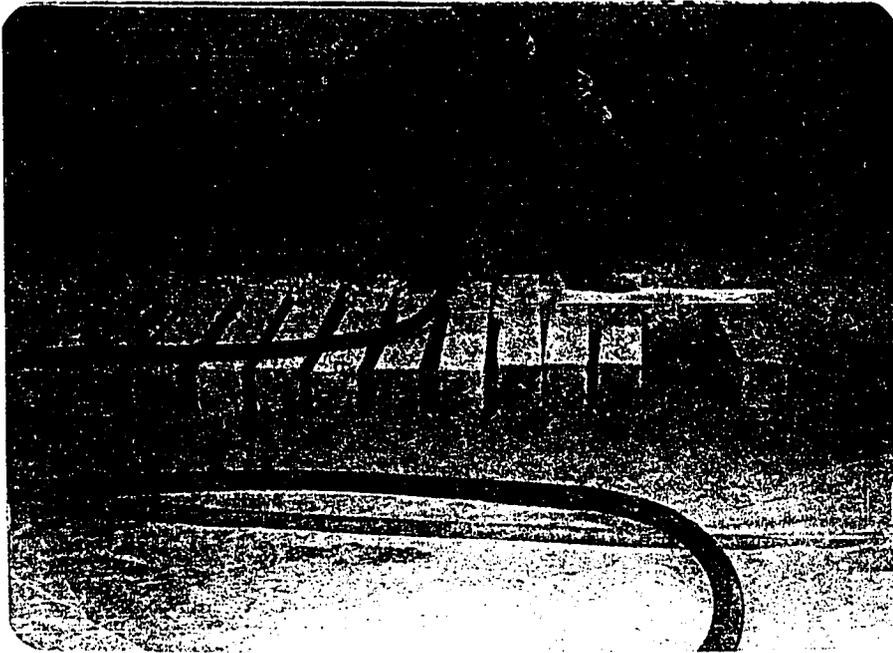


Plate 3.13: Roughening the Beam Surfaces Using Sand-Blasting Machine.

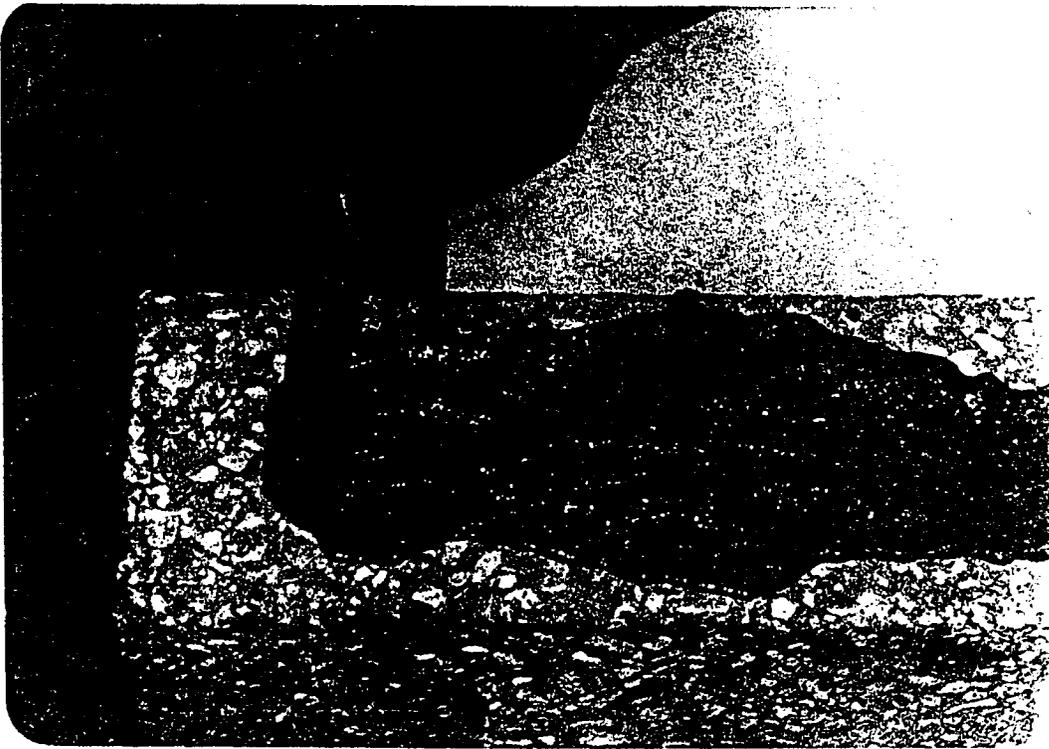


Plate 3.14: Application of the Epoxy on Beam Surface
Using Paint Brush.

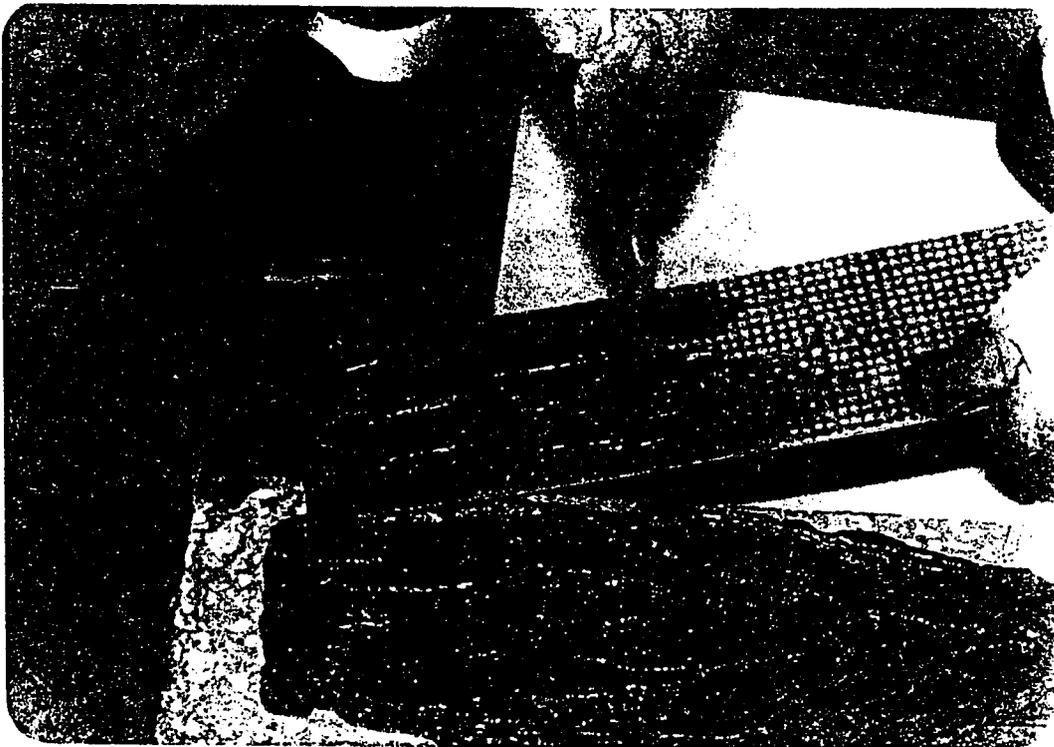


Plate 3.15: Application of the Epoxy on on the Plate Surface using Paint Brush.

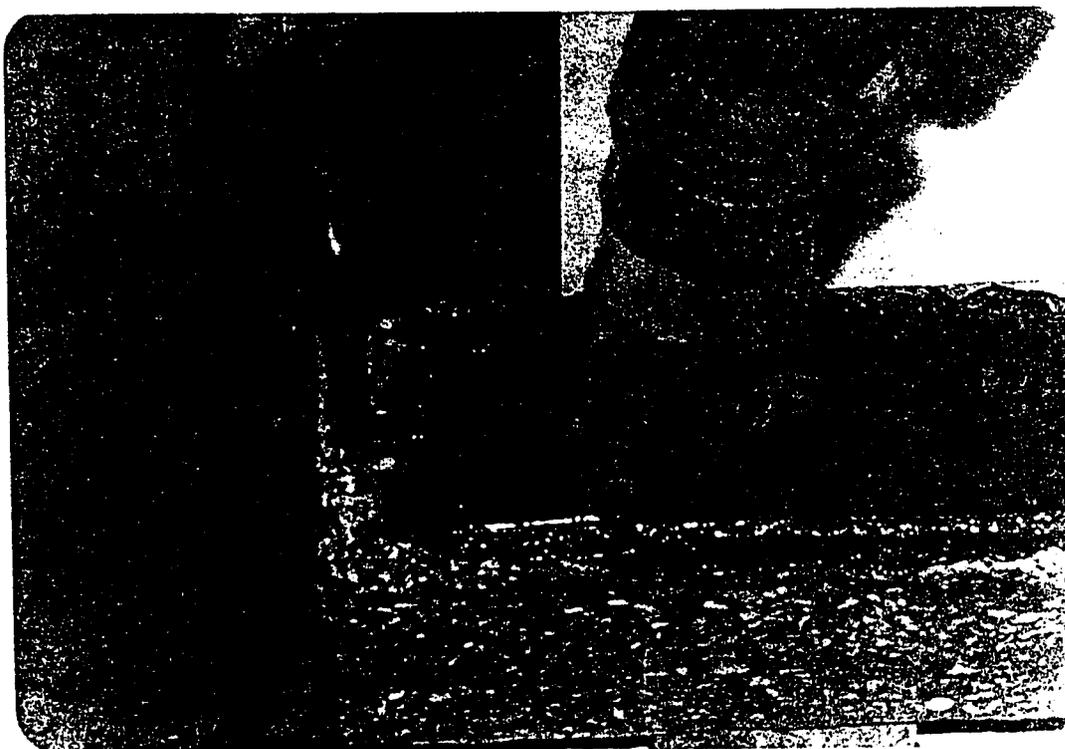


Plate 3.16: Placing the Fiber Glass Plate on the Beam Surface
and Pressing it With Hands to Force Excess Epoxy
From All Sides.

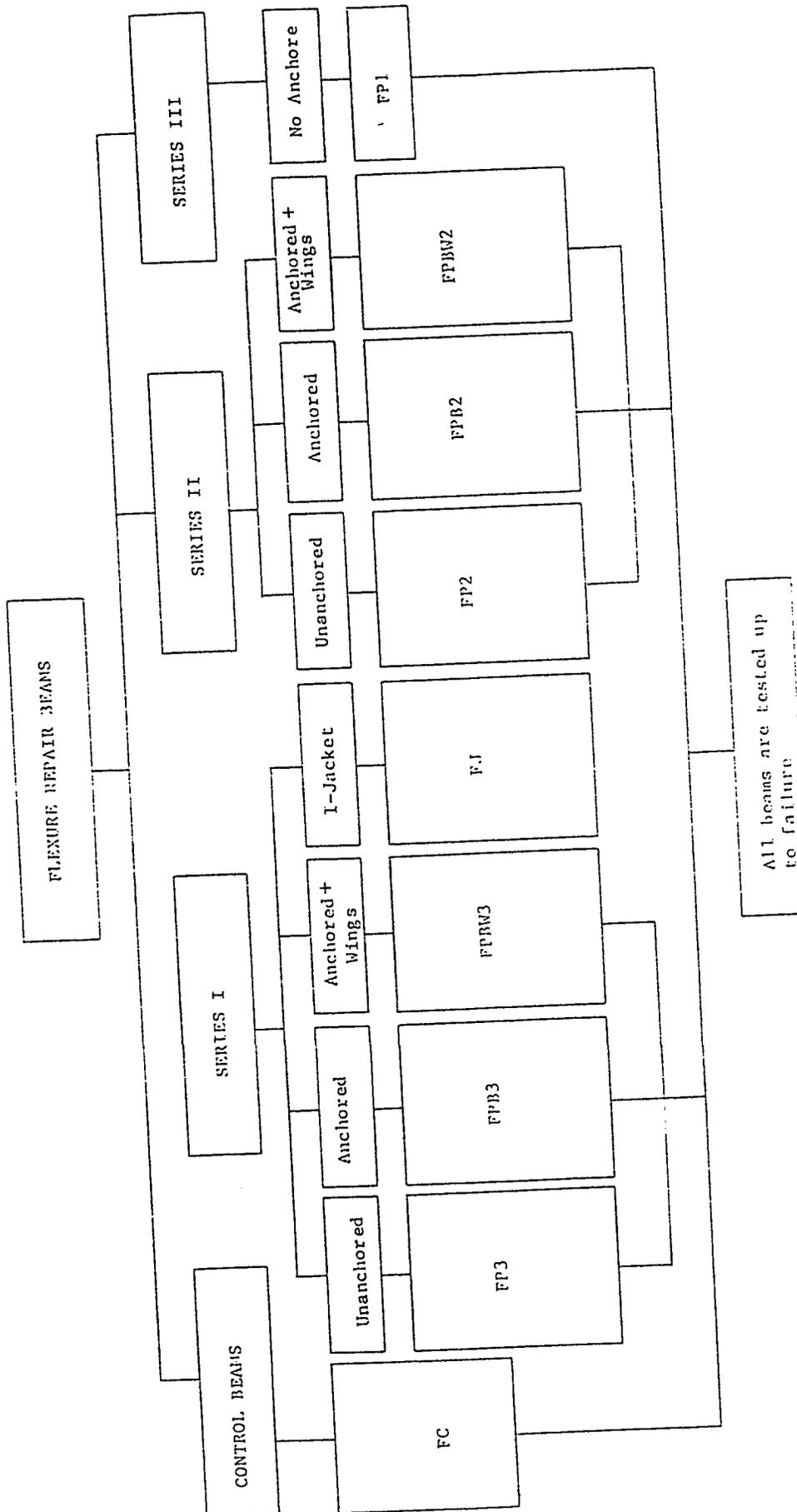


Fig. 3.14: Chart Diagram for Repaired Flexure Beams

Table 3.3: Flexurally Repaired Beams

Beam #	No. of Specimens	Plate Thickness (mm)	Mode of Repair	Illustration IN
FP3	3	3	Plate only	Fig. 3.15
FPB3	3	3	Plate + Bolts	Fig. 3.15
FPBW3	3	3	Plate + Bolts + Wings	Fig. 3.15
FP2	3	2	Plate only	Fig. 3.15
FPB2	3	2	Plate + Bolts	Fig. 3.15
FPBW2	3	2	Plate + Bolts + Wings	Fig. 3.15
FP1	2	1	Plate only	Fig. 3.15
FJ	2	3	I-Jacket	Fig. 3.16

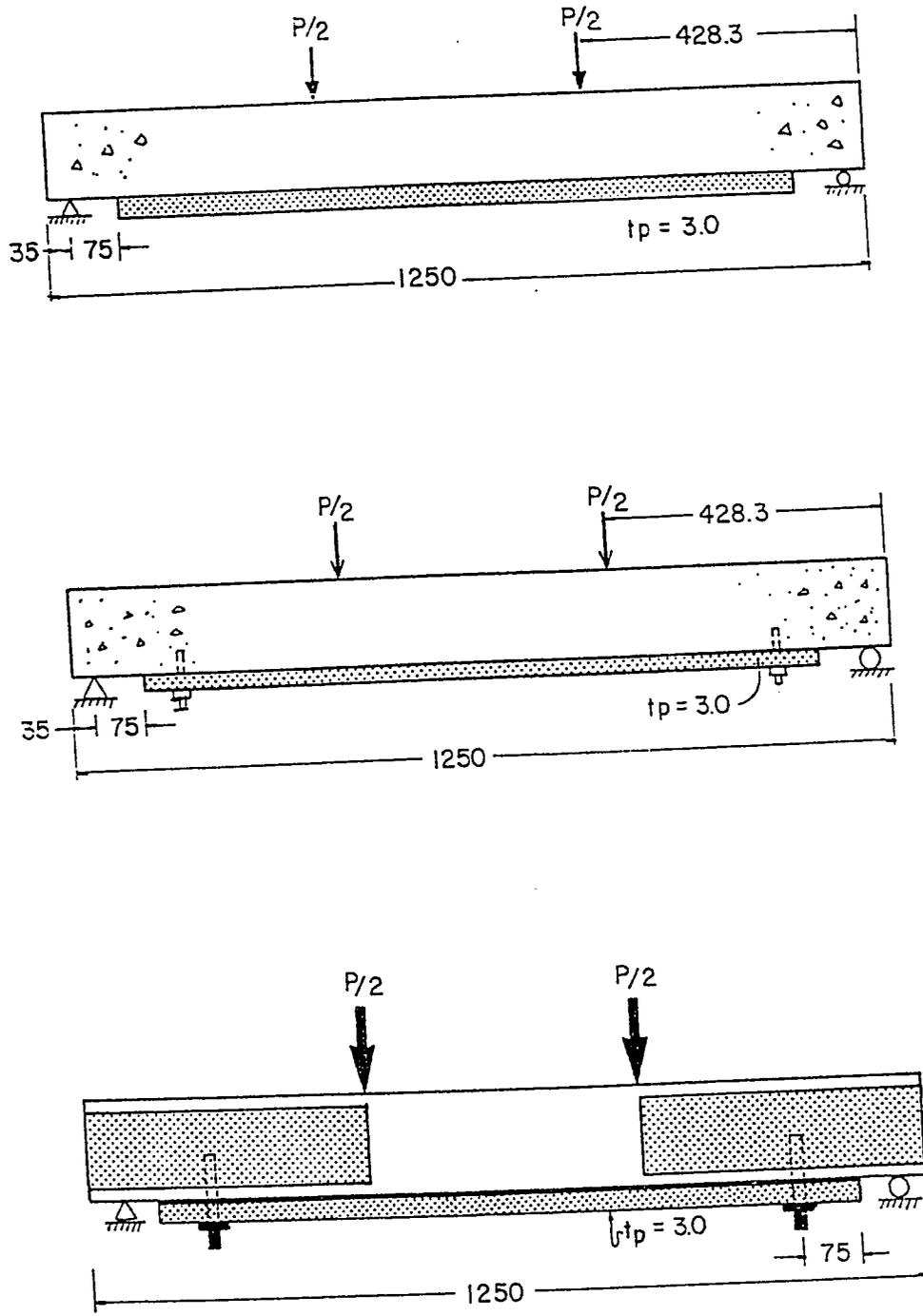


Fig. 3.15: Repair Sequence of Flexure Beams.

tion and diagonal tension cracking at the plate curtailment at the same time, Fig. 3.16. and plate 3.17.

End Anchoring System (Steel Bolts)

A special steel anchor bolts (12 x 100 mm) prepared in the Mechanical Engineering Workshop using ϕ 12 mm diameter and mild steel rebars to provide good adhesion with the epoxy, Plate 3.18. After the beams being preloaded, two holes 14 mm in diameter and 75 mm in depth ($h/2$) were drilled using an electrical drilling machine. The holes were located at 125 mm from the beam end (one hole at each end) along the centre line of the bottom face. The dust resulting from drilling process was removed by means of water jet. The holes were then left to dry before gluing the steel bolts.

3.6.2 Shear Beams

This part of the research is focused on repair of reinforced concrete beams weak in shear. The different modes of repair intended to improve their shear capacity and insure ductility. Twenty beams were strengthened in shear (i.e. applying additional external web reinforcement). The beams were classified into three series according to the type of the additional external web reinforcement applied as shown in Fig. 3.17 and Table 3.4.

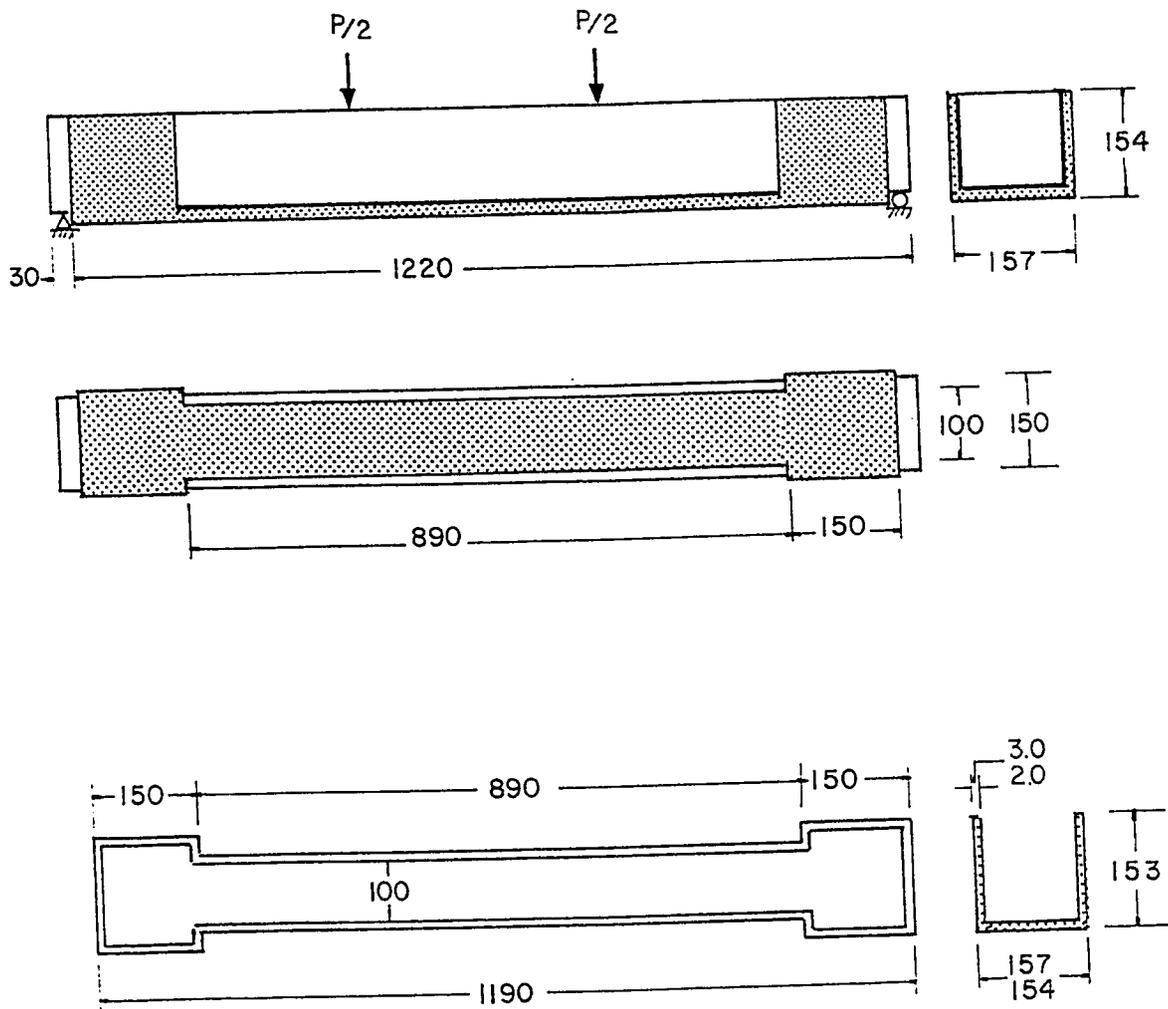


Fig. 3.16: Flexure Beams Repaired with I-Jacket.

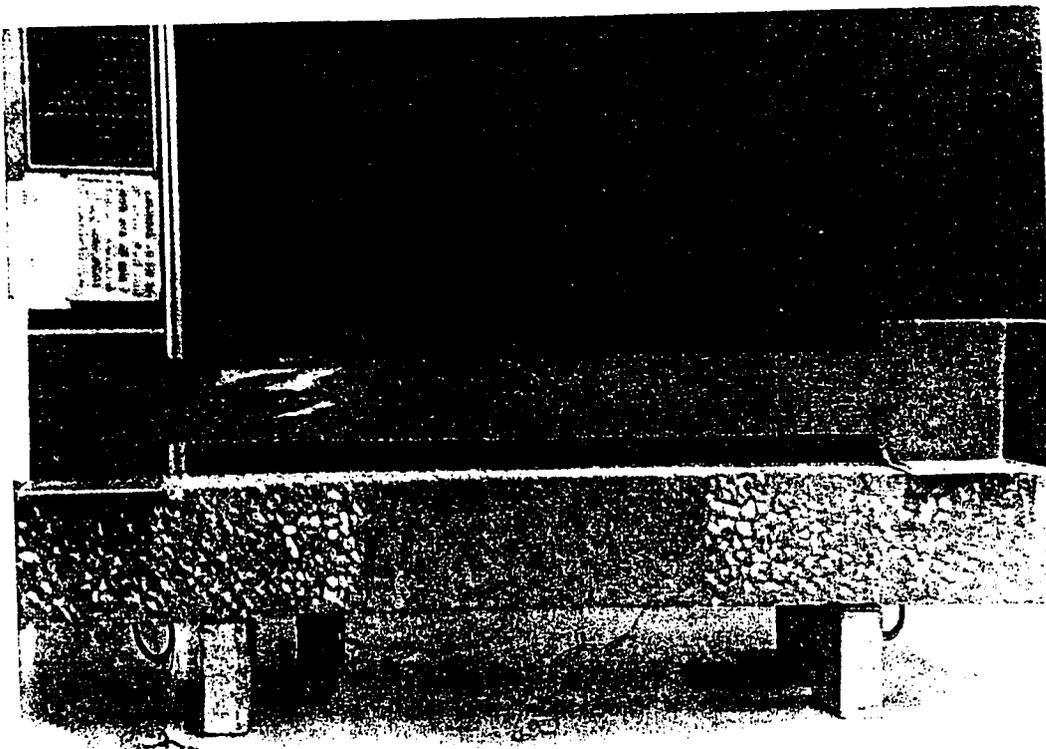


Plate 3.17: The I-Shaped Fiber Glass Jacket Used to Repair Beam (FJ).

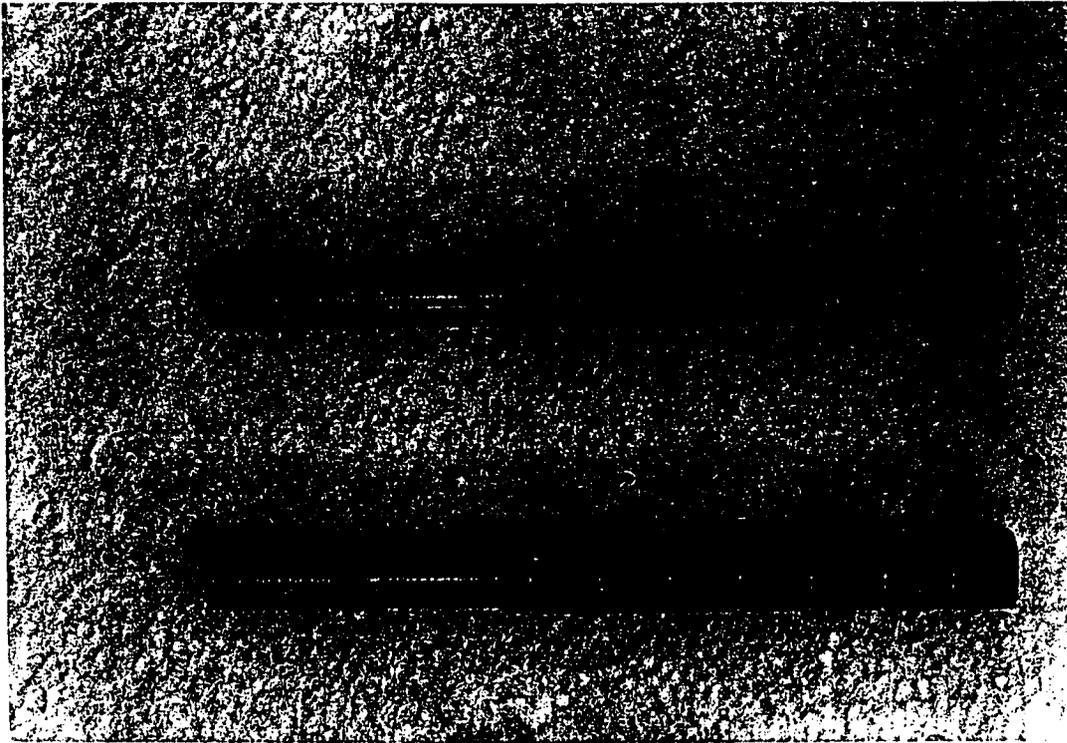


Plate 3.18: Steel Anchor Bolts Used to Anchor the Plate Ends

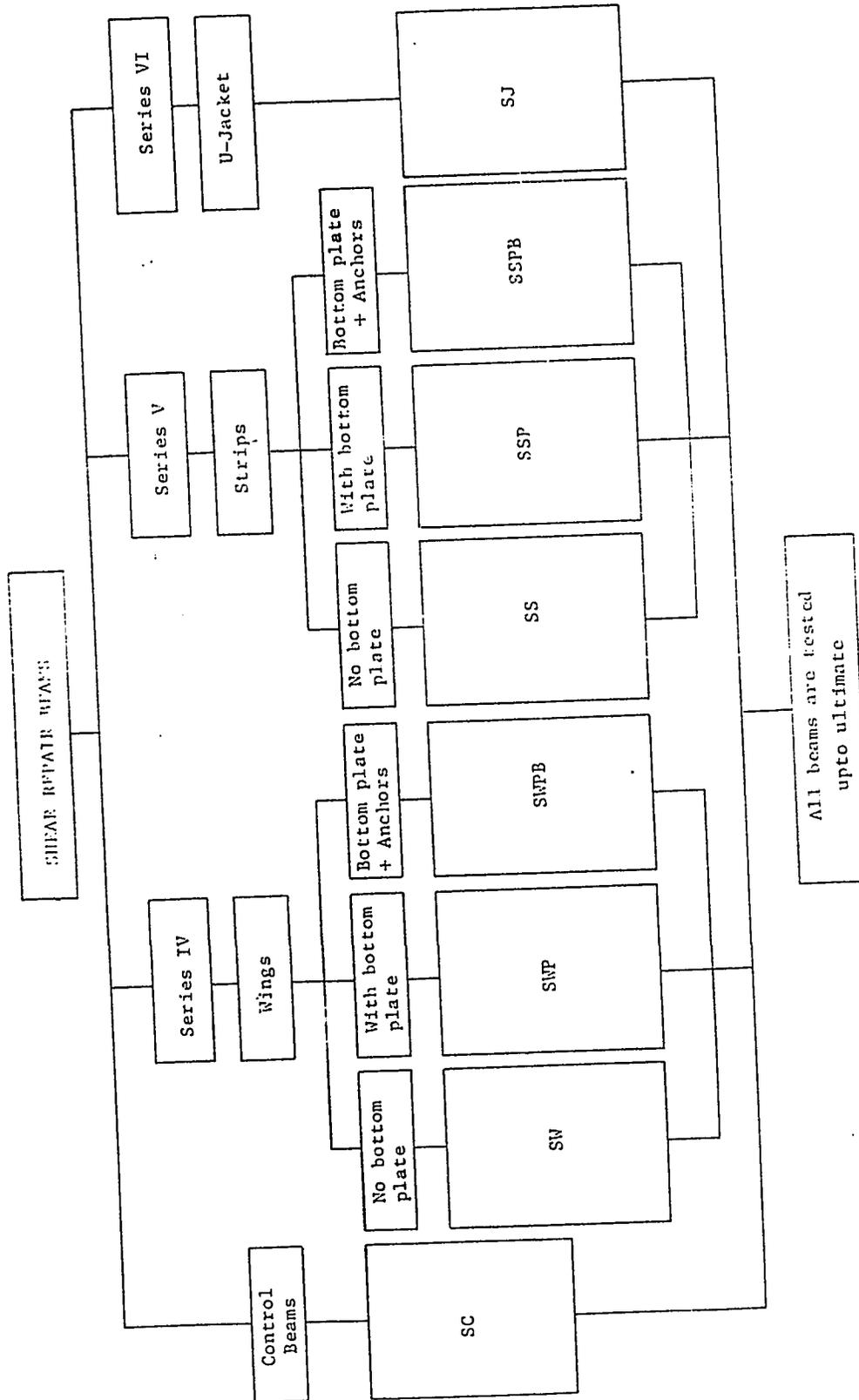


Fig. 3.17: Chart Diagram for Repair Shear Beams.

Repair Modes:**a) Repair by Wings (Series IV):**

A total of nine beams were strengthened using 3 x 120 x 420 mm side plates (wings) at the shear spans.

Three beams were strengthened using only wings (SW) to evaluate the effect of external web reinforcement on the shear capacity and the failure modes. Three other beams (SWP) were repaired with additional bottom plates glued to the soffit of beams to prevent longitudinal bottom cracks at high load levels. For the last three beams, the bottom plates were anchored with steel bolts to eliminate any possible separation for the bottom plate (SWPB). The repaired beams and sequence of repair are shown in Fig. 3.18.

b) Repair by Strips (Series V):

These beams were strengthened with 3 x 20 x 150mm strips in the shear spans from both faces. One strip was bonded at the end of each face, then others were bonded at 60mm center to center. The beams repaired with strips followed a similar sequence of repair as those repaired by wings. Three beams (SS) were repaired using only strips. Beams (SSP) were repaired by strips in addition to bottom plates glued to their soffits. The last group of beams (SSPB) were repaired using strips and anchored bottom

plates. The repaired beams and sequence of repair are shown in Fig. 3.18.

c) Repair by U-Jacket (Series VI):

A new technique was suggested to eliminate the debonding of the wings and strips in the form of U-shaped jacket Fig. 3.20 and Plate 3.19. Because of the brittle nature of the fiber glass material after hardening, it was difficult to form the U-jacket by bending the fiber glass plates. To overcome this problem a special wooden mould (158 x 154 x 1700mm) was prepared in the laboratory and transported to the local manufacturer. One complete U-channel of the fiber glass was casted in the same way as the fiber glass plates and then cut to the desired dimensions (154 x 158 x 420 mm), Plate 3.20.

These jackets were used to strengthen beam SJ. The glue layer used to bond the jackets was kept constant as before (1mm), this was maintained by bonding small metal spacers to the beam surfaces one day before bonding the jackets.

Bonding the jackets to the beam surfaces was carried out while the bottom face of the beam was up. The glue was applied to the jackets and beam surfaces using a brush. The jackets were then applied on the beam ends and the sides of the jacket were clamped using two pieces of wood and C-clamps. The beams were then inverted and supported on two concrete blocks. The own

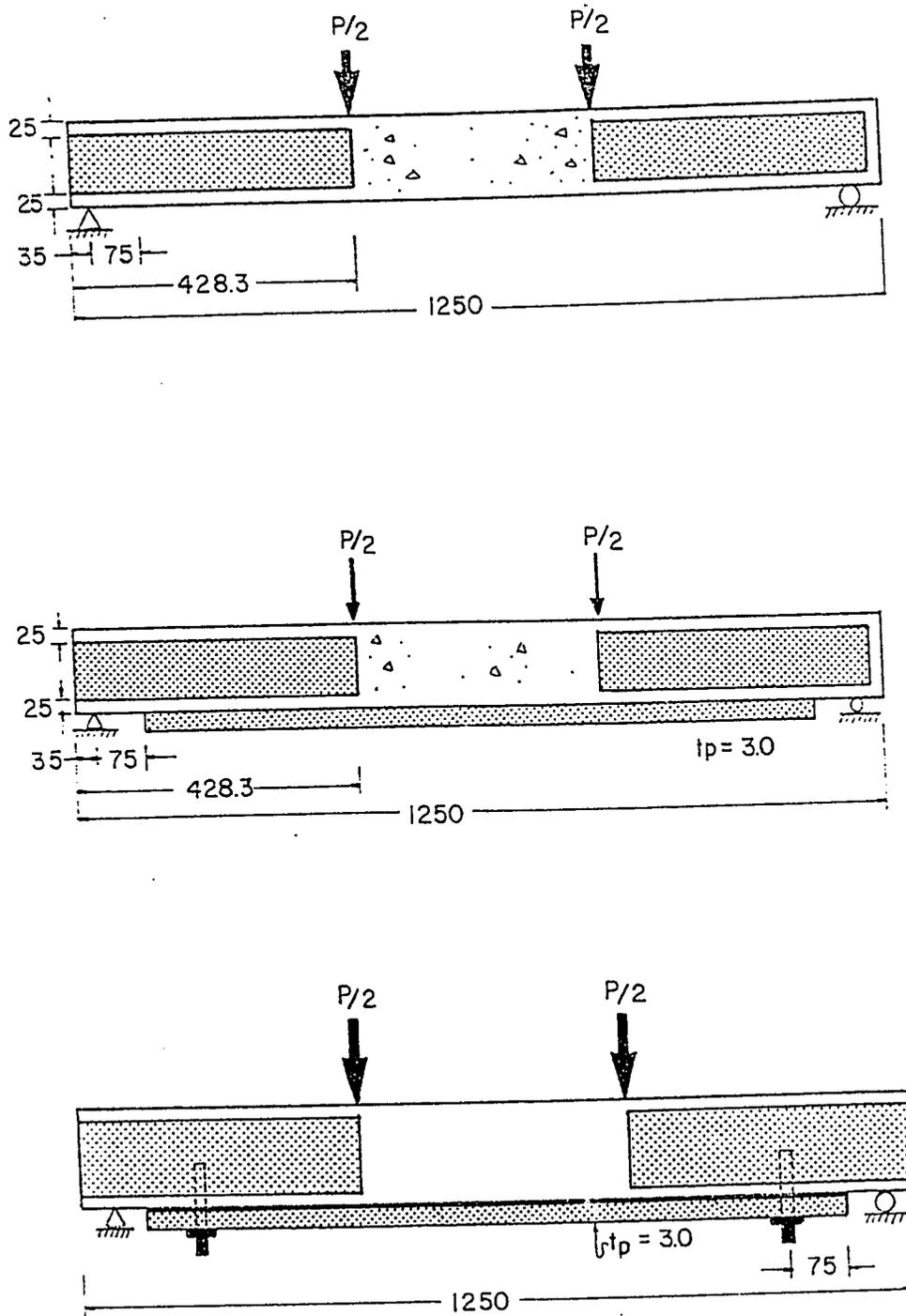


Fig. 3.18: Repair Sequence of Shear Beams Using Wings.

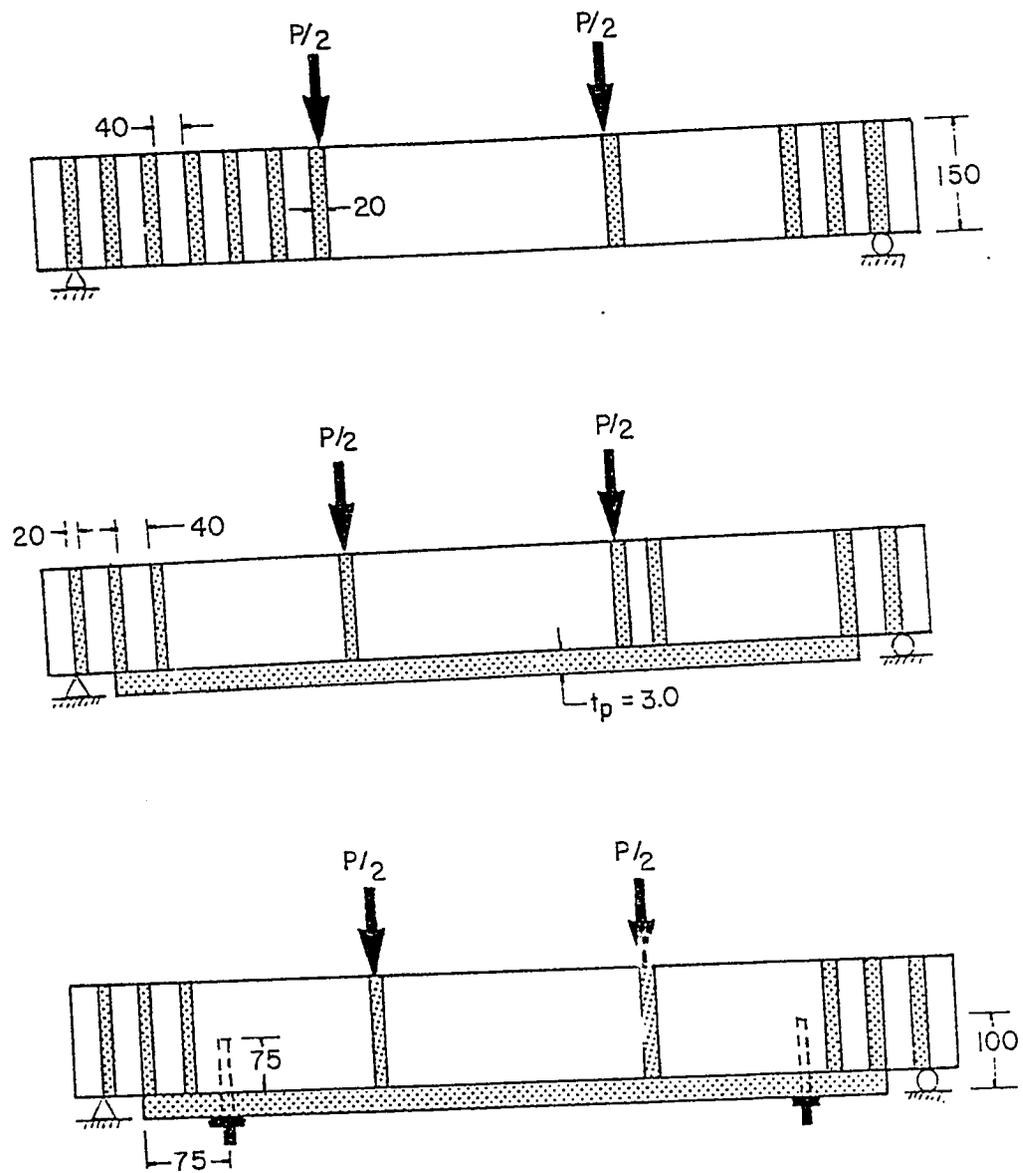


Fig. 3.19: Repair Sequence of Shear Beams Using Strips.

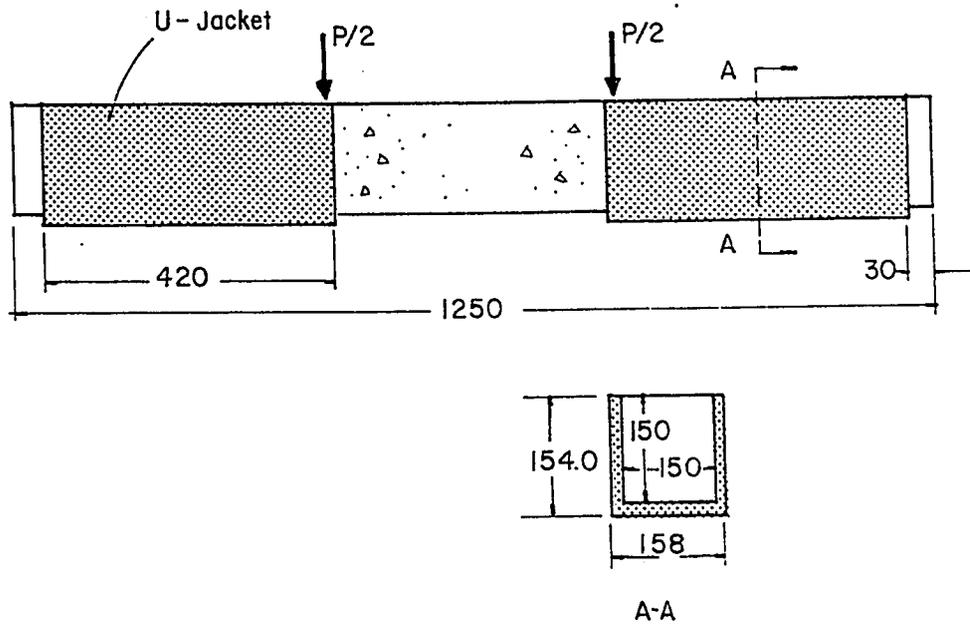


Fig. 3.20: Shear Beams Repaired Using U-Jacket.

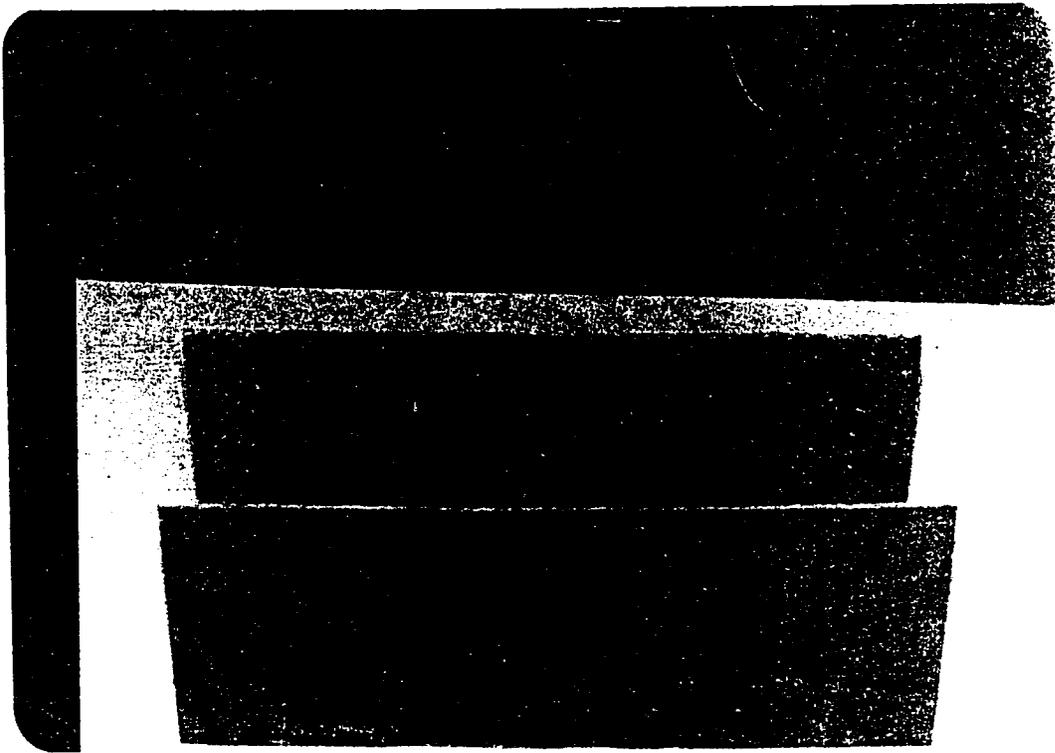


Plate 3.19: The U-Shaped Fiber Glass Jacket Used to Repair Beam (SJ).

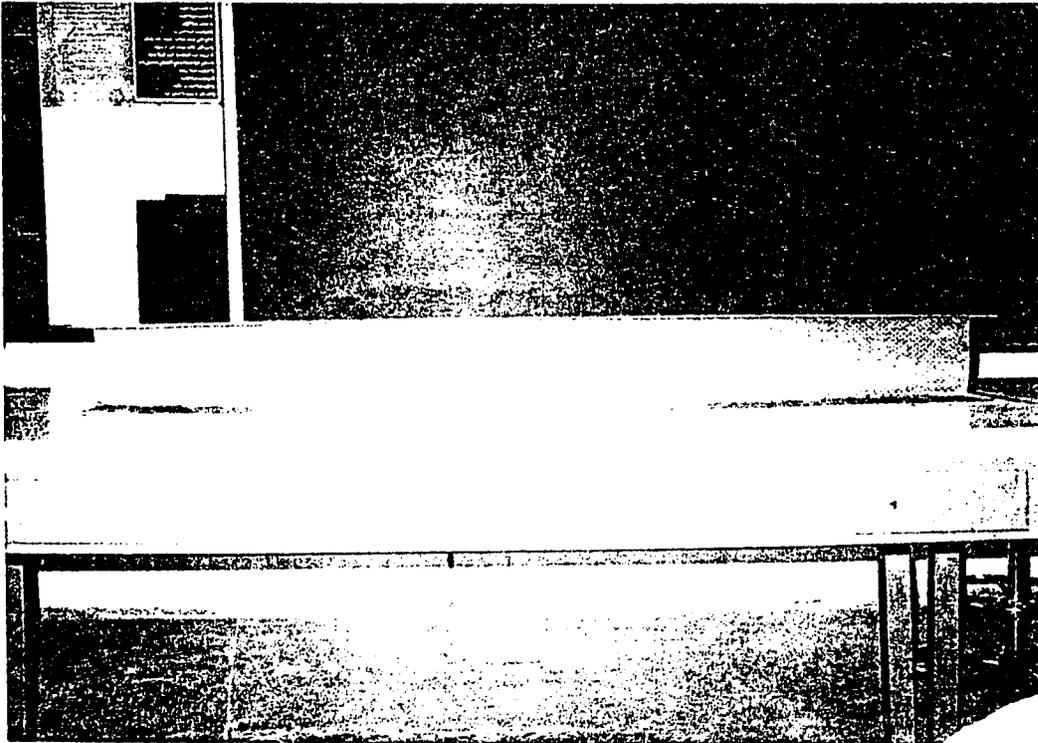


Plate 3.20: Acomplete U-Channel Fiber Glass Before Cutting
it to 420 mm U-Jackets.

weight of the beam was utilized as a constant pressure to hold the bottom surface of the jacket in place. The steps of repair are shown in Plates 3.21 through 3.24. Table 3.4 lists the repaired shear beams.

All repaired beams were loaded to failure. The testing procedures followed were identical to those discussed earlier in the preloading stage.

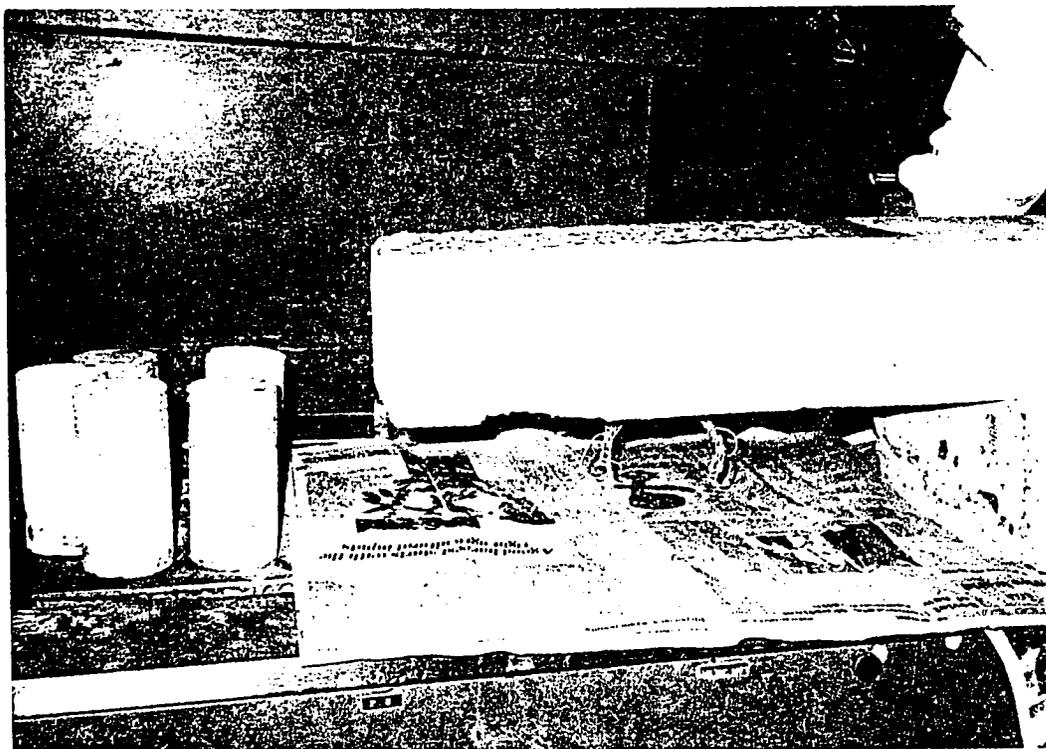


Plate 3.21: Application of the Epoxy to the Beam Surface
Using Painting Brush.

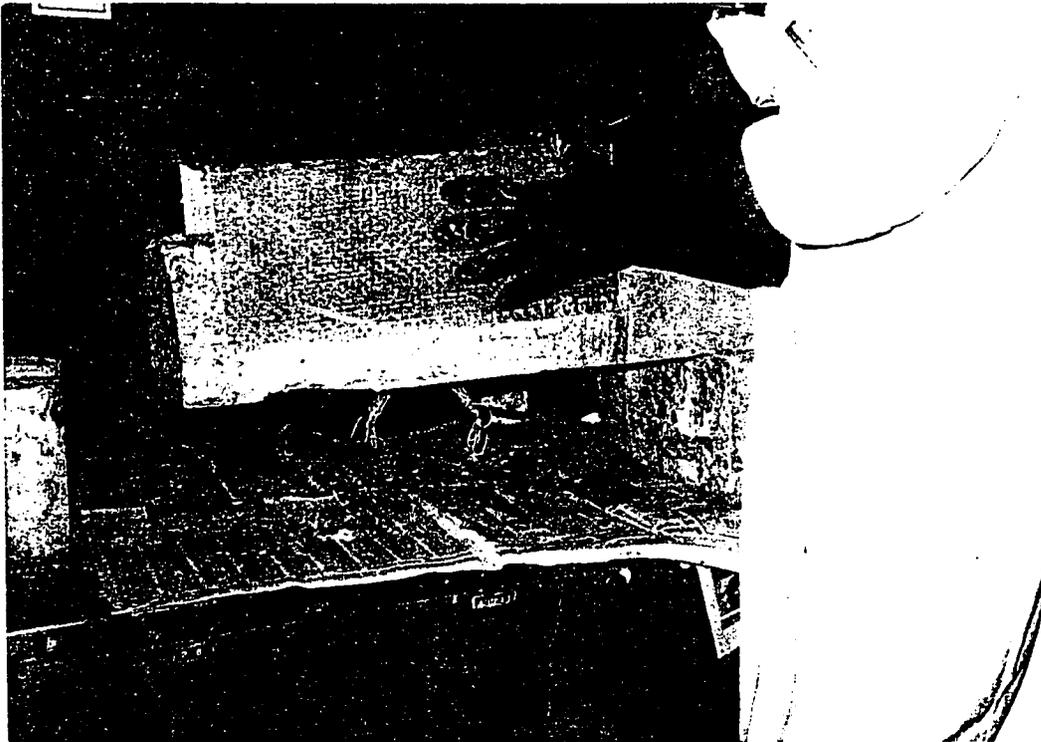


Plate 3.22: Encasement of the Shear Span of the Beam With
The U-Jacket.

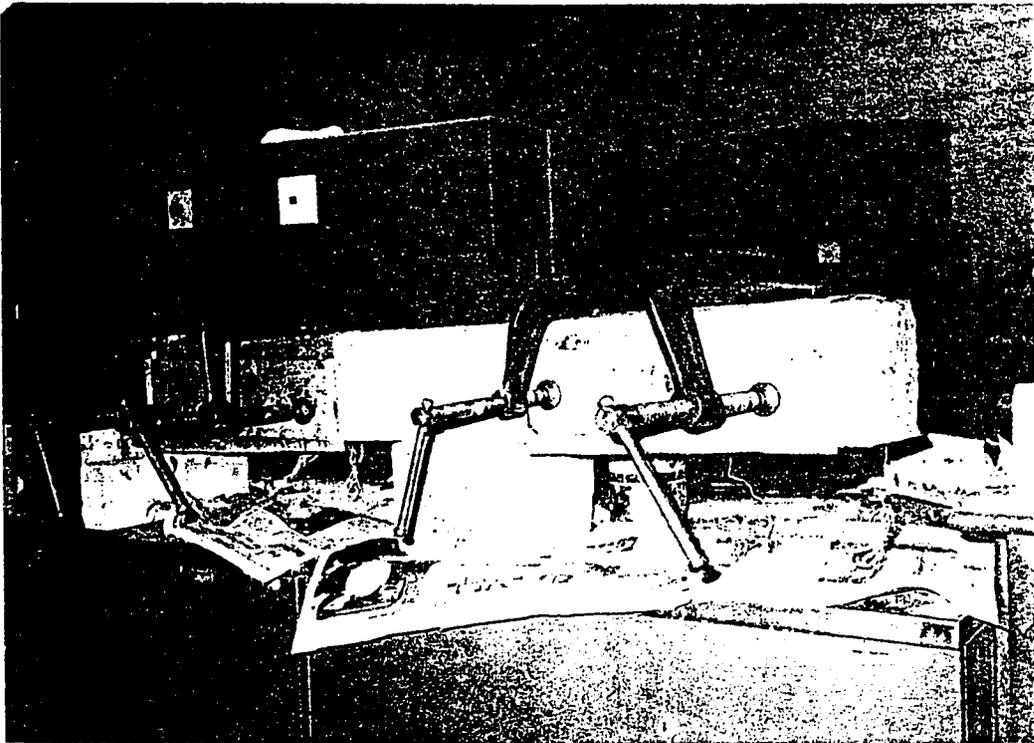


Plate 3.23: Holding the U-Jacket From Sides Using Two Pieces of Wood and C-Clamps.

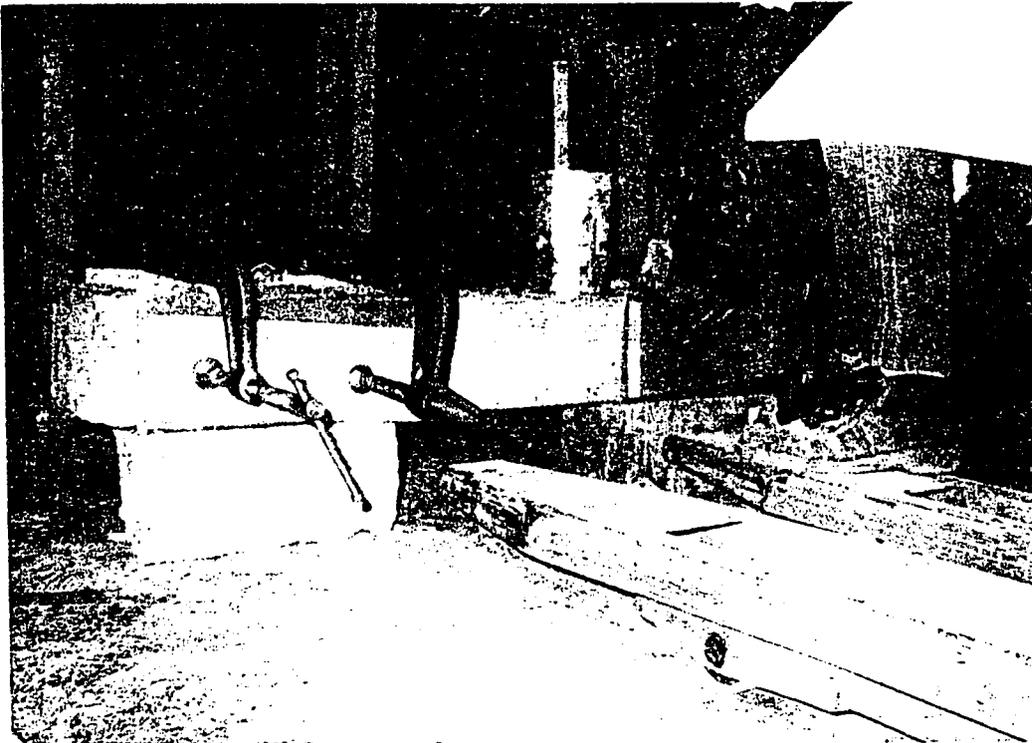


Plate 3.24: Resting the Beam on Concrete Blocks to Provide a Uniform Pressure on the Jacket Surface Utilizing the Self Weight of the Beam.

Table 3.4: Shear Repaired Beams

Beam #	No. of Specimens	Modes of Repair	Illustration IN
SW	3	Wings only	Fig. 3.18
SWP	3	Wings Bottom Plate	Fig. 3.18
SWPB	3	Wings +Anchored Bottom Plate	Fig. 3.18
SS	3	Strips only	Fig. 3.19
SSP	3	Strips +Bottom Plate	Fig. 3.19
SSPB	3	Strips +Anchored Bottom Plate	Fig. 3.19
SJ	2	U-Jacket	Fig. 3.20

Chapter 4

THEORETICAL CALCULATIONS

4.1 GENERAL

When existing damaged beams are repaired with external fiber glass plates either in flexure or in shear, their ultimate capacities will increase due to the additional external reinforcement applied. General expressions should be developed for calculating both the ultimate flexural and shear capacities.

4.2 ULTIMATE FLEXURAL CAPACITY

Assumptions:

- Full composite action (no slip)
- Concrete strength (ϵ_c) = 0.003 at ultimate

Steps:

- 1) Assume a fiber glass strain (ϵ_p) $\leq \epsilon_{up}$
- 2) Calculate the neutral axis (X) from the strain compatibility diagram (Fig. 4.1).

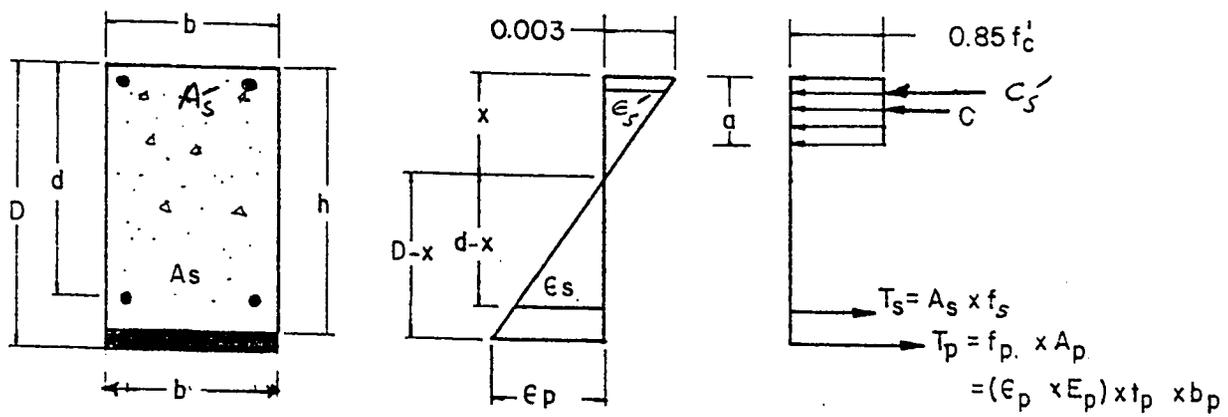


Fig.4.1: Strain Compatibility Diagram

$$\frac{0.003}{X} = \frac{\epsilon_p}{D - X}$$

$$X = \left(\frac{D - X}{\epsilon_p} \right) * 0.003$$

- 3) Calculate the strains in the tension steel and the compression steel (if it exists) as follows:

$$\frac{\epsilon_s}{(d - X)} = \frac{0.003}{X}$$

$$\epsilon_s = \frac{(d - X)}{X} * 0.003$$

$$\frac{\epsilon_s'}{X - d'} = \frac{0.003}{X}$$

$$\epsilon_s' = \left(\frac{X - d'}{X} \right) * 0.003$$

- 4) From the stress-strain curves for the steel and the fiber glass the following quantities are determined:

- The corresponding stress in the fiber glass plate (f_p)
- The corresponding stress in the tension steel (f_s)
- The corresponding stress in the compression steel (f_s')

- 5) From the equilibrium ($\Sigma H = 0$),

Calculate compression and tension forces as follows:

$$C = C_s' + C_c$$

$$T = T_s + T_p$$

or

$$C = 0.85 * f_c' * a * b + \epsilon_s' * f_s'$$

where,

$$a = \beta_1 * X$$

$$T = \epsilon_s * f_s + \epsilon_p * A_p$$

a) If $C = T$

6) Calculate the ultimate flexural capacity (M_u) from the following expression:

$$M_u = A_s * f_s * \left(d - \frac{\beta_1 * X}{2} \right) + A_s' * f_s' * \left(d' - \frac{\beta_1 * X}{2} \right) + A_p * f_p * \left(D - \frac{\beta_1 * X}{2} \right) \quad (1)$$

b) If $C \neq T$

adjust the value of ϵ_p and go back to step No. 2

Calculations of the ultimate flexural capacity are presented in Appendix (A).

4.3 ULTIMATE SHEAR CAPACITY

The ultimate shear capacity after repair can be generalized in the following form:

$$V_R = V_c + V_s + V_p$$

where,

V_R = the ultimate shear capacity after repair

V_c = the ultimate shear capacity carried by concrete

V_s = the ultimate shear capacity carried by stirrups

V_p = the ultimate shear capacity carried by fiber glass

$$V_c = \frac{1}{6} * \sqrt{f'_c} * b * d$$

$$V_s = \frac{A_v * f_y * d}{S}$$

Two different types of external web reinforcement will be discussed here, namely;

1) Strips

When the failure ultimately occurs, two different types of failure may be encountered, i.e. either rupturing or ripping off the strips from the concrete surface. Thus the ultimate shear capacity can be generalized as follows:

- a) When the failure occurs due to rupturing of the strips

$$V_p = \frac{2A_{vp} f_p d}{S_p}$$

$$= 2t b_{strip} f_p \frac{d}{S_p} \quad (a)$$

- b) When the failure is controlled by ripping off the strips

$$V_p = 2b d \tau \frac{d}{S_p}$$

$$V_p = 2A_{vp} \tau N \quad (b)$$

The smallest value from equation (a) or (b) should be selected to find the ultimate shear capacity from the following equation,

$$V_R = V_c + V_s + V_p$$

$$V = \frac{1}{6} * \sqrt{f_c'} * b * d + \frac{2 * A_v s * f_y * d}{S} + V_p \quad (2)$$

2) Wings

In case when the repair is to be carried out by wings the following two conditions should be checked:

a) Rupturing of the Wing

$$V_p = 2 * A_p * f_p$$

$$V_p = 2 * t * d * f_p$$

b) Ripping off the Wing

$$V_p = 2 * \{ \tau * d * d \}$$

$$V_p = 2 * \tau * d^2$$

The smallest value of V_p should be selected either from (a) or (b) and applied in Eq. No. (2)

The ultimate theoretical capacities for shear beams repaired either with wings or strips are shown in Appendix (A).

Chapter 5

RESULTS AND DISCUSSION

INTRODUCTION

The test results of this investigation are presented in Fig. 5.1 through 5.61 and Tables 5.1 through 5.13. The laboratory generated data fall in the following categories:

- Selection of the repair material
- Effect of thermal cycling on bond strength
- Flexural damaged repair
- Shear damaged repair

5.1 SELECTION OF THE REPAIR MATERIAL

The results as shown in Fig. 5.1 indicate that fiber glass type (I) and type (II) when subjected to tensile loads are behaving elastically up to the ultimate load. The first sign of damage under tensile loading is debonding of transverse fiber from the resin. At high loading the resin cracks which in turn cause debonding of longitudinal. As the resin cracks spread, the load is transferred to the fibers which eventually fracture or pull-out at

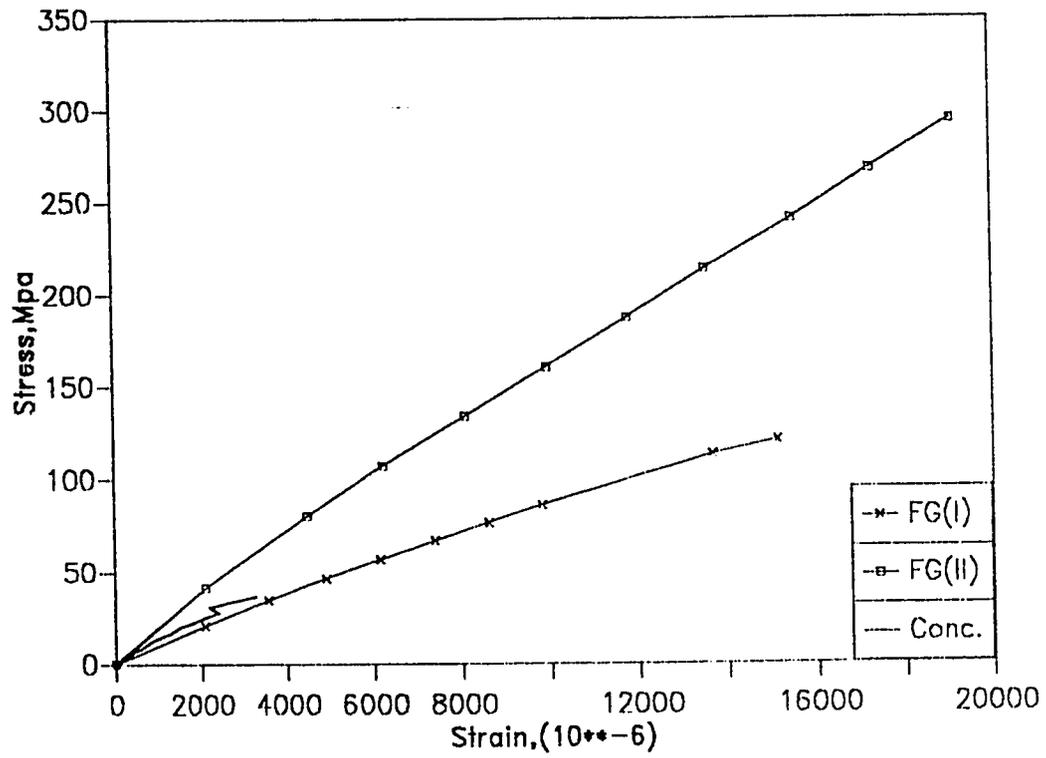


Fig. 5.1 Stress-Strain curves for Fiber Glass types and concrete

ultimate failure. Fiber glass Type (II) has higher modulus of elasticity (E_p) and strength than Type I. The ultimate strength and modulus of elasticity of type (II) is higher than that of type (I) by about 54%. Based on these results fiber glass type (II) was selected as the repair material to be used throughout this research. Fig. 5.2 shows the stress-strain diagram for both types of fiber glass relative to the steel reinforcement which indicates lower strength and modulus of elasticity.

The basic properties of concrete are given in Table 5.1.

5.2 EFFECT OF THERMAL CYCLING ON BOND STRENGTH

The results of the pull-out test for twelve prisms tested under axial tension are presented in Table 5.2 and Fig. 5.3. The results shown in Fig. 5.3 indicate a slight reduction in the bond strength during the first 60 cycles of heating and cooling. However, the bond strength is significantly reduced at 90 and 120 thermal cycles. A reduction of about 30% in the bond strength occurs at 120 thermal cycles. This reduction in the bond strength is due to the degradation of the epoxy layer between the fiber glass and concrete. Such degradation is attributed to the difference in the coefficients of thermal expansion of three different materials which result in different expansion and contraction. As a result of this repeated action the bond between the fiber glass

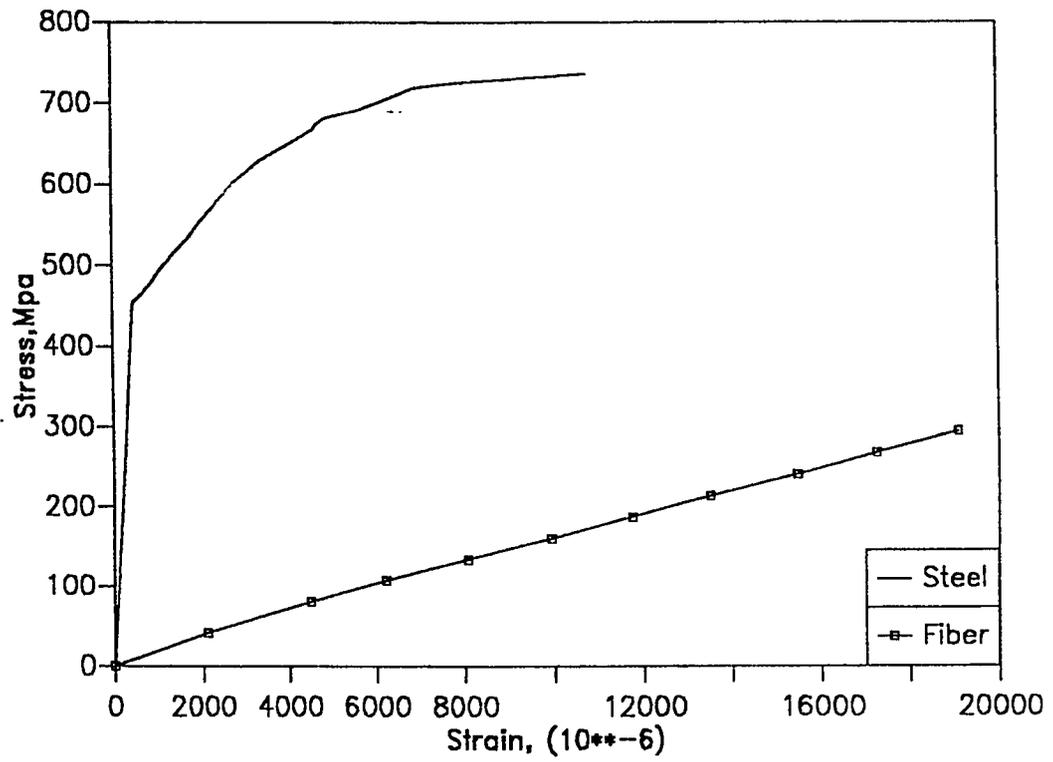


Fig. 5.2 Stress- Strain curves for Steel and Fiber Glass

Table 5.1: Basic Properties of Concrete

Compressive strength (f_c') MPa	37.7
Modulus of rupture (f_r) MPa	3.81
Modulus of elasticity (E_c) MPa	29042
Concrete slump (mm)	10

Table 5.2: Effect of Thermal Cycling on Bond Strength

Group	Sample #	No. of Thermal Cycles	Load (kN)	Bonded area mm ² (N/mm ²)	Bond Strength (N/mm ²)	% Reduction in Bond Strength
1	B1 B2 B3	60	15.3 15.5 14.8	3750	4.08 4.13 3.95	
	Av.		15.2		4.05	7.3
2	C1 C2 C3	90	12.1 11.9 12.0	3750	3.23 3.17 3.2	
	Av.		12.0		3.2	26.8
3	D1 D2 D3	120	11.1 11.5 11.3	3750	2.96 3.07 3.01	
	Av.		11.3		3.01	31.1
4	A1 A2 A3	0	16.2 16.3 16.7	3750	4.34 4.35 4.45	
	Av.		16.2		4.37	---

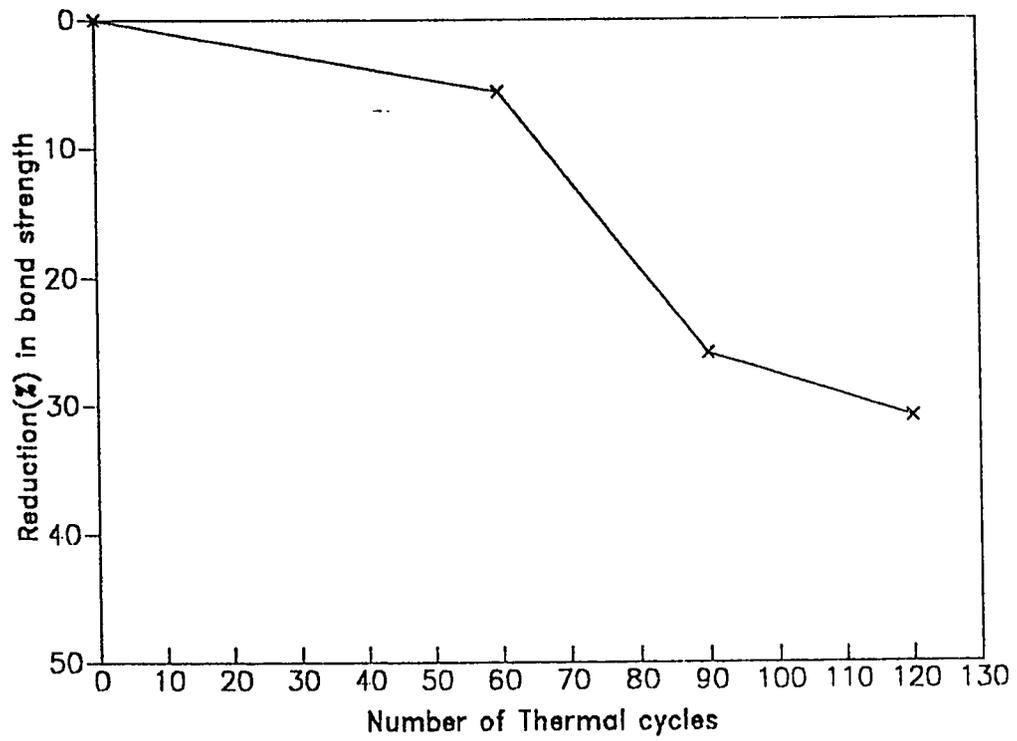


Fig. 5.3 Reduction(%) in bond strength vs. Number of thermal cycles

plates and the epoxy layer became weaker as the number of thermal cycles increased. In all control specimens failure occurred by ripping off a piece of concrete from the specimen surface (Plate 5.1). Group (1) specimens failed in the glue/concrete interface with small pieces of concrete ripped off with the glue layer (Plate 5.2). Failures in Group (2) and Group (3) specimens were in the glue/plate interface and more specifically by the plate separation from the glue layer (Plate 5.3). This clearly indicates that the bond strength between the fiber glass plate and the glue was very high and much greater than that between the glue and the concrete. After 60 thermal cycles the glue became weak and the bond dropped significantly resulting in the separation of the plate from the glue layer.

5.3 FLEXURAL DAMAGED REPAIR

The test results for flexural damaged are shown in Figs. 5.4 through 5.47 and Table 5.3 through 5.9.

5.3.1 Modes of Failure

1) 3mm Plate (Series I):

All beams repaired with 3 mm plate whether anchored or unanchored, showed similar behavior upto failure.

For beam FP3, flexural cracks appeared at 20 kN in the

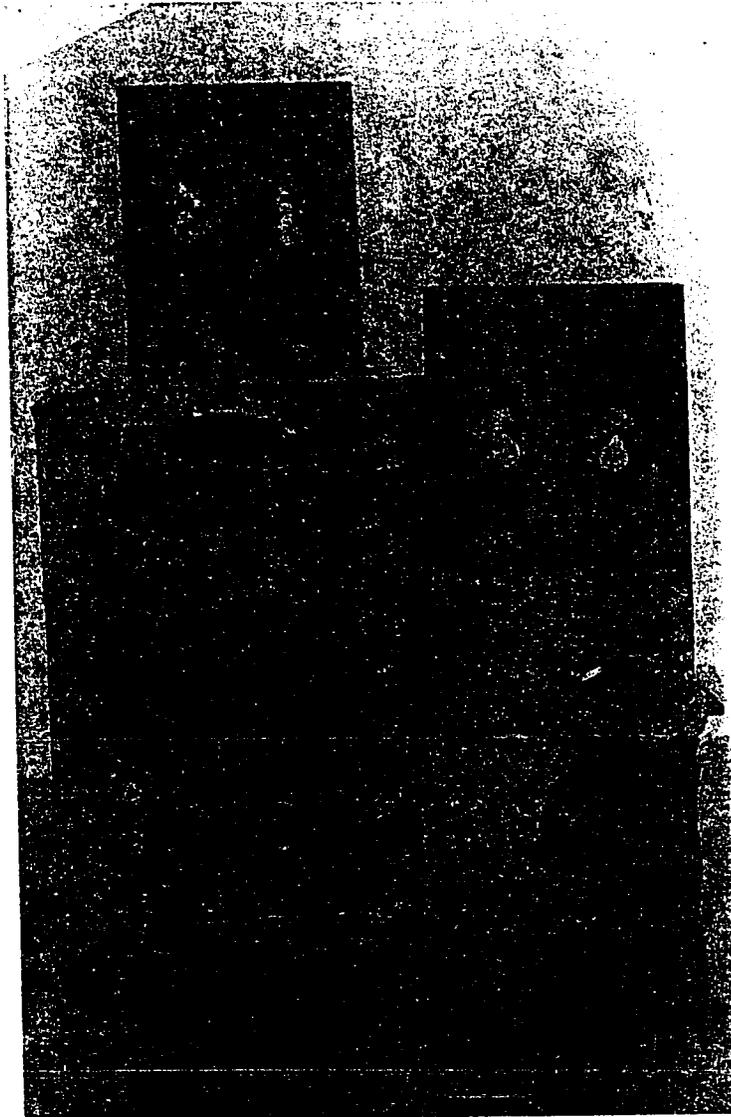


Plate 5.1: Failure Mode of Control Specimen (Ripping off the Concret.)

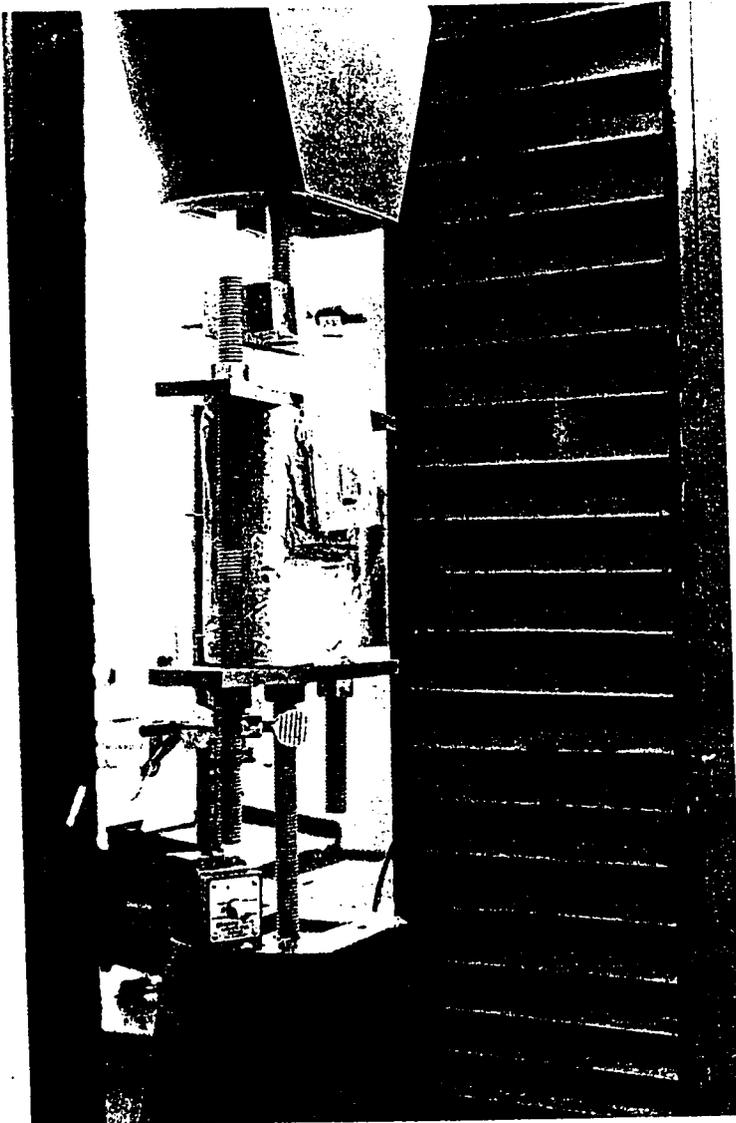


Plate 5.2: Failure Mode of Group (1) Specimens After 30 Thermal Cycles (Failure was in the Glue/Concrete Interface)

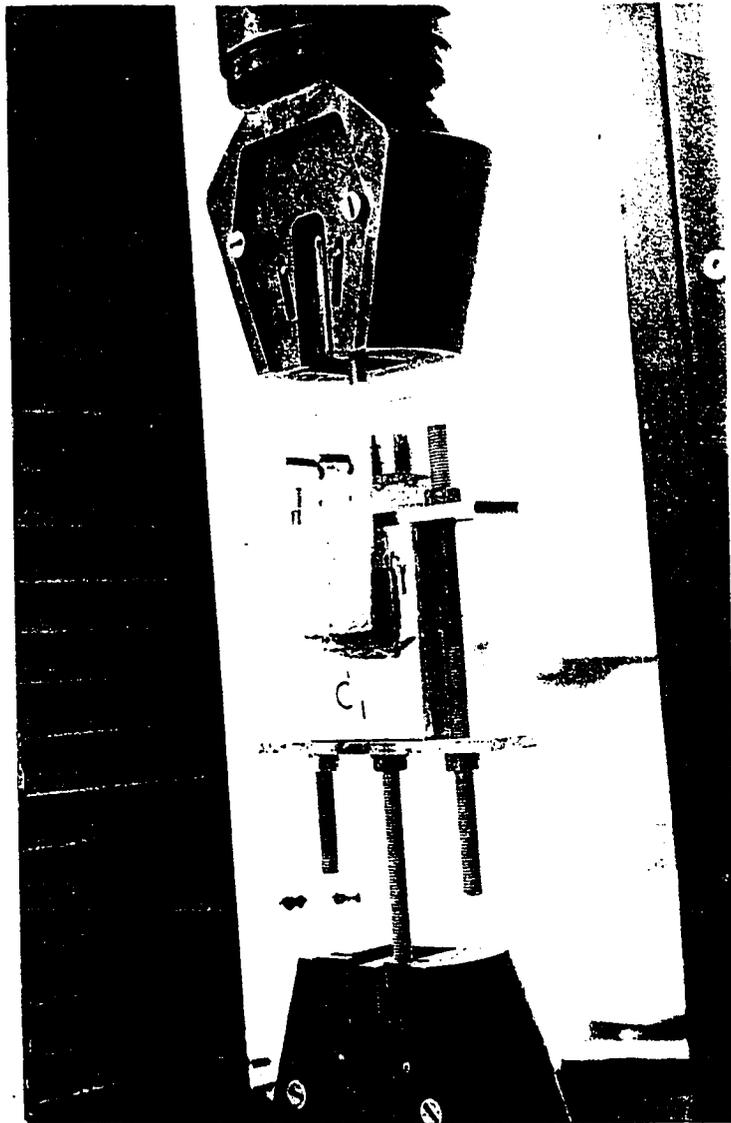


Plate 5.3: Failure Mode of Group (2) and Group (3) Specimens
(Failure in the Glue / Plate Interface).

shear span and more specifically near the plate curtailment. The original flexural cracks started to open at 30 kN load and they became wider and extended upward drastically as the load was increased. Finally the beam failed due to separation of the plate end along with tearing the concrete cover to the level of internal reinforcement at 66.1 kN load, Plate 5.4. This separation occurs because when the plate is terminated in the shear span, thus creating a critical section. The transfer of stresses from the plate to the bars in the region where the plate terminated results in a high gradients of stresses. Furthermore, the eccentricity between the tensile forces in the plate and the balancing bond forces in the epoxy layer results in normal forces which will tend to lift the plate (Fig. 5.4). The mechanism of this failure starts with the formation of a diagonal crack near the plate curtailment and once this takes place, the effect of the peeling force is magnified and the crack extends rapidly upwards. A large displacement of the concrete bounded by this crack and the plate then takes place in the direction of the peeling force. This relieves the bond stresses and peeling force at the end of the plate, moves the effective cut-off of the plate away from the support, and thus increases the distance between the plate cut-off and the support. Another diagonal crack is therefore produced immediately, since the conditions at the new cut-off are worse than before. This process is repeated rapidly along the length of the plate and results in a tearing effect in which shallow diagonal cracks are superimposed over any other



Fig. 5.4: System of Forces Acting on the Glue Interface Between the Plate and the Beam.

cracks and pieces of concrete are torn from the beam soffit, plate 5.4.

In beam FPB3 bolts were used to overcome the problem of the plate separation occurred in beam FP3. The behavior of this beam was similar to that of beam FP3 except that at 24 kN new vertical flexural cracks developed at the shear spans. At higher load level more vertical flexural cracks are formed in the shear span and propagated rapidly upward. A diagonal crack connects these flexural cracks, this crack became wider and opened up resulting in the failure of the beam at 71.7 Kn load, Plate 5.5. This failure is often encountered when the principal tensile stress exceeds the tensile strength of the concrete provided that the plate ends are anchored as it was the case in beam FPB3. The effective cut-off length between the support and the and the plate end is kept constant and the formation of any other diagonal crack is eliminated. Thus, the diagonal crack is keep on widening until the beam failed prematurely in a brittle manner, plate 5.5.

Wings were used to confine the shear span of beam FPBW3 and to eliminate the failure due to the diagonal tension crack developed in beam FPB3. Again this beam showed the same trend as beams FP3 and FPB3 during testing with a slight difference such as that the appearance of new cracks were detected at 28 kN load at the shear span ,Plate 5.6. The wings arrested the diagonal tension crack and the bolts prevented separation of the plate

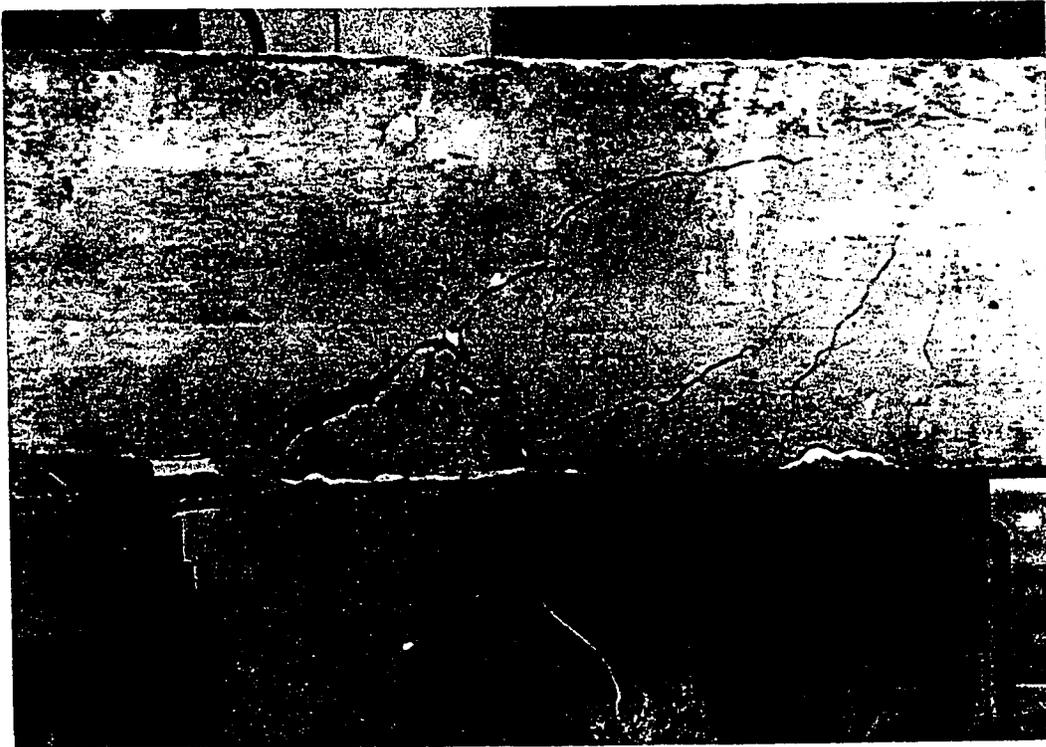


Plate 5.4: Failure Mode of Beam FP3 (Plate Separation With the Concrete Cover).

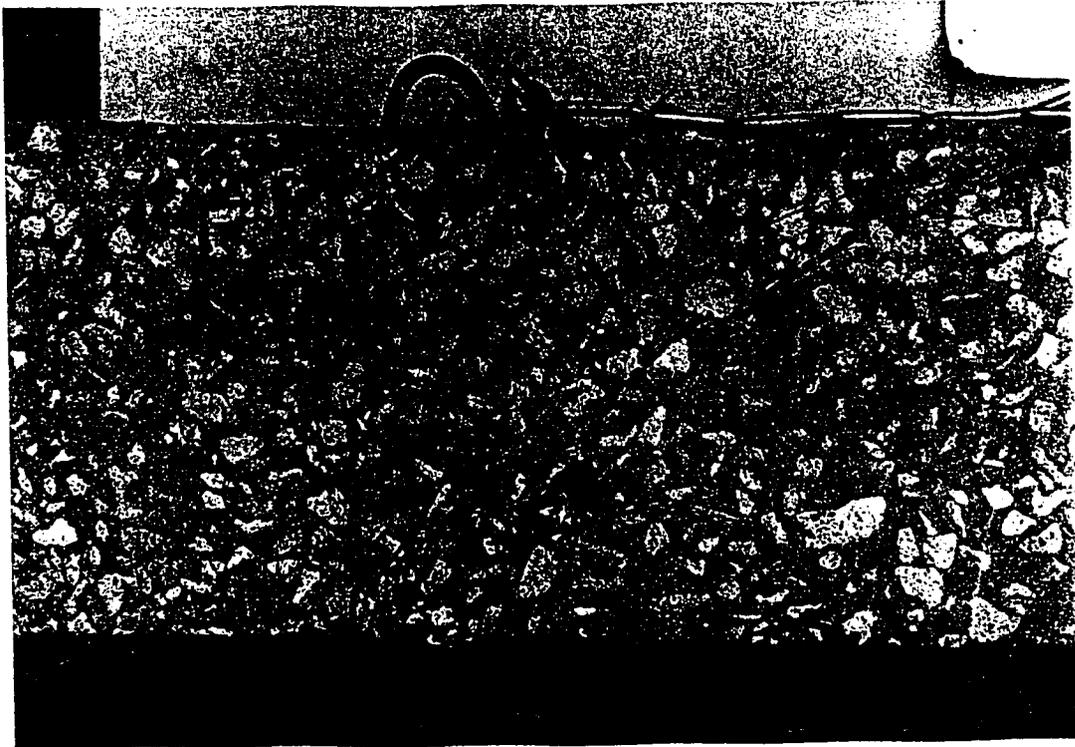


Plate 5.5: Failure Mode of Beam FPB3 (Diagonal Tension Crack and Debonding of the Plate).

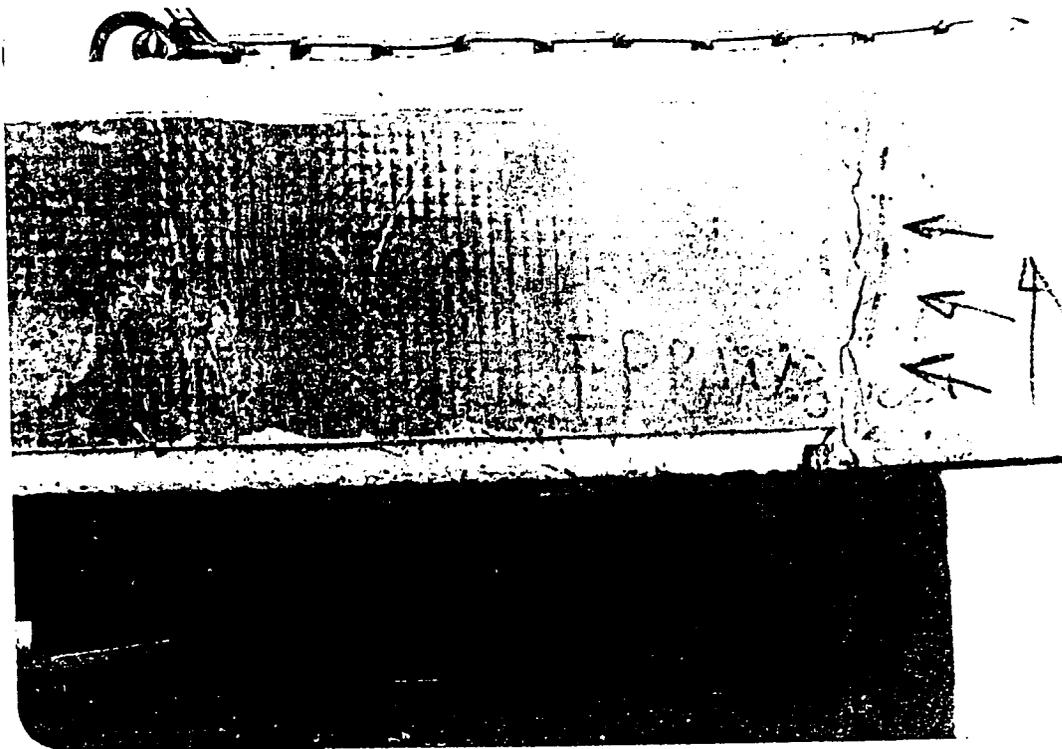


Plate 5.6: Failure Mode of Beam FPBW3 (Debonding of the Plate).

ends. However, at a load of 58 kN a crack appeared at the the lower edge of the wing and propagated horizontally up to the end of the wing and then extended upwards. The crack was observed closely and it became wider as the load is increased. At a load of 65 kN a similar crack appeared at the face of the other wing. These two cracks became wider until the beam failed at 71 kN load due to the debonding of the plate. The failure was in the glue/concrete interface.

Beam FJ showed a similar behavior like beam FP3, FPB3 and FPBW3. Old cracks started to grow at 20 kN load and new cracks started were detected at a load of 40 kN. The beam failed at 71 kN load due to rupturing of the plate at the face of the U-shaped portion and immediately followed by diagonal crack almost at the point where the plate is ruptured. The failure occurred because the strain in the plate reached its ultimate value due to the higher stresses concentration in the plate at the point of changing the plate cross sectional area, plate 5.7.

Beams of series (II) showed the same trend and they behaved during testing in a similar manner to those beams repaired with 3 mm plates.

Beam FP2 failed as the concrete cover with the plate separated along the steel reinforcement which immediately followed by crushing of concrete, Plate 5.8.

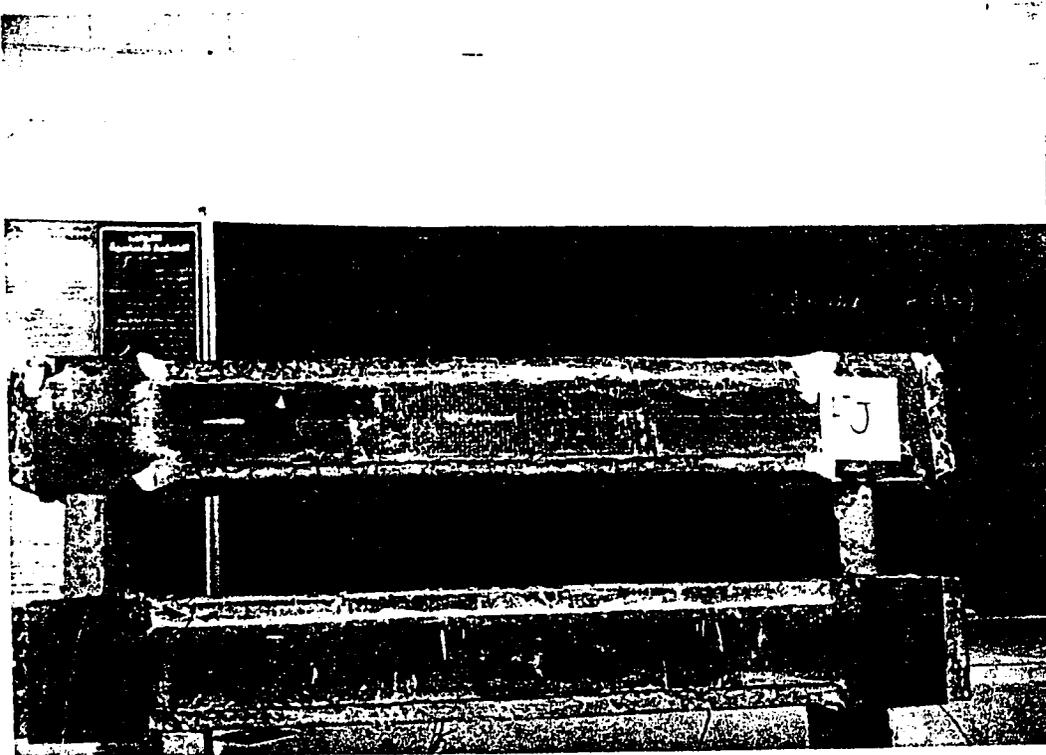


Plate 5.7: Failure Mode of Beam FJ (Rupturing of the Plate Followed by Diagonal Tension Crack at the point of Rupture).

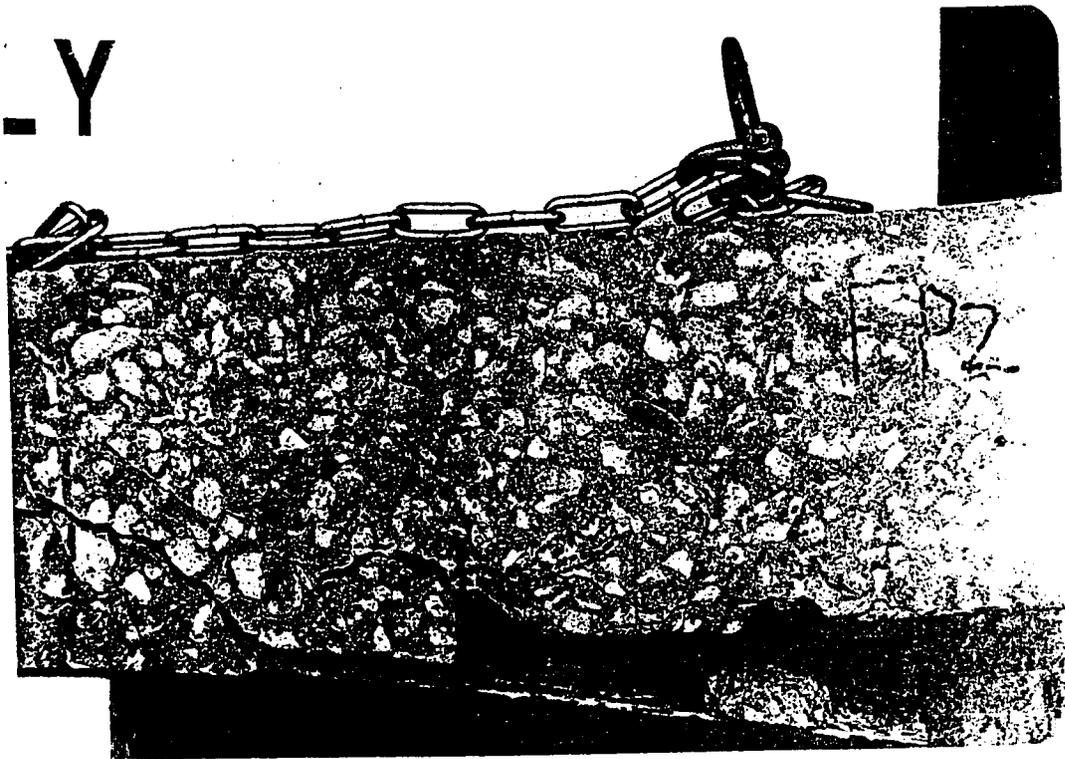


Plate 5.8: Failure Mode of Beam FP2 (Separation of the Plate and the Concrete cover Followed by crushing of Concrete).

Beam FPB2 failed due to extensive formation of flexural cracks (started at 24 kN) and connected by a diagonal crack at 62 kN load leading eventually to the failure of the beam and debonding of the plate, Plate 5.9.

The shear span of beam FPBW2 were effectively protected with wings against the occurrence of diagonal cracks and the plate was prevented from separation with the help of the bolts. Thus flexure failure was successfully obtained for beam FPBW2 by crushing of concrete in the constant moment region, plate 5.10.

3) *Imm Plate (Series III):*

Beam FP1 behaved in a similar manner as beam FP2 during testing. The only difference was that at ultimate load the flexural cracks were wider and the plate was ruptured at its centerline, Plate 5.11. The failure modes of flexure beams are listed in Table 5.3.

5.3.2 Ductility Measurements

Ductility is referred to the capacity or the capability of the member to undergo plastic (inelastic) deformation with out fracture. Ductility serves as warning of impending failures in reinforced concrete structures.

The load-deflection curves for beams of Series I, II and III are presented in Figs. 5.5 through 5.12 Each plot includes two

Table 5.3 : Theoretical Flexural Capacities and Ultimate Loads Carried for Flexural Beams

Beam #	Ultimate Experimental Load (KN)	Ultimate Theoretical Load (KN)	Failure Modes
FC	40.64	41.0	Yielding of the steel
FP3	66.1	91.8	Separation of the plate and the concrete cover
FPB3	71.7	91.8	Diagonal Tension crack at the plate cut-off
FPBW3	71.0	91.8	Debonding of the plate
FP2	64	80.8	Separation of the plate and concrete cover
FPB2	67	80.8	Diagonal Tension crack
FPBW2	78.5	80.8	Crushing of the concrete
FP1	62.4	59.0	Rupturing of the plate (1 mm)
FJ	71.0	91.8	Rupturing of the plate (3 mm)

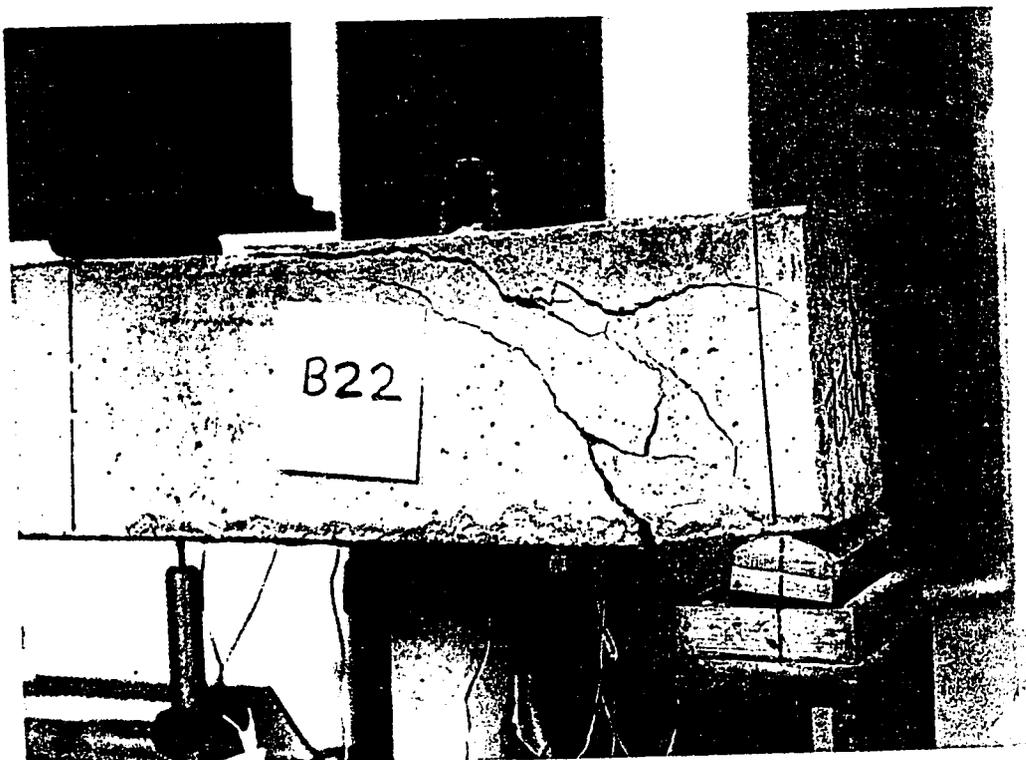


Plate 5.9: Failure Mode of Beam FPB2 (Diagonal Tension Crack Followed by Debonding of the Plate).

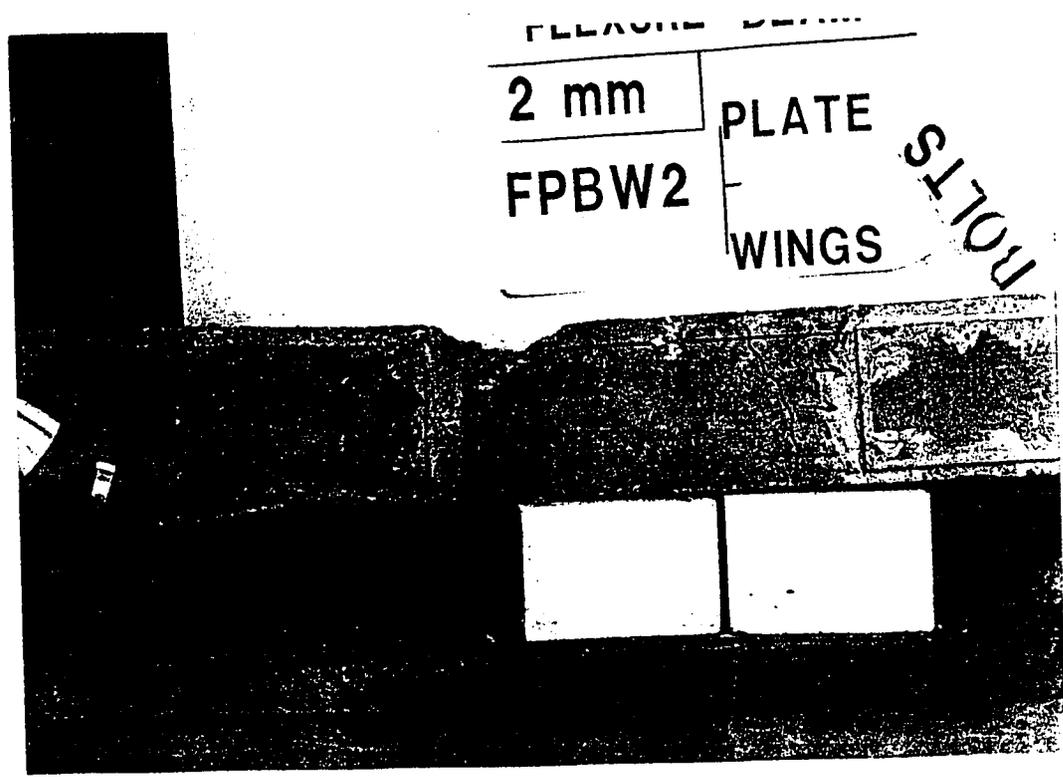


Plate 5.10: Failure Mode of Beam FPBW2 (Crushing of Concrete).

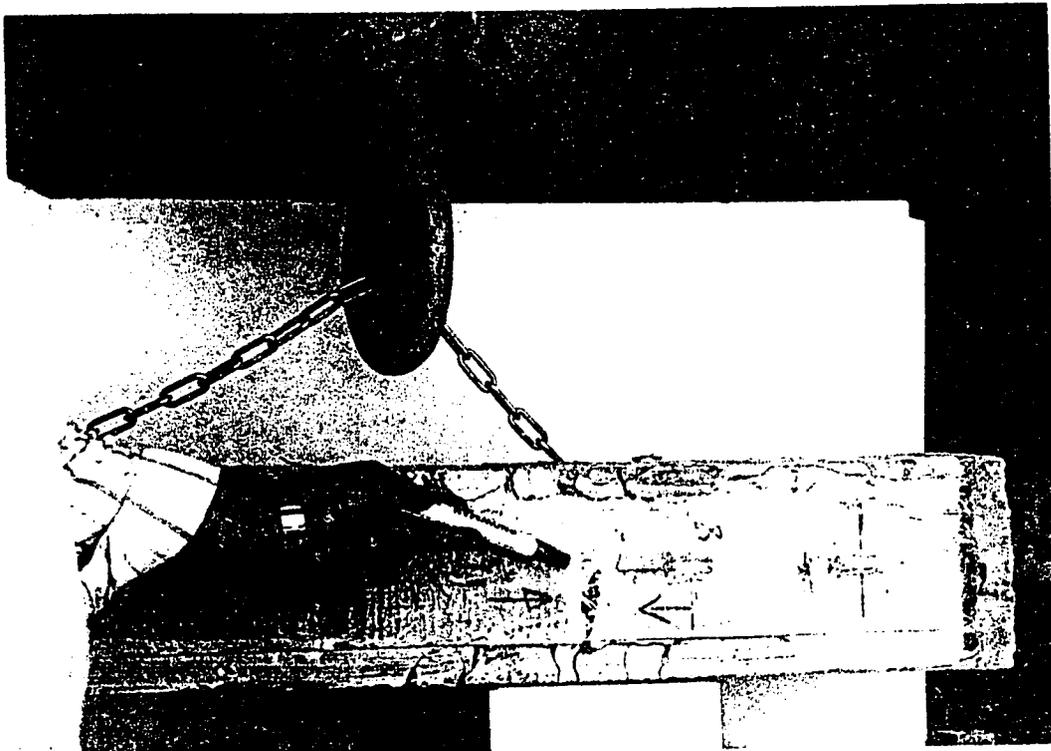


Plate 5.11: Failure Mode of Beam FP1 (Rupturing of the Plate Followed by Crushing of Concrete).

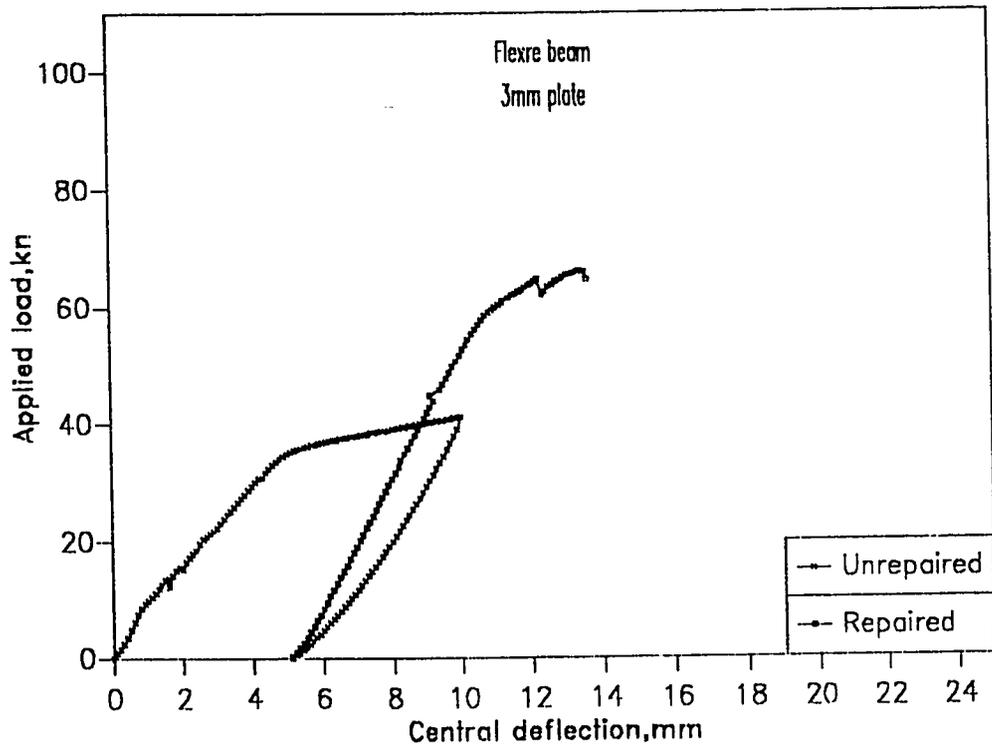


Fig. 5.5 Load vs. Central deflection (plate only)

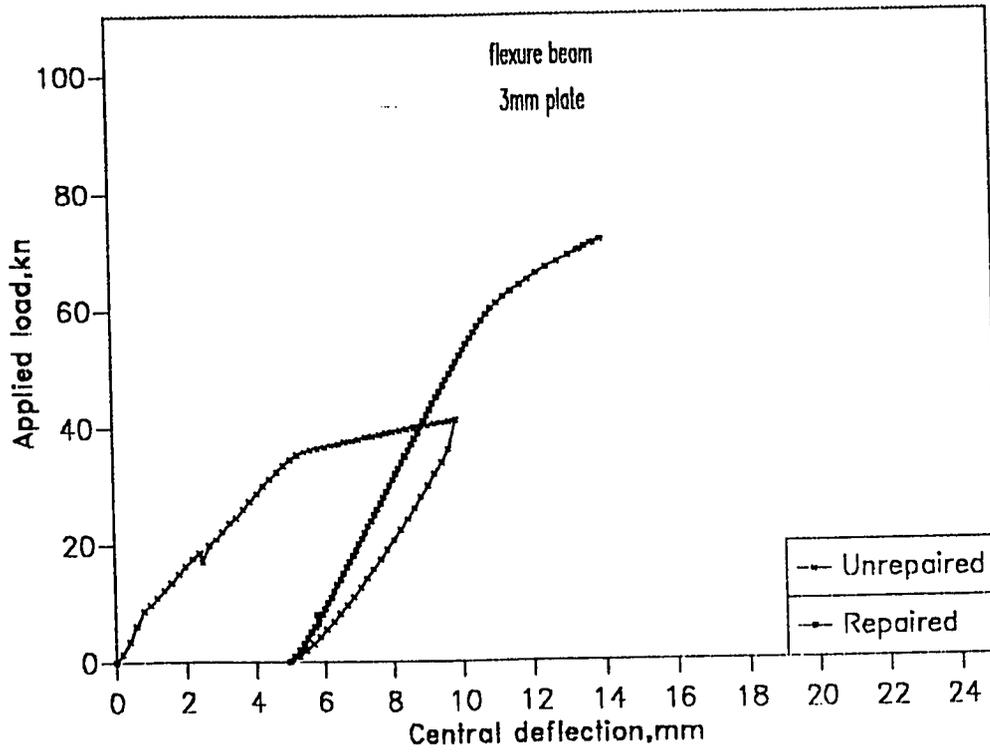


Fig. 5.6 Load vs. Central deflection (Plate + bolts)

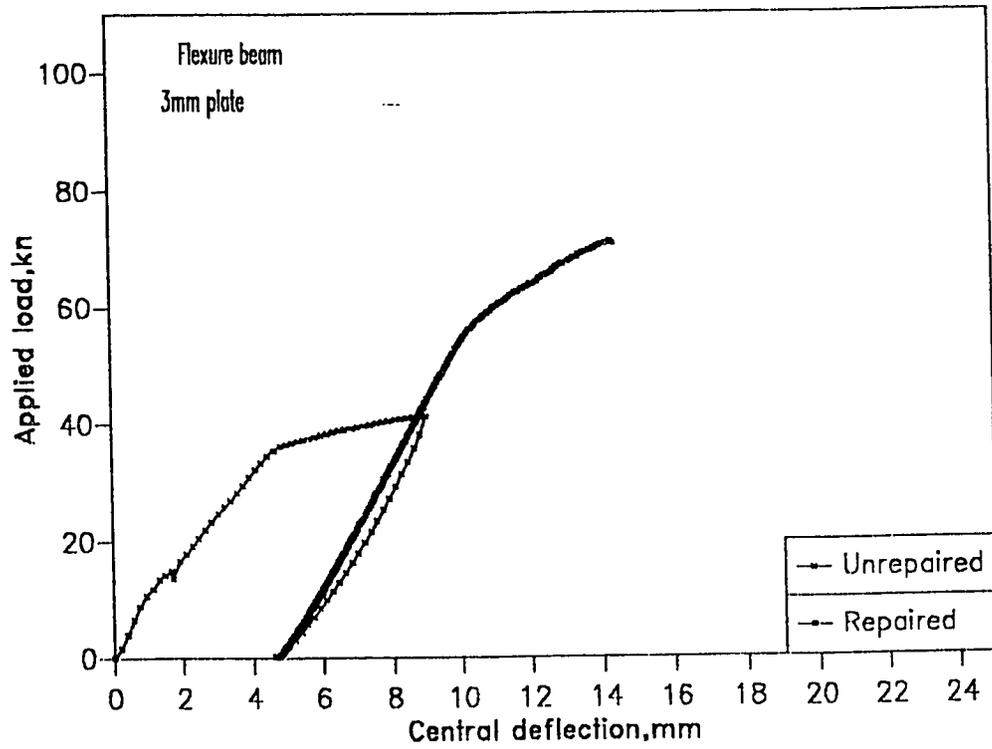


Fig. 5.7 Load vs. Central deflection (Anchored plate + wings)

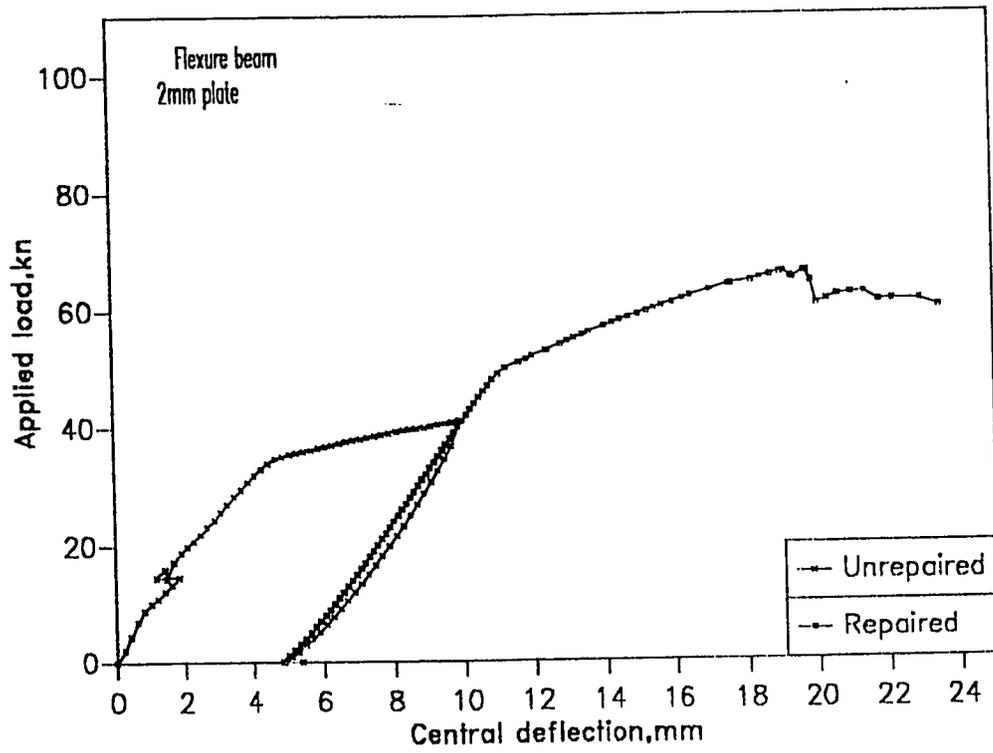


Fig. 5.8 Load vs. Central deflection (plate only)

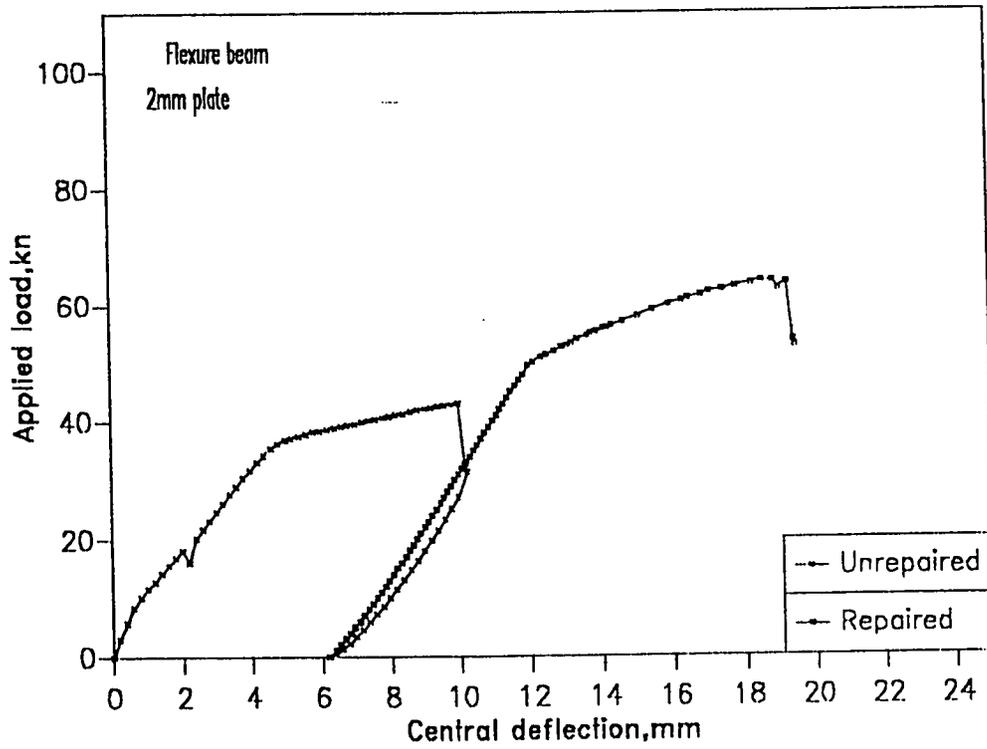


Fig. 5.9 Load vs. Central deflection (plate + anchor bolts)

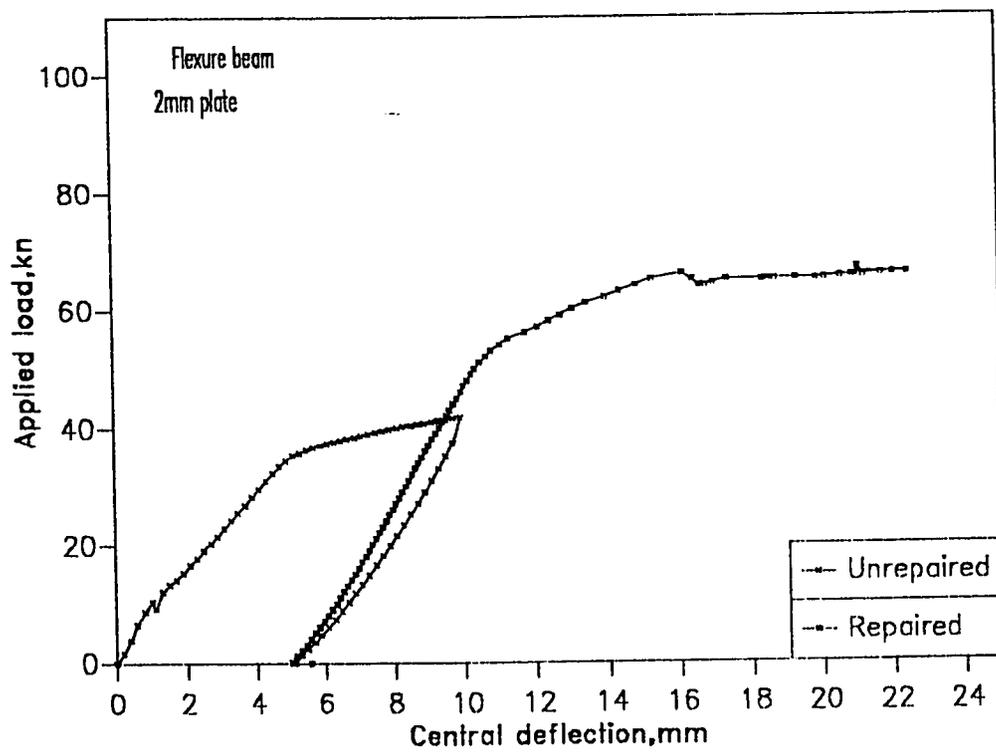


Fig. 5.10 Load vs. Central deflection (anchored plate + wings)

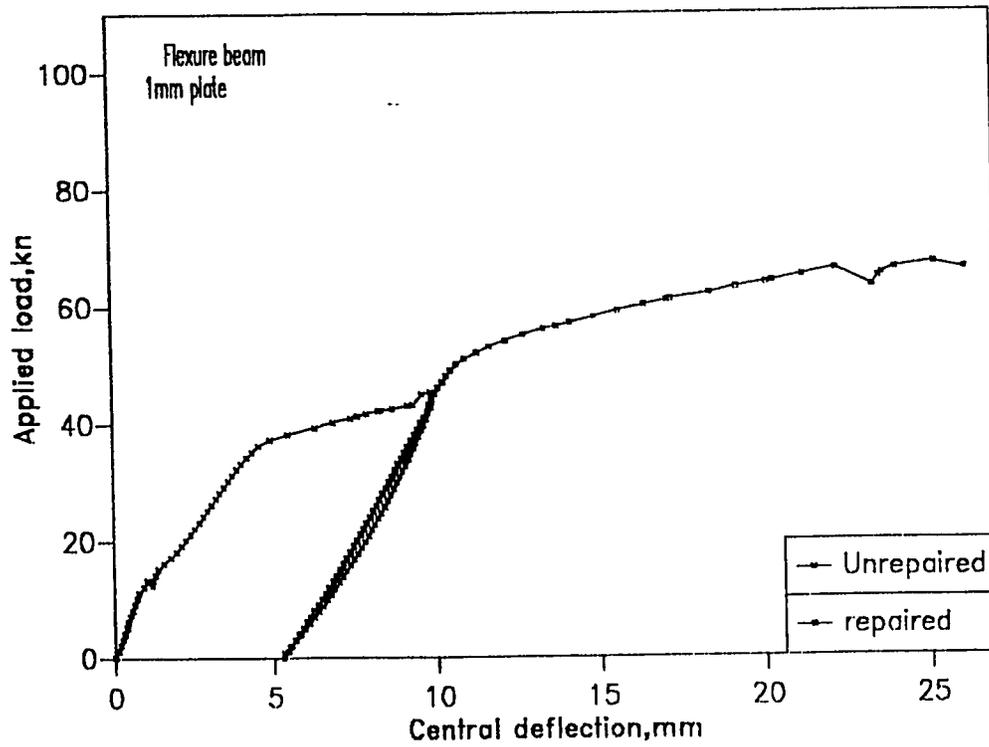


Fig. 5.11 Load vs. Central deflection (plate only)

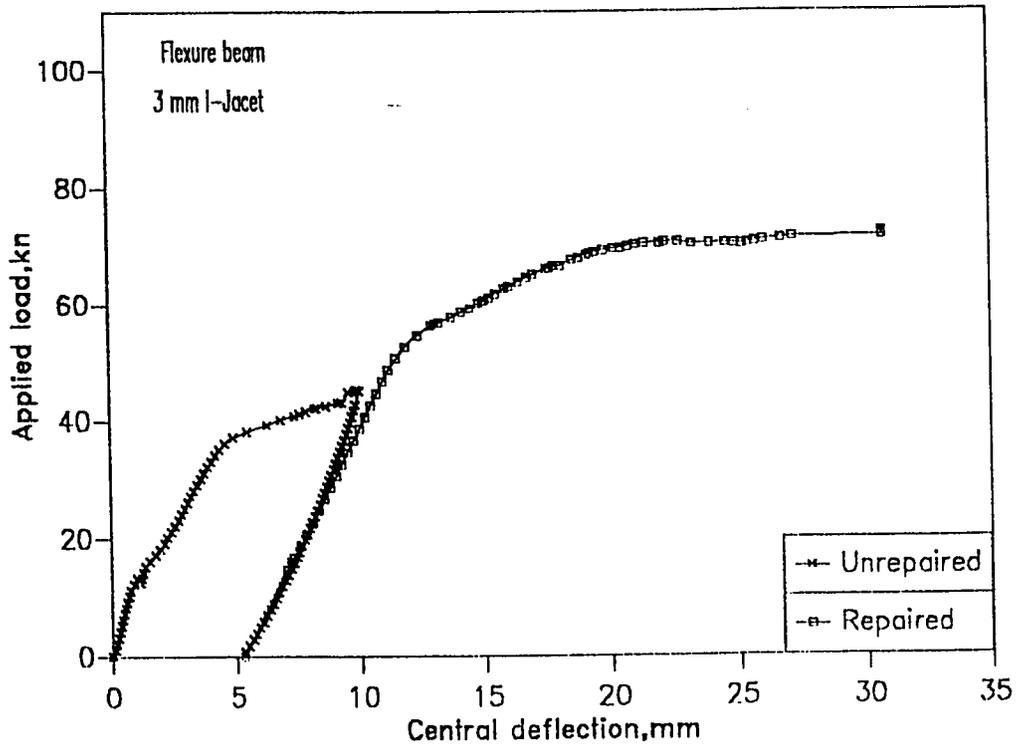


Fig. 5.12 Load vs. Central deflection (I-Jacket)

curves representing the beam specimen before and after repair. The ductility of unrepaired and repaired beams is calculated as the area under the P- Δ curves using an electronic planimeter. Initial stiffnesses K_i (kN/mm) are calculated before and after repair as the slopes of the linear part of the P- Δ curves. The detailed results are shown in Table 5.4. The ductility ratio (D.R. %) was calculated as the ductility of the repaired beam to the ductility of the controlled one, whereas the strength ratio (S.R. %) was calculated as the average ultimate load of repaired to the ultimate load of the controlled beam. Table 5.5 lists the values of both ductility and strength ratios for all flexure beams.

For beams of both Series I and Series II, beams which are strengthened with wings to confine their shear spans showed higher ductility ratio than anchored and unanchored beams, respectively. Figs. 5.13 to 5.15 show the ductility ratio vs. the plate thickness for unanchored, anchored and beams strengthened with wings in their shear span, respectively.

Fig. 5.13 clearly indicates that as the plate thickness increases the ductility ratio decreases. The behavior of anchored beams and beams strengthened with wings are shown in Figs. 5.14 and 5.15, respectively. The results confirm that ductility ratio decreases with increasing the plate thickness except for beam FJ repaired with 3mm I-jacket which showed the highest ductility

Table 5.4: Comparison of Control & Repaired Flexural Beams

Item	P_{cr} (kN)	K_i (kN/mm)		P_y (kN)		Δ_{ult}	Ductility Kn-mm	
		Control	Rep.	Control	Rep.		Control	Rep.
FP3	14.0	7.51	9.71	34.55	56.36	8.72	3381	4388
FPB3	17.3	8.75	10.00	35.00	60.0	12.30	1877	2657
FPBW3	15.2	7.74	10.00	36.00	56.00	9.7	2818	4510
FP2	13.6	9.6	15.65	36.00	54.00	18.6	1850	5723
FPB2	17.6	9.65	11.56	35.91	49.50	12.8	2900	5142
FPBW2	14.3	9.18	17.66	35.00	54.7	18.00	3542	5880
FP1	13.4	7.84	9.2	36.30	51.16	20.8	1867	6306
FC	16.4	5.90	-----	31.25	-----	-----	3970	-----

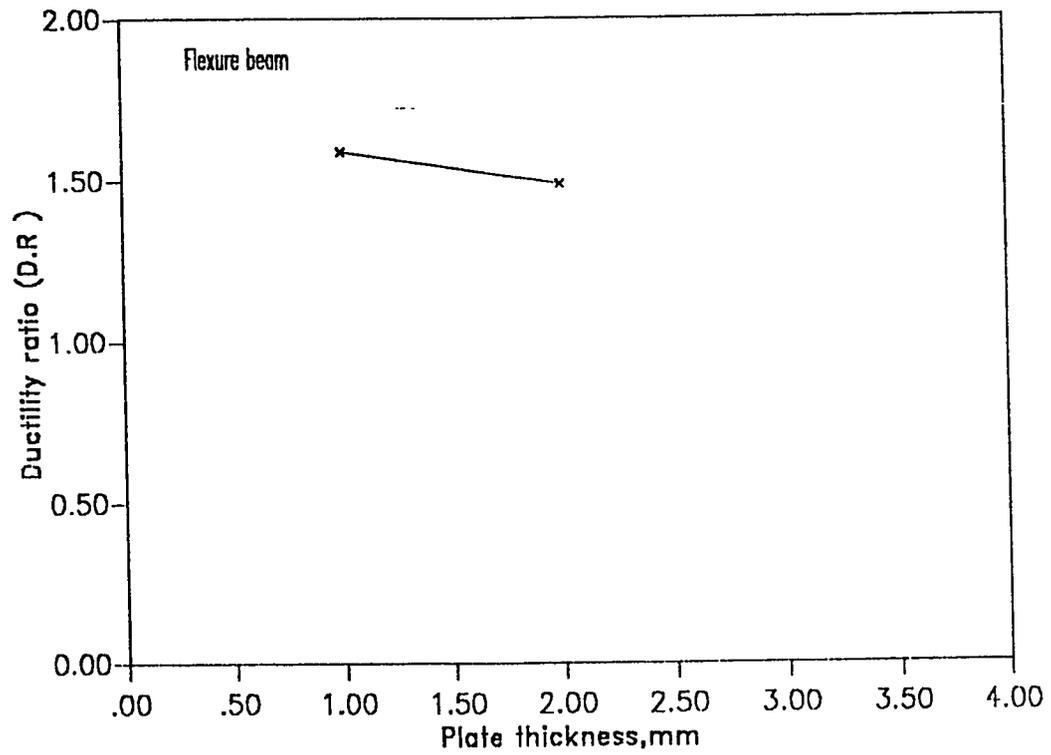


Fig. 5.13 Ductility ratio vs. Plate thickness (Plate only)

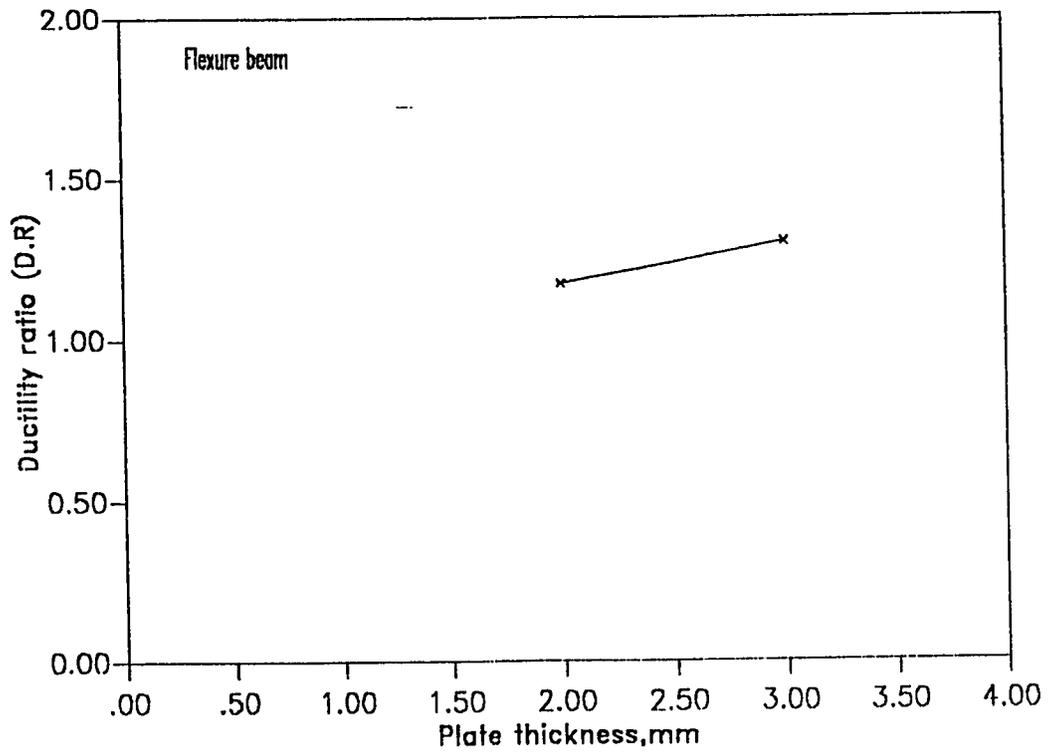


Fig. 5.14 Ductility ratio vs. Plate thickness (Plate only)

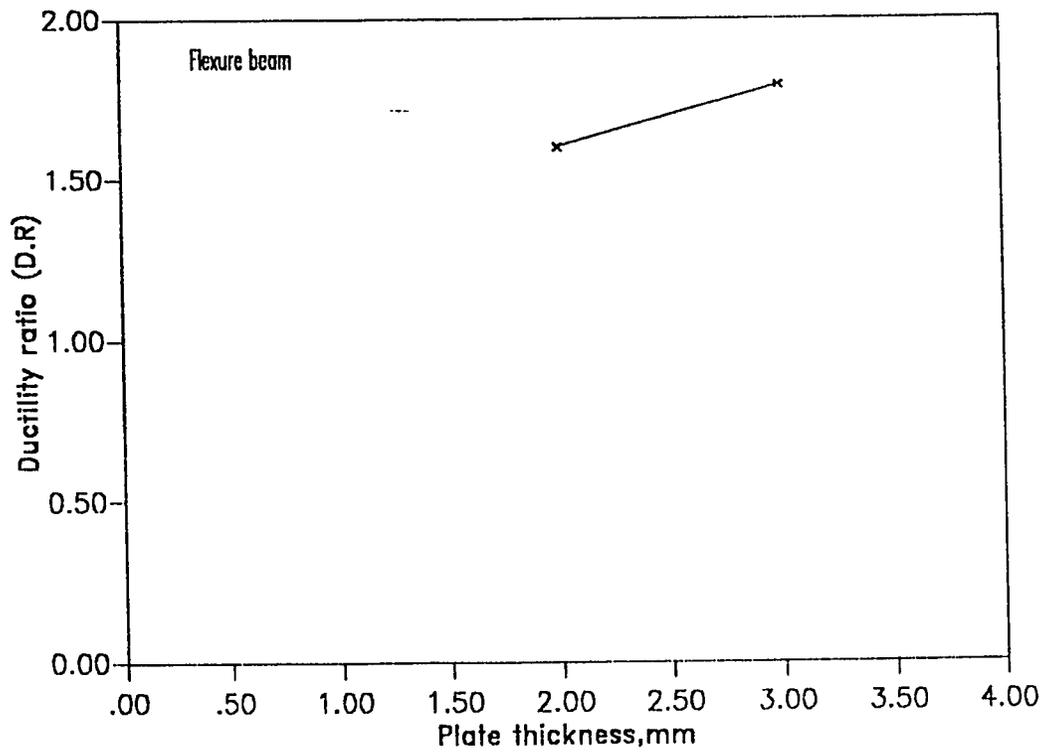


Fig. 5.15 Ductility ratio vs. Plate thickness (Anchored plate + wings)

PLEASE NOTE

Page(s) not included with original material
and unavailable from author or university.
Filmed as received.

133-134

University Microfilms International

ratio.

Figs. 5.16 through 5.18 show that the strength ratio increases with increasing the plate thickness. This is attributed to the increase in the reinforcement ratio in the form of external plates. It is clear from Table 5.5 that for any plate thickness used, anchored beams with bolts, and beams strengthened with wings and beams repaired with the I-jacket had higher strength ratio than unanchored beams.

5.3.2.1 Moment vs Curvature

Figs. 5.19 through 5.24 show the moment-curvature of beams for all series. The results of beams FP1, FP2 and FP3 shown in Figs. 5.19 to 5.21 respectively, indicate that the curvature of repaired beams are reduced relative to the controlled beam. Also, as the plate thickness increases, the beams stiffness increases and the curvature is reduced.

5.3.2.2 Rigidity:

The slopes of the $M-\phi$ curves represent the rigidities of the beams. Figs. 5.25 to 5.27 represent the rigidity (EI) vs. plate thickness for unanchored, anchored and beams strengthened with wings in their shear spans, respectively. The results indicate that for any type of repair the rigidity increases with increasing the plate thickness, Table 5.6. Surprisingly, the unan-

Table 5.5: Ductility and Strength Ratios of Flexural Beams for Different Plate Thickness

Plate Thickness (mm)	*Repair Mode	(Δ_c)ult (mm)	Ductility (kN - mm)	D.R.	Average Ultimate Load (kN)	S.R.
0	Control	17.8	3970	1.0	40.64	1.0
3.0	P	8.3	4388	1.11	65.70	1.61
"	P+B	8.9	4657	1.17	70.7	1.73
"	P+B+W	9.7	4810	1.21	71.00	1.79
"	I+J	27.0	8990	2.5	71.00	1.79
2.0	P	18.6	5923	1.49	63.5	1.56
"	P+B	12.8	5142	1.3	63.15	1.55
"	P+B+W	18.0	5810	1.46	65.3	1.6
1.0	P	20.8	6306	1.59	62.4	1.54

*P = Plate only, B = Bolts, W = Wings

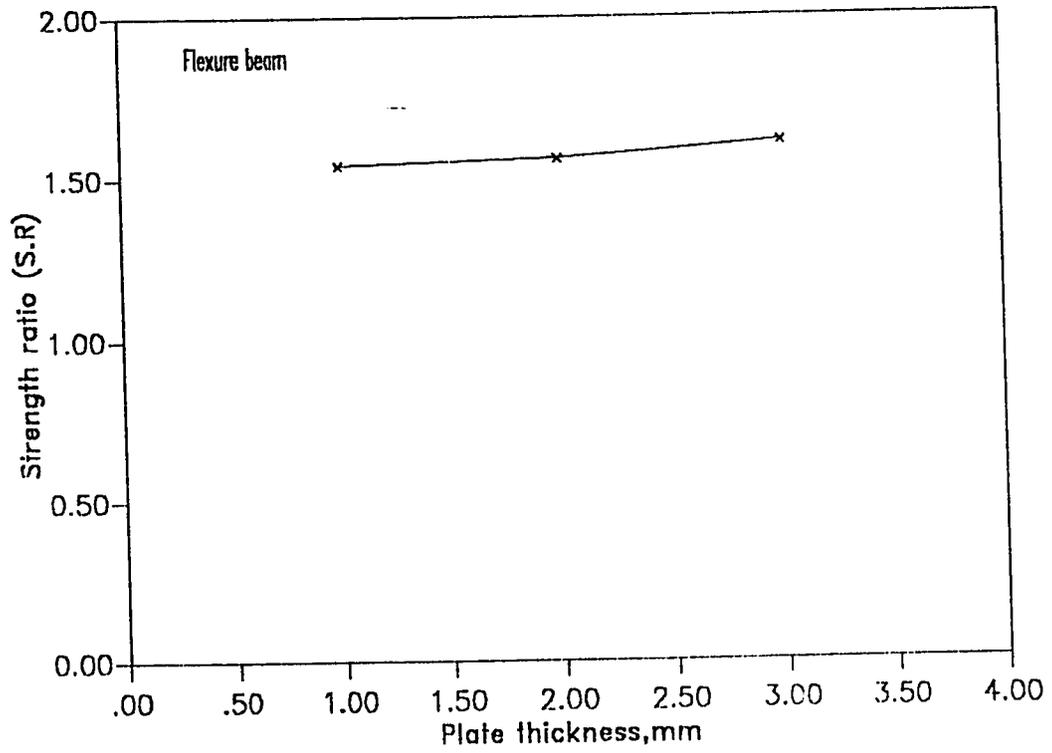


Fig. 5.16 Strength ratio vs. Plate thickness (Plate only)

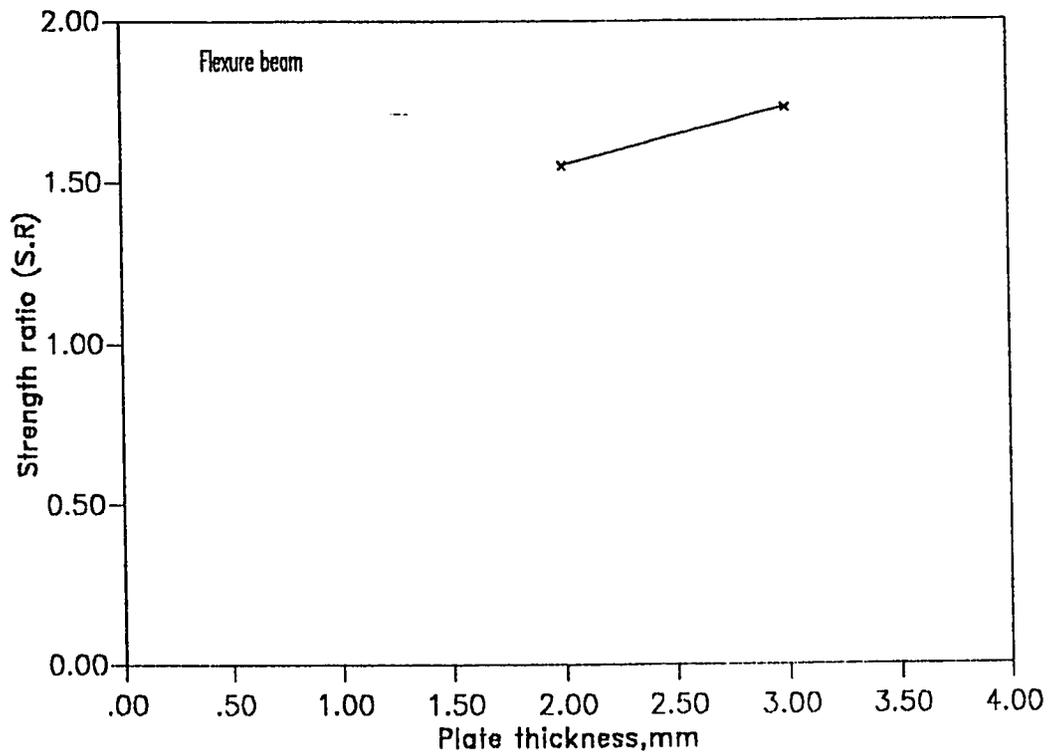


Fig. 5.17 Strength ratio vs. Plate thickness (Plate + Bolts)

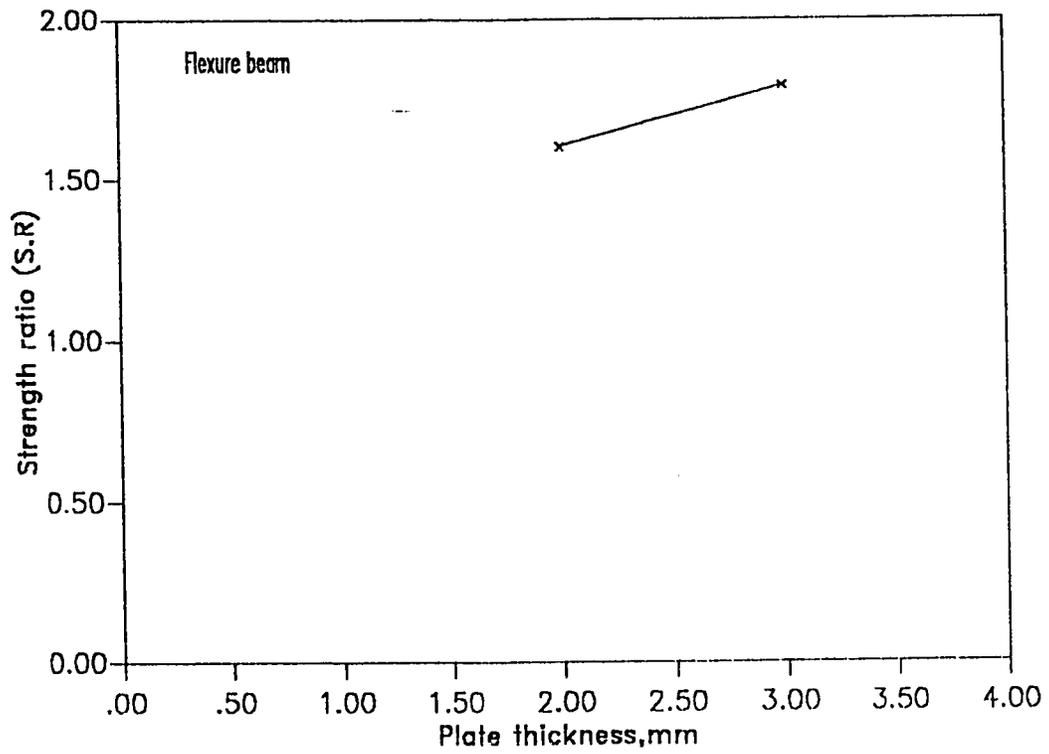


Fig. 5.18 Strength ratio vs. Plate thickness (Anchored plate + wings)

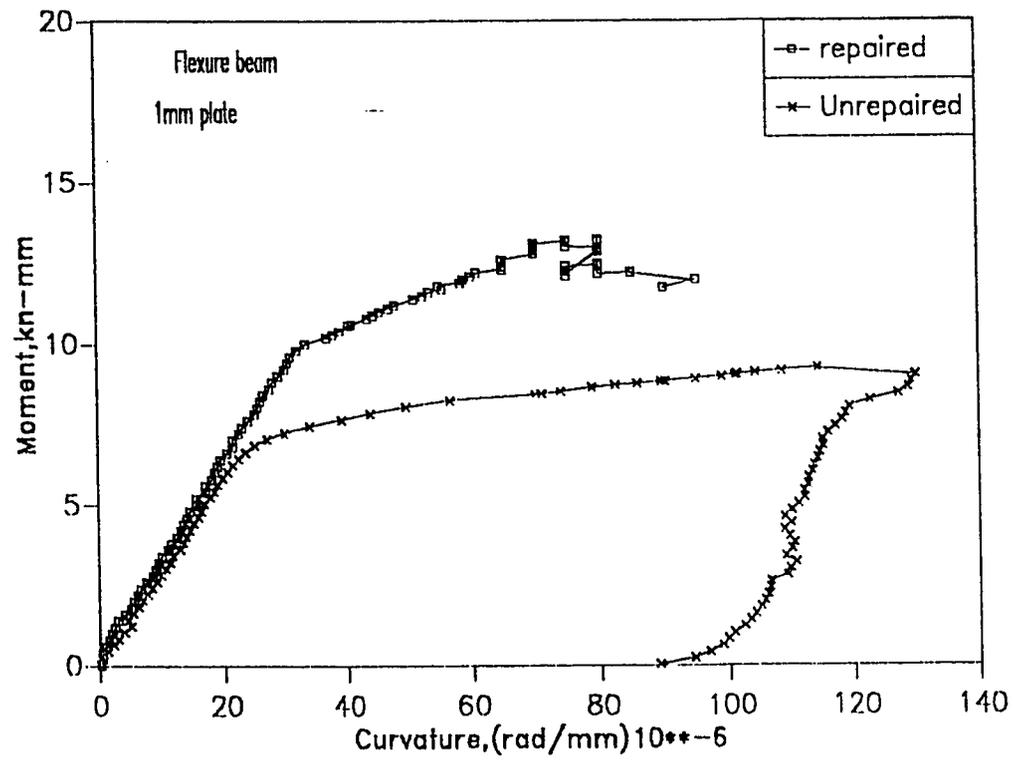


Fig. 5.19 Moment vs. Curvature (Plate only)

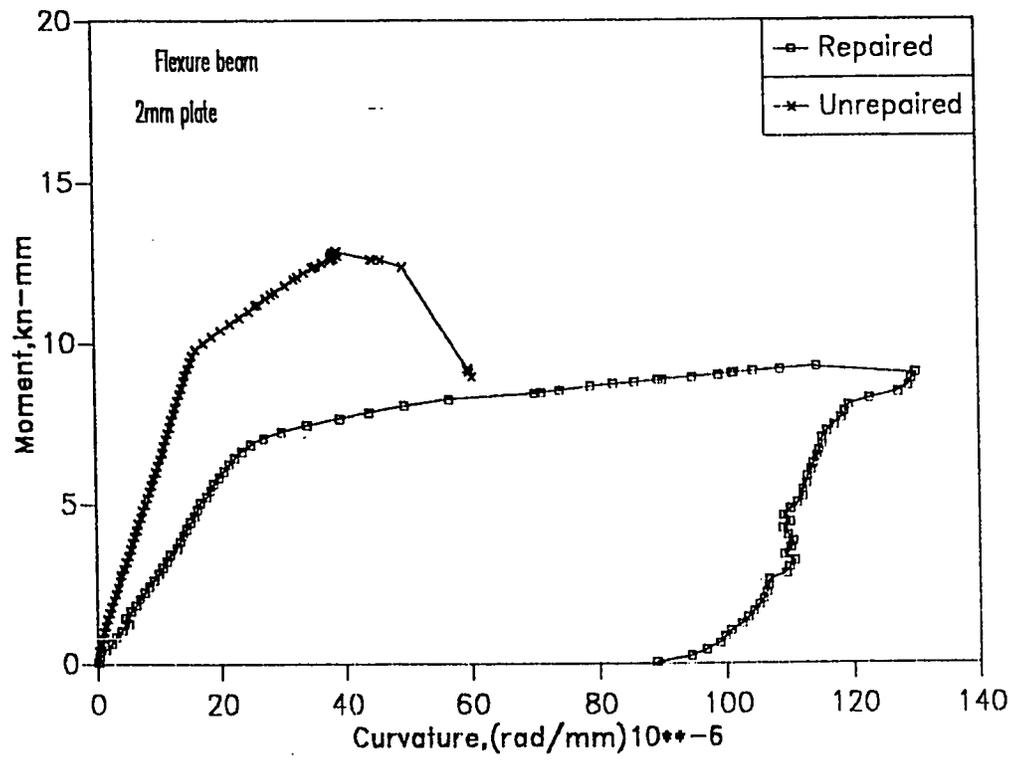


Fig. 5.20 Moment vs. Curvature (Plate only)

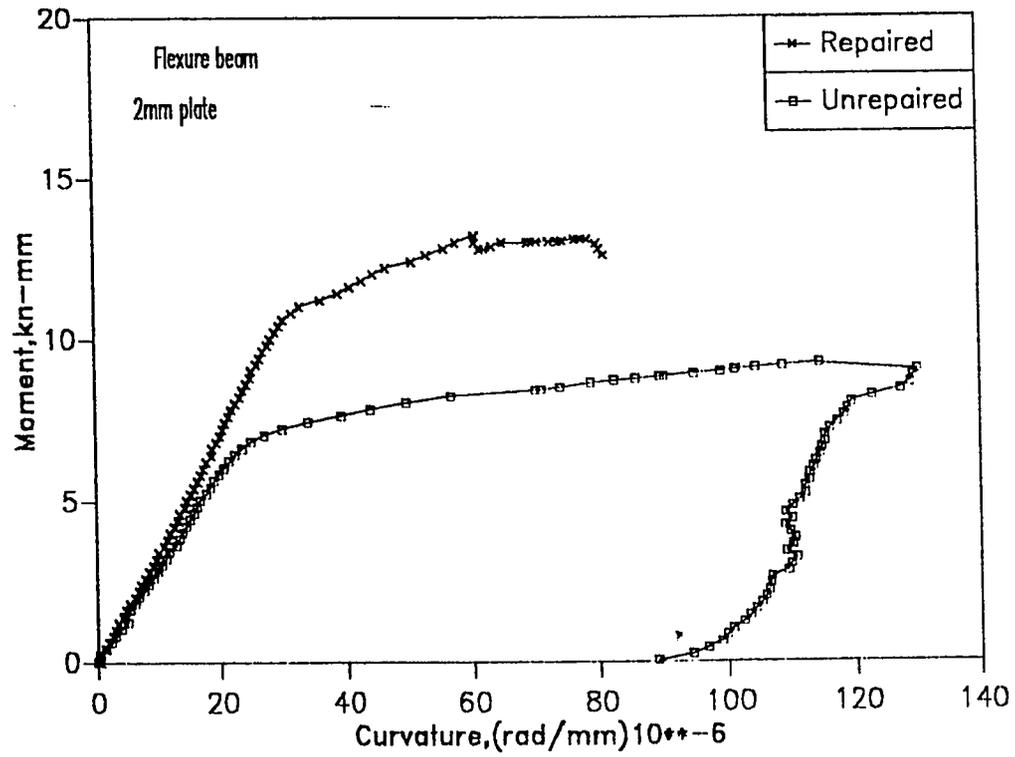


Fig. 5.21 Moment vs. Curvature (Plate +bolts)

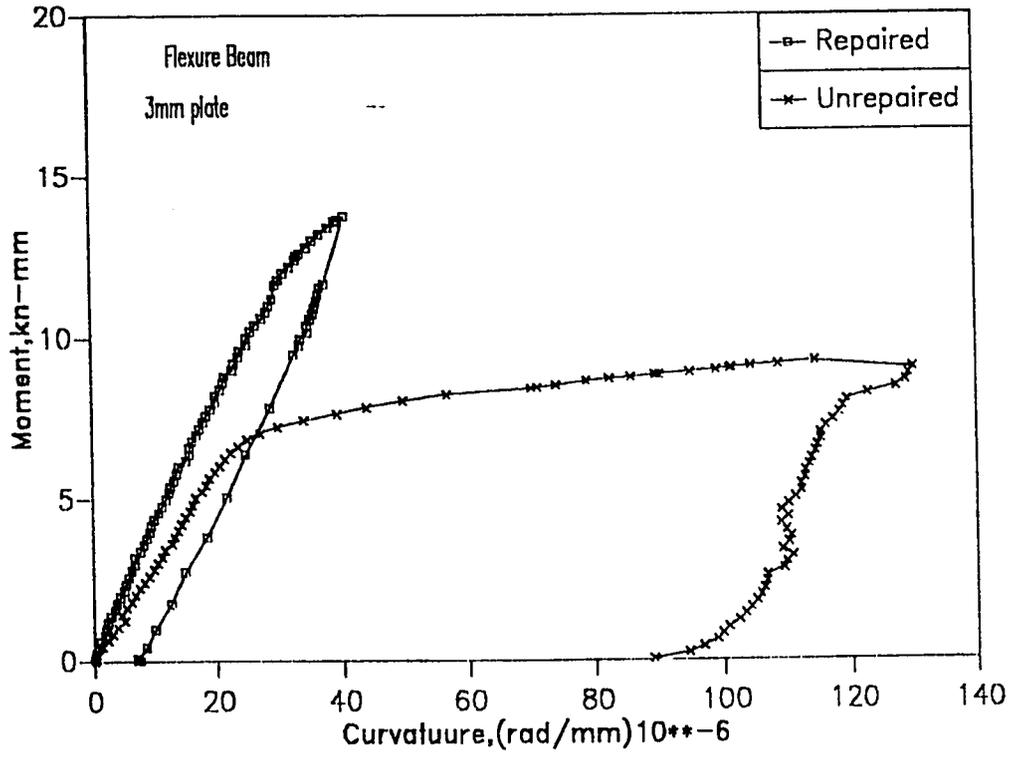


Fig. 5.22 Moment vs. Curvature (Plate only)

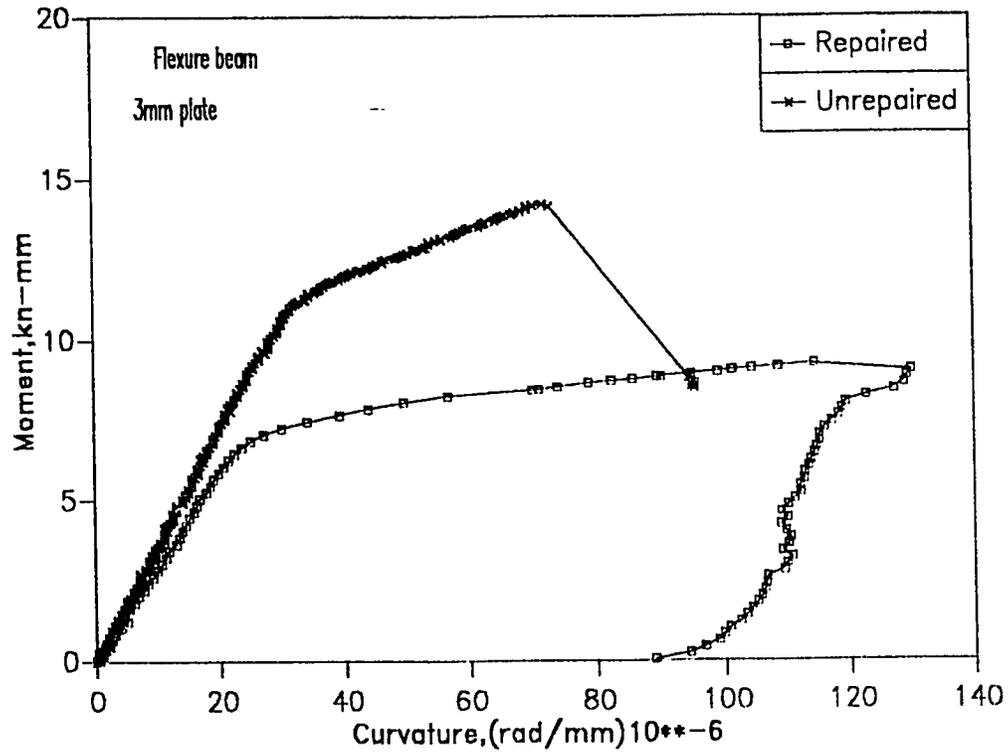


Fig. 5.23 Moment vs. Curvature (Plate + bolts)

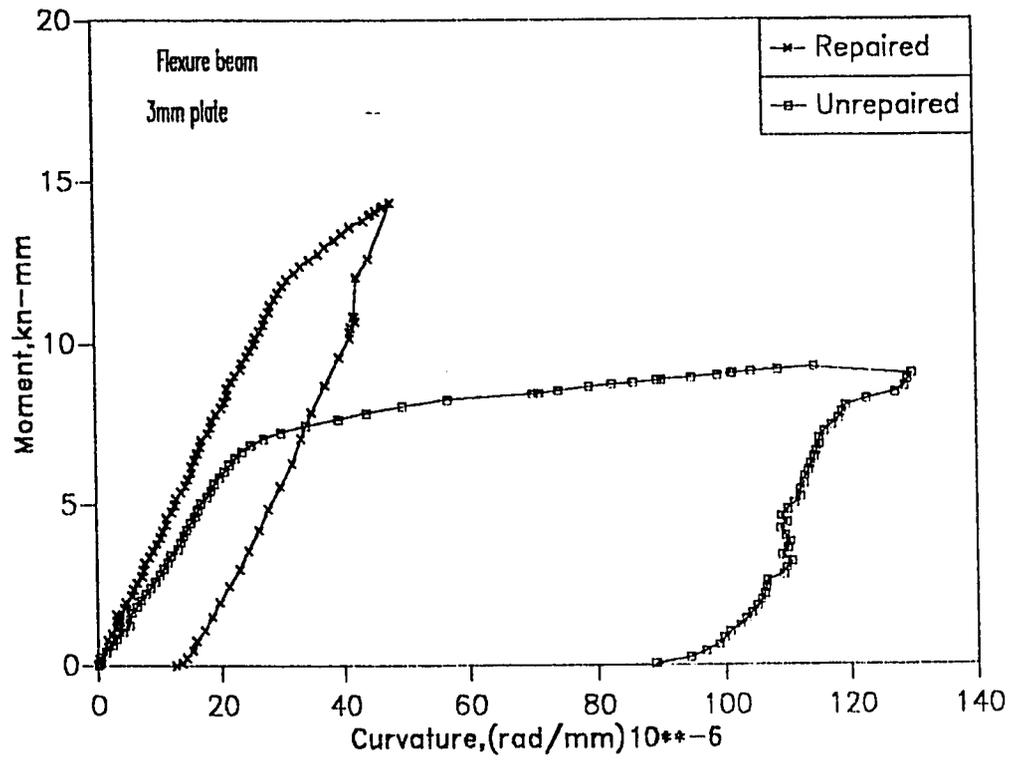


Fig. 5.24 Moment vs. Curvature (Anchored plate + wings)

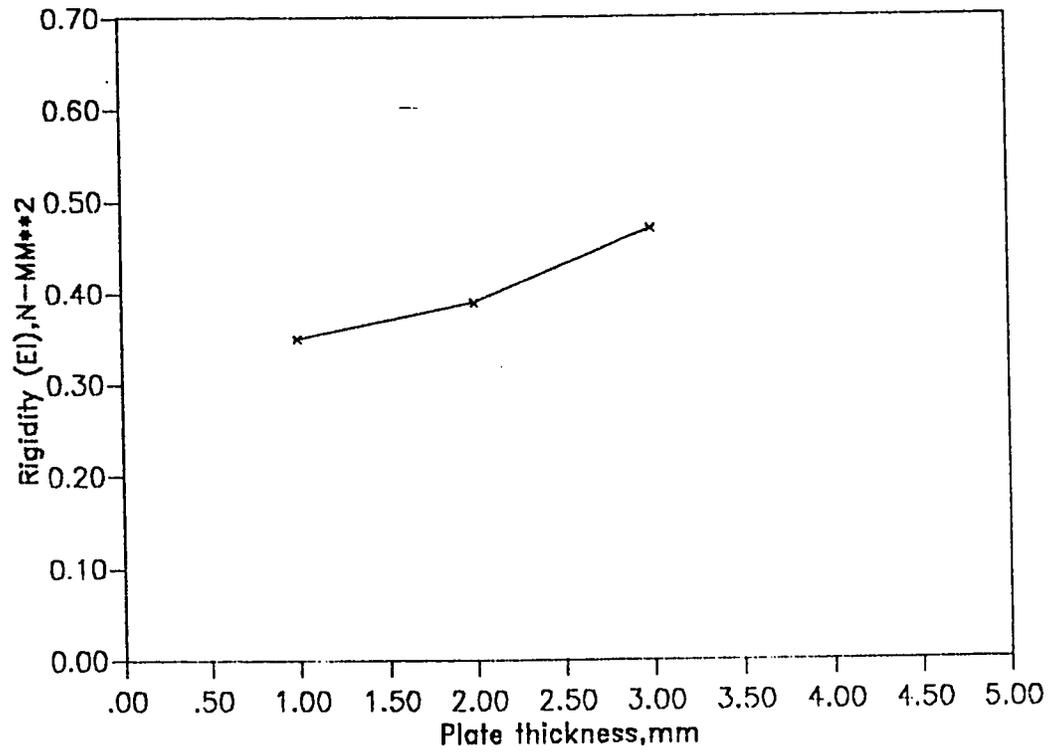


Fig. 5.25 Rigidity vs. Plate thickness (Plate only)

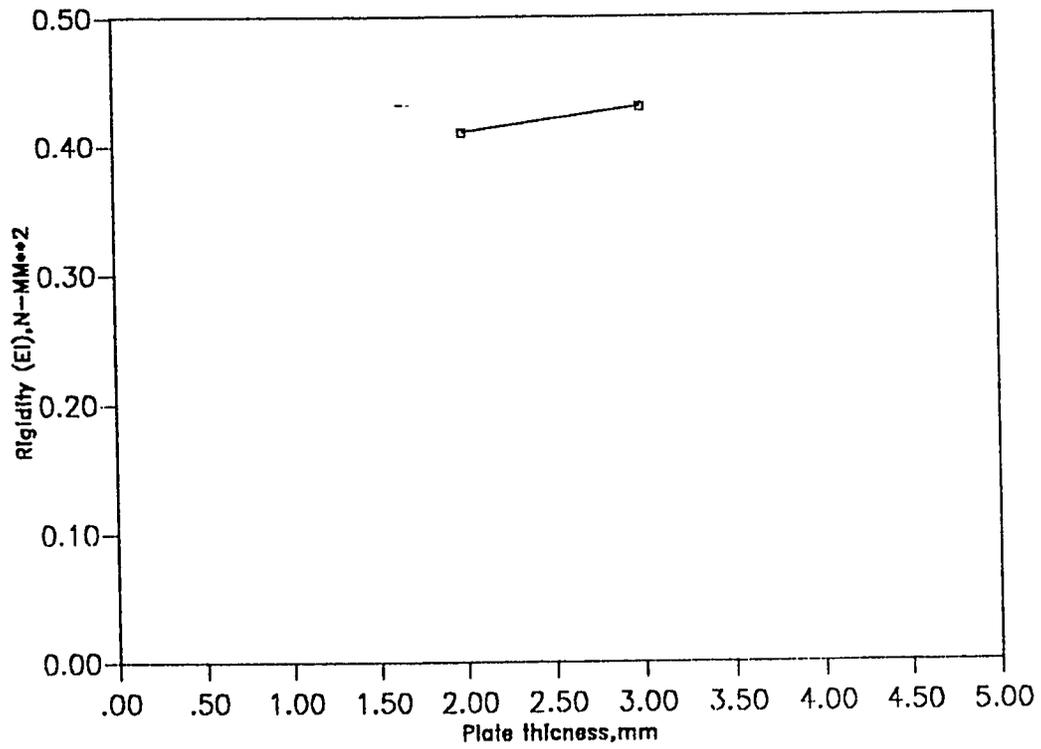


Fig. 5.26 Rigidity vs. Plate thickness (Plate + Anchor bolts)

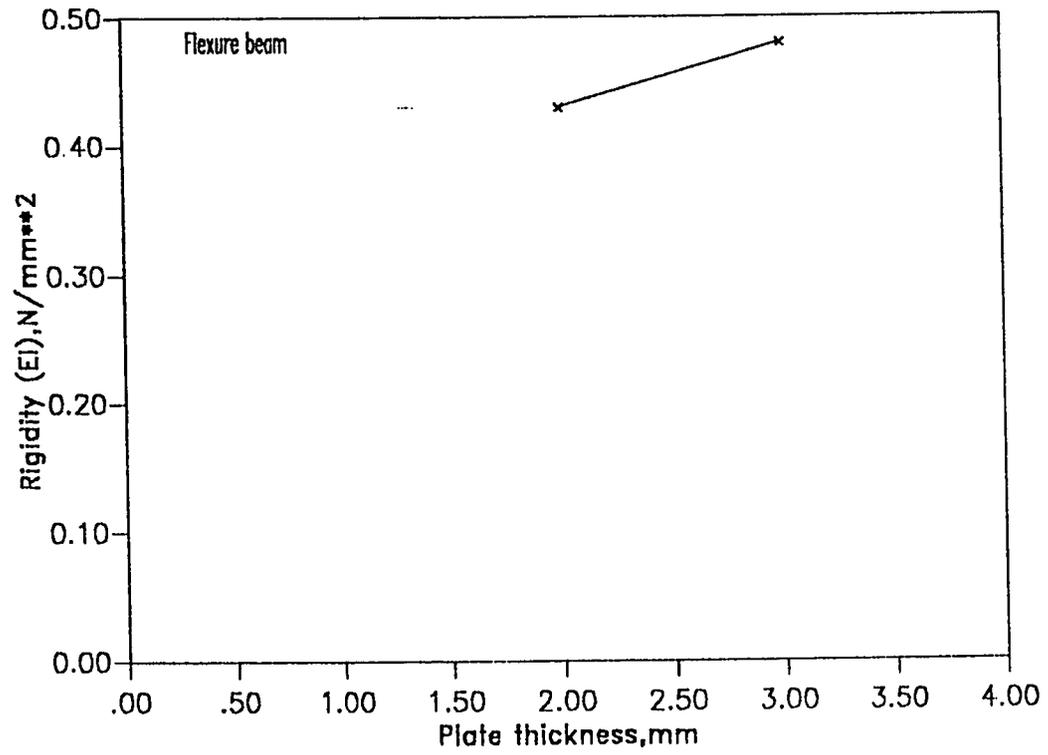


Fig. 5.27 Rigidity vs. Plate thickness (Anchored plate + Wings)

chored beams repaired with 3mm thick plates showed higher rigidity than beams FPBW3, FPBW2 and beam FJ. It should be noted that beams FPBW3, FPBW2 and FJ are expected to promote the highest rigidity. This was the case for beams FPBW3 followed by beams FJ.

5.3.3 Load Vs. Deflection

A) Effect of Repair Modes

The load-deflection curves for beams FP3, FPB3, FPBW3 and FJ are shown in Fig. 5.28. It is apparent from Fig. 5.28 that the behavior of all the beams are similar upto the end of the linear part of the $P-\Delta$ curve. The ultimate failure load was identical for beams FPB3, FPBW3 and FJ with an increase of 8.5% over beam FP3. This clearly indicates that, however, the use of bolts in case of beam FPB3, bolts with wings in beam FPBW3 and I-jacket for beam FJ changed the failure mechanism of the beams, but the ultimate load capacity was not increased so much.

All the beams could not reach the theoretical ultimate capacities given in Table 5.7 due to the occurrence of premature failure either due to separation of the plate or diagonal cracking. Also, the behavior of all the beams were identical at all levels of loading upto failure. The beams showed tremendous reduction in ductility, increase in the stiffness and the ultimate load capacity relative to the control beam except beam FJ which showed a

Table 5.6: Stiffness Values of Flexure beams

Beam No.	$\Delta_{ult.}$ (mm)	EI N-mm²	(%) Over FC
FC	17.8	0.39	--
FP3	8.3	0.47	20.5
FPB3	8.9	0.43	10.3
FPBW3	9.7	0.48	23.1
FP2	13.3	0.40	15.4
FPB2	18.6	0.43	10.3
FPBW2	16.0	0.43	10.3
FP1	20.8	0.39	2.50
FJ	27.0	0.46	17.95

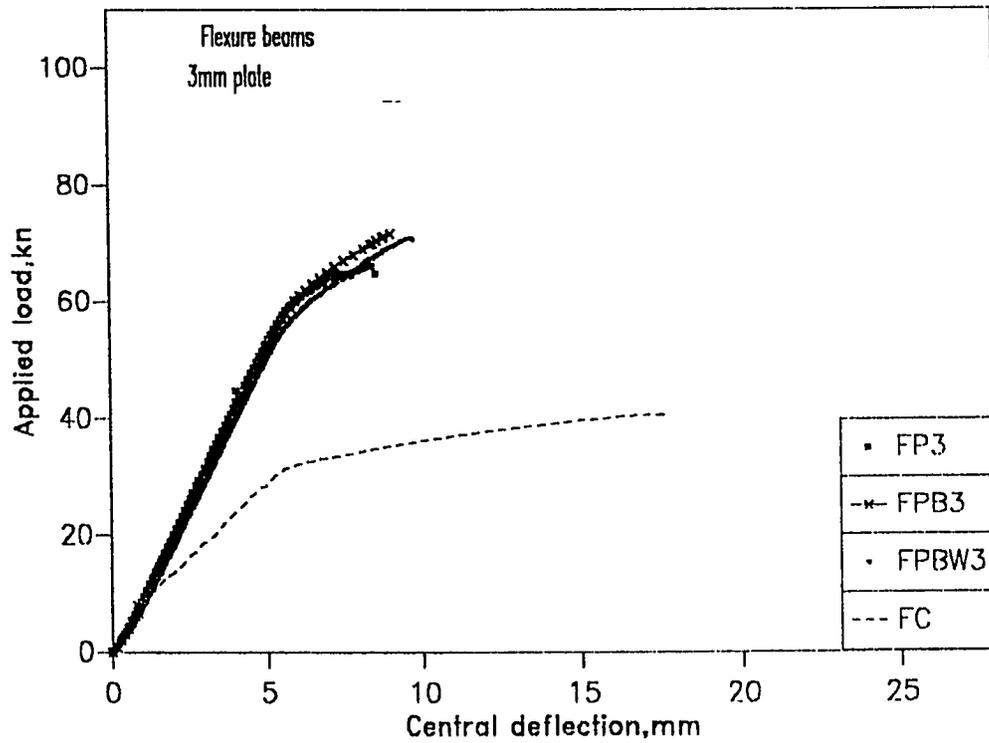


Fig. 5.28 Load vs. Central deflection (Different types of repair)

Table 5.7: Theoretical Capacity and Average Experimental Loads

Beam #	Theoretical Ultimate Capacity (kN)	Average Experimental Ultimate Capacity (kN)
FC	41.00	40.64
FP3	81.40	65.70
FP2	74.80	63.50
FP1	59.00	62.40
FJ	81.40	71.70

remarkable improvement in the ductility as compared to the repaired and control beams.

The results as shown in Fig. 5.29 indicate that beams (FP2, FPB2 and FPBW2) behaved almost in a similar manner at all load levels upto failure. Also, it can be seen from Fig. 5.29 that all repaired beams showed a remarkable increase in the ultimate flexural capacity and maintaining the original ductility as compared to the control beam FC. The stiffnesses of repaired beams were improved relative to the control beam, however, beam FPBW2 was slightly stiffer than beams FPB2 and FP2. All repaired beams behaved elastically almost up to 50 kN load.

It is clear from Figs. 5.28 and 5.29 that the anchoring has no great influence on the behavior of beams of both Series I and Series II. The behavior of these beams was more influenced by the plate thickness rather than the modes of repair. It is worth mentioning here that for thinner plate the effect of plate separation at both ends are eliminated and consequently the beam is capable to achieve its full theoretical flexural capacity.

The average ultimate capacity achieved for beams repaired with 3 mm plates was 65.70 kN with a reduction of 23.9 % as compared to the theoretical ultimate capacity ($P_{theo.} = 91.8$ kN). In the case of thinner plates the achieved average ultimate capacity was also less than the theoretical ultimate capacity. This is

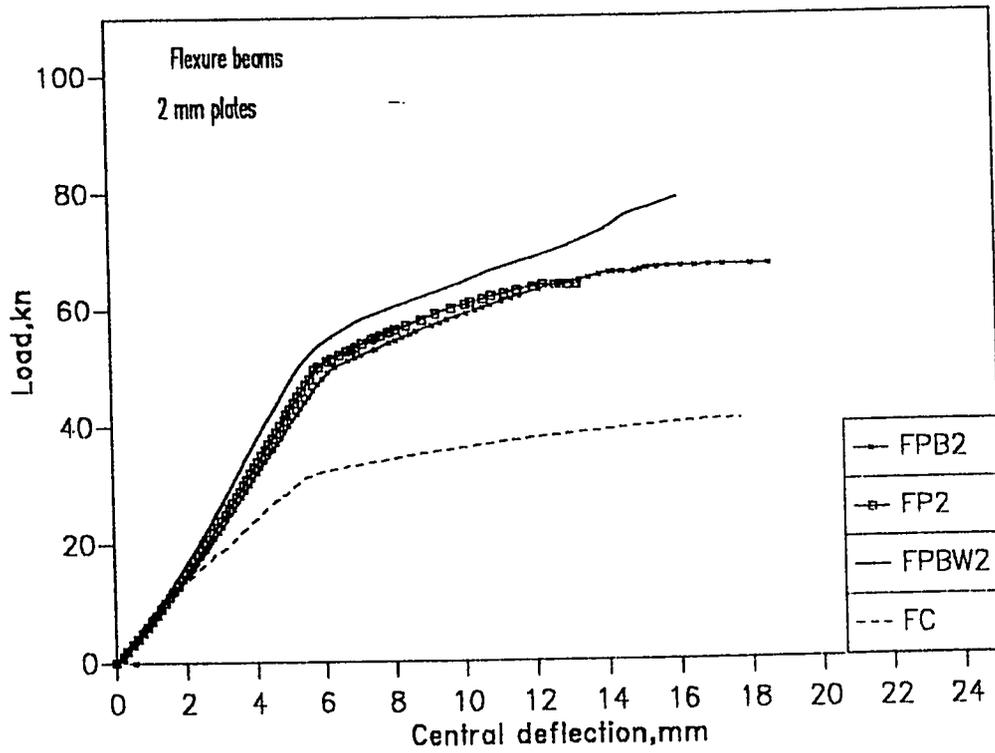


Fig. 5.29 Load vs. Central deflection (Different types of repair)

because the shear in the interface reached its maximum shear stress before any remarkable yielding of the plate leading to less composite action and plate separation. This did not enable the beams to achieve their full theoretical capacity.

B. Effects of Plate Thickness

The load-deflection curves in Fig. 5.30 show three different beams FP3, FP2 and FP1 repaired with 3, 2 and 1 mm plates, respectively. The results show that beams FP2 and FP1, showed more ductile behavior than the control beam except beam FP3 which failed prematurely by the plate separation and therefore could not reach its ultimate theoretical capacity.

Beam FP1 failed by rupturing of fiber glass plate and crushing of the concrete simultaneously. The beam showed high ductile behavior, however, this beam also could not reach its ultimate experimental capacity exceeded theoretical capacity due to rupturing of the plate (1 mm thick) in the constant moment region under high tensile stresses. Table 5.8.

The results as shown in Fig. 5.31 indicate that beam FPB3 is stiffer than beam FPB2. The average ultimate capacity of beam FPB3 is about 12% higher than beam FPB2. However beam FPB2 showed a significant increase in ductility about 44% over beam FPB3.

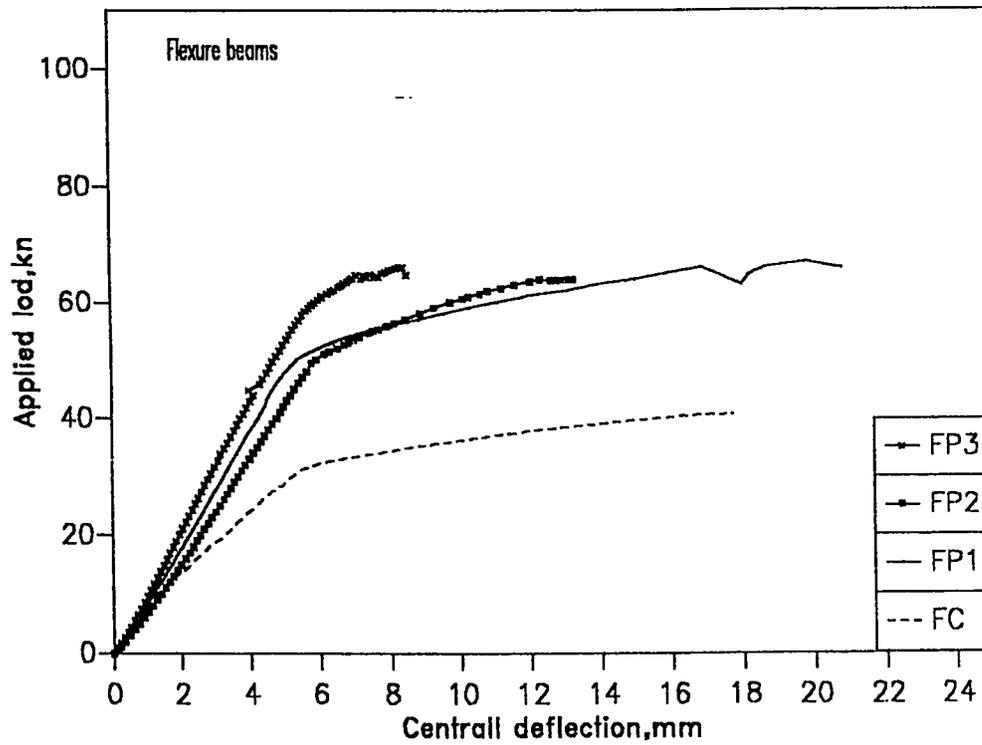


Fig. 5.30 Load vs. Central deflection (Plates only)

Table 5.8: Failure Loads and Strength Improvement

Beam No.	Failure Load (Kn)	% Over FC
FC	40.64	0
FP3	65.70	61.70
FPB3	70.7	74.0
FPBW3	71.0	74.7
FP2	63.5	56.3
FPB2	63.15	55.4
FPBW2	65.3	60.7
FP1	62.4	53.5
EJ	71.7	76.4

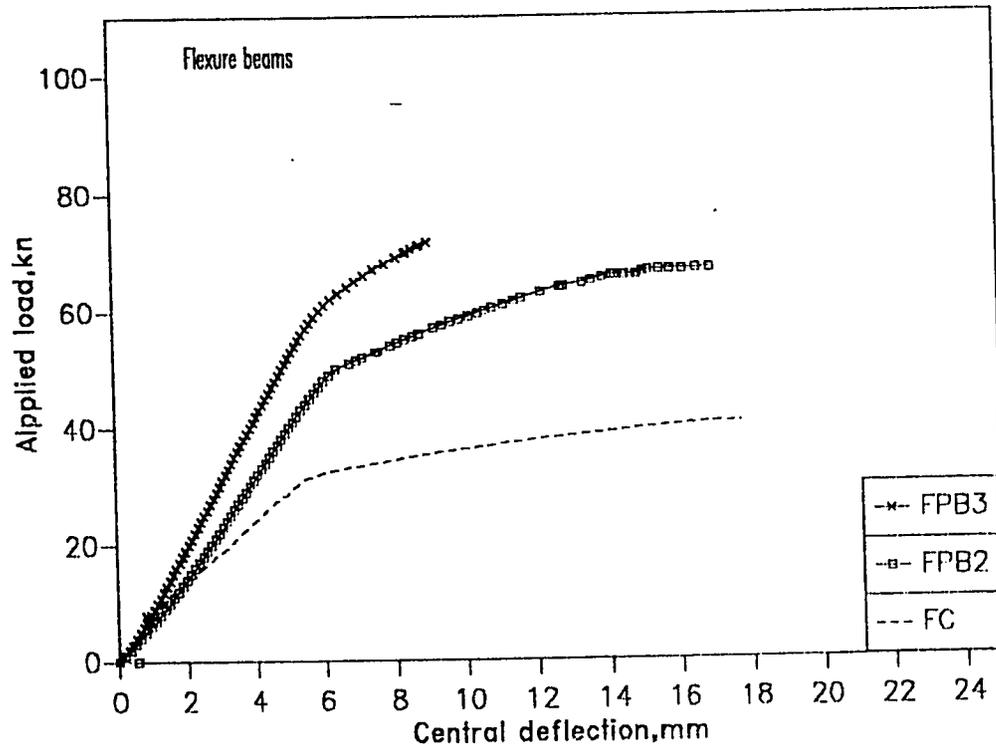


Fig. 5.31 Load vs. Central deflection (Plates + Anchor bolts)

Beams FPBW3 and FPBW2 in Fig. 5.32 again confirm the same results obtained earlier. Always thinner plate gives better ductility and a slightly lower ultimate capacity than thicker plate.

Beam FPBW2 underwent larger deflection than FPBW3 almost by 85.62% but with a slight reduction in the average ultimate strength in the range of 8.7%. Results of the theoretical calculations for all flexure beams are listed in Table 5.9.

5.3.4 Load vs Strain

Due to the nature of the fiber glass plates which are made of fibers dispersed in a resin medium, the fibers and/or the resin might tear or crack at the surface of contact under the strain gauges, thus, limited data were collected regarding the plate strains.

The strain distribution along the plate length for beams plated with 3mm plate at 40 kN and 60 kN loads are shown in Figs. 5.33 and 5.34 respectively. The results indicate that anchoring causes the plate ends to carry higher strains relative to the unanchored plate. The highest strain was achieved when the bottom plate was anchored with bolts and wings. The effect of anchoring by bolts only, showed no increase of strain relative to the unanchored plate at 60 kN loads. However, at 60 kN load higher strain are noticed at the end of the plate.

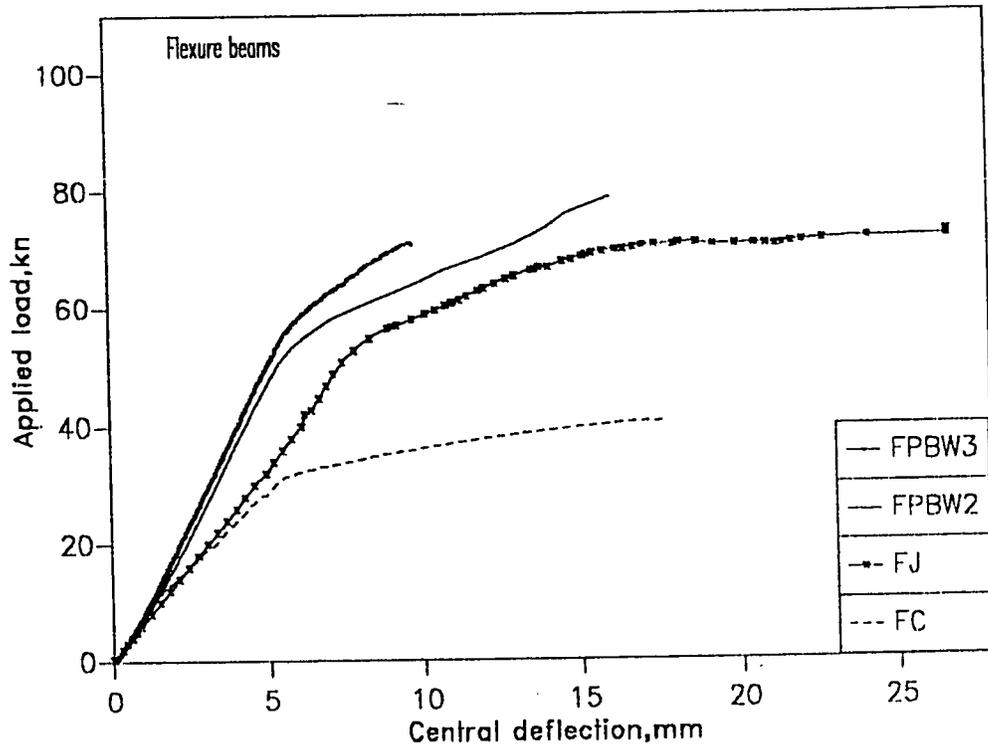


Fig. 5.32 Load vs. Central deflection (Anchored plates + wings)

Table 5.9 : Theoretical Ultimate Strength of Shear Beam Specimens

Beam #	Ultimate Shear Strength (KN)	Ultimate Flexure Strength (KN)
FC	123.2	41.0
FP3 FPB3	123.2	91.8
FPBW3	199.8	91.8
FP2 FPB2	123.2	80.1
FPBW2	199.8	80.1
FP1	123.2	59
FJ	199.8	91.8

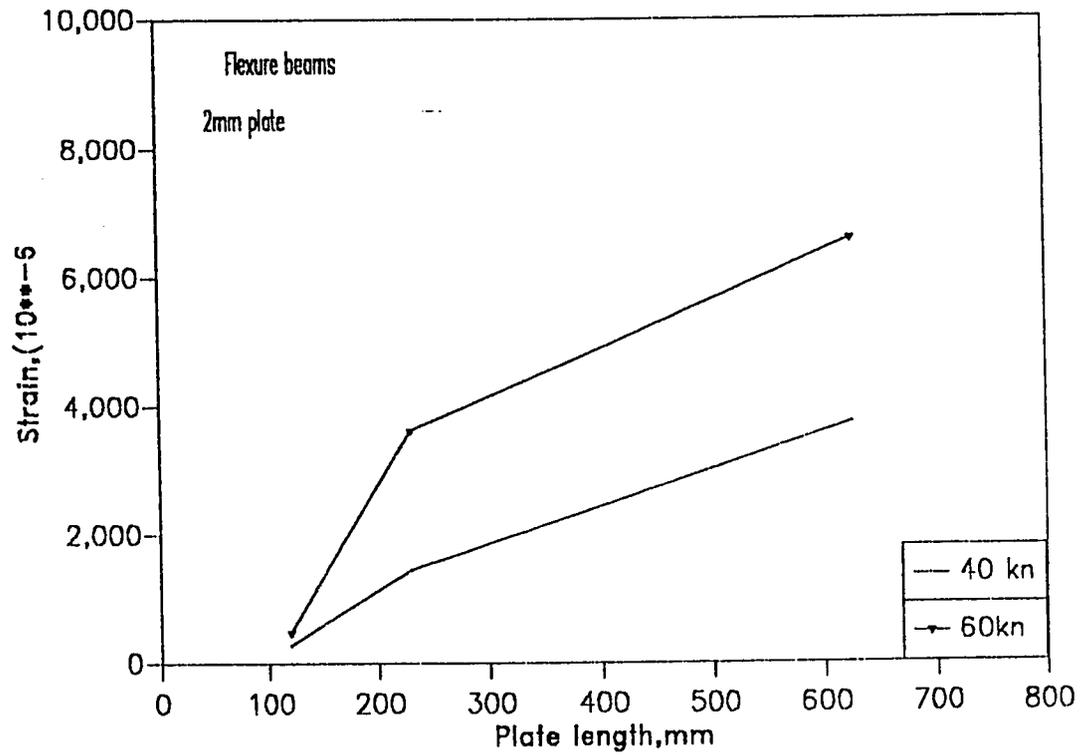


Fig. 5.33 Strain distribution along the plate length at different load levels

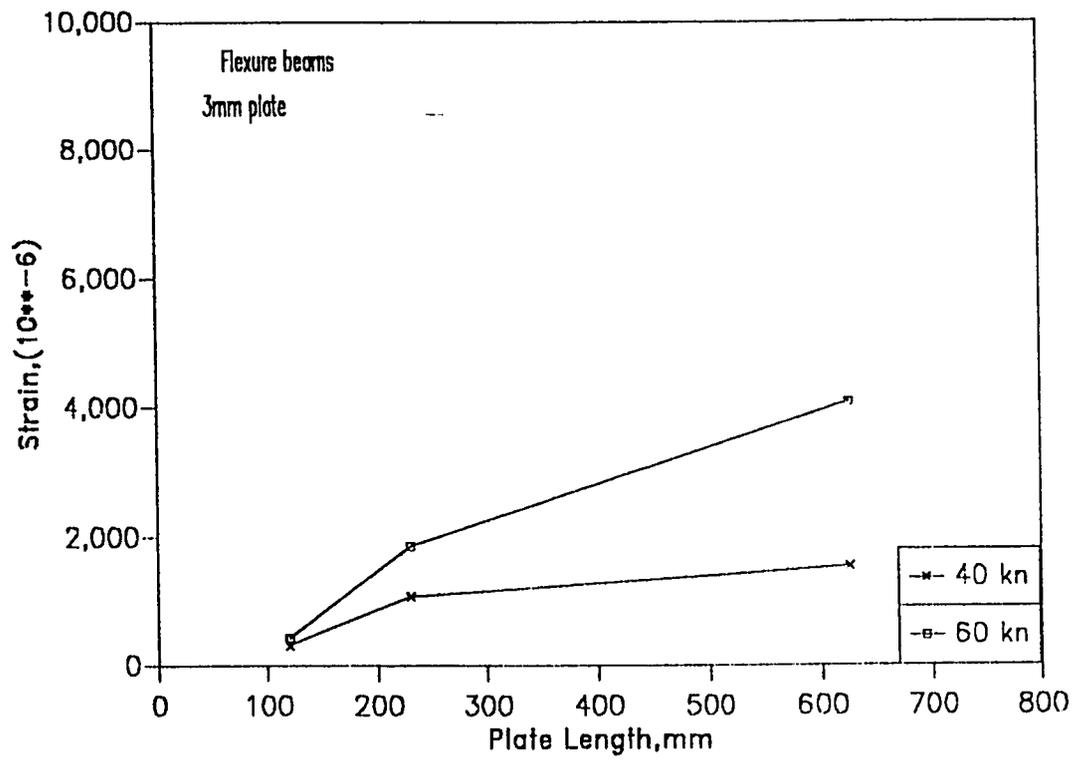


Fig. 5.34 Strain distribution along the plate length at different load levels

Figs. 5.35 and 5.36 show the strain distribution along the plate length for beams FP2 and FPB2 plated with 2mm plate. The results effect of plate anchoring on the end strain was less prominent than those beams bonded with 3 mm plate. At any location along the plate and for the same load level thinner plate shows higher strain than thicker one.

Figs. 5.37 and 5.38 represent the strain distribution along the plate length at 40 kN and 60 kN loads for beams FP3 and FP2 respectively. The results show that the strains at the plate end are almost the same for both load levels. Also, it is clear from Figs. 5.37 and 5.38 that the slopes of the curves increases as the load is increased.

Figs. 5.39 and 5.40 show the strain distribution at 40 KN and 60 kN loads for beams FP3 and FP2, respectively. The results confirm that thinner plates show higher strain than thicker ones at any location and at any load level.

Fig. 5.41 depicts the loads-strain curves at the middle of the plate for beams FP1, FP2 and FP3. As the results indicate only the strain in the plate of beam FP1 (1 mm) approached the ultimate strain while the strain the other plates (3 and 2 mm) did not but higher in case of 2 mm plate (FP2) which confirms the results stated that full composite action can be achieved with thinner plate and this will lead eventually to concrete crushing and

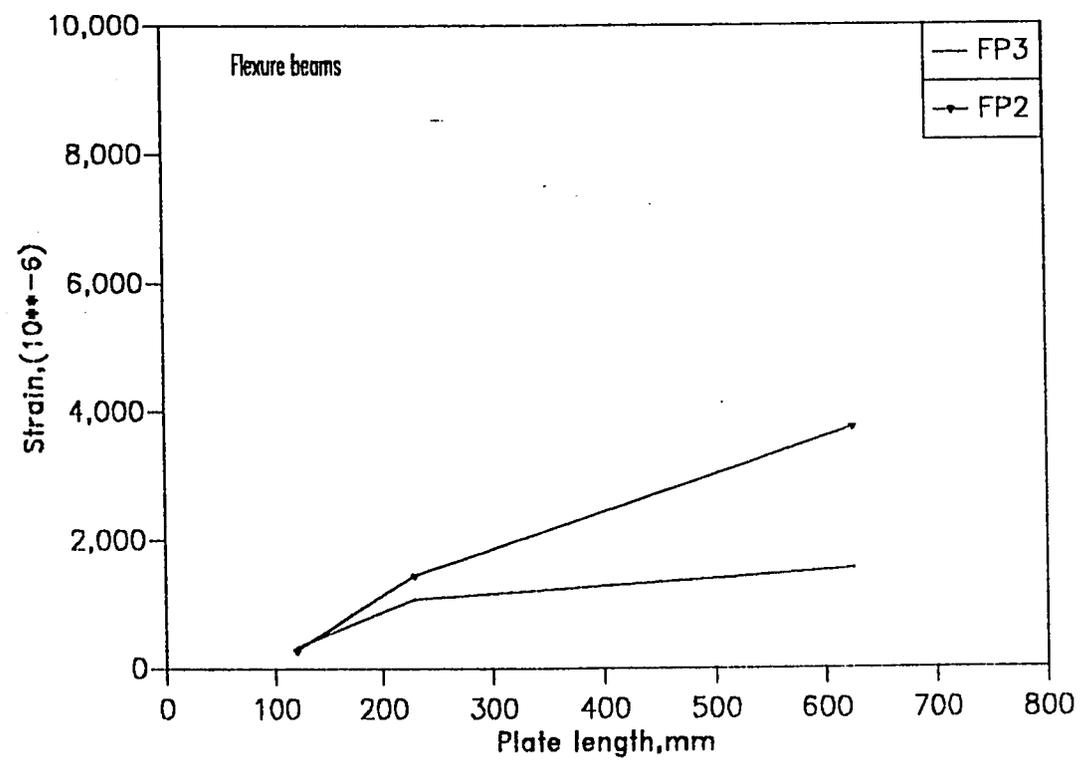


Fig. 5.35 Strain distribution along the plate length at 40 kn load (Diffrent plate thicknesses)

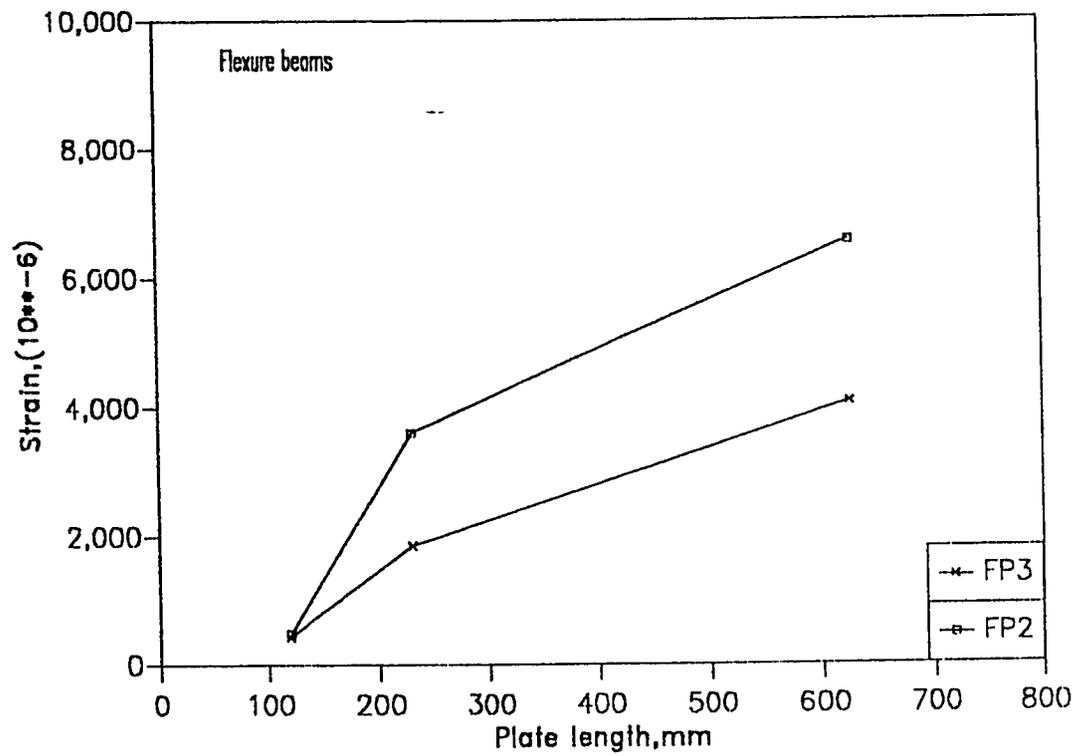


Fig. 5.36 Strain distribution along the plate length at 60 kn load (Different plate thicknesses)

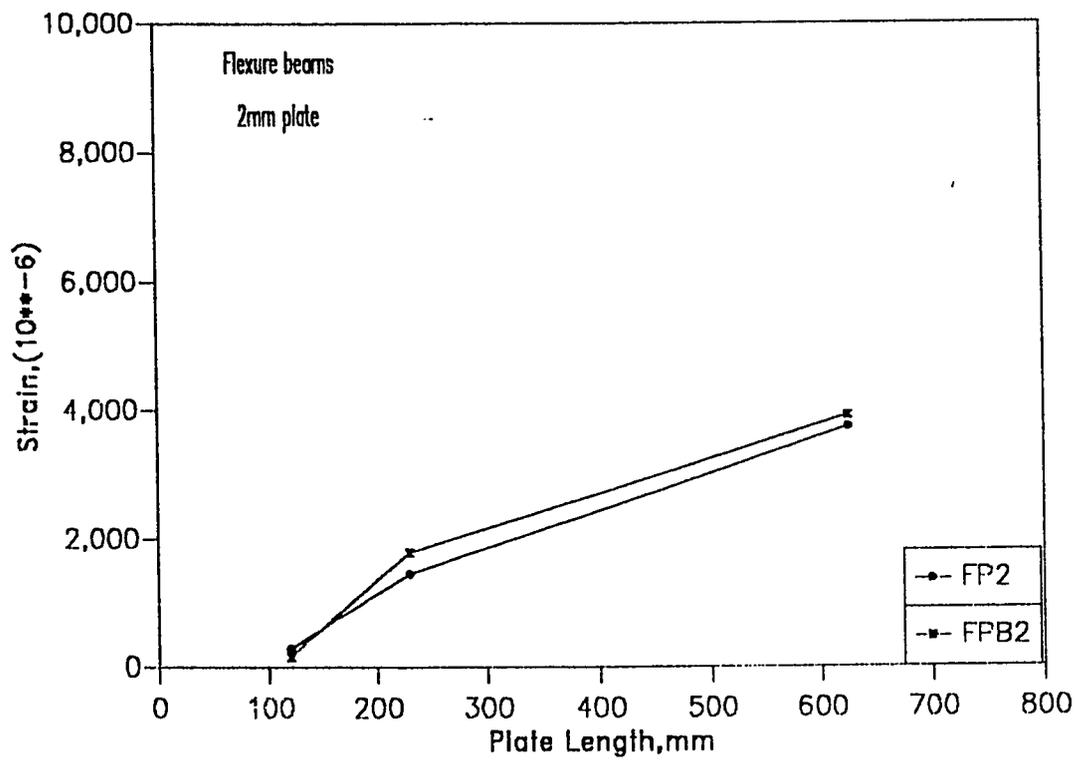


Fig. 5.37 Strain distribution along the plate length at 40 kn load (Different repair types)

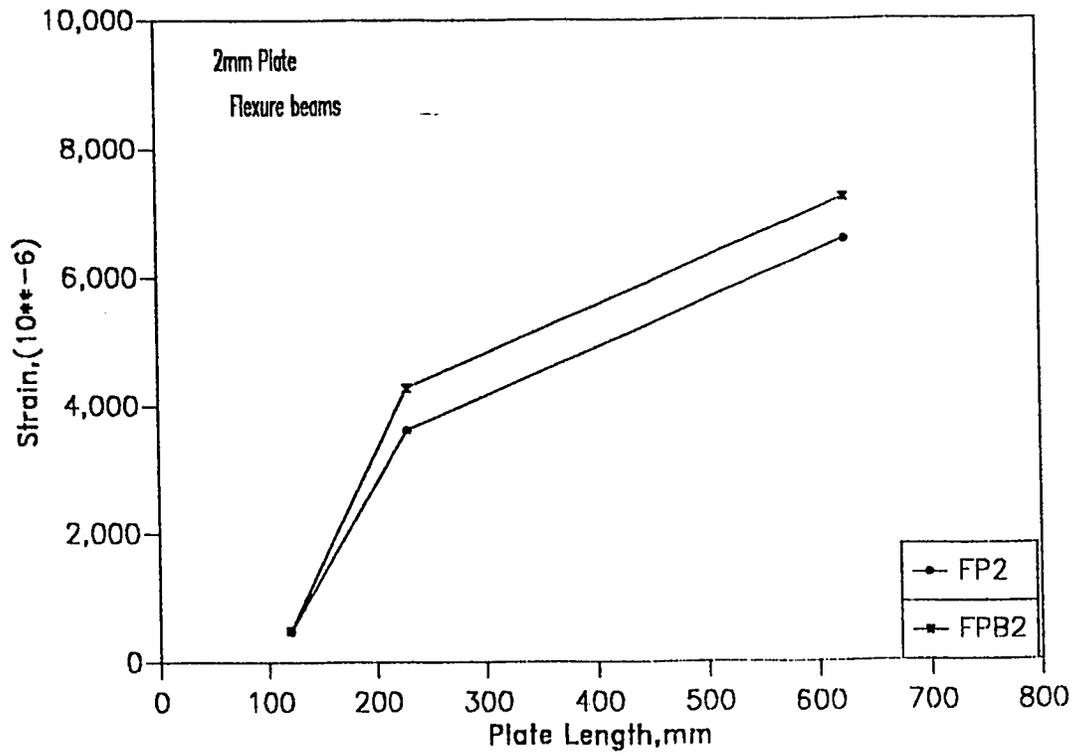


Fig. 5.38 Strain distribution along the plate length at 60 kn load(Different repair types)

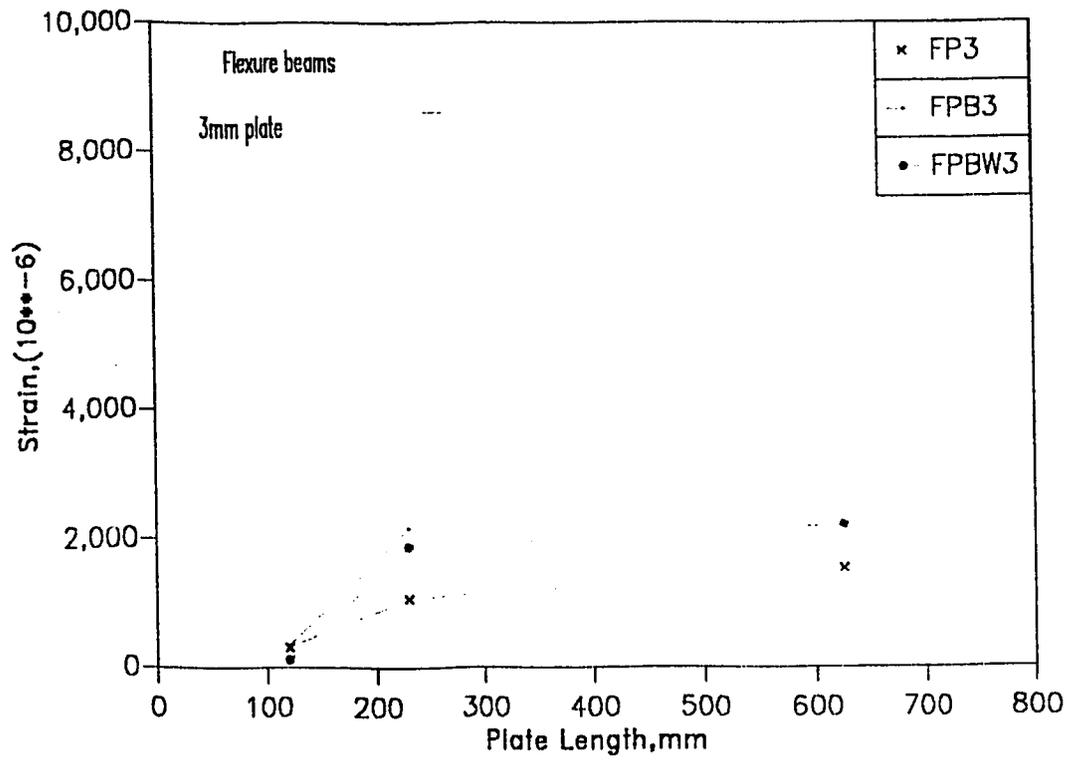


Fig. 5.39 Strain distribution along the plate length at 40 Kn load (Different repair types)

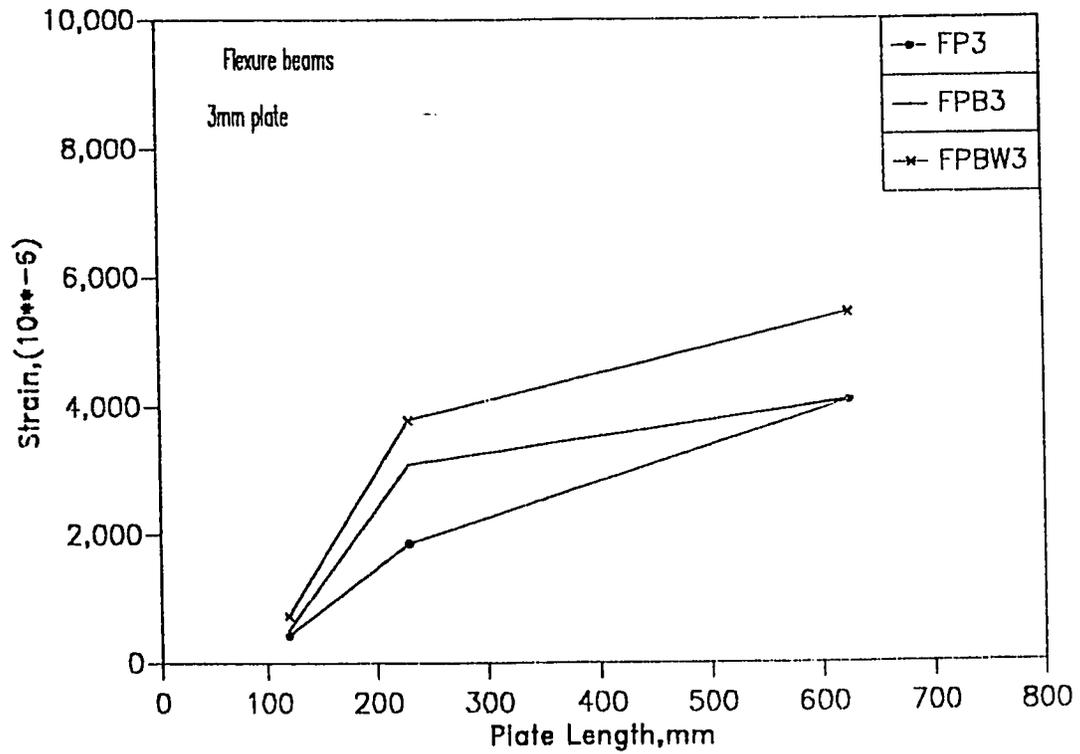


Fig. 5.40 Strain distribution along the plate length at 60 kn (Different repair types)

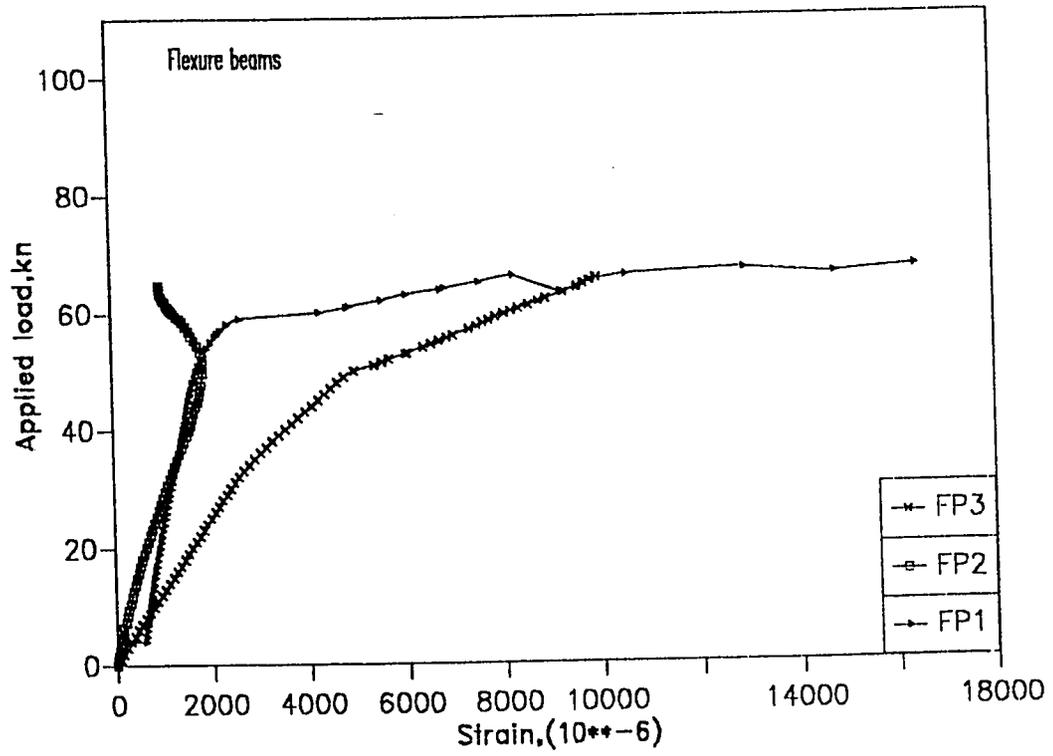


Fig. 5.41 Load vs.Strain at the plate center (Different plate thicknesses)

full ultimate flexural capacity. In thicker plates the shear stress in the interface reaches its maximum value before a significant yielding occur in the plates which leads to less composite action and ultimately to plate separation.

Figs. 5.42 and 5.43 show the strain in the rebars at 230 and 625 mm respectively from the end of beam FP3. The results clearly indicate that the steel yielded. The strains in the rebars for beams FP2 at the same locations are shown in Figs. 5.44 and 5.45. The strains obtained in case of beam FP1 is lower than that of beam FP2. Also, the strain in beam FP2 is lower than that of beam FP3. This is possibly due to the stiffening effect offered by the plate thickness, i.e. in thinner plates full composite action will be obtained and a lot of strain will be carried by the plates until failure while in thicker plates the composition action is less and debonding might occur at higher load levels which results in releasing strains to the rebars.

Fig. 4.47 indicates clearly that the steel already yielded even in the preloading stage with a high residual strain of $6,500 \times 10^{-6}$. In beam FP1 the plate failed by rupture and the strain of the steel rebar reached its ultimate strain.

5.4 SHEAR DAMAGED REPAIR

The data of shear beams are presented schematically in

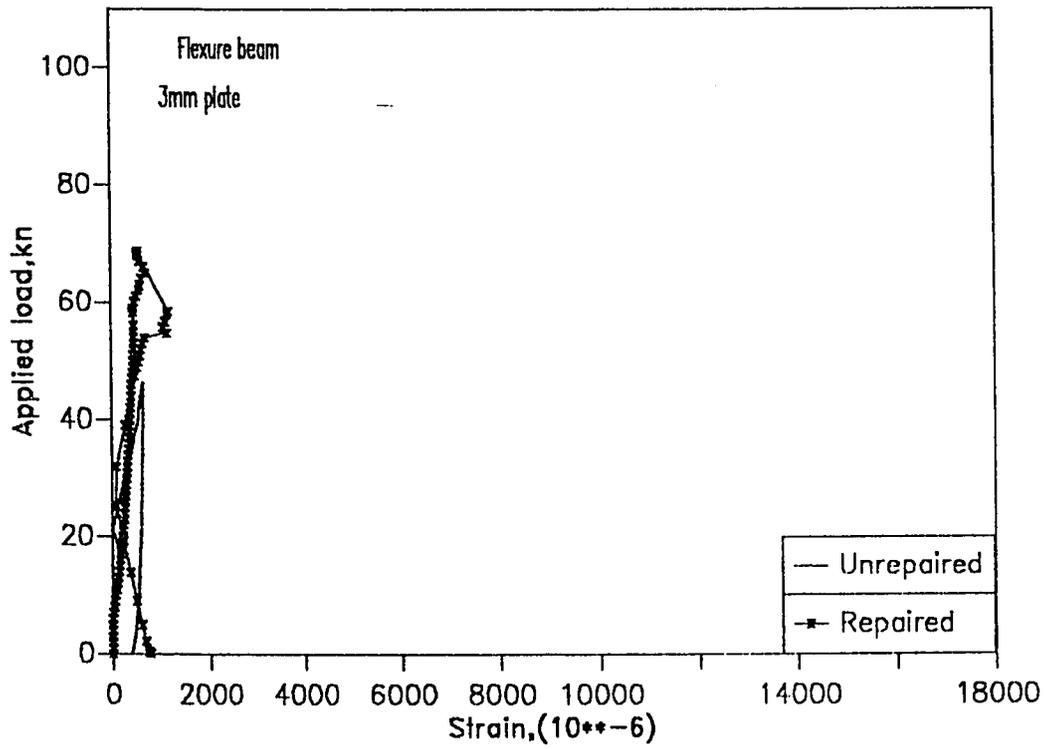


Fig.5.42 Load vs. Rebar strain at 120 mm from the beam end (Plate only)

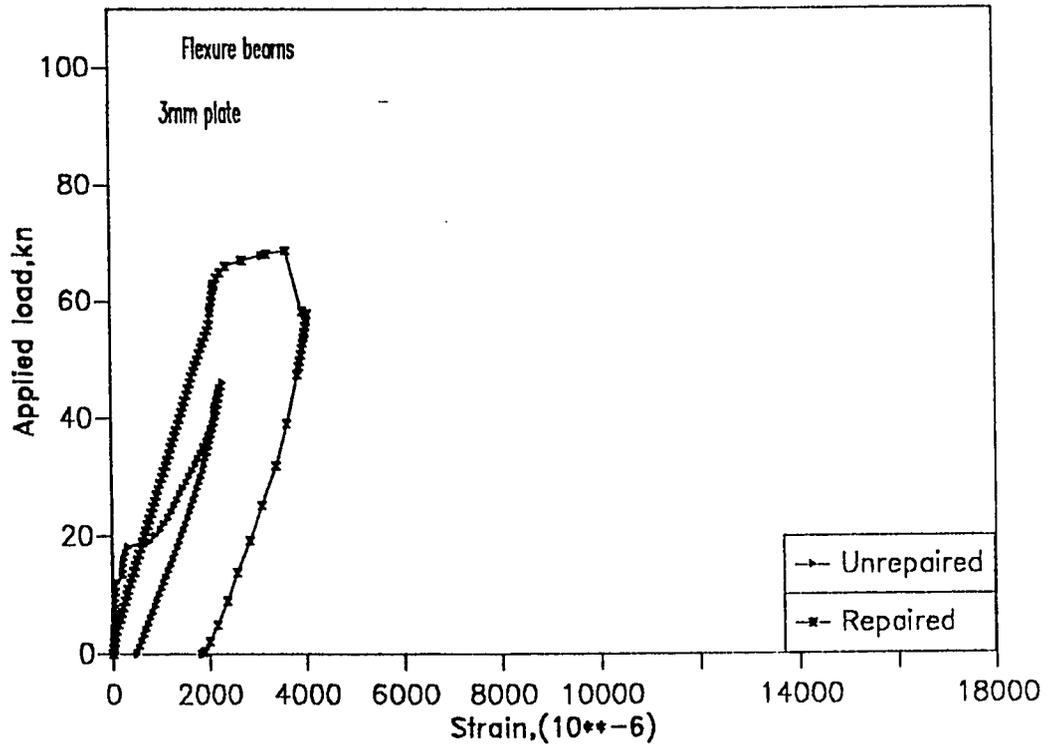


Fig. 5.43 Load vs.Rebar strain at 230 mm from the beam end (Plate only)

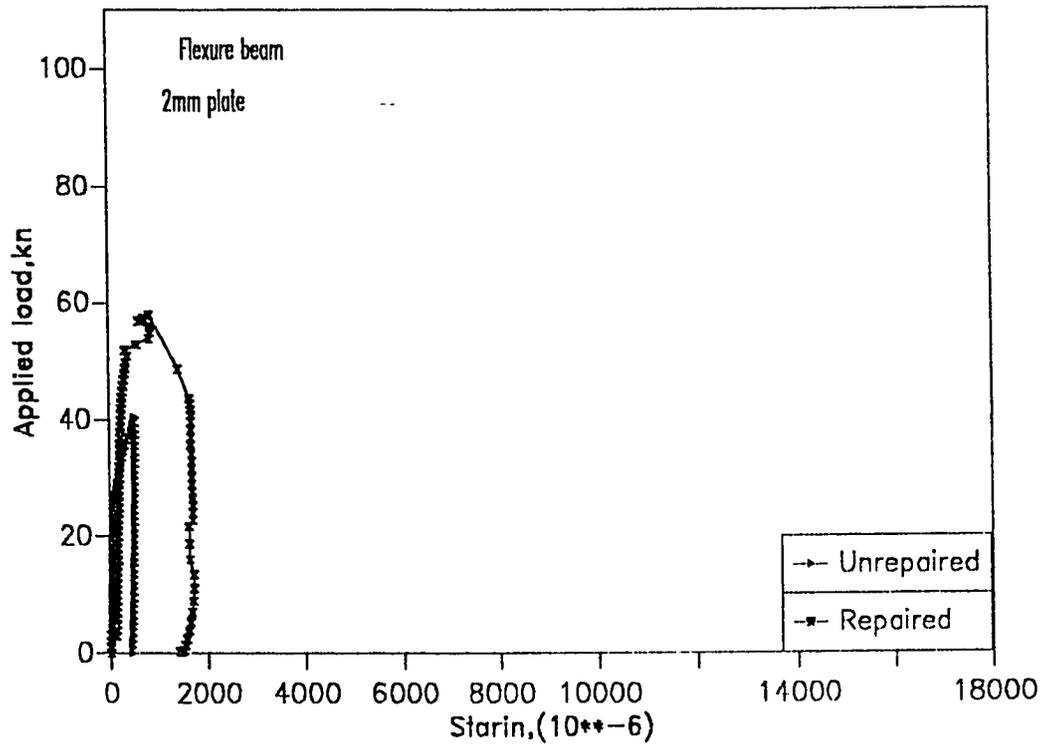


Fig. 5.44 Load vs.Rebar strain at 120 mm from the beam end (Plate only)

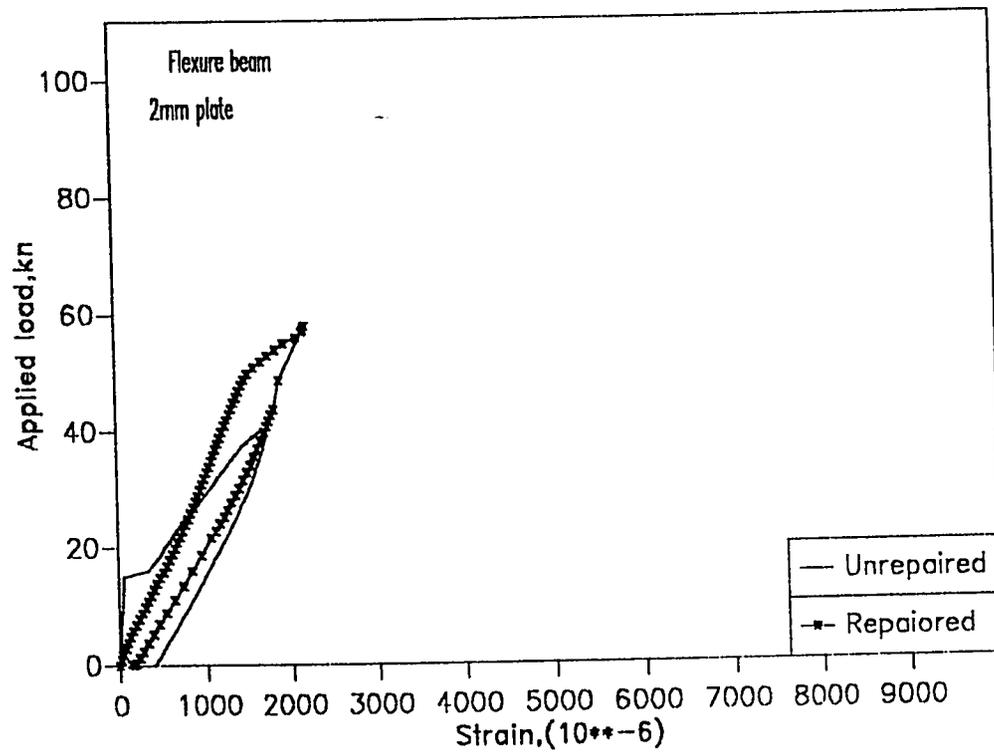


Fig. 5.45 Load vs. Rebar strain at 230 mm from the beam end (Plate only)

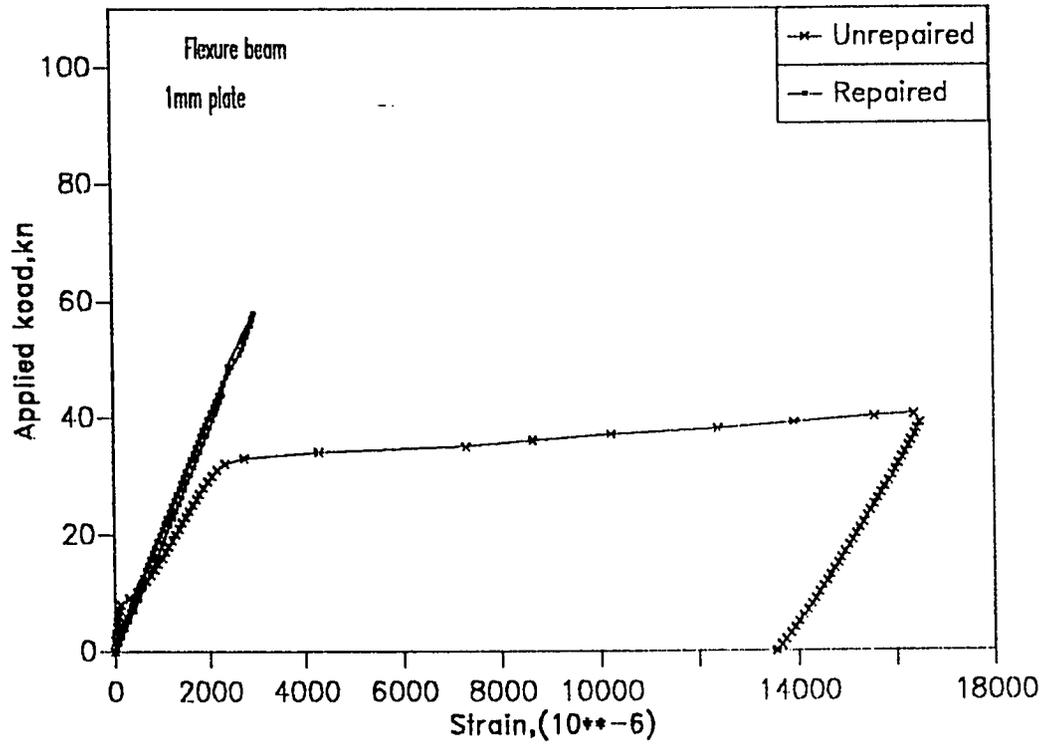


Fig.5.46 Load vs. Rebar strain at the middle of the rebar (Plate only)

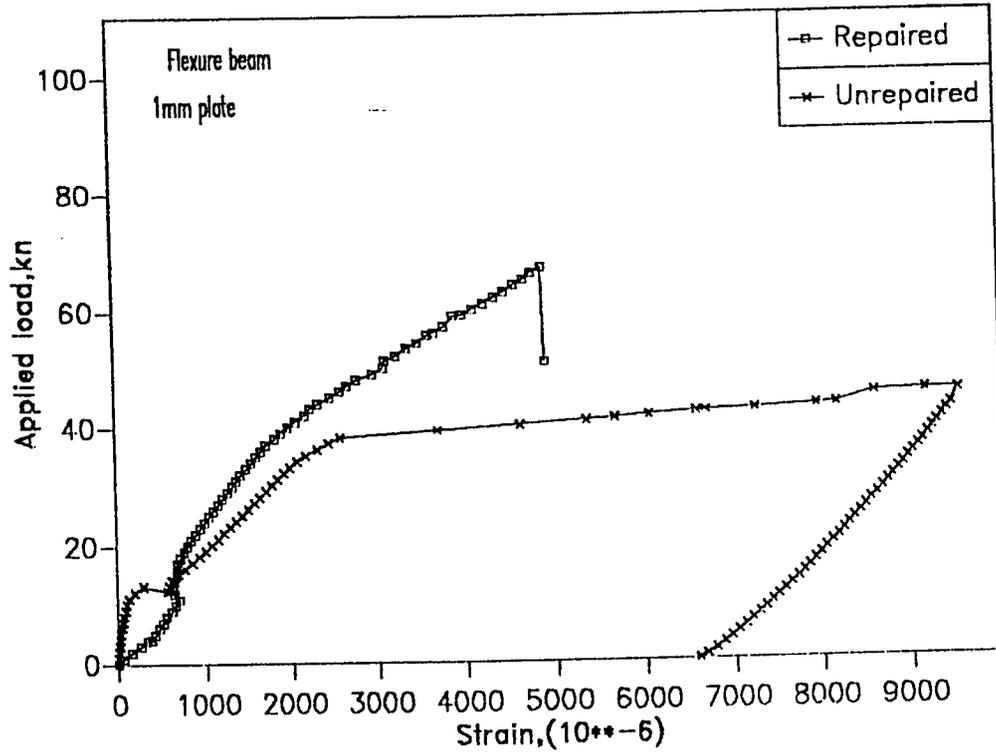


Fig. 5.47 Load vs.Rebar strain at 230 mm from the beam end (Plate only)

Figs. 5.48 through Fig. 5.61 and quantitatively in Tables 5.10 through 5.13.

5.4.1 Modes of Failure

It was observed from testing of shear beam SW, repaired by wings, that the original flexural cracks became wider and extended upwards as the load increased to 26 kN. As load reached 39 kN new flexural cracks at the shear spans appeared. At 70 kN longitudinal crack developed at the beam soffit and propagated horizontally towards the supports. This crack became wider at a load of 73 kN until eventually resulted in beam failure at a load of 75.8 kN, Plate 5.12.

The formation of such crack is probably due to the nature of the stresses resisted by the wings. Since the wings are subjected to a biaxial state of stress, they stiffened the beam and prevented shear compression failure to occur. This leads to the development of transverse tensile stresses exerted by the longitudinal steel at the beam soffit which cause flexural bond failure and splitting of the concrete at the beam soffit. The bond stress exerted by the rebars was 9.9 N/mm^2 which is higher than the allowable ultimate bond stress as recommended by the ACI code (5.4 N/mm^2), the flexural bond stress was 7.5 N/mm^2 compared to 4.0 N/mm^2 according to the ACI code.

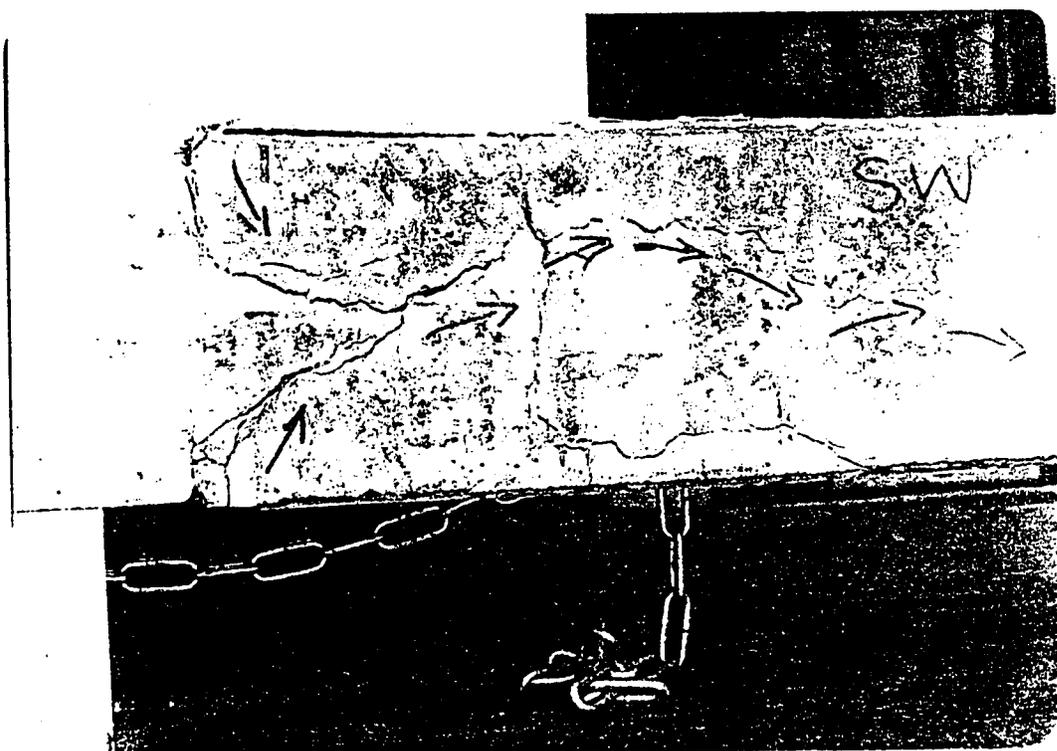


Plate 5.12: Failure Mode of Beam SW (Formation of Longitudinal Crack at the Beam Soffit Causing Transverse Splitting).

Beam SWP was then repaired by bonding plate at the soffit in order to arrest the longitudinal crack that developed in beam SW. The behavior of this beam was better than beam SW regarding the ultimate shear capacity. Several flexural cracks developed at shear span at 50 kN load. These flexural cracks initiated at the shear span, became wider at higher load levels and at failure load the cracks were wide enough so that the glue layer was damaged and the beam eventually failed at 89.9 kN load due to separation of the wings and simultaneous debonding of the plate. Ripping off the wings was due to a combination of tensile and shearing stresses along the wing faces. Because this part of the beam became very stiff as compared to the constant moment region thus, during bending the wings were subjected to twisting action resulting in ripping off the wings with the concrete, plate 5.13.

Beam SWPB represents the final stage of repair which was aimed to prevent the separation of the bottom plate. The steel bolts were then used to anchor the plate. It was observed that upto 84 kN load the beam behaved in a similar manner to beam SWP, however, at 94 kN load flexural cracks extended rapidly towards the N.A. Several shear cracks were observed at this load in the shear spans which were arrested by the wings. The flexural cracks at shear span became wider and at 107 kN load the beam failed due to transverse opening at its end and subsequent splitting of the concrete with the wings, plate 5.14. The failure

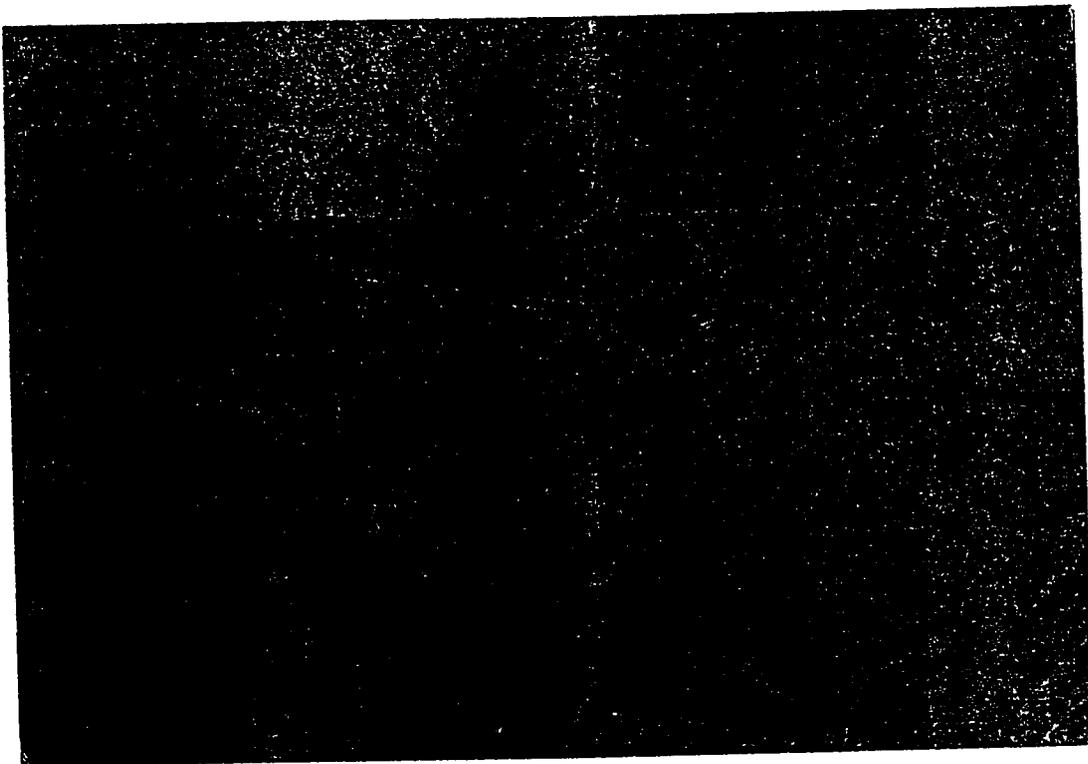


Plate 5.13: Failure Mode of Beam SWP (Separation of the plate End Followed by Ripping off the Wing With Chunks of Concrete).

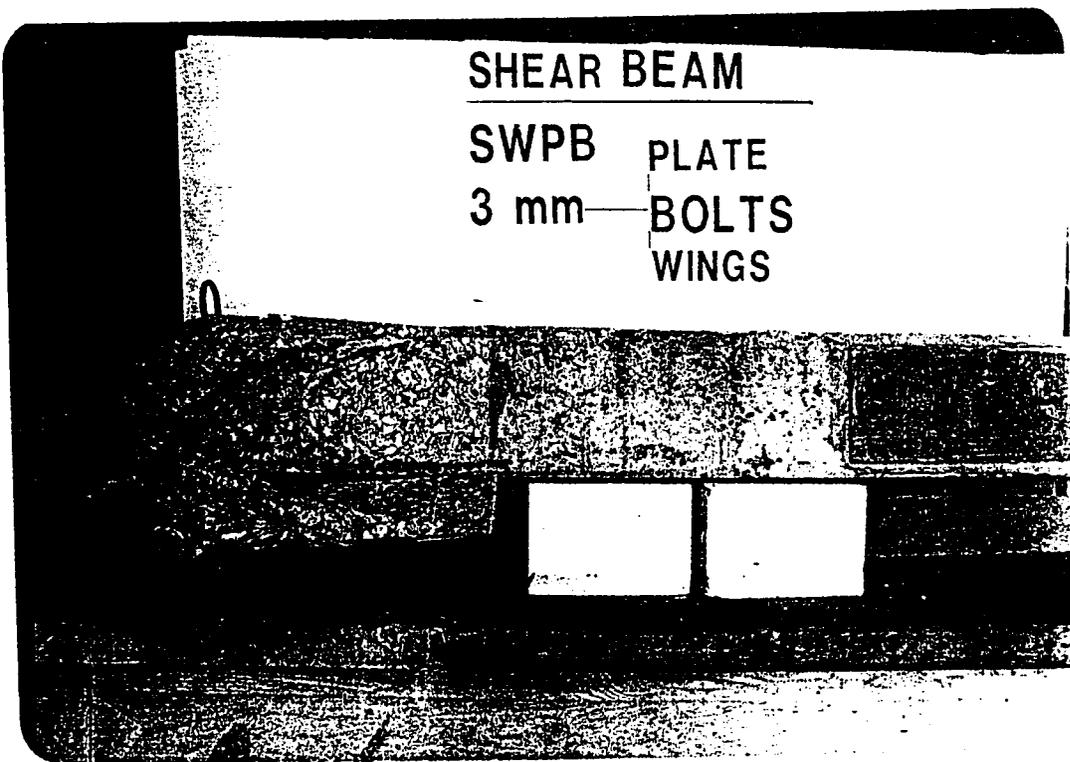


Plate 5.14: Failure Mode of Beam SWPB (Transverse Splitting and Subsequent Opening of the Beam End).

modes for these beams are listed in Table 5.10.

Beams repaired with strips, strips and plate with strips and anchored plate (SS, SSP and SSPB) behaved in a similar manner to those repaired using wings. The original flexural cracks from the preloading stage started to extend upward at a load of 24 kN. At a load of 40 kN new flexural cracks were developed in the shear spans and connected to form diagonal cracks propagated across the strips. The major common observation for all beams was the ripping off strips at failure load.

Beam SS failed due to the formation of longitudinal crack at the beam soffit. The failure was identical to that of beam SW. However, higher ultimate load capacity was obtained using the strips as compared to wings due to lower level of damage, Plate 5.15.

Beam SSP failed by ripping off the strips with concrete and plate separation. The failure was initiated by developing a new shear crack which widens across the strips as the loads levels increased, Plate 5.16.

Beam SSPB again failed by ripping off the strip but without plate separation, plate 5.17.

Beam (SJ) repaired using U-jacket failed in flexure by crushing concrete. The beam was loaded upto 98 kN, then the

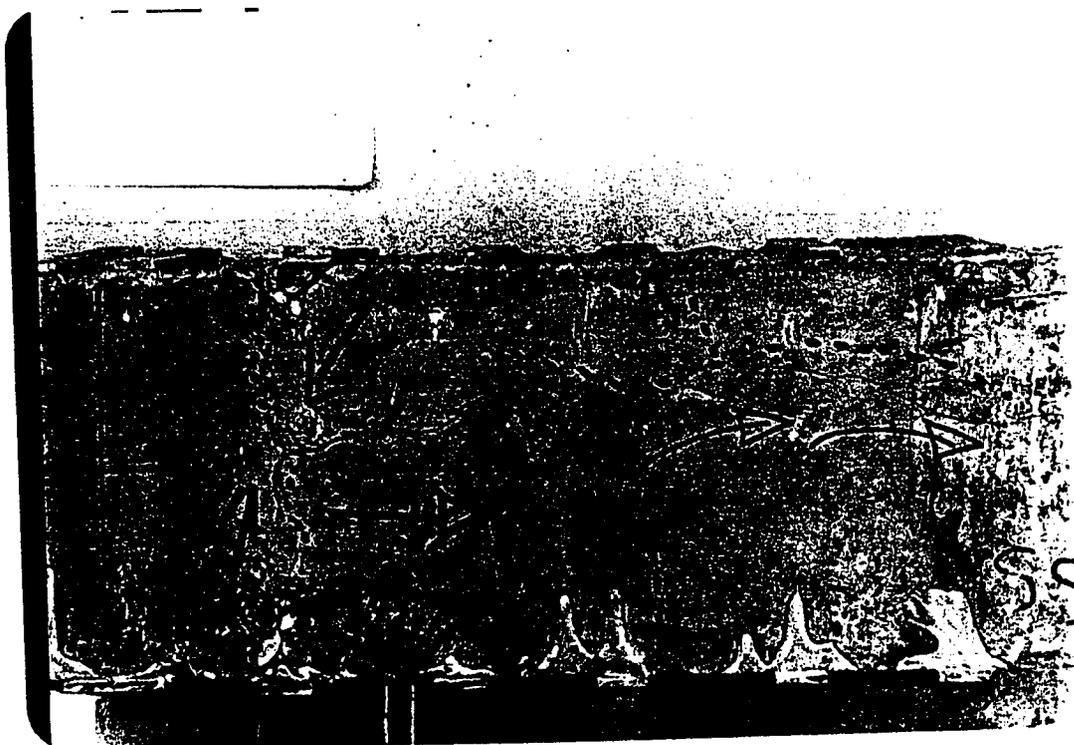


Plate 5.15: Failure Mode of Beam SS (Formation of Longitudinal Crack at the Beam Soffit Causing Transverse Splitting).

3 mm — PLATE

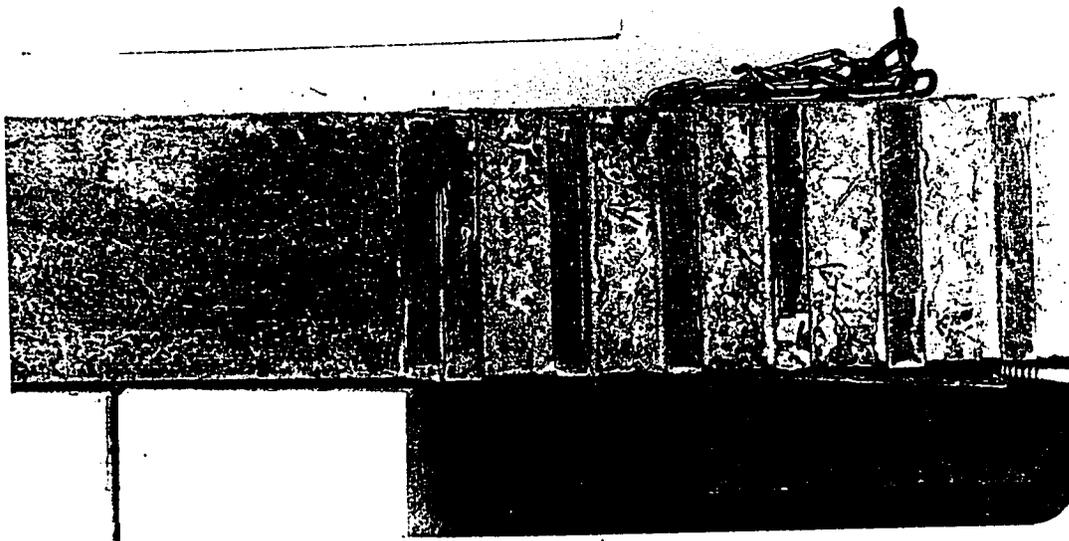


Plate 5.16: Failure Mode of Beam SSP (Ripping off the Strips With Concrete and Subsequent Plate Separation).

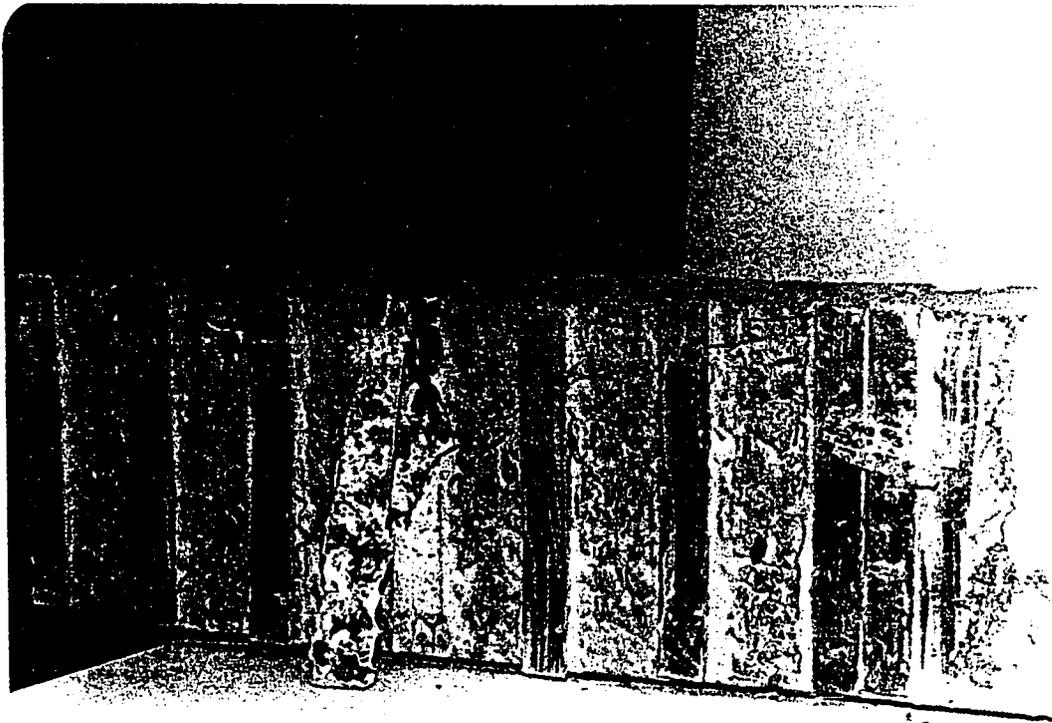


Plate 5.17: Failure Mode of Beam SSBP (Ripping off the Strips With Concrete).

machine was stopped and more precaution was taken before reloading to 105.9 kN load. The LVDTs were removed and the acquisition system was disconnected and the beam was loaded to failure in which the ultimate load reached was 107.0 kN. Wide flexural cracks were detected in the constant moment region, these cracks propagated rapidly upwards and no separation of the jackets were noticed at failure, Plates 5.18 and 5.19.

To confirm the failure mechanism obtained, another beam was tested and similar behavior was noticed. This type of shear repair clearly prevented the shear failure as well as any premature failure that would prevent achieving the full flexural capacity of the beam. The failure modes are shown in Table 5.10.

5.4.2 Load vs. Deflection

The load-deflection curves for shear beams repaired either with wings or with strips are presented in Fig. 5.48 through 5.54. Each plot includes two curves representing the behavior of the beams before and after repair. Fig. 5.48 to 5.50 represent the repair carried out by wings, for beams SW, SWP and SWPB, respectively. As the results show, beam SW was preloaded up to 81% of its ultimate capacity while beam SWPB and SSPB are preloaded up to 79% and 75% prior to repair, respectively

The repaired beams showed an increase in the ultimate capacity as the level of damage is reduced. Beam SS repaired with

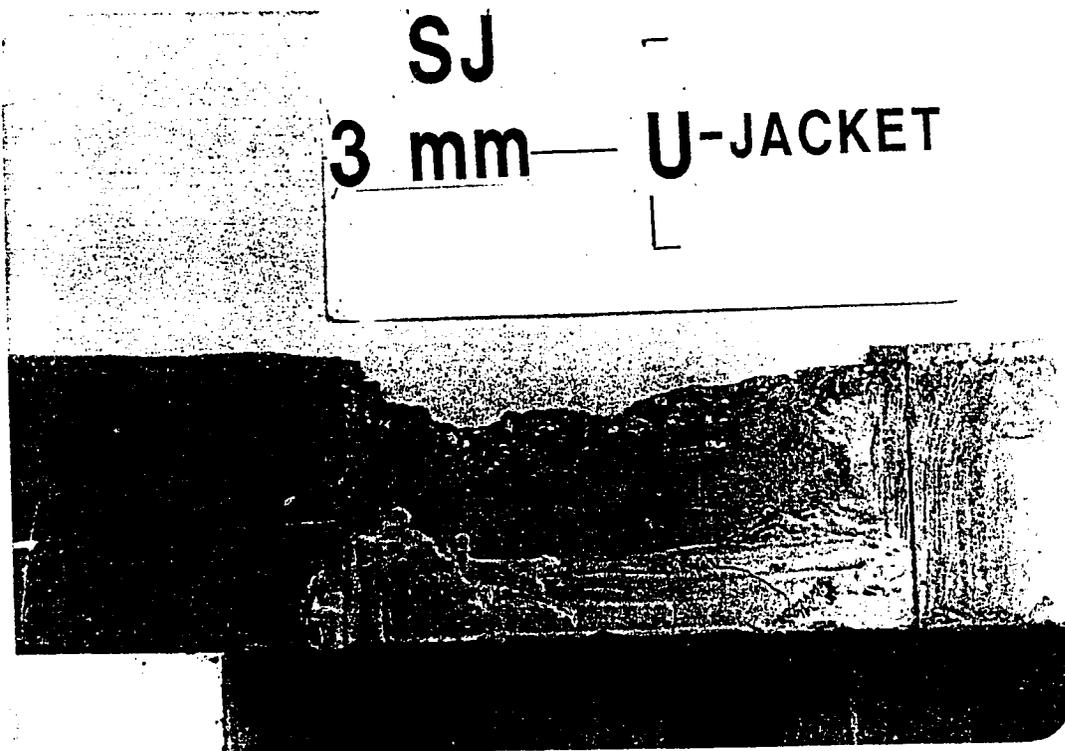


plate 5.18: Failure Mode of Beams SJ (Flexure Failure By
Crushing of Concrete).



Plate 5.19: The shear Span of Beam (SJ) after failure by Crushing of Concrete in the Constant moment Region.

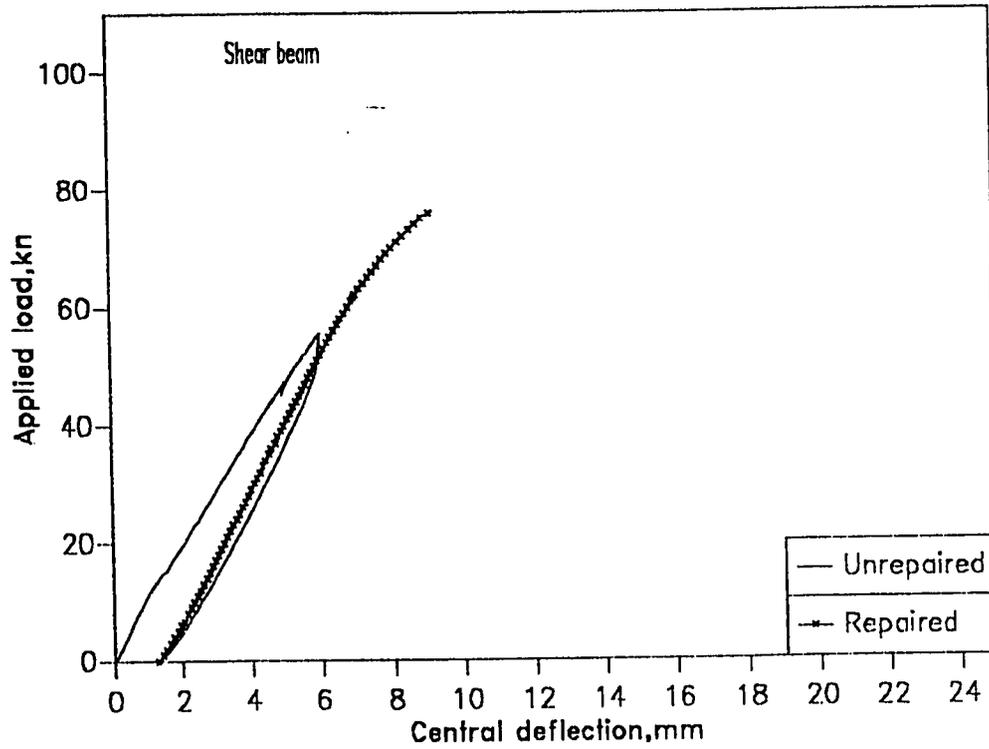


Fig. 5.48 Load vs. Central deflection (Wings only)

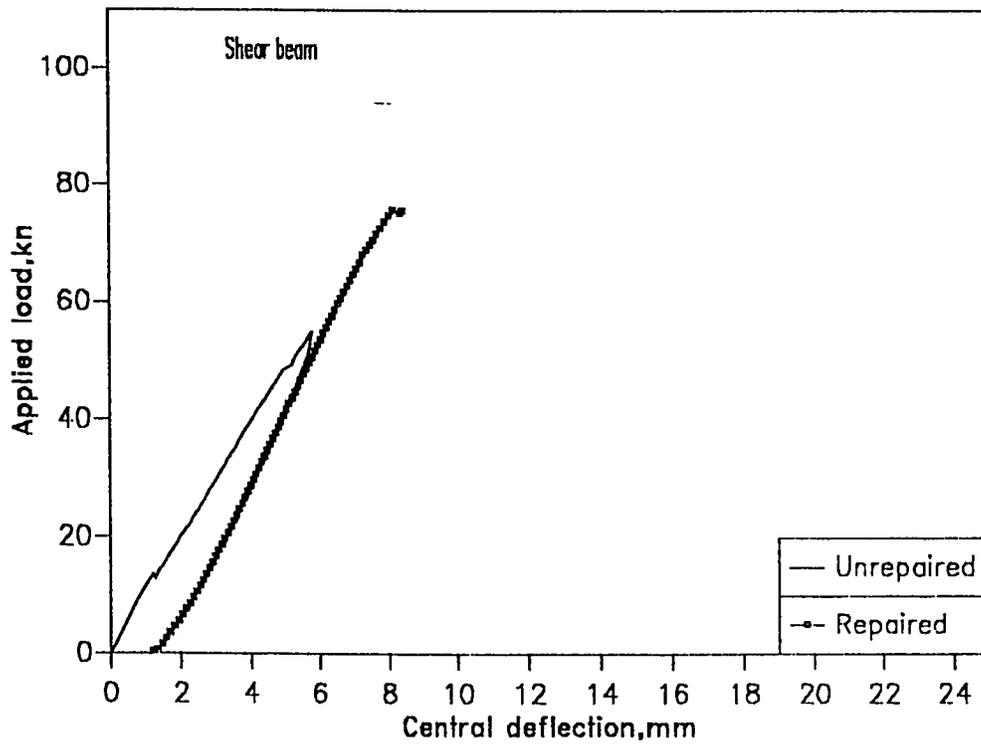


Fig. 5.49 Load vs. Central deflection (wings + bottom plate)

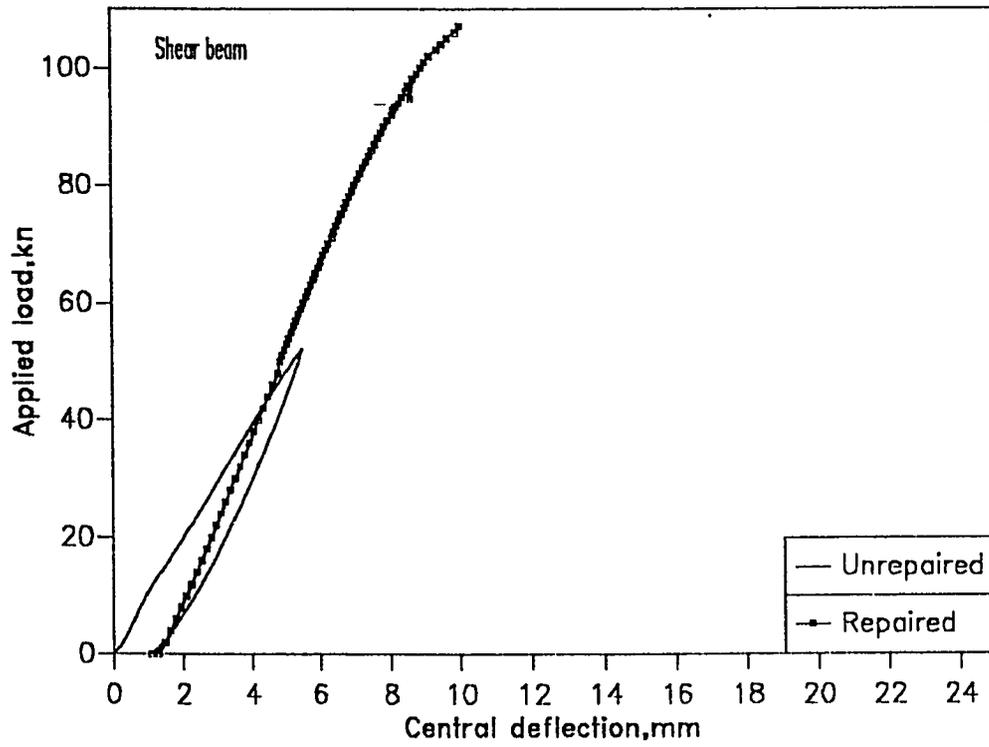


Fig. 5.50 Load vs.central deflection (Anchored plate + wings)

only strips is shown in Fig. 5.51. This beam was expected to achieve lower ultimate load than beam SW, but as it was damaged to lower level (48% of SC) compared to beam SW (81% of SC), Thus, it reached a higher load. Beams SSP and SSPB are shown in Figs. 5.52 and 5.53, respectively. The behavior of these beams was logical because they were preloaded up to the same level of damage like beams SWP and SWPB and for this reason they showed (SSP and SSPB) lower ultimate capacities than beams SWP and SWPB .

Fig. 5.54 shows a beam repaired with strips only after preloading it almost to failure. As the results indicate this beam did not show any improvement in the ultimate strength or in the ductility and could not even achieve the ultimate capacity of the control beam SC (69.1 Kn). The reason behind this is that the preloading level was very close to the ultimate load of the unrepaired beam (SC). Thus, the strips carried the load from the beginning of loading due to the absence of contribution from concrete.

A) Repair Modes:

The results as shown in Fig. 5.55 indicate that all repaired beams for shear showed a significant improvement in the shear capacity and a reduction in ductility compared to the control beam (SC). The behavior of beams SW and SWP were identical

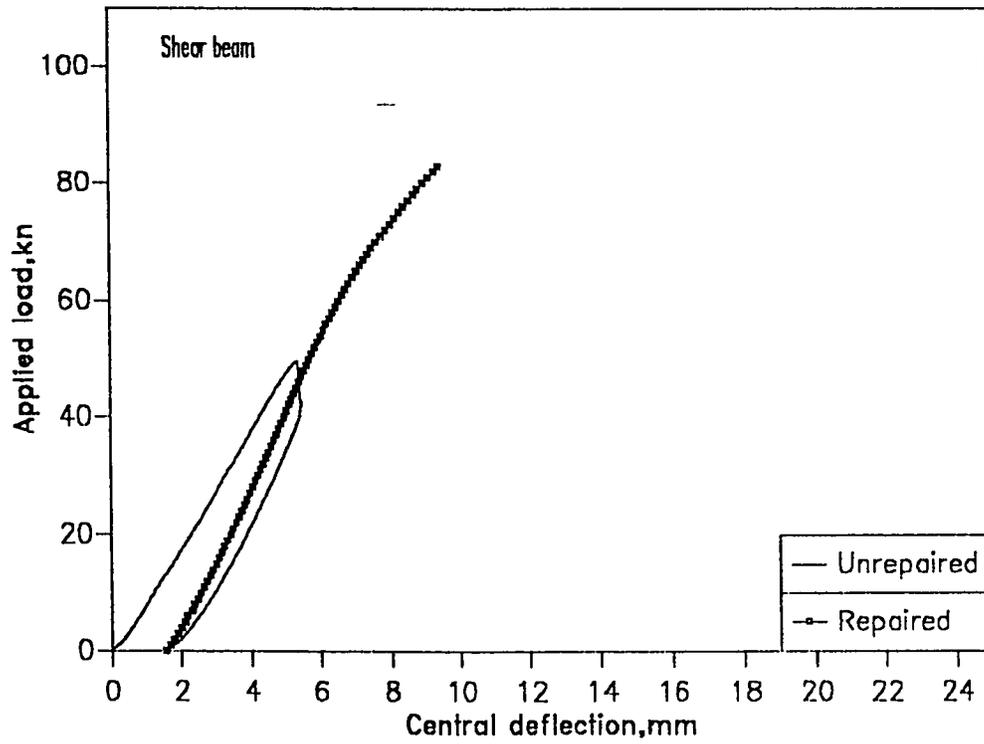


Fig. 5.51 Load vs. Central deflection (Strips only)

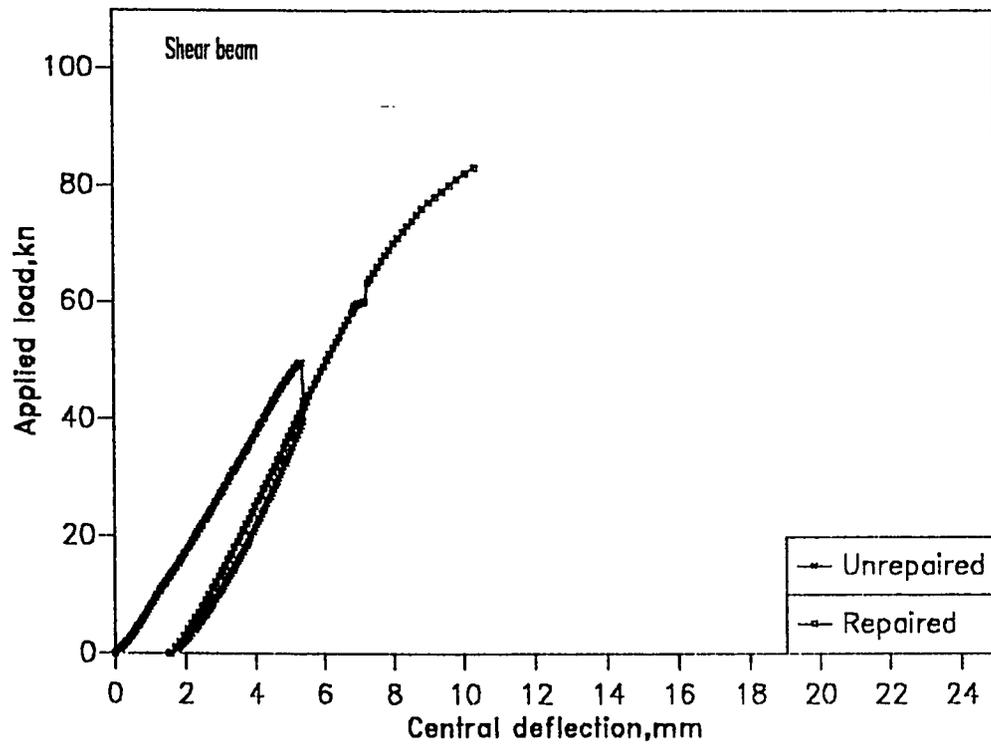


Fig. 5.52 Load vs. Central deflection (Strips + bottom plate)

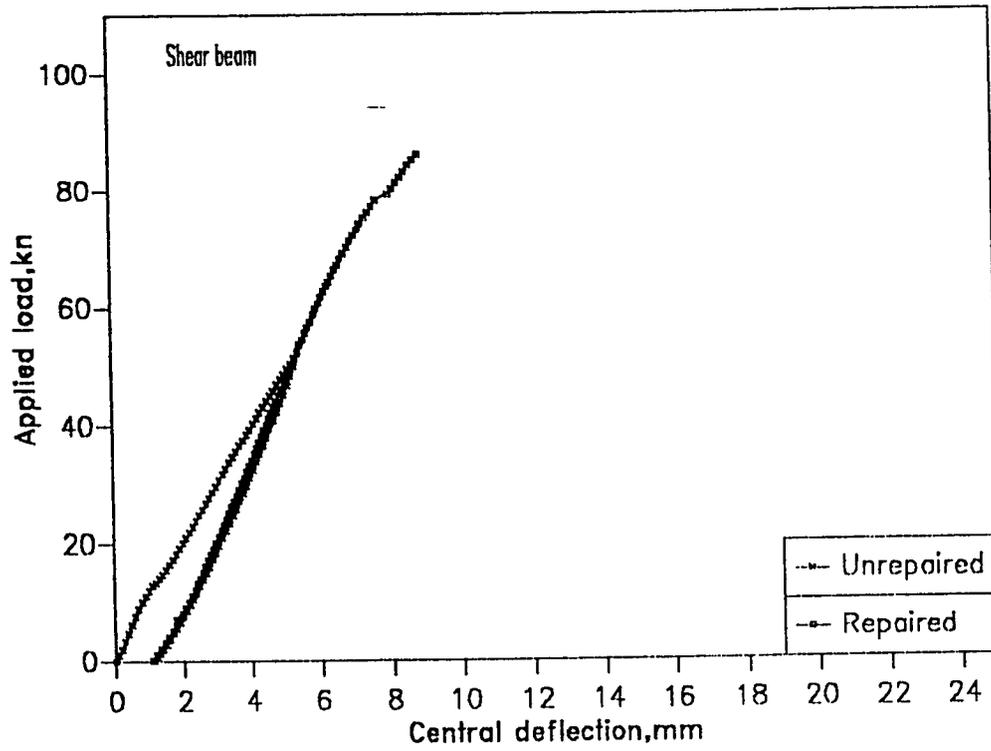


Fig. 5.53 Load vs. Central deflection (Strips + anchored Plate)

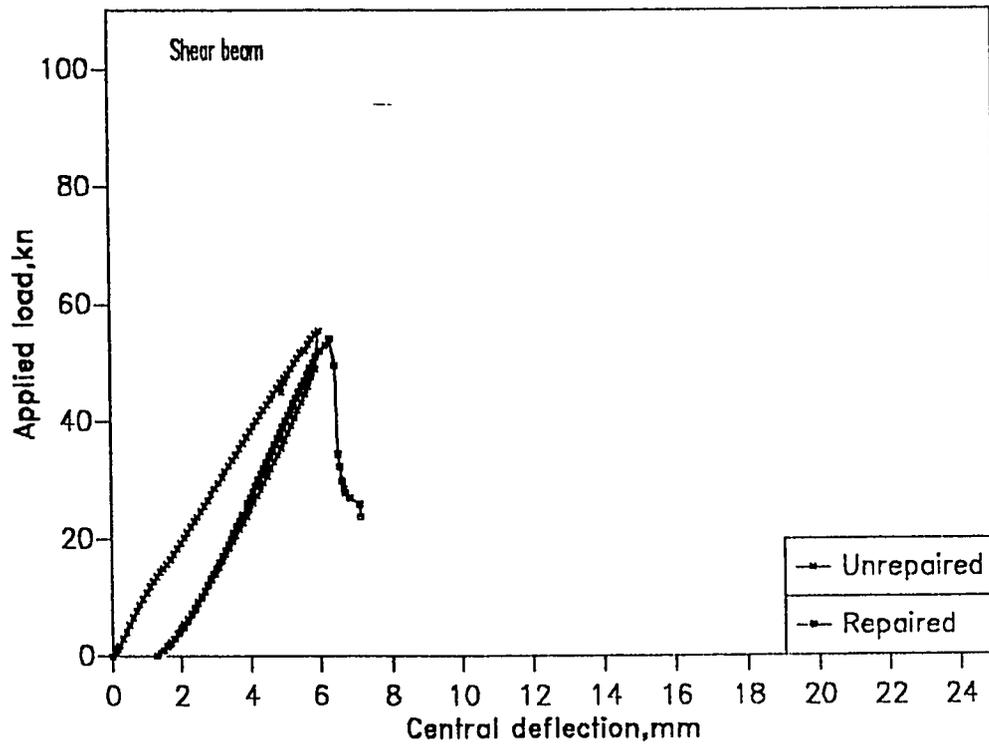


Fig. 5.54 Load vs. Central deflection (strips*)

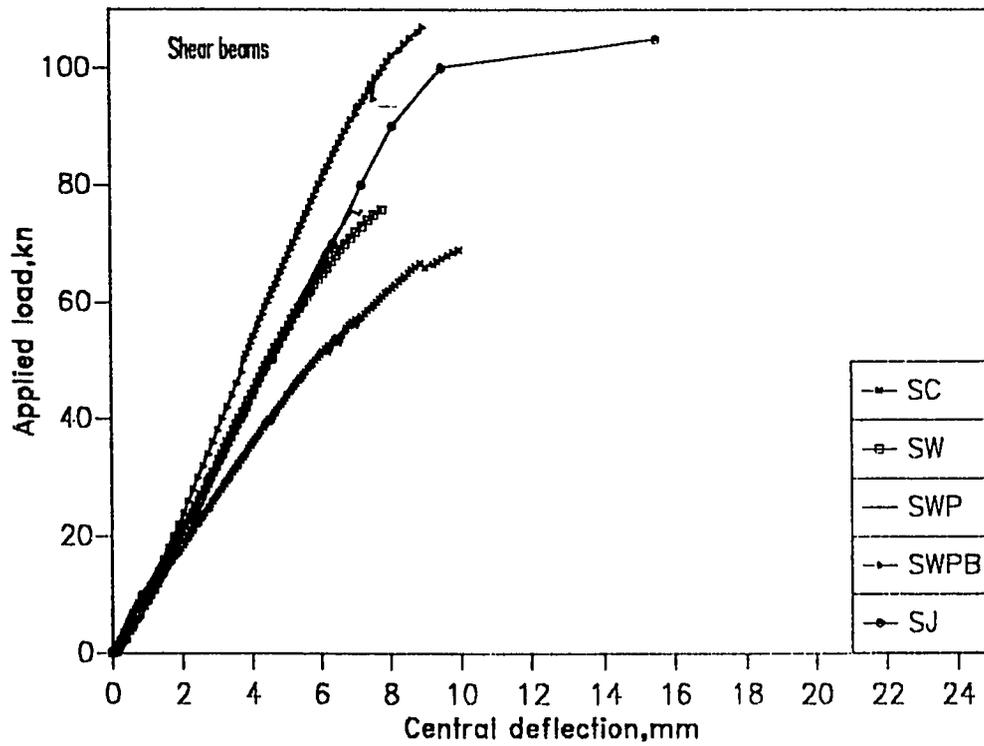


Fig. 5.55 Load vs. Central deflection (Wings and U-Jacket)

which clearly indicates that glueing a fiber glass plate to the tension face of beam SWP improved the shear capacity by 30.1% and reduced the ductility by 29.4%.

Beam SWPB showed a tremendous improvement in the shear capacity ($P_{ult} = 107$ kN), remarkable increase in stiffness and a slight reduction in ductility over beams SW and SWP. The bolts used to anchor the plate effectively arrested the plate debonding and prevented such premature failure. Also, due to the higher level of damage in case of beam SW.

Fig. 5.56 depicts the behavior of the beams strengthened with strips. All the beams showed a significant increase in the shear capacity and no improvement in ductility as compared to the control beam. Table 5.10

Beam SS provided the highest ultimate capacity and ductility compared to the other beams. This behavior was attributed to the small damaging level in the preloading stage. Beams SSP and SSPB behaved in a similar manner and with a remarkable reduction in ultimate strength and ductility relative to beam SS.

Beam SJ behaved in a very ductile manner. Fig. 5.55 shows that the behavior of beam SJ was identical to that of beams SW and SWP upto a load level of 71 kN at which they failed.

The behavior of beam SJ at all load levels was similar to

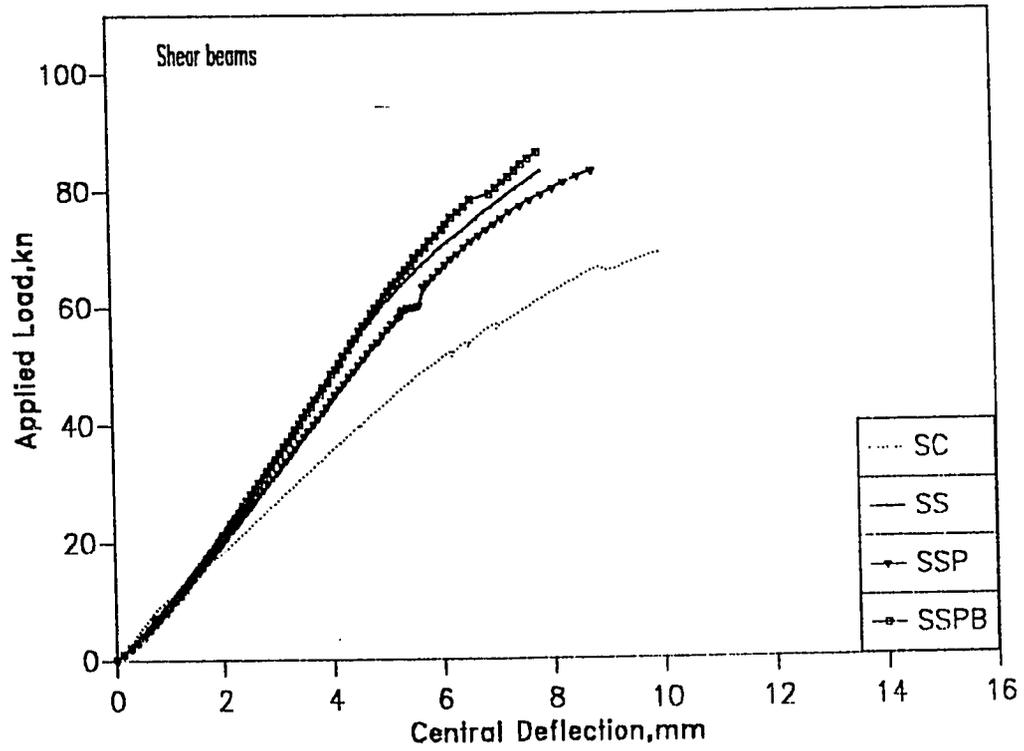


Fig. 5.56 Load vs. Deflection (Different types of repair using strips)

Table 5.10 : Experimental and Theoretical Ultimate Loads of Shear Beams

Beam #	Experimental Ultimate Load (KN)	Theoretical Ultimate Load (KN)	Failure Modes
SC	69.1	93.8	Shear failure (Diagonal crack)
SW	75.8	93.8	Formation of longitudinal crack at the beam soffit causing transverse splitting
SWP	89.9	120	Separation of the bottom plate end followed by ripping off the wings with chunks of concrete
SWPB	107.4	120	Transverse opening at the end of the beam subsequent splitting of concrete with strips
SS	83.0	93.8	Formation of longitudinal cracks at the beam soffit causing transverse splitting
SSP	82.4	120	Ripping off the strip with subsequent plate separation
SSPB	86.2	120	Ripping off the strips and concrete
SJ	107	93.8	Flexural failure by crushing of concrete

that of beam SWPB from strength point of view but its ductility was much more higher due to the efficient anchoring system offered by the jacket. Table 5.11.

The theoretical flexural and shear capacities for shear beams are shown in Table 5.12.

B) Comparison of Wings and Strips:

Fig. 5.57 shows a comparison between beam SW repaired with wings only and beam SS repaired with only strips along with the repaired beam SC. It can be seen from Fig. 5.57 that beam SS behaved in a ductile manner more than beam SW. It is also apparent that beam SS attained higher ultimate capacity than beam SW (9.5%). A possible reason for this is that wings will be subjected to bending as well as biaxial state of stress which tend to pull the wings out. This type of combined effect resulted in failing beam SW prematurely, in addition to that beam SW was damaged more than beam SS prior to repair.

In general, beams SW and SS showed an improvement in ultimate capacity of 9.7% and 20.1% respectively over the control beam SC.

The behavior of beams SWP and SSP is shown in Fig. 5.58 which clearly indicates that both of them behaved in a similar manner except a notable improvement in ductility in case of SSP over

Table 5.11: Improvements in Ultimate Capacity and Ductility for Shear Beams

Beam #	Exp. Ultimate Capacity(kN)	Δ_c mm	% Increase in Ductility	% Increase in Ultimate Capacity
SC	69.1	10.20	--	--
SW	75.79	7.80	-23.5	9.70
SWP	89.90	7.20	-29.4	30.10
SWPB	107.40	9.90	- 2.90	55.40
SS	83.00	10.30	1.00	20.10
SSP	82.4	8.80	-13.70	19.20
SSPB	86.90	7.81	-23.40	25.80
SJ	107.00	15.50	52.00	54.80

Table 5.12 : Theoretical Ultimate Strength of Shear Beam Specimens

Beam #	Ultimate Shear Strength (KN)	Ultimate Flexure Strength (KN)
SC	66.70	93.8
SW	143.3	93.8
SWP SWPB	143.3	120
SS	127	93.8
SSP SSPB	127	120
SJ	143.3	93.8

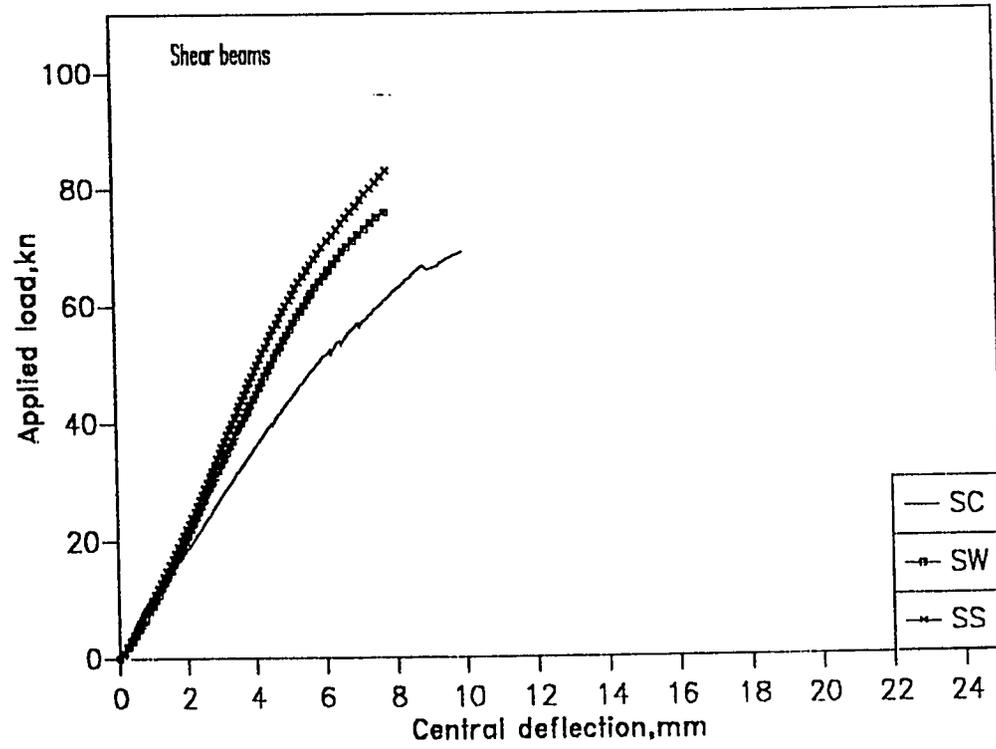


Fig. 5.57 Load vs. Deflection (Comparison between wings and strips)

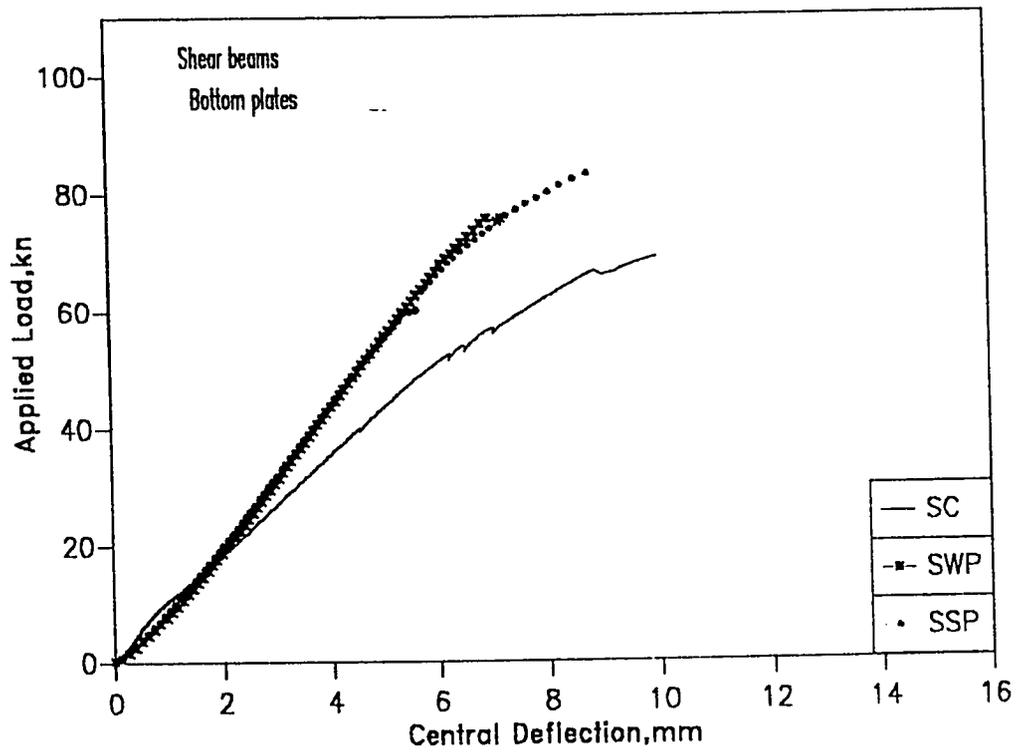


Fig. 5.58 Load vs. Central deflection (Comparison between wings and strips)

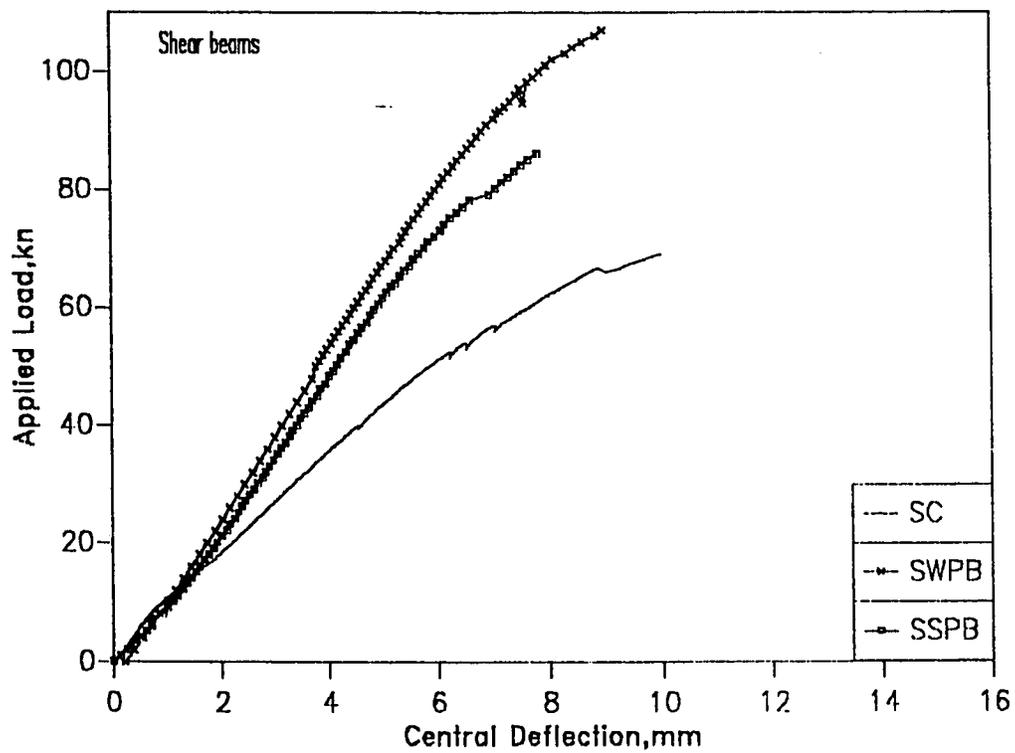


Fig. 5.59 Load vs. Central deflection (Comparison between wings and strips)

SWP in the range of 22.2%. However, the ductility of the beams SWP and SSP was reduced as compared to beam SC by 29.4% and 13.7% ,respectively.

The ultimate capacities of beams SWP and SSP were also improved over beam SC by 30.3% and 19.2%, respectively. Fig. 5.59 depicts the behavior of beam SWPB and SSPB. It clearly indicates that beam SWPB showed an improvement in the ultimate strength over the control beam SC by 54.8% with a slight reduction in ductility in the range of 3%. Beam SSPB offered only 25.8% as an improvement in the ultimate strength and 23.4% as reduction in ductility. Tables 5.11 and 5.13.

5.4.3 Load Vs. Strain

a) Strip Strains

Fig. 5.60 represents the measured strain at the center of the middle strip located at 210 mm from the support of beam SS. The strips started to support shear forces from the early loading stages because of the shear cracks existed in the preloading conditions. The strain in the strip almost reached the ultimate strain the fiber indicating the high force carried by the strip just before beam failure. The strain gauge worked properly upto failure, the reduction in strain beyond the 80 kN load was due to the relief of loads from the strip after its debonding from the beam. At failure the shear crack opened and caused the debonding of the strip.

Table 5.13: Comparison of Experimental and Theoretical Loads for Wings and Strips

Repair Mode	Exp. Load (kN)	Theo. Load (kN)
(Strips)		
a) Rupturing	--	146
b) Ripping	88.6	126
(Wings)		
a) Rupturing	--	210
b) Ripping	91	107.0

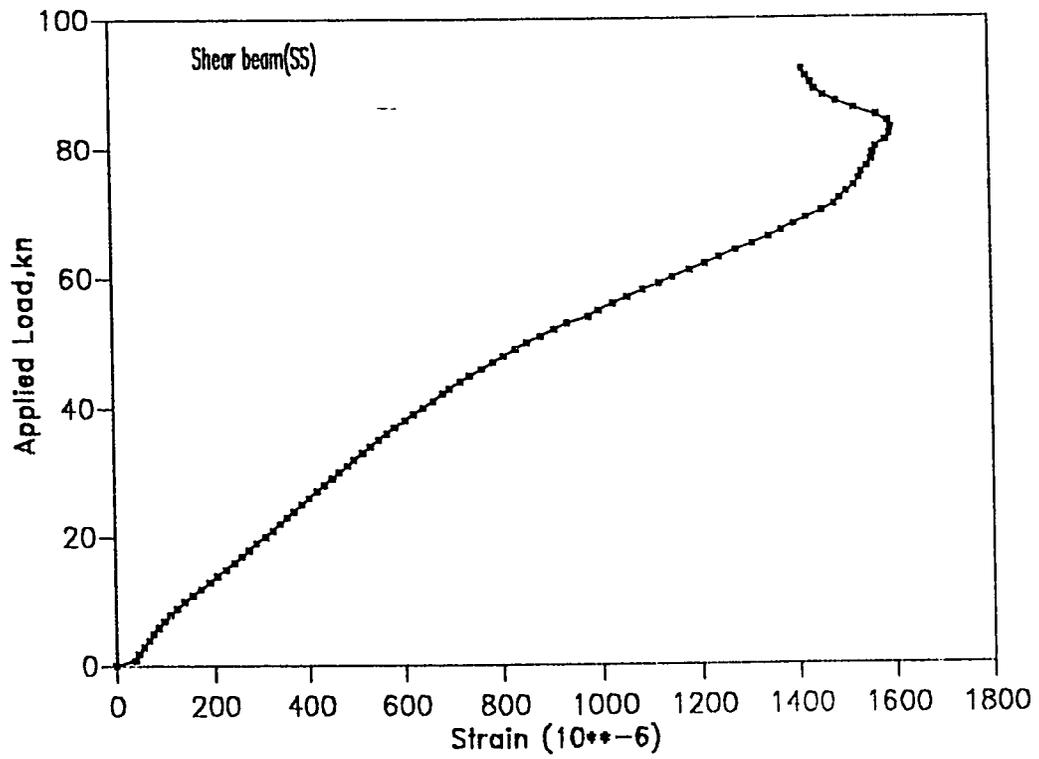


Fig. 5.60 Load vs. Strain at center of a strip located at 220 mm from the beam end

b) Rebar Strains

The load-strain curves for the strains along the rebars are shown in Fig. 5.61. The results indicate that the steel yielded at all locations which agrees with the under reinforced failure (crushing of concrete).

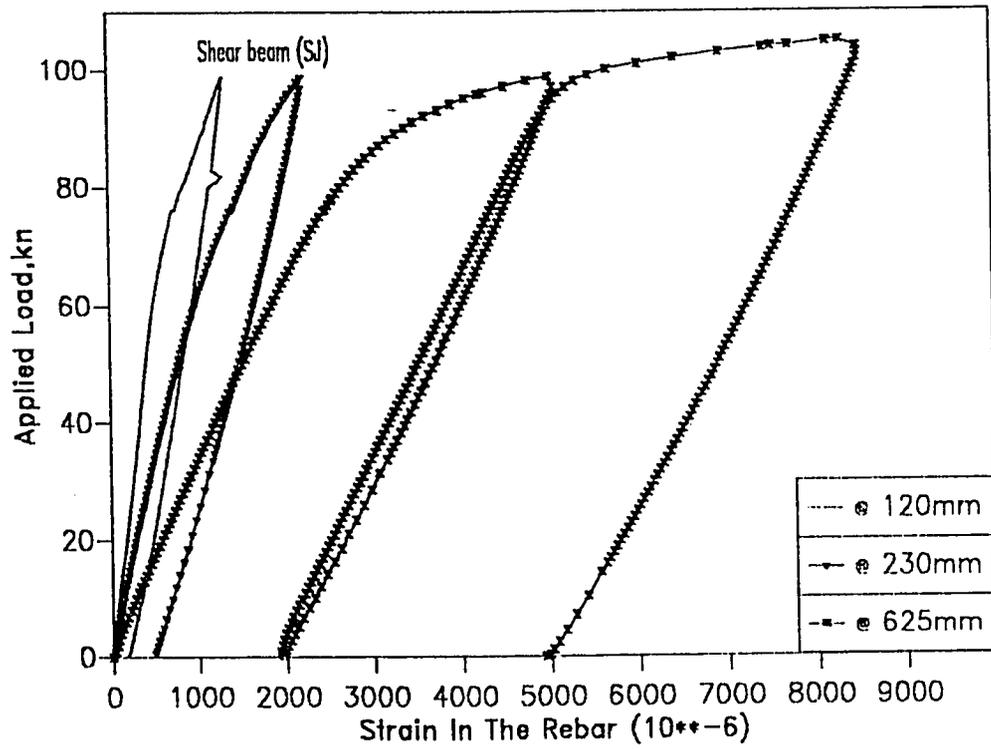


Fig 5.61 Load vs.Rebar strain at different locations for beam repaired with U-Jacket

Chapter 6

DESIGN CONSIDERATIONS FOR REPAIR IN FLEXURE

6.1 GENERAL

In recent years, systematic experimental investigations of various factors which influence the performance of plated concrete beams such as the plate thickness and the thickness of the adhesive layer, have been reported by many researchers [21,27,24,25,30]. These investigations show that the bonding of thin plates to the tension face of concrete beams can lead to a significant improvement in structural performance, under both service and ultimate load conditions. However, increasing the thickness of the plates may result in premature failure due to "ripping off" of the concrete cover along the level of conventional internal reinforcement, at the ends of the plate, Fig. 6.1.

6.2 EVALUATION OF THE PLATE THICKNESS

As shown in Figs. 6.2 and 6.3 the fiber glass is a ductile composite but did not have a defined yielding point and a plastic plateau similar to the steel behavior. The performance of the fiber glass plates depends on the glass content (%), type of the fiber glass material used and the amount of the resin (%) applied to bind

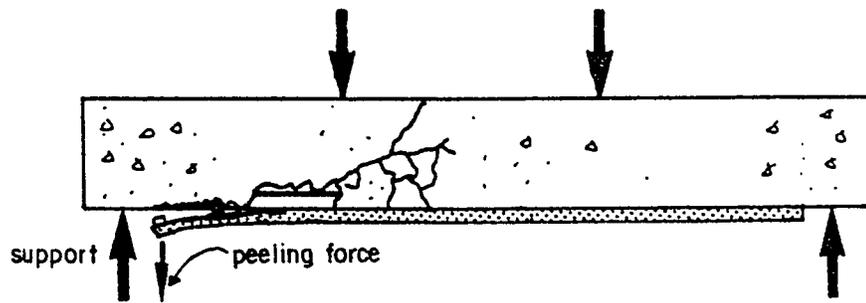


Fig.6.1: Peeling Force at The End of the Plate

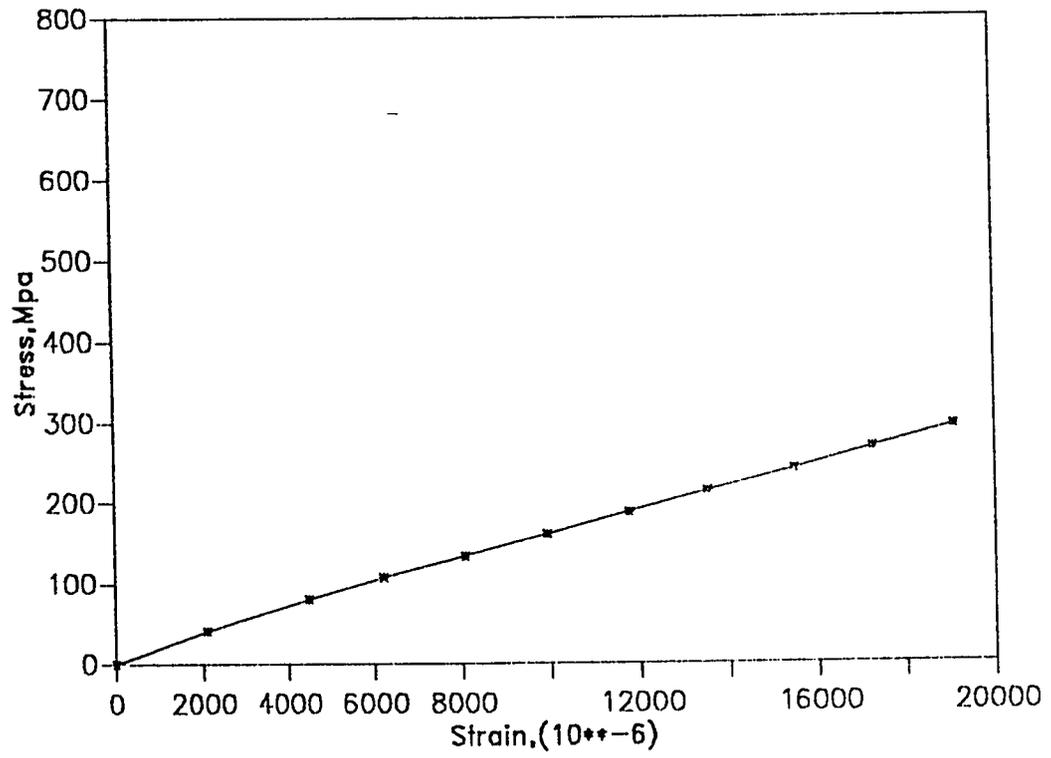


Fig. 6.2 Stree-Strain curve of the fiber glass material

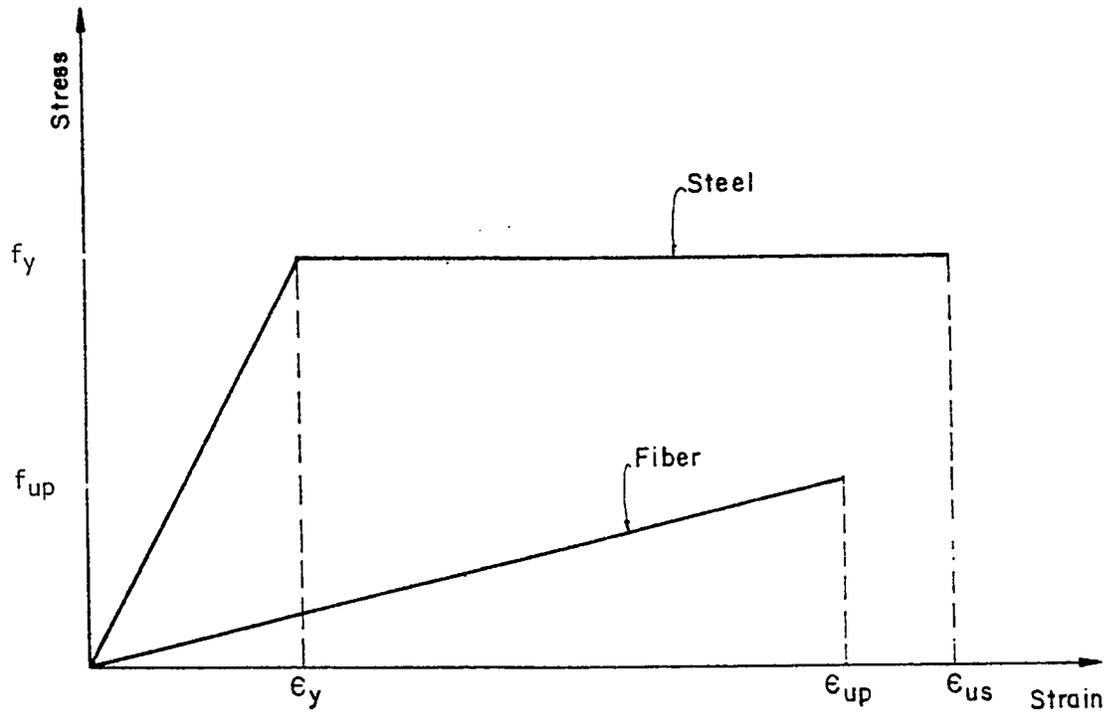


Fig. 6.3 : Idealized stress-strain curves for steel and fiber glass

the fiber glass. Thus each fiber composite has its own stress-strain curve, modulus of elasticity (E) and ultimate strain (ϵ_{up}) however, the overall behavior of the material is elastic upto failure. It is difficult to generalize an optimum thickness for the fiber glass plate to be used for repair any flexure beam in practice. Thus the plate thickness is designed based on the following:

A) Ultimate Flexural Capacity of the Section

Assumptions:

- Full composite action (no slip)
- Concrete strength (ϵ_c) = 0.003 at ultimate
- The fiber glass strain (ϵ_p) = ϵ_{up}

From compatibility and equilibrium of the section the plate thickness is evaluated as follows:

From equilibrium:

$$(\Sigma H = 0):$$

$$C_s' + C_c = T_s + T_p$$

$$A_s' * f_s' + 0.85 * f_c' * a * b = A_s * f_y + A_p * f_p$$

where:

$$a = \beta_1 * X_b \quad \text{and} \quad A_p = t_p * b$$

The plate width is taken as the width of the beam.

$$A_s' * f_s' + 0.85 * f_c' * \beta_1 * X * b = A_s * f_y + t_p * f_{up}$$

$$t_p = \left(\frac{A_s' * f_s' + 0.85 * f_c' * \beta_1 * X * b - A_s * f_y}{b_p * f_{up}} \right) \quad (3)$$

The plate thickness calculated from this expression is representing the minimum thickness (t_{min}) which is corresponding to the ultimate strain (ϵ_{up})

B) Maximum interface shear and normal stresses

Using Robert's formulation (31) to evaluate the plate thickness which yields the maximum shear and normal stresses. The maximum shear stress for the fiber glass (τ_0) was considered to be 2 N/mm^2 . The plate thickness is evaluated by trail and error because it is difficult to obtain it from the closed form of the formula. The thickness calculated from Robert's formulation is considered the maximum thickness which causes peeling of the plate.

The maximum shear and the normal stresses are given as follows:

$$\tau_0 = \left\{ F_0 + \left(\frac{k_s}{E_p * t_p * b_p} \right)^{\frac{1}{2}} * M_0 \right\} * \frac{b_p * t_p}{I * b_p} * (D - X)$$

$$\sigma_0 = \tau_0 * t_p * \left(\frac{k_n}{4 * I_p * b_a} \right)^{\frac{1}{4}}$$

where,

$$X = \frac{-B + (B^2 + 4 * A * C)^{\frac{1}{2}}}{2 * A} \quad (A_1)$$

$$A = \frac{E_c * b}{2 * E_p} \quad ; \quad B = A_s + b_p * d_p \quad (A_2)$$

$$C = d * A_s + D * d_p * b_p \quad (A_3)$$

$$I = \frac{E_c * b * X^3}{3 * E_p} + A_s * (d - X)^2 + b_p * d_p * (D - X)^2 \quad (A_4)$$

$$I_p = \frac{b_p * d_p^3}{12} \quad (A_5)$$

$$K_s = G_a * \frac{b_a}{d_a}$$

$$K_n = E_a * \frac{b_a}{d_a}$$

$$F_0 = \frac{P_{ult}}{2}$$

$$M_0 = F_0 * \frac{(h + d_p)}{2}$$

The calculated thicknesses in (A) and (B) representing the lower and the upper limits for the plate thickness to be used in repair. Thus, the beam which strengthened with a plate thickness within these two limits will be safe from rupturing as well as peeling.

Three different reinforced concrete beams loaded under the mid-third points will be presented here. Table 6.1 shows the dimensions and reinforcement of these beams. The methodology for evaluating the plate thickness is illustrated in Appendix (A) on the beam specimen used in the experimental investigation.

DISCUSSION OF THE RESULTS

Table 6.2 represents the results of the numerical examples which shows that the minimum plate thickness increases with increasing the beam cross section and the main steel. A practical plate thickness of 1 mm should be used due to manufacturing limitations. The recommended plate thickness to be used for a certain beam is the average value of the minimum and the maximum plate

Table 6.1: Numerical Examples Data

Item	Case 1	Case 2	Case 3
Concrete dimension	150x150	200x450	250x500
ρ_b	0.039	0.039	0.039
A_b	157mm ²	843mm ²	1170mm ²
ρ_s	24% ρ_b	24% ρ_b	24% ρ_b
ρ'	0.0	0.0	0.0
b	100mm	150mm	200mm

thicknesses causing rupturing and peeling of the plate ,respectively.

The expermintal load p_{exp} was compared with two different theoreticl values calculated using two different approaches as follows:

- 1) Theoretical load (P_f) based on crushing of concrete using the general form equation as described in chapter 4.
- 2) Theoretical load (P_{inf}) based on peeling or interface shear failure of the plate at its end using Robert's formulation (31).

As the results indicate , the ultimate load of the beam FP1 was not calculated by Robert's formulation because the failure of this beam was by rupturing of the plate rather than separation of the plate due to interface shear failure. It is clear that beam FP2 could not reach its ultimate theoretical capacity due to the premature failure occurred by plate separation which is also clear from the value calculated by Robert's equation (65.5 KN Compared to 63.5).

Beam FP3 also failed by plate separation but the ultimate load calculated by Robert's equation did not conform the value obtained expermintally which means that this equa-

tion doesn't give representative results at higher plate thicknesses. Table 6.3

Calculations of maximum interface shear stress and normal stress (appendix A) showed that the interface shear stress exceeded its limiting value ($\tau_0 = 2 \text{ N/mm}^2$) while the normal stress was less than the limiting value ($\sigma_0 = 2 \text{ N/mm}^2$). It is clear that using a plate thickness of 3 mm will result in peeling its end thus, for such beam the plate thickness to be used should be less than 3 mm and more than 1 mm. It is recommended to use an average plate thickness ($t_{\text{recommended}}$) or less due to economical considerations and to ensure a ductile behavior of the beam. Table 6.2

Table 6.2 Results of Numerical Examples

Case #	Concrete Dimensions	ρ_s	t_{min} (mm)	t_{max} (mm)	t_{opt} (mm)
1	150 * 150 mm	24% ρ_b	1	3	2
2	200 * 450 mm	24% ρ_b	1	4.5	3
3	250 * 500 mm	24% ρ_b	1	6.1	3.5

Table 6.3 : Comparison Between Experimental and Theoretical Loads

Beam #	Ultimate Experimental* Load P_{exp} (KN)	Ultimate Theoretical Load Base on Crushing of Concrete P_f (KN)	Ultimate Theoretical Load Using Robert's Eq. P_{inf} (KN)	Failure Modes
FP1	62.4	59.0**	61.9	Rupturing of the plate.
FP2	63.5	74.8	65.5	Separation of the plate and the concrete cover.
FP3	64.4	76.0	72.6	Separation of the plate and the concrete cover.

* P_{exp} should be smaller than the least of P_f and P_{inf}

** Based on rupturing of the plate.

Chapter 7

CONCLUSIONS AND RECOMMENDATIONS

CONCLUSIONS

A) Fiber Glass and Glue

- 1) Fiber glass is a brittle material with a very low modulus of elasticity and high toughness.
- 2) The epoxy used ensured excellent bond between the concrete surface and the fiber glass plate.
- 3) The effect of accelerated thermal cycling reduces the bond strength between the fiber glass plate and the concrete surface.

B) Flexure Damaged Repair

- 4) The ultimate strength of beams repaired for flexural damage generally increased by 60%.
- 5) The effect of peeling and debonding of the fiber glass plates at its curtailments prevent the beam from achieving the ultimate flexural capacity.

- 6) The peeling and shear stresses at the plate ends is directly proportional to the plate thickness.
- 7) Highest rigidity was obtained for repaired beams with anchored plates and wings in their shear spans.
- 8) The use of I-shaped fiber glass jacket for flexural repair proved the best performance in terms of anchoring scheme.

C) Shear Damged Repair

- 9) The external shear reinforcement used as wings or strips generally improved the shear strength of the repaired beams by 26%-32%.
- 10) Shear damaged beams repaired by strips and wings have not reached their ultimate flexural capacity due to ripping off fiber glass.
- 11) Shear damaged beams repaired by U-shaped fiber glass jacket reached the flexural capacity which showed high strength and ductility.

RECOMMENDATIONS

For further studies, the following points are suggested:

- 1) To investigate the Performance of repaired beams under

normal exposure.

- 2) To study the effects of cycling loading on repaired beams.

REFERENCES

- 1) Van Gemert, D.A. "Repairing of Concrete Structures by Externally Bonded Steel Plates", Proc. ICP/RILEM/IBK Internat Symposium on Plastics in Material and Engineering, Prague, June 1981; Elsevier Scientific Co., 1982, pp. 519-526.
- 2) Breson, J., "Realization Pratique d'un renforcement par Collage d'armatures", Annales de l'ITBTP, suppl. 278, February 1971, pp. 50-52.
- 3) Breson, J., "Realization par Collage d'armatures du passage inferieur du CD126 Sous l'autoroute du Sud", Annales de l'ITBTP, serie. Beton, Beton arme', suppl. 297, September 1972, pp. 3-24.
- 4) Iino, T., Otokawa, K., "Application of Epoxy Resins in Strengthening of Concrete Structures", Proc. Third Internal Congress on Polymers in Concrete, Koriyama, Japan, May 1981, Vol. II, pp. 997-1011.
- 5) Ryback, M., "Reinforcement of Bridges by Gluing of Reinforcing Steel", RILEM Materials and Structures, 16, No. 91, January 1981. pp. 13-17.
- 6) Fleming, C. J., King, G.E. M., "The Development of

Structural Adhesives for Three Original Uses in South Africa", RILEM Internat. Symposium, Synthetic Resins in Building Construction, Paris, 1967, pp. 75-92.

- 7) Hugenschmidt, H., "Epoxy Adhesive for Concrete and Steel", Proc. First Internat. Congress on Polymers in Concrete, London, May 1975, The Construction Press Ltd., Hornby, 1976, pp. 195-209.
- 8) Lander, M., Webber, C., "Concrete Structures with Bonded External Reinforcement", EMPA Report No. 206, Dübendorf, 1981.
- 9) Mander, R. F., "Bonded External Reinforcement, A Method of Strengthening Structures", Department of the Environment Report, Quinton Interchange of the M5 Motorway, 1974.
- 10) Davies, B. L., Powell, J., "Strengthening of Brinsworth Road Bridge, Rotherham", LABSE, 12th Congress, Vancouver, BC, September 1984, pp. 401-407.
- 11) Reinforcing Methods for Bridges, Proc. 23rd Annual Meeting of Civil Engineering, Nov., 1975, Public Works Institute, Ministry of Construction, Japan.
- 12) Raithby, K.D., "External Strengthening of Concrete Bridges with Bonded Steel Plates", Department of the Environment, Department of Transport, TRRL Supplementary Report 612,

Crowthorne, 1980, (Transport and Road Research Laboratory).

- 13) Calder, Ajj. "Exposure Tests on Externally Reinforced Concrete Beams Performance After 10 years", Department of the Environment, Department of Transport, TRRL RR 129, Crowthorne, 979 (Transport and Road Research Laboratory).
- 14) Breson, J., "Reinforcement par Collage d'ormatures du passage inferieur du CD126 Sous l'utoroute dy Sud", Annales de l'Institut Technique du Batiment et des Travaux Publics, serie. Beton, Beton arme', No. 122, Supplement No. 297, September 1972, pp. 3-24.
- 15) Breson, J., "Nouvelles Recherches et Applications Concernant l'utilisation des Collages dans les Structures", Beton Plaque, Annales de l'Institut Technique du Batiment et des Travaux Publics, serie. Beton, Beton arme', No. 116, Supplement No. 278, February 1971, pp. 23-49.
- 16) Hugenschmidt, H., "Epoxy Adhesive for Concrete and Steel", Proc. First Internat. Congress on Polymers in Concrete, London, May 1975, The Construction Press Ltd., Hornby, 1976, pp. 195-209.
- 17) Lander, M., "Field Measurements on Subsequently Strengthened Concrete Slabs", Douglas McHenry International Sympo-

- sium on Concrete and Concrete Structures, Publication SP-55, American Concrete Institute, Detroit, 1978. pp. 481-492.
- 18) Sommerard, T., "Swanley's Steel-Plate Patch-up", *New Civil Engineer*, No. 244, 16 June 1977, pp. 18-19.
 - 19) Irwin, C. A., "The Strengthening of Concrete Beams by Bonded Steel Plates", TRRL Supplementary Report 160 UC, Transport and Road Research Laboratory, Dept. of the Environment, Crowthorne, 1975, p. 8.
 - 20) Macdonald, M. D., "The Flexural Behavior of Concrete Beams with Bonded External Reinforcement", TRRL Supplementary Report 415, Transport and Road Research Laboratory, Dept. of the Environment, Crowthorne, 1978, p. 13.
 - 21) Jones, R., Swamy, R. N., Bloxham, J. and Bouderalah, A., "Composite Behavior of Concrete Beams with Epoxy Bonded External Reinforcement", *The International Journal of Cement Composites*, Vol. 2, May 1980, pp. 91-107.
 - 22) Jones, R., Swamy, R. N., Bloxham, J. and Bouderalah, A., "Crack Control of Reinforced Beams Through Epoxy Bonded Steel Plates", *Proc. International Conference on Adhesion Between Polymers and Concrete*, September 1986, pp. 542-555.

- 23) Swamy, R. N. Jones, R., Bloxham, J. W., "Structural Behavior of Reinforced Concrete Beams Strengthened by Epoxy-Bonded Steel Plates", The Structural Engineer, 65A, No. 2, February 1987, pp. 59-68.
- 24) Jones R., Swamy, R. N. Sharif, A., "Plate Separation and Anchorage of Reinforced Concrete Beams Strengthened by Epoxy-Bonded Steel Plates", The Structural Engineer, Vol. 66, No. 511, March 1988, pp. 85-94.
- 25) R. N. Swamy, R. Jones, A. Sharif, "The effect of External Plate Reinforcement on the Strengthening of Structurally Damaged RC Beams", Ph.D. Thesis, University of Sheffield, July 1983, 358 p.
- 26) Basunbul, I.A. Gubati, A. A., Al-Sulaimani, G. J. and Baluch, M. H., "Repaired Reinforced Concrete Beams", ACI Material Journal, Vol. 87, NO. 4, July-August, 1990, pp. 348-354.
- 27) Saadatmanesh, H. and Ehsani, M. R., "Fiber Composite Plates Can Strengthen Beams", Concrete International, March 1990, pp. 65-70.
- 28) Saadatmanesh, H. and Ehsani, M. R. (1990), "Fiber Composite Plates for Strengthening Bridge Beams", Elsevier Science Publishers Ltd., England.

- 29) Saadatmanesh, H. and Ehsani, M. R. (1991), "Strengthened with GFRP Plates I: Experimental Study", J. Struct. Engrg. ASCE, 117 (11).
- 30) Philip, A. Ritchie, David, A. Thomas, Le-Wu Lu and Guy M. Connelly, "External Reinforcement of Concrete Beams Using Fiber Glass Reinforced Plastics", ACI Structural Journal, Vol. 88, No. 4, July-August, 1991, pp. 490-500.
- 31) Roberts, T. M., "Approximate Analysis of the Shear and Normal Stress Concentrations in the Adhesive Layer of Plated RC Beams", The Structural Engineer, 67, No. 12, 20 June, 1989, pp. 229-233.
- 32) ACI Committee 503, "Use of Epoxy Compounds with Concrete", ACI Journal, September 1979, pp. 614-645.
- 33) Schutz, Raymond J., "Properties and Specifications for Epoxies Used in Concrete Repair", Concrete Construction, Oct. 1984, pp. 873-878.
- 34) Wang, Chu-kia and Salmon, Charles, G. "Reinforced Concrete Design", Third edition, New York, Harper and Row, Publishers, Inc., 1979.

APPENDIX

CALCULATIONS OF ULTIMATE CAPACITIES OF REPAIRED BEAMS

A) *Ultimate Flexural Capacity of Beam FJ*

The ultimate flexural capacity of beam FJ repaired with the I-Jacket can be determined from the general formula (eq. No.1) Due to the steel hardening the modulus of elasticity for the linear part of the stress-strain curve can not be used. Applying the assumptions and following the same procedures described in sec.(4.2), the ultimate capacity is calculated as follows:

$$\text{Let } (\epsilon_p) = (\epsilon_{up})$$

$$= 0.018615$$

From compatability, the depth of the neutral axis is (X) determined,

$$X = 32.3 \text{ mm}$$

Strain in the rebars is also determined from compatability;

$$\epsilon_s = 0.0075$$

From stress-strain curves for steel and fiber glass the cor-

responding stresses are determined;

$$f_p = 181.8 \text{ N/mm}^2$$

$$f_s = 736.0 \text{ N/mm}^2$$

Total Compression force (C) is found as follows;

$$C = 0.85 * 37.7 * 0.8 * 32.3 * 150$$

$$C = 1.24 \text{ KN}$$

Total Tension force (T) is found as follows;

$$T = 157 * 736.0 + 3 * 150 * 181.8$$

$$T = 1.974 \text{ KN}$$

$$C \neq T$$

Reduce the value of the plate strain (ϵ_p)

$$\epsilon_p = 0.3 * \epsilon_{up}$$

$$= 0.3 * 0.018615$$

$$= 0.005585$$

$$f_p = 100 \text{ N/mm}^2$$

$$X = 53.3 \text{ mm}$$

$$\epsilon_s = 0.00336$$

$$f_s = 581.8 \text{ N/mm}^2$$

$$C = 2.050 \text{ KN}$$

$$T = 1.363 \text{ KN} , \quad C \neq T \quad (\text{N.K})$$

Increase the value of the plate strain (ϵ_p)

$$\epsilon_p = 0.3 * \epsilon_{up}$$

$$= 0.5 * 0.018615$$

$$= 0.009308$$

$$f_p = 154.5 \text{ N/mm}^2$$

$$X = 37.2 \text{ mm}$$

$$\epsilon_s = 0.00611$$

$$f_s = 700.0 \text{ N/mm}^2$$

$$C = 1.430 \text{ KN}$$

$$T = 1.1.794 \text{ KN} , \quad C \neq T \quad (\text{N.K})$$

Reduce the value of the plate strain (ϵ_p)

$$\epsilon_p = 0.4 * \epsilon_{up}$$

$$= 0.3 * 0.018615$$

=

$$f_p = 127.3 \text{ N/mm}^2$$

$$X = 43.8 \text{ mm}$$

$$\epsilon_s = 0.004740$$

$$f_s = 709.0 \text{ N/mm}^2$$

$$C = 1.684 \text{ KN}$$

$$T = 1.685 \text{ KN} , \quad C = T \quad (\text{O.K})$$

From equation No.(1), the ultimate capacity is calculated as follows:

$$\begin{aligned} M_u &= 157 * 709.0 * \left(113 - \frac{0.8 * 43.8}{2} \right) \\ &+ 3 * 150 * 127.3 * \left(152.5 - \frac{0.8 * 43.8}{2} \right) \\ &= 18.36 \text{ KN-m} , \quad (0.4 \text{ m is the shear span of the} \\ &\text{beam}) \end{aligned}$$

$$M_u = \left(\frac{P * 0.4}{2} \right)$$

$$P = \left(\frac{18.36 * 2}{2} \right)$$

$$P = 91.8 \quad \text{KN}$$

B) Ultimate Flexural Capacity of Shear Beams with Bottom plates.

The ultimate flexural capacity of these beams repaired with only external web reinforcement and strengthened with bottom plates can be determined also from the general formula (eq. No.1).

$$\text{Let } (\epsilon_p) = (\epsilon_{up})$$

$$= 0.018615$$

From compatability, the depth of the neutral axis is (X) determined,

$$X = 32.3 \quad \text{mm}$$

Strain in the rebars is also determined from compatability;

$$\epsilon_s = 0.0075$$

From stress-strain curves for steel and fiber glass the cor-

responding stresses are determined;

$$f_p = 181.8 \text{ N/mm}^2$$

$$f_s = 736.0 \text{ N/mm}^2$$

Total Compression force (C) is found as follows;

$$C = 0.85 * 37.7 * 0.8 * 32.3 * 150$$

$$C = 1.24 \text{ KN}$$

Total Tension force (T) is found as follows;

$$T = 339 * 736.0 + 3 * 150 * 181.8$$

$$T = 3.3 \text{ KN}$$

$$C \neq T$$

Reduce the value of the plate strain (ϵ_p)

$$\epsilon_p = 0.3 * \epsilon_{up}$$

$$= 0.3 * 0.018615$$

$$= 0.005585$$

$$f_p = 100 \text{ N/mm}^2$$

$$X = 53.3 \text{ mm}$$

$$\epsilon_s = 0.00336$$

$$f_s = 581.8 \text{ N/mm}^2$$

$$C = 2.0 \text{ KN}$$

$$T = 1.98 \text{ KN} , \quad C = T \quad (\text{O.K.})$$

From equation No.(1), the ultimate capacity is calculated as follows:

$$\begin{aligned} M_u &= 339 * 581.8 * \left(113 - \frac{0.8 * 53.5}{2}\right) \\ &\quad + 3 * 150 * 100 * \left(152.5 - \frac{0.8 * 53.5}{2}\right) \\ &= 24 \text{ KN-m} \end{aligned}$$

$$M_u = \left(\frac{P * 0.4}{2}\right)$$

$$P = \left(\frac{24 * 2}{0.4}\right)$$

$$P = 120 \text{ KN}$$

C) Ultimate Shear Capacities of Shear Damaged Repair

The Theoretical capacities of shear beams repaired with

external web reinforcements either in the form of wings or strips are determined as follows:

$$V_c = \frac{1}{6} * \sqrt{37.7} * 150 * 113$$

$$= 17.35 \text{ KN}$$

$$V_s = \frac{2 * 28.3 * 414 * 113}{60 * 1000}$$

$$= 13.23 \text{ KN}$$

1) Strips

a) Rupturing of the Strips

$$V_p = \frac{2 * 3 * 20 * 265 * 150}{60000}$$

$$V_p = 79.5 \text{ KN}$$

$$V_R = 66.70 + 79.5$$

$$= 146.2 \text{ KN}$$

b) Ripping off the Strips

$$V_p = \frac{2 * 20 * 150 * 4 * 150}{60000}$$

$$V_P = 60 \text{ KN}$$

$$V_R = 66.70 + 60$$

$$= 126.7 \text{ KN}$$

2) Wings

a) Rupturing of the Wings

$$V_P = 2 * 3 * 265 * 113$$

$$V_P = 179.5 \text{ KN}$$

$$V_R = 66.70 + 179.5$$

$$= 246.2 \text{ KN}$$

b) Ripping off the Wings

$$V_P = 2 * 3 * 113 * 113$$

$$V_P = 76.6 \text{ KN}$$

$$V_R = 66.70 + 76.6$$

$$= 143.3 \text{ KN}$$

CALCULATION OF PLATE THICKNESSES

A) Based on Ultimate Flexural Capacity

Numerical Example (Experimental Beam Specimen)

$$\text{Let } (\epsilon_p) = (\epsilon_{up}) = 0.018615$$

From compatibility, the depth of the neutral axis (X) determined
 $X = 32.3 \text{ mm}$

The plate thickness (t_p) corresponding to the minimum plate thickness (t_{min}) is calculated by applying the equation of equilibrium, as described in chapter 4, as follows:

$$A_s' * f_s' + 0.85 * f_c' * \beta_1 * X * b = A_s * f_y + t_p * f_{up}$$

$$t_p = \frac{0.85 * f_c' * \beta_1 * x_b * b - f_y * A_s}{b_p * E_p * \epsilon_p}$$

E_p for fiber glass is 22727 N/mm²

$$t_p = \frac{0.85 * 37.7 * 0.8 * 32.3 * 150 - 414 * 157}{150 * 22727 * 0.018615}$$

$$= 0.9 \text{ mm}$$

Due to the fact that the fiber glass is built up of several layer binded with resin, the practical minimum thickness of the fiber glass plate should be at least 1 mm.

B) Based Maximum Interface Shear Stress

$$\tau_0 = \left\{ F_0 + \left(\frac{k_s}{E_p * t_p * b_p} \right)^{\frac{1}{2}} * M_o \right\} * \frac{b_p * t_p}{I * b_a} * (D - X)$$

$$X = \frac{-B + \{B^2 + 4 * A * C\}^{\frac{1}{2}}}{2 * A}$$

$$A = \frac{E_c * b}{2 * E_p} = \frac{(29 * 10^3) * 150}{2 * 22727} = 95.8 \text{ mm}$$

$$E_c = 29 * 10^3 \text{ N/mm}^2$$

$$B = A_s + b_p * t_p$$

$$\text{Take } t_p = 3 \text{ mm}$$

$$= 157 + 150 * 3.0$$

$$= 607 \text{ mm}^2$$

$$C = d * A_s + D * b_p * t_p \quad D = \left(h + 1 + \frac{t_p}{2} \right)$$

$$= 113 \times 157 + 152.50 * 150 * 3.0$$

$$= 86366 \text{ mm}$$

$$X = \frac{-607 + \left\{ (607)^2 + 4 * 95.80 * 13323 \right\}^{\frac{1}{2}}}{2 * 98.80}$$

$$X = 27.0 \text{ mm}$$

$$I = \frac{29 * 10^3 * 150 * (27.0)^3}{3 * 22727} + 157 * (113 - 27.0)^2$$

$$+ 3.0 * 150 (152.50 - 27.0)^2$$

$$= 9.5 * 10^6 \text{ mm}^4$$

where,

$$K_s = 16500 \text{ N/mm}^2, \text{ Try } t_p = 3 \text{ mm}$$

$$\tau_0 = \left\{ 21 * 10^3 + \left(\frac{16500}{22727 * 100 * 3.0} \right)^{\frac{1}{2}} * 932 * 10^3 \right\} * \frac{150 * 3.0}{150 * 9.5 * 10^6} (152.50 - 27.0)$$

$$\tau_0 = 2.3 \text{ N/mm}^2 > 2 \text{ N/mm}^2$$

$$\sigma_0 = \tau_0 * t_p * \left(\frac{k_n}{4 * E_p * I_p} \right)^{\frac{1}{4}}$$

$$K_n = 23333 \text{ N/mm}^2$$

$$I_p = \frac{b_p * t_p^3}{12}$$

$$= \frac{150 * (3.0)^3}{12} = 337.5 \text{ mm}^4$$

$$\sigma_0 = 2.3 * 3.0 \left(\frac{42000}{4 * 22727 * 337.5} \right)^{\frac{1}{4}}$$

$$= 1.33 \text{ mm} < 2 \text{ mm}$$

FIBER GLASS MATERIAL

Introduction

The use of reinforced plastics as material for engineering applications is steadily increasing as engineers acquire more confidence in them. The advances made by organic chemists during recent decades have led to the emergence of the new man-made materials commonly known as plastics. The possibilities of using these plastic materials in engineering situations are now being extensively examined, and in the case of structural engineering such development is taking place mainly in their use as glass fiber-reinforced plastics, the plastic material most widely used being polyester resin. Thus the abbreviation 'GRP', although usually thought of as meaning 'glass-reinforced plastics', should strictly be interpreted as 'glass-reinforced polyesters'.

The strength properties of plastics are reasonably good in civil engineering forms but their stiffness, when measured by their modulus of elasticity, is low. For structural applications, in which both the strength and stiffness of the material are critical, it is therefore, necessary to combine plastics with other material into composites whose properties transcend those of the constituents.

The most commonly employed component is a particulate or fibrous form. In the particulate composites, particles of a specific material or materials are embedded in and bonded together by a

continuous matrix of low modulus of elasticity. In fibrous composites, fibers with high strength and high modulus are embedded in and bonded together by the low modulus continuous matrix. The fibrous reinforcement may be oriented in such a way as to provide the greatest strength and stiffness in the direction in which it is needed, and the most efficient structural forms may be selected by the mouldability of the material. In the construction industry, glass fiber and polyester resin are used to form the fibrous composite which is then known as glass reinforced polyester (G.R.P.). In the past this abbreviation has referred to glass reinforced plastics in general, but now it refers specifically to polyesters. This material has been developed since the Second World War with the main growth interest and technology beginning in the 1960's.

The production of resins, catalysts, accelerators which cure at room temperature has facilitated the manufacture of G.R.P. by relatively straight forward techniques, using the open mould process without the need to provide presses and steel moulds.

G.R.P. is now well established in the construction industry and takes its place alongside materials such as metal and timber; it can not be considered as cheap substitute for other materials. Two sophisticated G.R.P. structures have played a major role in the development of this material; these are the dome structures erected in 1968 in Benghazi and the roof structure of the Dubai Airport built in 1972. The design and fabrication for the latter

structure took in the U.K. and the units were shipped to Dubai.

1. Mechanism of Reinforcement in Fiber Reinforced Plastics

The reinforcement of a low modulus matrix with high strength, high modulus fibers uses plastic flow of the matrix under stress to transfer the load to the fibers, this results in high strength, high modulus composite. The aim of the combination is to produce a two phase material in which the primary phase which determines stiffness and is in the form of particles of high aspect ratio (i.e. fiber) is well dispersed and bonded by a weak secondary phase (i.e. matrix). The principal constituents which influence the strength and stiffness of the composites are the reinforcing bars, the matrix and the interface. Each of these individual phases has to perform certain essential functional requirements based on their mechanical properties so that a system containing them may perform satisfactorily as composite.

Fibers

The desirable functional requirements of the fibers in a fiber reinforced composite are:

- 1) The fiber should have a high modulus of elasticity in order to give efficient reinforcement.
- 2) The fiber should have a high ultimate strength.

- 3) The variation of strength between individual fibers should be low.
- 4) The fibers should be stable and retain strength during handling and fabrication.
- 5) The diameter and surface of the fibers should be uniform.

Plastic Matrix

The plastic part of the composite in glass-reinforced plastics consists of a liquid resin which, when combined with a chemical catalyst and accelerator, sets into a comparatively rigid material. There are two main types of resins which can be hardened in this way, namely polyesters and epoxy-based resins. In glass-reinforced plastics we are concerned mainly with the polyester types of resin for which glass reinforced plastics is the major application. The matrix is required to fulfil the following functions:

- 1) to bind together the fibers and protect their surfaces from damage during handling, fabrication and during the service life of the composite;
- 2) to disperse the fibers and separate them so as to avoid any catastrophic propagation of cracks and subsequent failure of the composite;

- 3) to transfer stresses to the fibers efficiently by adhesion and/or friction (when composite is underload);
- 4) to be chemically compatible with fibers over a long period; and
- 5) to be thermally compatible with fibers.

The interface between the fibers and the matrix is an isotropic transition region exhibiting a gradation of properties. It must provide adequate chemically and physically stable bonding between the fibers and the matrix.

2. NATURE OF REINFORCED PLASTICS

Glass fiber reinforced plastics (GRP) have advantages as structural materials over both unreinforced plastics and glass fibers used alone. Unreinforced plastics have low density and are easily processed. They have good weathering properties and require no surface protection. Disadvantages which limit their use in structural applications, are low stiffness, low strength and creep under load. Glass fibers are stiff and strong but so brittle that the high stiffness and strength can not be fully utilized. By fabricating a composite material of glass fiber embedded in a plastic matrix it is possible to combine many of the desirable properties of both constituents. These glass reinforced plastics are light,

strong constructional materials with weather resistant surfaces which are easily fabricated into complex shapes. The glass fibers enhance the poor stiffness, strength and creep resistance of the plastic matrix, whose purpose is to transmit the load into the stiff fibers and to protect them from damage. A range of different GRP materials is available depending on the choice of matrix material and the method of glass reinforcement. There are two principal types of plastics, thermoplastics and thermosetting materials. Thermoplastics such as polypropylene and polystyrene are solids which soften and flow on heating and return to the solid state on cooling because of their chain-link nature. Thermosetting materials such as epoxies and polyesters are usually supplied as viscous syrups which set to a hard solid when activated by a catalyst, but remain solid on further heating because of the nature of the material which are linked together producing a mere structure that has a greater resistance to temperature effects.

It is the second type of plastics, especially the polyester resins that has been most frequently used in structural engineering applications. As materials in themselves plastics are unsuitable for major structural stiffness and ultimate strength values are relatively low and their ability to creep is not negligible. These adverse properties are, of course, analogous to the adverse effect of the low tensile strength of plain concrete which makes it unsuitable for applications in which tensile stress is developed. Thus

for the same reason that plain concrete must be 'reinforced' to produce a material with sufficient tensile strength, so plastics must be similarly reinforced if they are to provide. The reinforcement most commonly used in plastics, because of its good bonding characteristics with the resin and its high strength properties, is glass fibers. A unique feature of GRP materials is that they are usually formed during fabrication of a component.

Traditionally, this is by hand lay up in which glass fiber reinforcement is placed on a mould and impregnated with catalysed resin. The required thickness is built up in layers, the resin left to cure and the finished article removed from the mould. To facilitate this process glass fibers, are supplied in sheet form, of which there are three types.

3. TYPES OF FIBER GLASS

3.1 Woven Roving (WR)

Woven roving are a coarse glass fabric made by weaving untwisted rovings almost in plain weave. They are made in a variety of fineness and weights from 200 gm/m² to 850 gm/m² and nominal thickness from 0.2 mm to 0.9 mm. They may have equal or unequal weights for rovings in each direction. The use of woven rovings enables the highest glass contents and therefore strengths, to be achieved. Resin/glass ratio in the range 1:32.5

can be obtained.

3.2 Chopped Strand Mat (CSM)

Chopped strand mat consists of chopped glass strands 25-30 mm in length, distributed in random pattern in the plane of the mat and held together by a small amount of resin binder. The glass content obtainable with this form of reinforcement is considerably less than that using woven roving materials and resin/glass ratios in the range 2:1 to 3:1 are typical.

3.3 Surface Tissue

Surface tissue is a little like chopped strand mat except that it is made using much finer fibers and is quite thin. It is used to reinforce moulded surfaces to improve the resistance to cracking or crazing or to form a finer surface on the non-mould side of a layed-up laminate.

4. Advantages of GRP

Glass reinforced-plastics has taken its place as a proven material in wide range of industries, including marine and land transport, aerospace, building and chemical process plant. It has made these breakthroughs largely because applications have been selected in which reinforced plastics offer distinct advantages which may be summarized as follows:

- 1) Excellent corrosion resistance in a wide range of aggressive environment.
- 2) High strength/weight ratio
- 3) Light weight, easy to handle
- 4) Easy to maintain
- 5) Easy to fabricate to complex shapes
- 6) Good surface weathering properties
- 7) Good abrasion resistance.

5. Glass Manufacture

Glass fibers are manufactured for the reinforced plastics industry by the rapid drawn of molten glass marbles from an electrically heated furnace continuously and at high speed through platinum brushing. The filaments cool from the liquid state, at a temperature of 1200°C , to room temperature in approximately 10^{-5} sec. On emerging from the brushings 204 filaments are bundled together and these filaments are bonded to each other by a lubricant to reduce the abrasive effect of filaments rubbing against one another. The process of manufacturing the glass fibers is shown schematically in Fig. (B-1). Glass reinforcement used in GRP is formed from those very thin filaments which are assembled in dif-

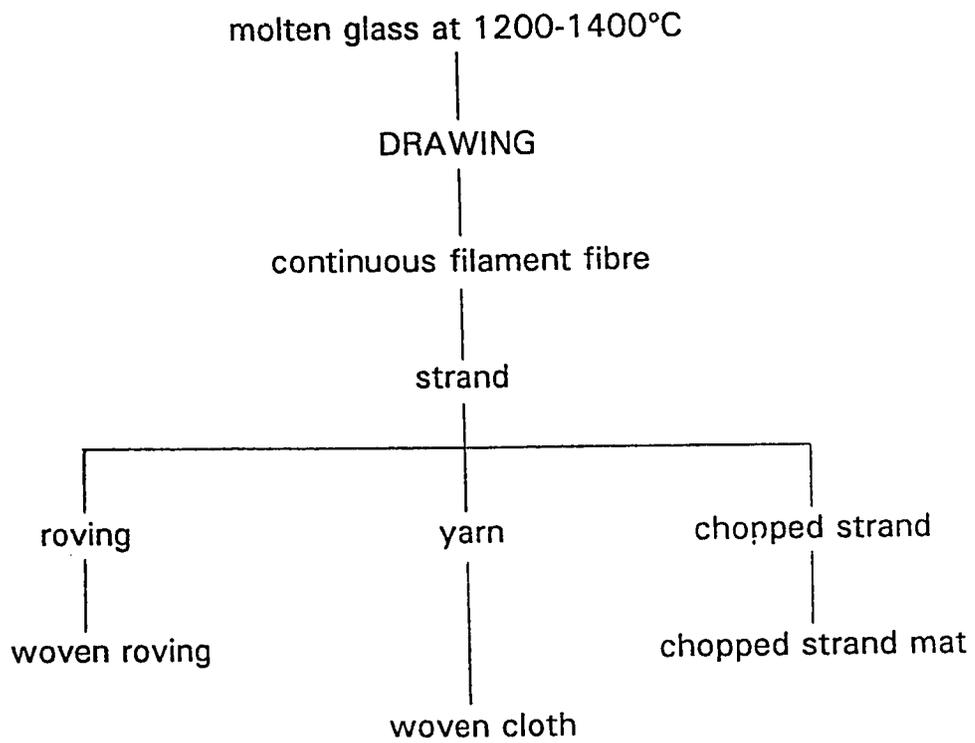


Fig. B-1 : Schematic diagram for the manufacture of glass fibre

ferent forms of strands, and bundles called rovings, the filaments are in the range of 5-10 14 μm in diameter. Because filaments of this size can not be handled separately they are combined in various forms suitable for use in reinforced plastics. Strands may also be twisted to form several types of yarns; rovings or yarns may either be used individually or in the form of woven fabric. The strength of finely-drawn filaments is much greater than glass in bulk, having tensile strength in the range of 3250 to 3650 N/mm^2 . Glass fibers are dimensionally stable, inert, incombustible, and do not creep. The two types of basic glass are known as 'E' and 'A' types. Glass type 'E' is a borosilicate having a low alkali content, under 1% calculated as Na_2O . It has higher strength, better electrical properties and greater moisture resistance than type 'A' glass. 'E' glass is the type used principally in GRP work. Type 'A' has higher silica and sodium contents; lower strength but better acid resistance than type 'E' glass. Comparative typical constituents and properties are shown in Tables B-1 and B-2

Thermosetting Plastics

Thermosetting resins are in liquid or plastic stage once, and then hardened irreversibly when suitably catalysed to form a hard solid. This chemical reaction is known as poly addition, polymerization or curing, and on completion of this reaction the material can not be softened or made plastic again without change

of molecular structure. The principal resins in use with glass fiber reinforcement are polyester resin. Unreinforced thermosetting plastics are resistant to corrosion and attack by many acids and alkalis. However, they are brittle materials with relatively low stiffness and strength and for enhancing their mechanical properties glass fiber reinforcement is needed. Typical mechanical properties of cured polyester resin are given in Table (B-3).

6. GRP MANUFACTURE METHODS

There are various techniques for the manufacture of GRP and these may be considered under two main headings. The first one is the open mould system in which, during moulding operation, the material is in contact with the mould on one surface only and this is the one generally adopted for civil engineering and structural applications. The second one is the closed mould technique in which the composite is shaped between the male and female moulds. This method is generally employed for the manufacture of small components which are not necessarily associated with the building trades.

6.1 Open Mould System

As the name implies, these processes use only one mould, and hence only the surface of the product in contact with the

mould is able to attain two advantageous characteristics of polyester resin, namely that in standard environments neither heat nor pressure is essential to attain complete curing, although at times their application may supplement the nature cure.

6.2 Hand Lay-up:

This method, the oldest, simplest and the most common technique for the production of components in fiber-reinforced plastics, is ideally suited to the production of small number of similar components such as commonly occur in structural engineering practice. The mould is first treated with a suitable release agent, such as a mineral oil, to ensure that the final product can be easily removed from the mould without damage when this has been allowed to dry, an even layer of resin up to about 0.5 mm thick, often containing additives and pigments to give weathering resistance and color to the surface, and some time reinforced with a surface tissue mat, is applied to the mould surface and allowed to cure partially. This layer is known as the 'gel coat', it serves two purposes. Firstly to protect the glass fiber from external influences, the main one being moisture penetration to the interface of the fiber and matrix, with consequent breakdown of interface bond, and secondly to provide a smooth texture of the mould, Fig. (B-2) shows the hand lay-up operation. After the gel coat has become tacky but firm, a liberal coat of resin is brushed over it and the first layer of glass reinforcement is placed in position and

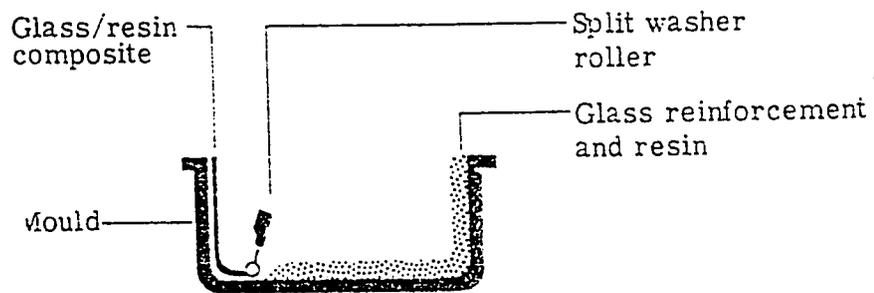


Figure B-2 Hand lay-up moulding method

consolidated with brush and roller. The glass fiber may be in the form of chopped strand mat, woven rovings or both. Subsequent layers of resin and reinforcement are then applied until the required thickness of the composite is reached.

6.3 Spray-up Method

The spray up technique is less labour intensive than the hand lay-up method. During the spray-up operation, glass fiber roving is fed continuously through a chopping unit, and the resulting chopped strands are projected on to the mould in conjunction with a resin jet. The glass fiber resin matrix is then consolidated with rollers. The technique requires considerable skill on the part of the operator to control the thickness of the composite and to maintain a constant glass/resin ratio, Fig. (B-3) shows the spray-up moulding technique.

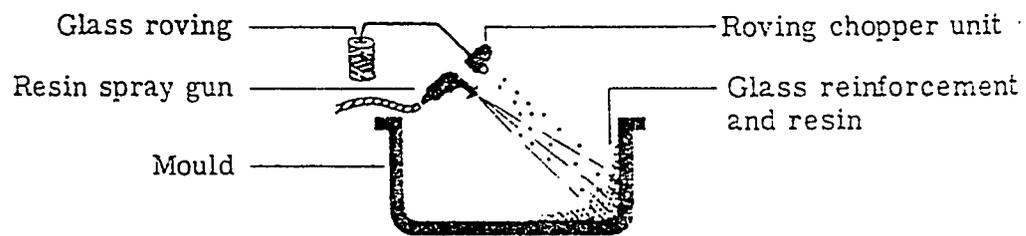


Figure B-3 Spray-up moulding technique

a) Constituents:

Composite	Type E	Type A
% silica	52	73
% Boron Acid	11	0
Sodium Potassium Oxides	1	14
Aluminum/Iron/Calcium/ Magnesium Oxides	36	13
Total	100%	100%

b) Properties:

Property	Type E	Type A
Specific Gravity	2.55	2.45
Tensile Strength of filament	3650 N/mm ²	3250 N/mm ²
Young's Modulus	76000 N/mm ²	7000 N/mm ²
Coefficient of Thermal Expansion	$5 \times 10^{-6} / ^\circ\text{C}$	$7 \times 10^{-6} / ^\circ\text{C}$
Poisson's Ratio	0.2	--

Table B-1 : Typical Constituents and properties of Fiber Glass Materil

Specific Gravity	1.28
Tensile Strength	45-90 N/mm ²
Compressive Strength	100-250 N/mm ²
Impact Strength	18-24 kg/mm ²
Elongation at Break	2%
Coefficient of Thermal Expansion	100-110x10 ⁻⁶ /°C
Shrinkage	0.005-0.008

Table B-2: Typical Mechanical Properties of Curved Polyester Resin

	Anchored Plate	193
5.51	Load Vs. Central Deflection for Unrepaired and Repaired Beams with Strips Only	195
5.52	Load Vs. Central Deflection for Unrepaired and Repaired Beams with Strips and Bottom Plate Only	196
5.53	Load Vs. Central Deflection for Unrepaired and Repaired Beams with Strips and Bottom Anchored Plate	197
5.54	Load Vs. Central Deflection for Unrepaired and Repaired Beams with Strips Only	198
5.55	Load Vs. Central Deflection for Beams Repaired with Wings and U-Jacket.....	199
5.56	Load Vs. Central Deflection for Beams Repaired with Different Repair Types Using Strips	201
5.57	Load Vs. Central Deflection for Comparison Between Beams Repaired with Wings and Strips Only.....	206
5.58	Load Vs. Central Deflection for Comparison Between Beams (with bottom Plates) Repaired with Wings and Strips	207
5.59	Load Vs. Central Deflection for Comparison Between Beams (with Anchored Bottom Plates) Repaired with Wings and Strips.....	208
5.60	Load Vs. Strain for Beams Repaired with Strips Only	211
5.61	Load Vs. Rebar Strains at Different Locations for Beam Repaired with U-Jacket	213
6.1	Peeling Force at the end of the Plate	215
6.2	Stress-Strain Curves for Fiber Glass Plates.....	216
6.3	Idealized Stress-Strain Curve for Steel and Fiber Glass.....	217